R-01-02

Modelling of future hydrogeological conditions at SFR

Johan G Holmén, Martin Stigsson
Golder Associates

March 2001

Svensk Kärnbränslehantering AB
Swedish Nuclear Fuel
and Waste Management Co
Box 5864
SE-102 40 Stockholm Sweden
Tel 08-459 84 00
+46 8 459 84 00
Fax 08-661 57 19
+46 8 661 57 19

ISSN 1402-3091
SKB Rapport R-01-02

Modelling of future hydrogeological conditions at SFR

Johan G Holmén, Martin Stigsson
Golder Associates

March 2001

Abstract

Holmén, J., G. and Stigsson, M. (2001) "Modelling of Future Hydrogeological Conditions at SFR, Forsmark", SKB R-01-02, Swedish Nuclear Fuel and Waste Management Co. Box 5864 SE-10240 Stockholm, Sweden.

Purpose. The purpose is to estimate the future groundwater movements at the SFR repository and to produce input to the quantitative safety assessment of the SFR. The future flow pattern of the groundwater is of interest, since components of the waste emplaced in a closed and abandoned repository will dissolve in the groundwater and be transported by the groundwater to the ground surface.

Methodology. The study is based on a system analysis approach. Three-dimensional models were devised of the studied domain. The models include the repository tunnels and the surrounding rock mass with fracture zones. The formal models used for simulation of the groundwater flow are three-dimensional mathematical descriptions of the studied hydraulic system. The studied domain is represented on four scales – regional, local, semilocal and detailed – forming four models with different resolutions: regional, local, semilocal and detailed models. The local and detailed models include a detailed description of the tunnel system at SFR and of surrounding rock mass and fracture zones. In addition, the detailed model includes a description of the different structures that take place inside the deposition tunnels. At the area studied, the shoreline will retreat due to the shore level displacement; this process is included in the models. The studied period starts at 2000 AD and continues until a steady-state-like situation is reached for the surroundings of the SFR, at ca. 6000 AD.

Predicted tunnel flow. The models predict that as long as the sea covers the ground above the SFR, the regional groundwater flow as well as the flow in the deposition tunnels are small. However, due to the shore level displacement the shoreline (the sea) will retreat. Because of the retreating shoreline, the general direction of the groundwater flow at SFR will change, from vertical upward to a more horizontal flow; the size of the groundwater flow will be increased as well. The present layout of the SFR includes five deposition tunnels: SILO, BMA, BLA, BTF1 and BTF2. The predicted groundwater flow at SFR and the flow through the deposition tunnels will increase with time until a steady-state-like situation will be reached; the detailed model predicts the following flows. For the waste domain of the BLA, the flow increases from 10 to 40 m^3/year; for the waste domain of the BTF tunnels, the flow increases from 2 to 8 m^3/year. For the waste domains of the SILO and the BMA, the flow is less than 0.3 m^3/year.

Flow path lengths and breakthrough times. The models predict that as long as the sea covers the SFR, the flow paths from the deposition tunnels are short and nearly vertical from the deposition tunnels to the ground surface (below the sea). When the general direction of the groundwater flow changes to a more horizontal flow, the lengths of the flow paths increase, as the flow pattern becomes more complicated. The average lengths increase from being less than a 100 m (minimum is ca. 66 m) to a few hundred meters. Considering flow paths from the deposition tunnels, the breakthrough times vary from a few tenths of years up to a few hundred years, but the slowest paths may take more than a thousand years. On the average, the shortest breakthrough times are at approximately 3000 AD – 4000 AD, during this period the groundwater flow is larger than at 2000 AD, and the flow paths are still short.

The study also includes the following topics, which are not discussed in this Abstract.
• *Location of discharge areas for flow paths from SFR and dilution at those areas.*
• *Hydraulic interaction between deposition tunnels.* • *Origin of water in deposition tunnels.*
• *Importance of fracture zones as conductors of flow.* • *Extended tunnel system at SFR.*
• *Effects of theoretical wells at SFR.* • *Tunnel flow and degradation of tunnel plugs.*
• *Flow of a failed SILO.* • *Flow of a failed or breached section of the BMA and BTF1 tunnels.*
• *Effects of small changes in the topography, caused by sediment accumulation.*
• *Groundwater saturation of the SFR repository.* • *Discussion of uncertainties.*

Abstract (in Swedish)

Holmén, J., G. and Stigsson, M. (2001) "Modelling of Future Hydrogeological Conditions at SFR, Forsmark", SKB R-01-02, Swedish Nuclear Fuel and Waste Management Co. Box 5864 SE-10240 Stockholm, Sweden. (Report in English).

Syfte. Syftet är att uppskatta det framtida grundvattenflödet vid SFR-förvaret och producera indata till den kvantitativa säkerhetsanalysen av SFR. Det framtida flödesmönstret för grundvattnet är av intresse eftersom beståndsdelar av avfallet, som förvaras i ett stängt och övergivet förvar, kommer att lösa sig i grundvattnet och transporteras med grundvattnet till markytan.

Metodik. Studien är baserad på en systemanalytisk metod. Det studerade systemet är grundvattenflödet i tunnlar och bergmassa vid SFR. De upprättade modellerna är tre-dimensionella tidsberoende matematiska beskrivningar av detta system. Modellerna representerar tunnelsystemet vid SFR och omgivande bergmassa med regionala och lokala sprickzoner. Det studerade området representeras i fyra skalor som bildar fyra modeller, vilka har olika upplösning: regional, lokal, semilokal och detaljerad modell. De lokala och detaljerade modellerna omfattar en detaljerad beskrivning av tunnelsystemet vid SFR och av omgivande bergmassa och sprickzoner. Dessutom innehåller den detaljerade modellen en beskrivning av de olika strukturer som förekommer inuti förvarstunnlarna. På grund av strandlinjeförskjutningen (landhöjningen) kommer strandlinjen att dra sig tillbaka vid det studerade området och denna process är inkluderad i modellerna. Den studerade perioden börjar vid 2000 AD och fortsätter tills stationär-liknande förhållanden erhålls för området kring SFR, vid ca. 6000 AD.

Predikterade tunnelflöden. Modellerna predikterar att så länge som havet täcker SFR, så länge kommer både det regionala grundvattenflödet och tunnelflödena att vara små. Emellertid kommer havet att dra sig tillbaka på grund av strandlinjeförskjutningen och därför kommer den generella flödesriktningen för grundvattnet vid SFR att förändras, från att ha varit riktat nästan vertikalt uppåt till att blir mer horisontellt, och storleken på grundvattenflödet kommer också att öka. För närvarande består SFR av fem förvarstunnlar SILO, BMA, BLA, BTF1 och BTF2. Grundvattenflödet och tunnelflödena kommer att öka med tiden tills dess att stationärliknande förhållanden erhålls och den detaljerade modellen predikterar följande flöden: För avfallsdomänen i BLA ökar flödet från 10 till 40 m^3/år; för avfallsdomänen i BTF ökar flödet från 2 till 8 m^3/år. För avfallsdomänerna i SILO och BMA är flödet mindre än 0.3 m^3/år.

Längd på flödesvägar och genombrottstider. Modellerna predikterar att så länge som havet täcker SFR, så länge kommer flödesvägarna från förvaret att vara korta och nästan vertikala, från förvarstunnlarna till markytan under havet. När den generella flödesriktningen för grundvattnet vid SFR förändras till ett mer horisontellt flöde förändras också flödesvägarna, som blir längre och mer komplicerade. Medelvärdet för flödesvägarnas längd ökar från att ha varit kortare än 100 m (minimum är ca. 66 m) till att bli flera hundra meter. Med avseende på flödesvägarna från förvarstunnlarna, varierar genombrottstiderna mellan några tiotals år till flera hundra år, men de långsammaste flödesvägarna kan ta mer än 1000 år. De kortaste genombrottstiderna erhålls vid ca. 3000 AD – 4000 AD; under denna period är grundvattenflödet större än vid 2000 AD, och flödesvägarna är fortfarande korta.

Studien omfattar också följande områden, vilka inte är diskuterade i detta Abstract
• *Utströmningsområden för flödesvägarna från SFR och utspädning i dessa områden.*
• *Hydraulisk interaktion mellan tunnlar.* • *Ursprung för vattnet i tunnlarna.* • *Betydelsen av sprickzoner som bärare av flöde.* • *Ett utökat tunnelsystem.* • *Effekter av teoretiska brunnar vid SFR.* • *Tunnelflöden och degradering av tunnelpluggar.* • *Flöde genom en kollapsad SILO.*
• *Flöde genom en kollapsad sektion i BMA och BTF1.* • *Betydelsen av små förändringar i topografin orsakade av sedimentackumulation.* • *Grundvatten-mättnad av SFR-förvaret.*
• *Diskussion av osäkerheter.*

Executive summary

Purpose. The purpose of the study is to estimate the future groundwater movements at the SFR repository for low- and intermediate-level nuclear waste, and to produce input data to the quantitative safety assessment of the SFR. The future flow pattern of the groundwater is of interest, since components of the waste emplaced in a closed and abandoned repository will dissolve in the groundwater and be transported by the groundwater to the ground surface.

Methodology

Method and numerical code. The study is based on a system analysis approach. Three-dimensional models were devised of the studied domain. The models include the repository tunnels and the surrounding rock mass with fracture zones. The formal models (the mathematical models) used for simulation of the groundwater flow are three-dimensional mathematical descriptions of the studied hydraulic system. To set up the formal models we used the numerical code GEOAN, which is based on the finite difference method.

Scales and models. The studied domain is represented on four scales – regional, local, semilocal and detailed – forming four models with different resolutions: a regional model, a local model, a semilocal model and a detailed model.

Models and representation of rock mass. To represent the heterogeneity of the fractured rock mass, the regional model uses the stochastic continuum approach for the rock mass between large fracture zones, and the large regional fracture zones are defined deterministically. The effective conductivity of the rock mass in the regional model is set equal to the equivalent conductivity of rock mass and local fracture zones in the whole local model. The local and the detailed models use deterministic fracture zones together with a homogeneous rock mass. The conductivity of the rock mass in the local model is set as uniform and derived from a calibration procedure. The conductivity of the rock mass in the detailed model is identical to that in the local model.

Models and representation of tunnels. The layout of the tunnel system at SFR is given in Figure 3.1 (page 19). In the local and detailed models, the tunnels are represented as separate continuous structures of connected cells. The layout of the tunnel system and the fracture zones at SFR is given in Figure 5.1 (page 26) and Figure 5.2 (page 27). The local model includes a detailed description of all tunnels at SFR and of the surrounding rock mass and fracture zones (Figure 6.3 page 42). Except for the access ramp, all tunnels are also represented in the detailed model, and in addition the detailed model includes a description of the different structures that occurs inside the deposition tunnels (barriers, encapsulations etc), see. Figure 9.3 through Figure 9.7 (pages 77 through 81).

Boundary conditions. As far as possible, the boundary conditions of the regional model coincide with the naturally occurring hydraulic boundaries (physical boundaries). The local model and the semilocal model, on the other hand, have boundary conditions

provided by the regional model, and the detailed model has boundary conditions from the local model. This modelling approach is called telescopic mesh refinement (Figure 2.4, page 13). Shore level displacement (the sum of land uplift and sea level change) is included in the model (Figure 2.3, page 8). The boundary conditions of the models are therefore time-dependent.

Establishment and simulation order of models. The models are built from the tunnel system outwards, hence from the detailed and local domains to the regional domain. The models simulate the time-dependent flow system in an order starting with the regional domain, and then based on the results of the regional domain, the flow conditions within the local and detailed domains are simulated. Hence, the order is from the regional model to the local model and from the local model to the detailed model (see Figure 2.6, page 14).

Predicted tunnel flow

Predicted tunnel flow - general evolution. Generally, the models predict that as long as the sea covers the ground above the SFR, the regional groundwater flow as well as the flow in the deposition tunnels is small. However, due to shoreline displacement the shoreline will retreat, and in around 2800 AD the shoreline will be above the deposition tunnels. As a consequence of the retreating shoreline, the general direction of the groundwater flow at SFR will change, from vertically upward to a more horizontal flow; the size of the groundwater flow will increase as well. Hence, the predicted regional groundwater flow at SFR and the flow through the deposition tunnels will increase with time, but a steady-state-like situation will be reached in around 5000 AD.

Predicted tunnel flow – details. The purpose of the detailed model is to predict the flow through the closed deposition tunnels in detail, considering the internal structures of the tunnels, such as flow barriers and encapsulations. The detailed model predicts that most of the water that flows in the deposition tunnels will flow in the highly permeable parts of the tunnels, e.g. in the top fills. These highly permeable structures will partly act as flow barriers and lead the flow away from the waste encapsulation. However, it is only in the BMA tunnel that highly permeable flow barriers surround the encapsulation on all sides; the BMA is the only tunnel at SFR that has a complete hydraulic cage protecting the waste encapsulation. The other deposition tunnel at SFR with an efficient system of flow barriers is the SILO, which is protected by low-permeable bentonite flow barriers on all sides. The tunnel with the least barriers is the BLA tunnel, which contains no waste encapsulation.

For the encapsulation in the SILO and the BMA tunnel, very small values of flow are predicted. For the BMA, this is the result of the efficient hydraulic cage that surrounds the BMA encapsulation. However, the hydraulic cage will only work efficiently if it surrounds the encapsulation on all sides. If, for example, the highly permeable gravel bed at the base of the BMA tunnel is replaced with a concrete floor, similar to that in the BTF and BLA tunnels, the flow through the BMA encapsulation will be about 20-40 times the flow of the present layout.

In the detailed model, total flow versus time has been calculated for the different internal structures of the deposition tunnels separately, the definition of the internal layout of the tunnels is given in Section 7. The flow of the different structures is given

in Table 10.2 through Table 10.10 (pages 88 through 96), as well as in Figure 10.1 and Figure 10.2 (page 91). A summary of the total flow as predicted by the established models and a comparison with the results of the previous modelling studies of the SFR is given in Table 10.12 (page 101). This study predicts much smaller flow values than the previous studies. This is partly a consequence of the much more detailed representation of the tunnel system in this modelling study, compared to the coarse representation used in previous studies.

Analytical estimate of tunnel flow. The purpose of the analytical model is to estimate the magnitude of the groundwater flow through the deposition tunnels and thereby check that no fundamental error has been included in the numerical models. The methodology of the analytical method is briefly presented in Section 7.11. The results of the analytical estimate and the corresponding results of the local model are given in Table 10.11 (page 99). The table demonstrates that the analytical predictions are fairly close to the predictions of the local model.

Results of flow path analysis

Length of flow paths from deposition tunnels. The models predict that as long as the sea covers the ground above the SFR, the flow paths from the deposition tunnels are short and more or less vertical from the deposition tunnels to the ground surface. When the general direction of the groundwater flow changes, from a vertical to a more horizontal flow, the lengths of the paths increase, as the flow pattern becomes more complicated. For the five different deposition tunnels, the length of the flow paths versus time has been calculated for each tunnel separately. Considering the base case, in which the topography remains the same in the future, the results for time-independent flow paths are given in Figure 11.9 (page 113) as well as in Table 11.1 through Table 11.5 (pages 111 through 112). A visualisation of the flow paths are given in Figure 11.1 through Figure 11.8 (pages 107 through 110)

Breakthrough times for flow paths from deposition tunnels. Generally, the models predict that the shortest breakthrough times will be in around 3000 AD for BMA, BLA, BTF1 and BTF2, and in 4000 AD for the SILO; during this period there will be a large groundwater flow as well as short flow paths. Earlier, in 2000 AD, the flow paths are short, but the size of the groundwater flow is small too. In 4000-5000 AD and later, the flow is large but the flow paths are long as well. For the five different deposition tunnels, the breakthrough times of the flow paths versus time have been calculated for each tunnel separately. Considering the base case, in which the topography remains the same in the future, the results for time-independent flow paths are given in Figure 11.10 and Figure 11.11 (pages 119 and 120), as well as in Table 11.6 through Table 11.14 (pages 116 through 118).

Fracture zones as conductors of flow paths from deposition tunnels. By investigating which fracture zones occur along a predicted flow path, we can estimate the importance of the different zones as conductors of the flow from the deposition tunnels. The general trend is that the importance of the zones as conductors of flow paths increases with time. In 2000 AD, the only important zone is zone 6; in 7000 AD zones H2, 3, 6, 8 and 9 are all involved in the pattern of the flow paths from the deposition tunnels. The

results for time-independent flow paths are given in Figure 11.12 and Figure 11.13 (pages 123 and 124). The figures present the results with a focus on the distribution of the flow in the different zones. Focusing on the distribution of flow from the deposition tunnels, the results are given in Table 11.16 through Table 11.20 (pages 121 and 122). The importance of fracture zones is also discussed in Section 17.3 (page 240)

Hydraulic interaction between deposition tunnels. By investigating which tunnels occur along a predicted flow path from a deposition tunnel, it is possible to estimate the hydraulic interaction between the different deposition tunnels. The general conclusion is that for the studied base case (with intact barriers etc.) the hydraulic interaction between the deposition tunnels is limited. To a limited extent, flow paths from BTF1 pass through BTF2, and flow paths from BTF2 and BMA pass through BLA. In the case studied, no more than 10 percent of the flow from a deposition tunnel will pass through another deposition tunnel. The largest interaction takes place between 3000 AD and 4000 AD. The results for time-independent flow paths are given in Figure 11.14 (page 126), as well as in Table 11.21 and Table 11.22 (page 125).

Origin of water in deposition tunnels. During the period from 2200 AD until 3000 AD, the retreating shoreline will pass above the SFR and as a consequence the groundwater flow pattern will change. Since the flow pattern of the groundwater changes, the origin of the groundwater that reaches the tunnels changes as well. And since the origin of the groundwater changes, the chemical composition of the groundwater that reaches the deposition tunnels also changes. The models predict that during the first 750 years of the lifetime of the SFR, the type of groundwater that will reach the deposition tunnels will change, from an old groundwater (e.g. high chloride content, low oxygen content) coming from great depth, to a young groundwater (e.g. no chloride, some oxygen) coming from recharge areas in the immediate surroundings of the SFR. The main change will take place between 2300 AD and 2750 AD. The situation with local recharge areas providing nearly all the groundwater (i.e. a young groundwater) flowing through the deposition tunnels will persist after 2750 AD as the sea (shoreline) continues to retreat. This will be the final situation as the groundwater flow system evolves into a steady-state-like condition. Details of the results discussed above are given in Section 11.7 and Figure 11.15 (page 129). The results are based on both steady and transient paths.

Location of discharge areas for flow paths from deposition tunnels –base case. The models predict that the discharge areas for the flow paths from the deposition tunnels will change with time. This is because shoreline displacement will change the flow pattern of the groundwater. The most important factors for the location of the discharge areas are the topography and the position of the sea. The models predict that most discharge areas occur along low-lying parts of the topography. The greatest discharge occurs along permeable fracture zones and especially where permeable fracture zones intersect, at low-lying parts of the topography.

In 2000 AD, the main discharge area is directly above the deposition tunnels. With time the main discharge areas move north of the SFR. Considering the length of the period studied, it is possible that the topography will change somewhat due to different processes, e.g. sedimentation. In the base case of this study no such changes have been included. However, the effects of sedimentation are included in a special case discussed below.

Assuming that the topography remains the same in the future (the base case), the main discharge area is approximately 500 m north of the deposition tunnels in 5000 AD (steady-state-like conditions). The discharge area for the SILO is not the same as the main discharge area, since the flow paths from the SILO and some flow paths from the BTF1 discharge in separate discharge areas east of the main discharge area. For the SILO there is also a separate discharge area above the SILO.

In the studied base case (in which the topography remains the same in the future), all discharge will be within a horizontal distance of approximately 700 m from the deposition tunnels. The results are given in Figure 11.16 and Figure 11.17 (pages 134 and 135).

Discharge distribution and dilution in discharge areas. The amount of flow from the deposition tunnels that discharges above and below the sea will be different at different times. In 2000 AD, all water from the repository will discharge below the sea. Assuming that the topography remains the same in the future (the base case), all discharge will take place above the sea in 4000 AD. In between, discharge will take place close to the shoreline. In discharge areas above sea level, where water from the repository will discharge, water that has not passed through the repository will also be discharged. The actual groundwater discharge will be a mixture of groundwater from the repository (polluted water) and groundwater that has not been inside the repository (non-polluted water). We have estimated the ratio between polluted water and non-polluted water in the discharge areas, and hence estimated the dilution that will take place in the discharge areas. However, as the groundwater finally discharges and forms a part of the surface water flows, there will probably be further mixing and dilution with non-polluted surface water flows; this dilution is not included in this study. The results of the estimate of groundwater dilution demonstrates that water from the deposition tunnels typically comprises only a few percent of the total discharge of groundwater in a discharge area. These results are average values for the whole areas where the flow paths from the deposition tunnels terminate. The results are given in Table 11.23 through Table 11.25 (pages 132 and 133).

Effects of theoretical wells at SFR

The purpose of the well-cases was to study the effects of a small well on the future groundwater flow field in the environs of the SFR; conclusions are given below. The conclusions below correspond to a situation when the sea has retreated from the areas surrounding the repository.

- In the case of a well located upstream of the SFR, the probability that such a well will be contaminated is very small, unless it is situated extremely close to the repository tunnels.
- In the case of a well located inside the SFR, it is likely that such a well will receive most of the contaminated water produced by the flow through the repository, but probably not all of it. A well inside the tunnel system will also give rise to a large increase of flow through the tunnels. Normally a well collects water along its entire length. However, if a well intersects a deposition tunnel and the well receives all its water from this tunnel only, which is very unlikely, all of the well discharge will be contaminated water, and no dilution will take place in the well. If the well intersects an access tunnel, dilution with non-contaminated water will take place in the well.

- If a well downstream of SFR is located along the flow routes from the repository or below a discharge point for the groundwater flow from the repository, it may intercept and collect contaminated water from the SFR, even if the well is a very weak sink. If such a well is a strong sink, it may collect a large amount of the water coming from the repository, but if the well is located outside of the flow paths and the discharge areas it will have to be a very strong sink to divert the natural flow field and receive water from SFR.

It is however unlikely that a single well will be capable of being a very strong sink and change the groundwater flow pattern on a large scale. This is due to the large potential recharge in the present climate and the small conductivity of the rock mass. In the base case in this study, we assume that the topography will remain the same in the future. For such a case it is not possible for a single well to collect all the contaminated water from the SFR, since the flow paths of the undisturbed flow from the deposition tunnels will spread out over a large domain. Dilution with uncontaminated water will also take place in a well, unless the well is located inside a deposition tunnel and collects all its water from that tunnel. A summary of the results is given in Table 12.14 and Table 12.15 (pages 159 and 160). For the positions of the wells studied see Figure 12.2 (page 143).

It is possible to define a risk area as the area within which a well might be contaminated with water coming from the SFR repository or an area within which a well may intersect the deposition tunnels. Based on a simple comparison between (i) the size of the risk area and (ii) the current well density in the SFR area, it is possible to estimate the probability that a well will be drilled within the risk areas (assuming that the well is located in a uniformly random way). The resulting probability of a well being located in a way that its discharge may become contaminated (Risk Area 1) is 0.18, which is the same as 18 percent. Consider a borehole intersecting a deposition tunnel. For a vertical bore hole (Risk Area 2) the resulting probability is 0.07 percent; and for an inclined borehole (Risk Area 3) the resulting probability is 4 percent. The values of probability given above correspond to the probability of a well being drilled within a given risk area. Hence it is not the same as the probability that a well discharge will be contaminated (Risk Area 1), or that a well will intersect a deposition tunnel (Risk Areas 2 and 3). Risk Area 1 is an area for which there is a significant probability that a well located within this area will collect contaminated water, and Risk Areas 2 and 3 may be regarded as estimates of upper and lower bounds for the probability of a well intersecting a deposition tunnel. See Figure 12.6 (page 155) and Figure 12.7 (page 157)

Extended tunnel system

There are plans for expansion of the SFR repository to make place for the disposal of radioactive waste from the decommissioning of the nuclear power plants. The purpose of the model study of the extended tunnel system is to estimate the future flow through the closed deposition tunnels of the extended tunnel system. During the design and construction of the SFR repository, when the original layout of the extended tunnel system was determined, the occurrence and extent of the local fracture zones was not known to the same degree as it is today. The layout of the extended tunnel system (see Figure 13.3 page 167) was therefore not designed to avoid the local fracture zones. Consequently, from a hydrogeological point of view, the layout of the new horizontal deposition tunnels is not optimal and can probably be improved. It follows that the groundwater flow through the new tunnels will be greater than for the old tunnels, and the flow paths from the new tunnels to the ground surface will also be shorter than for

the old tunnels. The general trend of the flow in the extended tunnel system is the same as for the model representing the present tunnel system. Hence, the predicted regional groundwater flow at SFR and the flow through the deposition tunnels will increase with time, but a steady-state-like situation will be reached in around 5000–6000 AD. It should be noted that the presence of the new tunnels will influence the flow in the old tunnels. The flow in the new deposition tunnels is generally much larger than the flow in the old deposition tunnels. For the different deposition tunnels, total flow versus time has been calculated for each tunnel separately. The results are given in Table 13.2 (page 172).

Sensitivity cases –failure of barriers

Tunnel flow and degradation of tunnel plugs. As a sensitivity case it is assumed that the plugs that separate the horizontal deposition tunnels from the access tunnels, as well as the plugs in the access ramp, will completely degrade over a given time period. During the period of degradation, the flow in the deposition tunnels will increase due to the evolution of the regional groundwater flow pattern, which is discussed in previous sections. In addition , the degradation of the plugs will produce a further increase of flow inside the tunnels. However, the degradation of the plugs will also change the direction of flow through the tunnels, which will also affect the size of the total flow.

- Considering the total flow through the whole of the tunnels, the detailed model predicts that complete degradation of the plugs will produce a total flow in the BMA, BLA and BTF tunnels that will be approximately two to three times the total flow in the same tunnels with intact plugs. In the SILO, the increase of flow in the top fill is much greater. The flow in the situation without the plugs will be 30 times the flow with plugs.
- Considering the total flow through the waste domains (encapsulations) in the tunnels, the detailed model predicts that the complete degradation of the plugs will produce a total flow in the tunnels as follows: In the BTF tunnel the flow wll be somewhat less than the flow with plugsas a result of the change in flow direction in the tunnels. In the BLA and BMA tunnels the flow will be two to three times greater than the flow with plugs. In the SILO the flow will be less than the flow with plugs, as long as the regional flow is vertical; in the case of horizontal regional flow (after 4000 AD) the flow will be somewhat greater than the flow with plugs.

The results are given in Table 14.1 through Table 14.5 (page 181 through 183). As the land above the access ramp rises above the sea, a water divide will be created in the access ramp. One consequence of the groundwater divide in the ramp is that the plugs in the ramp will be of little importance for the groundwater flow in the tunnels of the repository. Hence, with or without plugs in the ramp, the groundwater flow through the tunnel system will be nearly the same. Because of the groundwater divide in the access ramp, the large regional fracture zone (the Singö zone) will not have a great impact on the flow in the SFR tunnel system, even if all the plugs are completely degraded.

Flow in a failed SILO. As a sensitivity case we have studied the flow through a failed SILO encapsulation. This case represents a situation in which the concrete barriers and the bentonite barriers of the SILO encapsulation have been breached. The groundwater flow through a failed SILO encapsulation is much greater than the flow through an intact encapsulation. But as the SILO after the collapse still has some resistance to flow; the

flow through the failed SILO will not be the same as the flow through a completely empty SILO cavern. The detailed model predicts that a failed SILO, having a conductivity equal to 1 x 10^{-8} m/s, produces a total flow in the waste domain of the SILO between 3 and 10 times the total flow in the waste domain of an intact SILO, depending on the shoreline. The largest differences occur in 3000 AD. As far as the flow through the other deposition tunnels is concerned, the change in flow due to a failed SILO is very small if the other parts of the tunnel system are intact. Results of the detailed modelling of this sensitivity case are given in Table 14.7 (page 185) and Table 14.8 (page 186).

Flow in a failed or breached section of the BMA encapsulation. The BMA encapsulation is divided into different sections separated by concrete walls. As a sensitivity case we have studied the flow through an assumed failed or breached section. Compared to the base case, the difference is that a limited part of the encapsulation, located close to Zone 6, is defined as having the same conductivity as the surrounding backfill (1 x 10^{-5} m/s).

The groundwater flow through a breached section of the BMA encapsulation is greater than the flow in the same section with intact concrete walls, because a certain amount of the flow in the surrounding barriers will be redirected through the breached section. However, as the intact parts of the encapsulation are still low-permeable (separated by intact concrete walls), the size of the flow through the intact parts of the encapsulation will change very little. Hence, the change in flow will primarily take place in the breached section. The flow in the BMA will increase due to the evolution of the regional groundwater flow pattern, which is the same behaviour as in the base case discussed in previous sections. The flow in the intact parts of the encapsulation is nearly the same as the flow in the encapsulation in the base case.

Considering the flow in the breached section and the flow in the whole of the encapsulation, the detailed model predicts that the total flow in the breached section makes up about 97 percent of the total flow in the encapsulation. The model predicts that the breached section studied will cause a total flow in the encapsulation that is between 30 and 37 times the total flow in an intact encapsulation. When flow values calculated for other parts of the BMA tunnel – e.g. top fill, side fill etc. – are compared with the flow values of the base case, the change in flow values are small, because the properties of the surrounding materials are not changed. The effect of the breached section is mainly to redirect some of the flow that occurs in the backfill and hence provide a short cut through the encapsulation. When the predicted flow in other deposition tunnels is considered, the values predicted for this case are the same as the values predicted for the base case. The results of the detailed modelling of this sensitivity case are given in Table 14.10 (page 189).

Flow of a failed or breached section of the BTF1 tunnel. As a sensitivity case we have studied the flow through a failed or breached section of the BTF1 tunnel. The flow through such a section is larger than the flow in the same section when intact, because a certain amount of the flow in the surrounding area will be redirected through the breached section. Compared with the base case of the detailed model, the difference is that a limited part of the BTF1 tunnel, located close to Zone 6, is assumed to be breached and is defined as having the same conductivity as the highly permeable top fill (1x10^{-5} m/s). For this case we have studied two different alternatives, as regards to what extent the different barriers of the BTF1 tunnel are breached. In Alternative 1, only the waste domain (encapsulation) of the section studied is failed or breached; the floor and the side fills (concrete) are intact. In Alternative 2, all parts of the tunnel at the section

studied are breached or failed, including the floor and the side fills. The results of the simulations demonstrate that the flow in BTF1 will increase due to the evolution of the regional groundwater flow pattern, which is the same behaviour as for the base case, discussed in previous sections.

- Considering Alternative 1, the total flow in the encapsulation increases with time and reaches a steady value in about 6000 AD. The total flow in the breached part makes up about 60 percent of the total flow of the encapsulation. In comparison with a completely intact encapsulation (the base case), the flow of the breached encapsulation is about 1.6 times larger (in 3000 AD the flow is 2.3 times larger).
- Considering Alternative 2, the total flow in the encapsulation increases with time and reaches a steady value in about 6000 AD. The total flow of the breached parts makes up about 90 percent of the total flow of the encapsulation. In comparison to a completely intact encapsulation (the base case), the flow of the breached encapsulation is about 5 times larger (in 3000 AD the flow is 6.3 times larger).

Considering the predicted flow in other deposition tunnels (SILO, BMA, BLA, BTF2), the values predicted for this sensitivity case are very close to the values predicted for the base case. The results of the detailed modelling of this sensitivity case are given in Table 14.12 and Table 14.13 (page 192)

Sensitivity case – effects of small changes in the topography

Discharge areas, flow paths from the repository and sediment accumulation. The flow paths of the groundwater that has passed the repository will terminate at the ground surface, in discharge areas located north of the repository. The topography and the sea level are the main factors determining the locations of these discharge areas. In the simulations in Chapter 16 (which starts at page 217) we have assumed that with time sediments of both of biological and geological origin will accumulate in the discharge areas north of the repository, as these areas rise above the sea, which will change the topography and cause a build-up of the groundwater heads in these areas, which in turn will force the groundwater to discharge in other areas with lower groundwater heads, closer to the shoreline. Thus, the accumulation of sediments will change the location of the discharge areas for the flow paths coming from the repository, and slowly force these discharge areas to move with the retreating shoreline. As a result, the flow paths coming from the repository have a tendency to follow the retreating shoreline.

The simulations of Chapter 16 demonstrate that that it is not the permeability of the sediments that is the most important parameter with regard to the movement of the discharge areas (assuming that the permeability is not extremely large), but the rate at which the sediments accumulate. The calculated total sediment accumulation for the different cases studied is dependent on the maximum rate of sediment accumulation, but it is not directly equal to this rate, since in the model sediment accumulation will only take place in groundwater discharge areas, and only as long as the area remains a discharge area.

- The type of landscape and biological environment where the discharge takes place are of importance when calculating the effects of a release of radioactive nuclides. The flow paths from the repository will have a tendency to follow the retreating shoreline (especially if sediments accumulate in discharge areas). The different rates of sediment accumulation defined for the different cases studied resulted in different movements of the discharge areas. For the different cases of sediment accumulation

studied , we have analysed which type of discharge area the flow paths from the repository will discharge into. As a rule, there are two different situations : the discharge will either be directly into large open bodies of surface water (discharge below the sea, at the shoreline or in a lake), or the discharge will be above the shoreline and not into a lake, but into creeks and wetlands etc.

- For the case with no sediment accumulation, the discharge will be into open water or at the shoreline between around 2000 AD and 3900 AD. From then on the discharge will take place above the shoreline, see Figure 16.6 (page 237)
- For the cases studied with significant sediment accumulation in discharge areas, the discharge will be into open water or at the shoreline between around 2000 AD and 4600 AD. Between around 4600 AD and 5200 AD, the discharge will be above the shoreline, but still close to the shore, the maximum distance to the shore being about 200 m. After around 5200 AD, the discharge will be into a small lake; from then on the situation will depend on the rate of sediment accumulation in this small lake. If sediment accumulation occurs in this small lake, the lake will probably turn into a mire (bog) within a few hundred years, which may force the flow paths from the repository to move to the larger lake located north of the small lake, see Figure 16.6 (page 237).

We are aware of the fact that the geological and biological process that was studied in Chapter 16 (accumulation of sediments) is difficult to quantify and will add some uncertainty to the analysis; such processes have therefore not been included in the other analyses of this study.

Groundwater saturation of the SFR repository

At present the tunnels of the SFR are kept dry; however, some time after the repository is abandoned, the tunnels will be filled with groundwater. One purpose of this study is to simulate the transition period during which the tunnels are being filled with water (the saturation period). We have estimated the length of the saturation period based on different analytical and numerical methods. The detailed model was defined with a porosity that varied for the different structures inside the tunnels (see Table 15.4, page 200). A transient numerical modelling of the saturation period was carried out by use of the complete chain of models (regional–local–detailed).

The last part of the deposition tunnels to become saturated is the void inside the SILO encapsulation; it may take 25 years to saturate this structure. The time necessary for the complete saturation of the BMA, BLA and BTF tunnels is a few years. The detailed results are given in the following tables and figures: Table 15.6 (page 203) through Table 15.10 (page 204), as well as Figure 15.2 (page 205) through Figure 15.6 (page 207).

Analytical solutions of the transient course of saturation have also been derived. The good agreement between (i) the inflow as predicted by the numerical GEOAN model and (ii) the inflow as predicted by the analytical solutions demonstrates that no fundamental error has been included in the numerical model.

Discussion of uncertainties

The uncertainty in the conceptual model and the uncertainty stemming from generalisations and simplifications applied in the formal models will give rise to uncertainty in the predictions. To minimise the uncertainties we have used calibration procedures and sensitivity analyses when establishing the formal models and when selecting the case used for detailed studies. The calibration procedure and sensitivity analysis will not eliminate the uncertainties, but will provide us with a plausible model for which the uncertainties are limited considering the knowledge available for the system being studied. Sensitivity analysis will provide us with an estimate of the importance of different parameters.

The predicted flows through the deposition tunnels should be regarded as estimates, and since we do not know the uncertainty in the conceptual model, it is not possible to estimate a confidence interval for these results. In Chapter 17 (page 239) we have discussed uncertainties due to unknown regional properties, the importance of fracture zones and the conductivity of the rock mass, as well as the uncertainty stemming from the numerical procedure. If we add these uncertainties together it is possible to estimate a probable total uncertainty for the flow through the deposition tunnels. The uncertainty is approximately plus 100 percent and minus 50 percent; it should however be noted that this is only an estimate.

The uncertainties in the locations of the discharge areas are small, assuming that the current topography does not change in the future. The discharge areas are approximately the same for all the cases simulated, with or without fracture zones, or with a negligible rock mass conductivity (but with fracture zones), assuming the topography remains the same. Hence, the topography and the position of the shoreline are the main factors that determine the location of the discharge areas. This means that for a given topography, the uncertainty is limited when a calculated representative value of the flow path lengths is considered. However, in view of the length of the period studied, even small changes in the topography (a few millimetres per year) will lead to changes in the locations of the discharge areas and thereby in flow path lengths. The predictions of breakthrough times are very uncertain, as they depend not only on the length of flow paths and size of groundwater flows, but also on the effective porosity.

Table of contents

1. Introduction and purpose

The Swedish Nuclear Fuel and Waste Management Co. (SKB) is operating the SFR repository for low- and intermediate-level nuclear waste. SKB has launched the project, SAFE (Safety Assessment of Final Disposal of Operational Radioactive Waste), the aim of the project is to update the safety analysis of SFR and to prepare a safety report that will be submitted to the Swedish authorities. This study is a part of the SAFE project, and concerns the future hydrogeological conditions at the SFR repository.

1.1 General purpose of study

The general purpose of this study is to estimate the future groundwater movements at SFR and to produce input to the quantitative safety assessment of the SFR. The future flow pattern of the groundwater is of interest, since components of the waste emplaced in a closed and abandoned repository will dissolve in the groundwater and be transported by the groundwater to the ground surface.

1.2 Method

The study is based on a system analysis approach, and the studied system is the groundwater flow at SFR. To reach the objectives of the study, different mathematical models were devised of the studied domain; these models will, in an idealised and simplified way, reproduce the present and predict the future groundwater movements. The models include a detailed description of the repository tunnels and of the surrounding rock masses with fracture zones. The formal models (the mathematical models) used for simulation of the groundwater flow are three-dimensional, time-dependent mathematical descriptions of the studied hydraulic system. To set up the formal models we used the numerical code GEOAN, which is based on the finite difference method.

1.3 Detailed objectives

The safety analysis of the SFR repository regards a period of many thousands of years into the future. The SFR is located below the sea and about 600 meters off the shoreline. Considering the length of the time period studied, and the localisation of the repository, the analysis needs to include the effects of the shore displacement (the sum of the land uplift and the sea level change) as the shore displacement will influence the groundwater flow at the repository area. The established models will predict the groundwater conditions until steady-state-like conditions prevails at SFR, which means for a time period of about 5000 years into the future. The results of the study include:

- Magnitude and direction of groundwater flow.
- Details of the flow inside the deposition tunnels, size and distribution of flow etc.

- Length of flow paths from repository
- Breakthrough times of flow paths from repository
- Importance of fracture zones as conductors of flow
- Evaluation of hydraulic interaction between tunnels
- Development of discharge areas and dilution at discharge areas, considering transport and flow from the repository
- Origin of the water that reaches the deposition tunnels
- Flow in tunnels considering, (i) degradation of tunnel-plugs, (ii) collapse of a section of the encapsulation of the BMA and BTF1 deposition tunnels and (iii) different values of permeability of the backfill surrounding the encapsulation of the BMA deposition tunnel as well as (iv) collapse of the SILO encapsulation.
- Effects of theoretical wells at the SFR area.
- Flow of the tunnels of a future extended tunnel system.
- Details of the groundwater saturation of the tunnel system, after the repository is closed, length of saturation period, distribution of flow etc.
- The effects of sediment accumulation as regards flow paths coming from the SFR
- Uncertainties and sensitivity analysis as regards e.g. importance of fracture zones and the size of the excess heads measured before the construction of SFR.

Hydrogeological modelling work was suggested in the study, "Update of the SFR-1 safety assessment. Phase 1." Andersson *et al* (1998). The following was proposed:

The objectives of repository scale analysis is to evaluate the groundwater flow situation on the repository scale under varying conditions and thereby to:

- *Provide estimates of the groundwater flow needed in the source term modelling.*
- *Identify the portion of rock where far-field migration may take place, identify regions for discharge into the biosphere.*
- *Provide estimates of the evolution of groundwater discharge and recharge areas.*
- *Assess the uncertainties in the predictions, which are caused, by the uncertainties in the adopted modelling approach.*

It was also suggested in the study by Andersson *et al* (1998) that the objectives of a hydrogelogical modelling should include:

- *The effects of wells and the possibility for dilution in wells placed in the repository region.*
- *The distribution of incoming water between the SILO and the different caverns during the saturation phase and in the long-term perspective considering the hydraulic properties of barriers in the SILO and in the caverns.*
- *The distribution of the water flow between the different barriers within the caverns considering the hydraulic properties of the different barriers.*

1.4 Layout of report

This study is divided into19 chapters and three appendices. The first part of the study concerns the methodology, the conceptual model (a description of the system studied) and the established formal models (used for simulations); this part of the study is given in Chapters 2 through 9. The results of the study are given in Chapters 10 through 16. A discussion of uncertainty is given in Chapter 17 and general conclusions are given in Chapter 18.

2. Methodology

2.1 The system analysis approach

In this study the limited part of the reality that we are investigating is called *the system*. *The model* is an idealised and simplified description of the studied system. This study is based on *the system analysis approach*. This is a method for solving complicated problems by: (i) establishing a model of the studied system, (ii) using the model for simulations which imitate the behaviour of the studied system and (iii) based on the results of the simulations, determine a solution to the investigated problem.

Based on the objectives, and on available information of the system studied, a conceptual model is established. *The conceptual model* includes information of the studied media (repository and rock mass) and the physical processes governing the groundwater flow, but it includes only information relevant as regards the objectives of the study. Based on the conceptual model a formal model is established. *The formal model* is a mathematical description of the conceptual model, it is established by the use of a computer code. The formal model is used for simulations.

2.2 Original flow equation

The formal model is a three-dimensional, time-dependent mathematical description of the studied hydraulic system. Groundwater flow will be calculated with the use of Darcy's law (Darcy, 1856). Darcy´s law assumes a non-deformable flow medium and that the inertial effects and the internal friction inside the fluid are negligible; these generalisations are applicable, considering the flow system studied. We will also assume that the fluid has a constant density, this is motivated by the small differences in salt concentrations measured in the groundwater at the SFR, and as previous calculations have shown that the density effects are not significant (Stigsson et al, 1998).

Hence, the governing equation for groundwater flow in a continuous medium is the following differential equation (presuming constant fluid density, the X-direction and the Y-direction is in the horizontal plane, the Z direction is in the vertical plane).

$$\frac{\partial}{\partial x}\left(K_x \frac{\partial \phi}{\partial x}\right)+\frac{\partial}{\partial y}\left(K_y \frac{\partial \phi}{\partial y}\right)+\frac{\partial}{\partial z}\left(K_z \frac{\partial \phi}{\partial z}\right)-VF = Ss \frac{\partial \phi}{\partial t} \qquad (2.1)$$

K_x , K_y , K_z = *Hydraulic conductivity along axes* [$L\ t^{-1}$]
ϕ = *Hydraulic head (Piezometric head, Groundwater head)* [L]
VF = *Volumetric flow (flow per unit volume, inflow and outflow of water)* [T^{-1}]
Ss = *Specific storage of medium* [L^{-1}]
t = *Time* [T]

The head (hydraulic head) is defined as the sum of pressure and elevation. The development of Equation 2.1 from Darcy's law and from the continuity equation is well known, see for example Bear and Verruit (1987).

Equation 2.1 constitutes, together with initial conditions and boundary conditions, a mathematical representation of a flow system. Analytical solutions to the equation normally exist only for very idealised and simplified cases. Consequently, models representing tunnels with complicated properties, or models representing a heterogeneous flow medium, have to be models based on numerical methods - in this study the finite difference method.

2.3 Numerical and analytical approach, computer codes

The formal models are mathematical descriptions of the studied hydraulic system. The formal models are based on a numerical approach and established by use of the GEOAN computer code. This is a computer code based on the finite difference numerical method. The finite difference method and the GEOAN code are briefly presented in Holmén (1997); the code was first presented by Holmén (1992). We will also use an analytical approach, based on a method originally proposed by Carslaw and Jaeger (1959), the method is presented in Holmén (1997).

2.4 Mathematical approach to the flow media – the heterogeneity of the flow media and the models

The established models represent the tunnels of the repository and the surrounding rock mass. The SFR is located in a fractured crystalline rock mass. Groundwater flow in such a rock occurs in fractures and in fracture zones of different size and significance. These fractures and fracture zones determine the heterogeneous and anisotropical hydraulic properties of the rock mass (see Sec.5.2.1).

There are different ways of making a mathematical description of a fractured medium. In this study we will use the continuum approach, which replaces the fractured medium by a representative continuum in which spatially defined values of hydraulic properties can be assigned to blocks of a given size. A large number of blocks represent the studied media (the rock mass and the tunnels). We will in this study not discuss in detail the concept of the continuum method; for a detailed presentation of the continuum method we refer to Bear and Verruit (1987) and Bear and Bachmat (1990).

Properties may be assigned to the blocks in a deterministic way, if the detailed information is available i.e. *a deterministic continuum model*. If we replace a heterogeneous property (e.g. the conductivity) with an average value and assign that value to the blocks of a model, we will get a model that we will call *a uniform continuum model*. If detailed information of the hydraulic properties are unknown and we want to include the heterogeneity into the model, we can use *a stochastic continuum model*. In a stochastic continuum model the hydraulic properties of the blocks are described by probability distributions, selected to fit the size of the studied blocks. The

different methods should be regarded as different ways of idealising and simplifying the system studied, when establishing a mathematical model representing the system.

For the system that we will study, it is possible to identify three different types of flow media: the rock mass between large fracture zones, the large fracture zones and the tunnels. What type of fracture zones that will be defined as "large" depends on the scale of the model used for representation. We will use the following approach considering the continuity and the conductivity of the different identified flow media:

- The rock mass between large fracture zones will be defined as continuous, having either: (i) a homogeneous conductivity by use of representative averages values of conductivity or (ii) a heterogeneous conductivity by use of the stochastic continuum approach. We will in this study not discuss in detail the concept of the stochastic continuum approach; the method is discussed in many studies, e.g. Neuman (1987) and (1988). A review of the theory is given in Follin (1992).
- Large fracture zones will be defined as separate continuous structures, by use of an implicit formulation as regards the conductivity of the different volumes defining the geometry of the models (the cells). The conductivity of the zones is defined as being homogeneous, by use of representative average values of conductivity.
- The tunnels will be defined as separate continuous structures, by use of an explicit formulation as regards the conductivity of the different volumes defining the geometry of the models.

For the very close surroundings of the tunnel system, the heterogeneity of the flow media is rather well known, as the local fracture zones are known. Consequently, for this domain, the large important structures of the heterogeneity are known and included in the models, and the remaining heterogeneity is probably of less importance considering average representative results. If we want to include the remaining heterogeneity, in the models representing the very close surroundings of the tunnel system, such a heterogeneity has to be specified as rather limited, as it otherwise may create local fracture zones in the models that are actually not present in the close surroundings of the SFR repository. Such a limited heterogeneity will probably be of a minor importance considering representative results. Hence, for the local domain that surrounds the tunnel system, the rock mass between known fracture zones is defined as homogeneous in the models, and the fracture zones are defined as homogeneous as well, but with a different (larger) conductivity.

We have much less knowledge of the heterogeneity of the regional domain. The only known fracture zones of this domain are some large regional zones, a few of them are known from structural geological investigations by drilling, but most of them are only interpretations based on topographic maps. For the regional domain we have included the heterogeneity of the rock mass between the large fracture zones for some of the studied cases and not included this heterogeneity for other cases. For the cases with heterogeneity between large fracture zones, the heterogeneity was included by use of the stochastic continuum method.

For some of the objectives of this study, the unknown and not included heterogeneity of the rock mass (the heterogeneity that is not represented by the fracture zones), is of less importance -these objectives are the predictions of the flows inside the tunnels. The not

included heterogeneity of the flow media outside of the tunnels is of less importance considering the flow inside of the tunnels, because the models will be calibrated to reproduce the actual measured inflow to the tunnels and because the flow inside the tunnels will be inside the tunnels (sic!) and for the tunnels the properties are known and included in the models.

For other objectives, the unknown and not included heterogeneity might be of more importance – such objectives are typically based on an analysis of simulated flow paths in the rock mass, e.g. length of flow paths from the repository to the discharge areas and breakthrough times. Considering the results of the flow path analysis, the approach used for the local domain, with a homogeneous rock mass between given fracture zones having different but homogeneous properties, will provide us with good estimates considering average representative results. However, the actual variation of results caused by the local heterogeneity of the rock mass and especially by the heterogeneity inside the fracture zones, is not included in this study. To calculate such a variation also the heterogeneity of the rock mass and the fracture zones need to be included and as such heterogeneity has not been included in this study no such variation is calculated.

2.5 Salt water and the importance of variable density flow

The salinity of the Baltic Sea has fluctuated during the last 10 000 years, this has been investigated by several authors e.g. Westman (1997). Today the salinity of the sea water outside of Forsmark (SFR) is about 0.5 percent, (Marine Ecosystem Modeling group, 1996). Kautsky (1998) predicted that the salinity of the sea water at Äspö will be constant for the next 5000 years. SFR is 400 km North of Äspö; the bottom topography of the Baltic Sea makes SFR situated north of a topographic threshold. According to Stigsson *et al* (1998) it is likely that these topographic conditions will make the seawater at SFR less saline in the future, as the heavy saline seawater will have difficulties to pass this topographic threshold.

Samples have been taken of the groundwater at SFR. Representative values of the undisturbed chemical conditions were taken by use of bore-holes drilled from the sea, during the pre-investigation phase, the chloride content varied between 1375 and 4360 mg/litre (Axelsson (1997), based on Hagconsult, 1982).

Stigson *et al* (1998) investigated the importance of variable density flow at SFR, by use of two-dimensional models, representing a large vertical cross-section. A large number of different cases were studied. The changed parameters were:
- Permeability.
- Porosity.
- Change in long term evolution of the salinity in the sea-water.
- Presence of vertical and/or horizontal structures.

The most important conclusions were:
- The porosity has a large impact on the results since higher porosity means that the transport time is longer and that more saline water has to be flushed out.

- As the model becomes more complex (i.e., incorporating heterogeneity structures, etc) the spatial differences in salinity and the difference in flow through the SFR, between variable-density and uniform-density flow, becomes less significant.
- Differences between modelling groundwater as a variable-density flow or a uniform-density flow with salt (chloride) as a tracer at the SFR is negligible.

Thus, based on the conclusions by Stigsson *et al* (1998), we have not included density dependent flow in the models of this study.

2.6 A qualitative assessment of the groundwater development and its representation in the formal models

2.6.1 Introduction

It is necessary to make a qualitative assessment of the past and future development of the groundwater system, because the formal models need to be established in a way that they are capable of representing the development that we assume as the most likely. For example, as we assume that the shore level displacement has occurred and that it will continue, we need to describe the past and future shore displacement and establish models that are time-dependent and capable of representing this phenomenon. It follows from the time-dependent models that we need an initial condition, this condition must be based on the assessment of the past groundwater system. Hence, the results of this study depend on the assumed development of the groundwater system, as the models will be established in accordance with these assumptions.

2.6.2 The shore level displacement - the land uplift

During the latest glacial period large amounts of water were tied to the ice mass, which had a maximum thickness of about 3 km. When the ice began to melt both the levels of the land and the water levels of the seas became higher. The interplay between land, ice and the water has resulted in different water levels and different types of water in the Baltic Sea as well as in the Baltic shield rock. In some periods the Baltic Sea was a freshwater lake while in others it was a saline sea. The sum of the ground level changes and the sea level changes is called shore level displacement. We assume that a shore level displacement has occurred in the past and that it will continue in the future. Påsse (1996) presented a mathematical model of these phenomena.

The shore level displacement in the models of this study, will be defined in accordance with the estimations given by Påsse (1996), see Figure 2.1 and Figure 2.2. The models must be time-dependent to be able to reproduce the changing flow pattern of the groundwater, caused by the shore level displacement. In the models, the shore level displacement will be simulated as a lowering of the level of the seawater table, a lowering in relation to a fixed reference system. The topography and the different positions of the Sea are given in Figure 2.3 as well as in Figure 11.16 and in Figure 11.17. The topography of this study does not include piers, embankments and quays of

the SFR harbour. Considering the purpose of this study, the presence of these constructions are not very important, furthermore it is possible that the piers and embankments of the SFR harbour will be removed, before the closure of the repository.

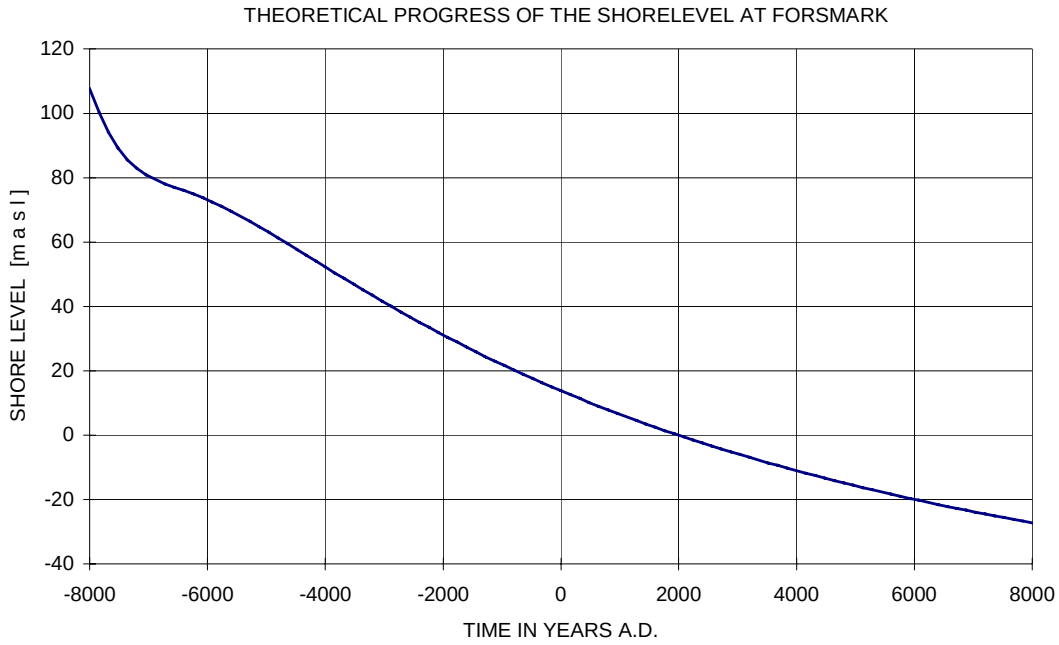

Figure 2.1 *The shore level displacement as a result of land-rise and sea level change, Påsse (1996).*

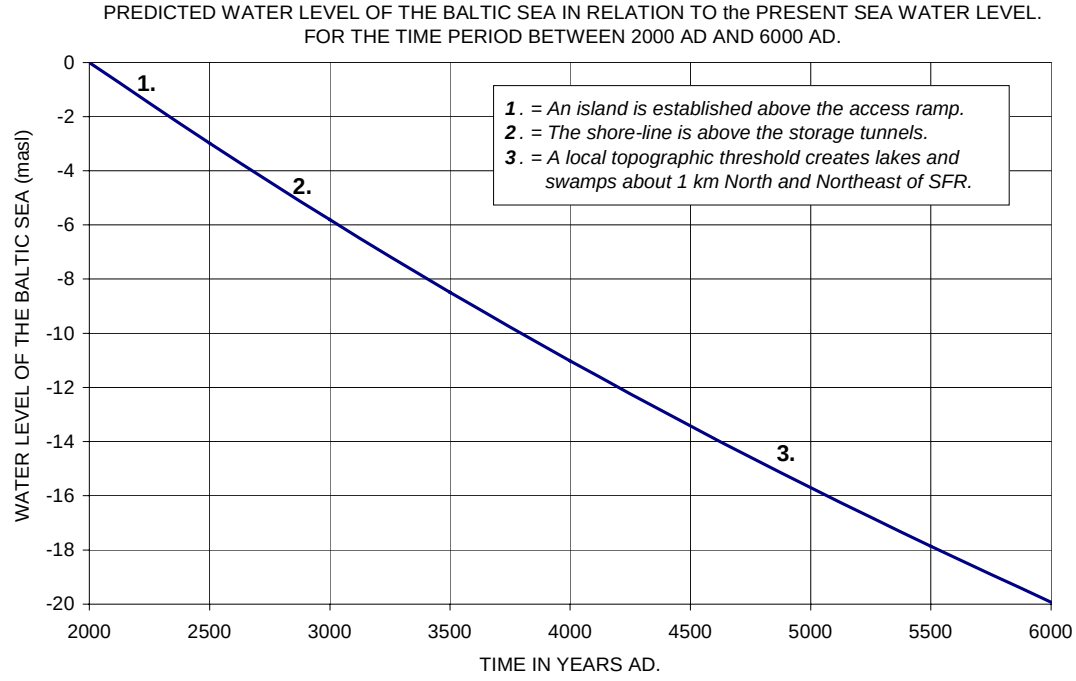

Figure 2.2 *Water level of the Baltic Sea versus time. For the time period from present and until 6000 AD. Prediction based on the shore level displacement as predicted by Påsse (1996).*

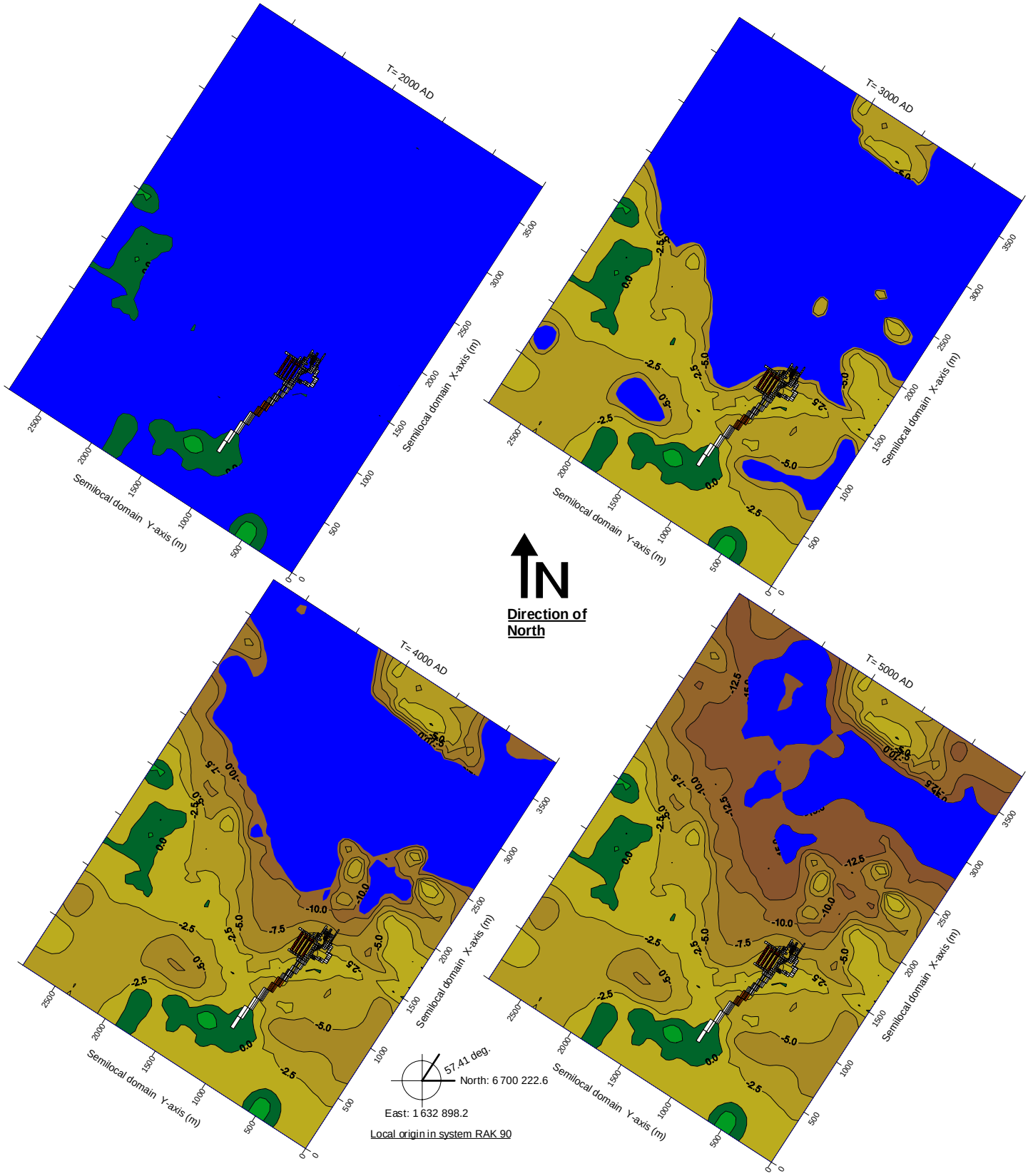

Figure 2.3 *Semilocal domain, the topography, the retreat of the shoreline and the position of the SFR repository.*

The figure gives the following situations: upper left is 2000 AD, upper right is 3000 AD, lower left is 4000 AD and lower right is 5000 AD.
The position of the SFR repository is denoted as:

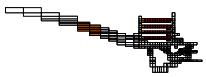

The studied time period starts with an initial condition at time equal to the year 0 AD and continue until steady-state-like conditions are reached for the groundwater system at SFR, which means until about 5 000 AD – 7 000 AD. At present, the depth of the sea is about 2 - 6 meters at the area where the SFR deposition tunnels are located, and the deposition tunnels are about 600 meters off the shoreline. We will predict the groundwater flow at the SFR area for the present situation and for a time period of 6000 years into the future. In relation to the length of the time period studied, the seabed above the repository will rise above the sea level in the near future. As the shore level retreats from the present position, the first part of the seabed that will rise above the sea is the ridge above the Northeast part of the access ramp (see Figure 2.3); at present a pier is located along this ridge. Already at 2250 AD, when the sea water level is 1.5 m lower than the present level, with or without the pier this part of the seabed has risen above the sea and formed a small island. The shoreline will be above the main deposition tunnels at about 2800AD.

It follows from the regional topography at the Forsmark area, that the shoreline will be several kilometres away from the repository at 7000 AD. However, as the shore level withdraws towards lower elevations, local lakes and mires will be established because of topographic thresholds. At about 4800 AD it is likely that such a topographic threshold will create a lake (and some smaller lakes and mires) about 1 km North and Northeast of the SFR repository. The exact water level of these lakes and mires is somewhat uncertain, as it depends on the future elevation of a certain topographic threshold; it is however likely that the water level will be at about -15 masl. The extension of these lakes is given in Figure 2.3. The topography will be discussed further in Chapter 4.

2.6.3 Initial condition

The models needs an initial condition, the initial condition is an assumed state of the studied system at the start of the time-dependent simulation. The actual condition of the system at past times is not known, consequently we will have to assume an initial condition. As a robust approach we will set the initial condition to a situation when the whole of the model is below the sea, and assume isostatic groundwater heads for this situation. Based on the analysis by Påsse (1996) regarding the shore level displacement, we note that all of the regional model will be below the seawater table at year 0 AD (except a few small islands close to west boundary of the regional model). We will set this time to the start point of the time-dependent simulation. For this start point (initial time) we will assign the model a generalised condition for the groundwater heads, everywhere in the models we will set the groundwater heads equal to the seawater level -this is the initial condition.

2.6.4 Future development of the groundwater flow field

From the initial condition, the shore level displacement will continue and as a consequence the land will successively rise from the sea. The groundwater heads will change and an increased groundwater flow will take place. Because of the land uplift and the moving shoreline, the groundwater flow will be increased close to the shoreline. Initially, below areas no longer covered by the sea, the main flow direction of the groundwater will be towards the ground surface and towards the retreating shoreline.

With time, as the shoreline moves further away, the groundwater flow will develop into a steady-state-like situation, with recharge and discharge areas primarily controlled by the local topography.

2.6.5 Flow condition in the tunnels

The purpose of this study is to estimate the future groundwater flow at SFR. At present the tunnel system is kept dry, all the water that leaks into the tunnels are pumped to the ground surface. In the close surrounding of the tunnels the groundwater flow is directed towards the empty tunnels. However, in the future the repository will be closed and abandoned and the tunnels will not be kept dry.

The present conditions at SFR, with dry tunnels, have lead to groundwater drainage and a lowering of the groundwater head in the rock mass surrounding the SFR tunnels, compared to undisturbed conditions (without the tunnels). When the tunnels are abandoned and no longer kept dry, the groundwater head will rise in the tunnels and in the surrounding rock mass, after some time the tunnels will be filled with water. The groundwater system will after some time reach a new equilibrium, in which most of the tunnels will act as permeable conductors of the groundwater flow. There will be a transition period when the tunnels are being filled with water and the local groundwater situation develops into a steady-state-like situation (with respect to the flow in the tunnels). This steady-state-like situation and local equilibrium should not be confused with the slow change in flow conditions caused by the shore level displacement.

We will simulate the present situation for the calibration of the local model. For the predictive simulations, the models will imitate the flow through closed and abandoned tunnels that are not kept dry. The models will simulate a situation when all tunnels are filled with groundwater and the groundwater situation has reached a steady situation as regards the transition period when the tunnels are filled with water. The transition period is not reproduced in the main predictive simulations, but in a separate analysis.

2.7 Chain of models

2.7.1 Chain of models and the representation of the flow domain

We will use a chain of different models at different scales, representing the studied system (the flow domain). This is because the numerical methods put practical restrictions on the amount of information represented in a single model. We will use a regional model, a local model, a detailed model and a semilocal model. All models include the same information as regards the tunnel system and the local fracture zones, however to what degree of details this information is included in the models depends on the resolution of the model. The regional model represents the system on a regional scale; this model will have a regional resolution. The local model represents the system on a local scale; this model will have a local resolution. The local model represents a much smaller domain than the regional model. However, the regional model also represents this small domain, in a simplified way, at the centre of the regional model,

see Figure 2.4 and Figure 6.1. The purpose of the detailed model is to represent the tunnel system in such a detail that also important internal features of the tunnel system will be included in the model. As far as possible, the boundary conditions of the regional model coincide with the naturally occurring hydraulic boundaries (physical boundaries). The local model and the semilocal model, on the other hand, has boundary conditions provided by the regional model and the detailed model has boundary conditions provided by the local model. This approach of modelling is often called the nestled approach or the approach of telescopic mesh refinement.

2.7.2 Chain of models and the time-dependent approach

The purpose is to represent a time-dependent course. The regional model will be used for fully time-dependent simulations. The local model will not. Instead, the local model will be given boundary conditions that are taken from the regional model (from the time-dependent regional simulation), these conditions represents different moments in time. For each studied moment, defined by the boundary conditions, the local model will be solved until an acceptable mass balance is reached, based on the condition that no storage or release of fluid will take place in the local model; the same method is used for the detailed model, except that the given boundary conditions comes from the local model, see Figure 2.5. The solution of the local model and the detailed model is not a fully time-dependent solution, as time-dependent internal storage/release of fluid will not take place in the models. This approach is an acceptable simplification, as the driving force of the flow system in the local and detailed models are the boundary conditions, and the boundary conditions are time-dependent as they come from the time-dependent regional model. The advantage of this approach is that we will have a good control of the accuracy of the numerical solution of the local and detailed models. The local and detailed models will contain a complicated three-dimensional system of permeable tunnels and fracture zones, and it is very important to ensure a good numerical solution for such a complex system. The semilocal model, which is not a part of the primary chain of models, will be solved under fully transient conditions, but this model will also include time-dependent boundary conditions, taken from the regional model, which represents the change in the regional groundwater flow.

2.7.3 Chain of models, the establishment order and the calibration

The formal models will be built in the following order. First we will start with the tunnel system at SFR and its close surrounding, from there on the models will be built outwards. The local model will be established first, because we have detailed information of the local domain. The local model will be calibrated based on the present flow situation, with local boundary conditions representing the present situation. The regional model will be established after the local model. When establishing the regional model, the results of the calibration of the local will model will be considered, Figure 2.6 illustrates the order of establishment.

2.7.4 Chain of models and the simulation order

The formal models will be used for simulations. The simulation will be carried out in the following order. First the regional model is used for fully time-dependent simulations; producing time-dependent head values at the boundary of the local domain.

The local model will be used for simulations after the regional model has performed its simulation and the detailed model will be solved after the local model, Figure 2.5 and Figure 2.6 illustrates the order of simulations.

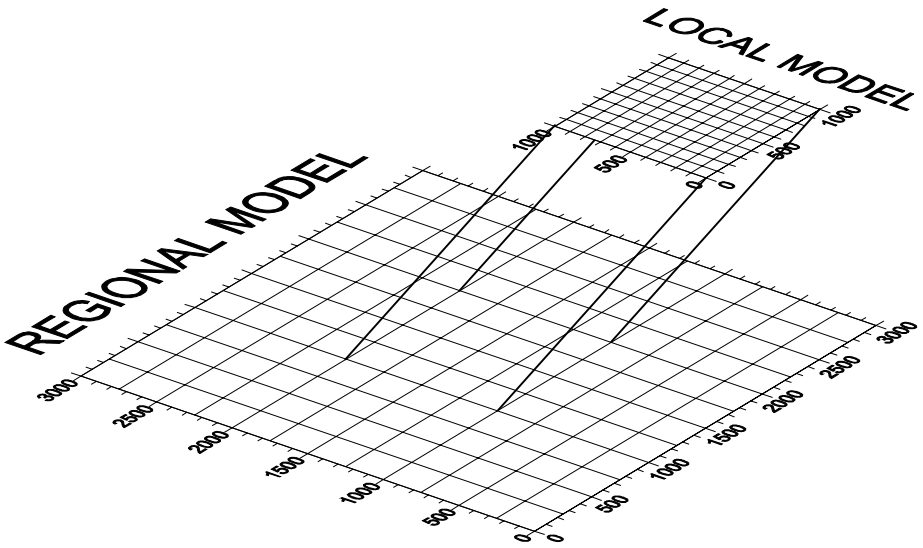

Figure 2.4 *The principle of the chain of models as regards the spatial domain.*

The telescopic approach -the large regional model and the small local model. The local model represents a part of the regional model, in the local model the resolution is higher than in the regional model. The figure demonstrates the principle only, the actual models used in this study are large 3D-models.

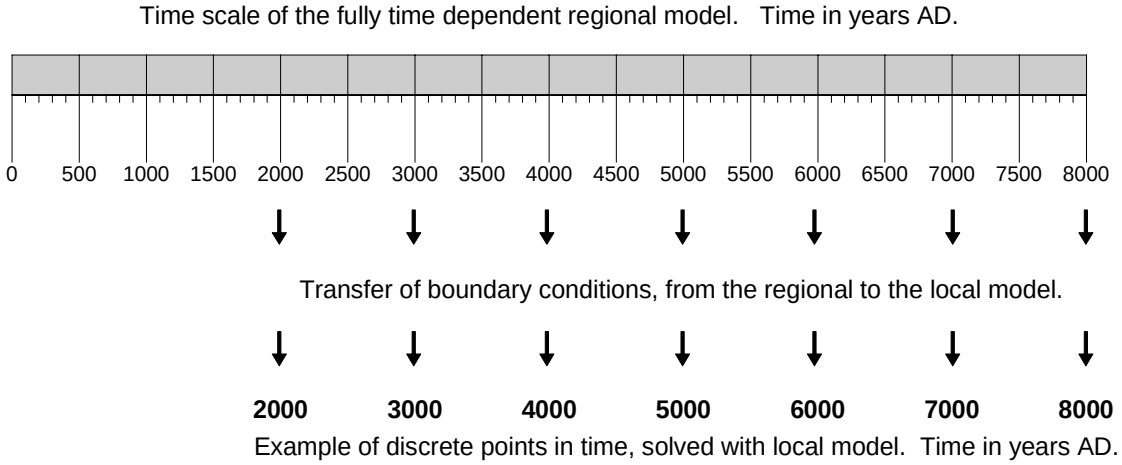

Figure 2.5 *The principle of the chain of models as regards the time domain.*

The fully time-dependent regional model provides the local model with time-dependent boundary conditions. At specific points in time, boundary conditions are transferred from the regional model to the local model, and the local model is solved for these specific moments in time only. The same method is used for the detailed model. At specific points in time, boundary conditions are transferred from the local model to the detailed model, and the detailed model is solved for these specific moments in time only. The semilocal model is a fully time-dependent model but it is solved after the regional model and it uses the results of the regional model for representation of the regional groundwater flow.

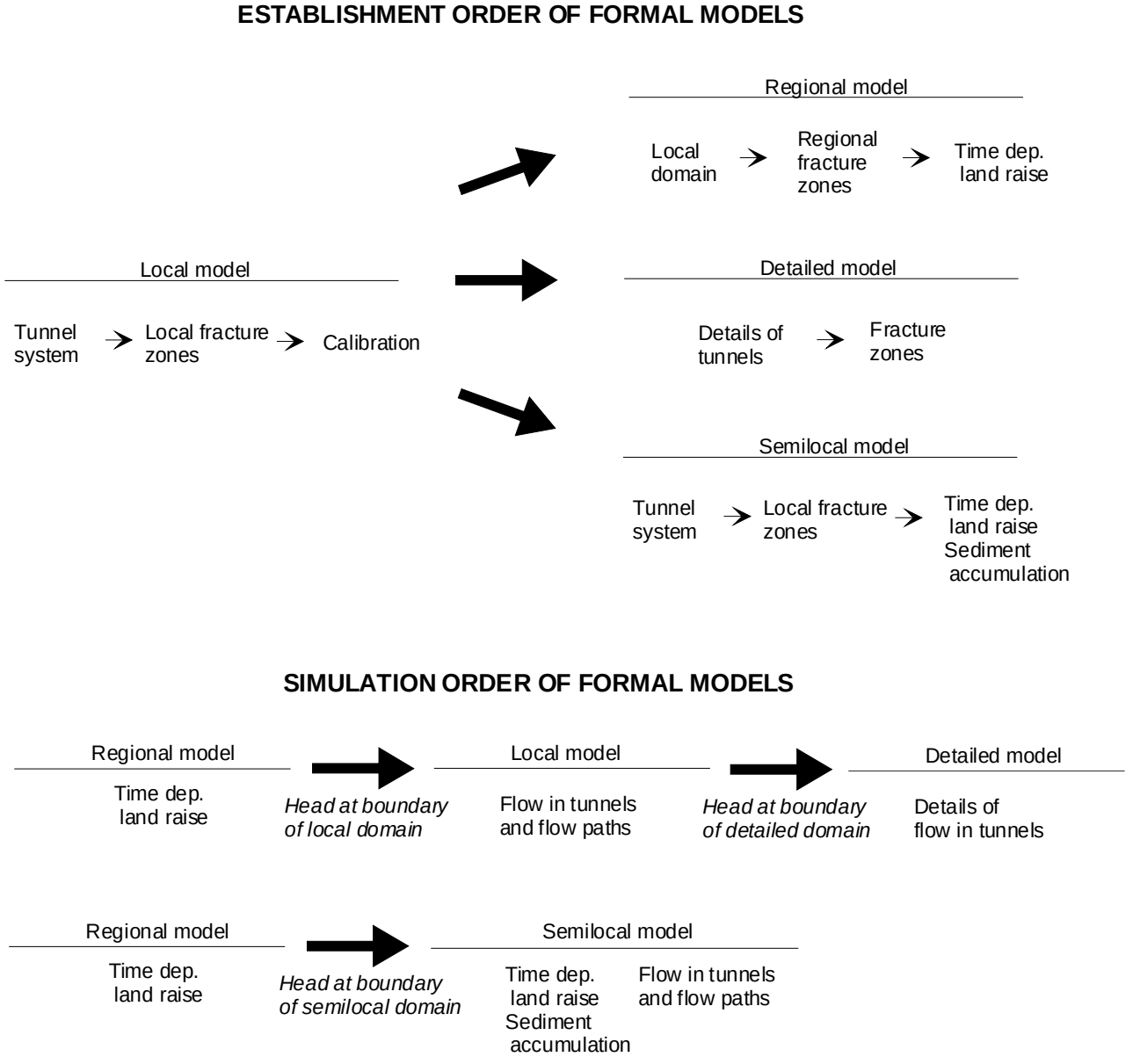

Figure 2.6 *The principle of the chain of models as regards establishment and simulations.*

The order in which the formal models are established, and the order in which the simulations are performed. The models are built from the tunnel system and outwards The local model is the first model to be established, and it is also the model for which the calibration was performed, hence, the properties of this model is included in the regional, the detailed and the semilocal models. After the establishment and calibration of the local model, the regional and the detailed as well as the semilocal models were established. The models simulate the time-dependent flow system in an order starting with the regional domain and then based on the results of the regional domain, the flow conditions within the local domain are simulated, hence, from the regional domain to the local domain. Based on the results of the local domain, the details of the flow inside the tunnels are calculated by use of the detailed model. The semilocal model is a fully time-dependent model but it is solved after the regional model and it uses the results of the regional model for representation of the regional groundwater flow.

2.8 The concept of flow in a tunnel

This study investigates the flow in closed tunnels that are abandoned and no longer kept dry. Under such conditions a tunnel receives water from the rock mass at different sections along the tunnel, and gives water to the rock mass at other sections along the tunnel. Thus, the flow and velocity of water inside the tunnel varies along the tunnel. We note that the tunnel is not a tube that receives water at one end and gives it away at the other end, it receives water along an upstream part (inflow part) and gives it away along a downstream part (outflow part). What is upstream and downstream depends on the direction of the tunnel and the direction of the regional groundwater flow.

The flow of water in a tunnel can be studied based on two different concepts: "specific flow" and "total flow". In accordance with Holmén (1997), we will in this study use the following definitions of these two concepts of flow.

Specific flow, is defined as a flow per unit area [$L^3 / (L^2\ T) = L / T$]. The specific flow gives information about the flow at a local point. As the specific flow normally varies inside a tunnel, the specific flow of a tunnel it is often given as an average value.

Total flow, in a tunnel is defined as the flow that enters and/or leaves a tunnel [L^3 / T]. The calculation of total flow is based on a mass balance taken over the envelope of the studied structure (e.g. a tunnel). The total flow gives information about the amount of water that "visits" the tunnel. If the tunnel system is complex, it is possible that water, which previously has been inside the tunnel system, re-enters the tunnel system at some other point downstream. Such water will be added to the total flow every time it enters the tunnel system. The total flow provides no information of the length of the flow paths in the tunnels, a short path or a long path, will both add to the total flow. The total flow depends on both the magnitude of the flow in the surrounding rock mass and on the direction of that flow, as well as on the hydraulic properties of the tunnel.

Different aspects of flow in closed tunnels are discussed in Holmén (1997). The following is stated in that study

> From a general point of view, as regards direction of the regional flow, the flow of a tunnel will vary in the following way.
>
> •*Specific flow.* If the tunnel has a larger conductivity than the surrounding rock mass, the largest average specific flow inside a tunnel will occur when the regional flow is along the tunnel (along the main axis of the tunnel) or in an angle close to the direction of the tunnel. And the smallest average specific flow inside a tunnel occurs when the regional flow is directed at right angles to the tunnel (along the short axis of the tunnel). If the tunnel has a smaller conductivity than the surrounding rock mass, the variation of specific flow will be the reverse of the variation given above.
>
> •*Total flow.* It is more difficult to predict the total flow than the specific flow as the total flow depends on the exposed area in the direction of regional flow, as well as on the tunnel conductivity.

- If the conductivity of the tunnel is small compared to the conductivity of the rock mass, or slightly larger than that of the rock mass, maximum total flow will occur when a large area of the studied tunnel is exposed to the regional flow (regional flow along short axis) and minimum total flow will occur when a small area is exposed (regional flow along main axis).
- If the conductivity of the tunnel is large compared to the conductivity of the rock mass, maximum total flow will occur when the regional flow is directed along the tunnel (along the main axis) and minimum total flow will occur when the regional flow is directed at right angles to the tunnel (regional flow along short axis).

If the tunnel has a small conductivity, the flow in the tunnel will be small, if the conductivity is large the flow in the tunnel will be large. However, an increase of the conductivity of the tunnel will only have a large effect on the flow in the tunnel, if the tunnel conductivity is small. If the conductivity of a tunnel is large, a much more conductive tunnel will not have a much larger flow, as the flow in such a tunnel is mainly dependent on the conductivity of the surrounding rock mass.

3. Description of the SFR repository

3.1 The general layout

The SFR repository is located in Forsmark in the northern part of Uppland, close to the Forsmark nuclear power plant. The tunnel system of the repository consists of access tunnels and five deposition tunnels; the radioactive waste is placed in the deposition tunnels. The deposition tunnels are located in the bedrock, approximately 60 m below the seabed and about 600 meters off the coast. The underground part of the repository is accessed through two tunnels, called the access ramp. The SFR is designed for the final disposal of low and intermediate level nuclear waste from the Swedish nuclear power plants and from the CLAB (central interim storage for spent nuclear fuel) as well as from other industries, research and medical care. In total the present layout of the SFR is intended for 90000 m^3 of waste. There are plans for expansion of the SFR to make place for the disposal of radioactive waste from the decommissioning of the nuclear power plants. The layout of the SFR is given in Figure 3.1 and Figure 3.2. Generally the repository consists of a large number of different access tunnels and of the five different deposition tunnels. Four of the deposition tunnels are horizontal, they are called: BMA, BLA, BTF1 and BTF2. The fifth deposition tunnel has the shape of a cylinder with its main axis in the vertical plane, this tunnel is called the SILO. For a more detailed description of the SFR we refer to Andersson *et al.,* (1998) and SKB (1993) *Slutlig säkerhetsrapport*. The layout of the deposition tunnels is also discussed in Sec.9.

3.2 The deposition tunnels, the SILO and the tunnel plugs

3.2.1 SILO

The main part of the radioactivity of the SFR-waste is intended for disposal in the SILO. The SILO deposition tunnel has a cylindrical shape with a height of approximately 69.5 m and a diameter of approximately 29.5 m; the uppermost part has a diameter of 31 m. The total volume of the cavern is approximately 47 500 m^3. Inside the cavern a cylindrical concrete construction is installed (the encapsulation), with a height of 50 m, the volume of the encapsulation is ca. 40 000 m^3. The waste will be stored in vertical shafts in the encapsulation. On all sides a bentonite flow barrier protects the encapsulation. The SILO is designed for approximately 18 500 m^3 of conditioned waste.

3.2.2 BMA deposition tunnel

The radioactivity in the waste that is deposited in the BMA tunnel is mainly lower than the activity in the waste intended for the SILO. The BMA tunnel has a length of 160 m, a width of 19.5 m and a maximum height in the roof wall of 16.5 m, the height of the

vertical walls are 11.5 m. The cross-section area is approximately 300 m^2. The total volume of the tunnel is approximately 47 600 m^3. A concrete construction is installed in the tunnel (the encapsulation); the waste containers will be stored in this encapsulation. On all sides of the encapsulation a highly permeable backfill will be installed, forming a hydraulic cage. The BMA is designed for approximately 13 400 m^3 of conditioned waste

3.2.3 BLA deposition tunnel

The waste deposited in BLA is mainly low level waste placed in standard steel containers. The BLA tunnel has a length of 160 m, a width of 15 m and a maximum height in the roof wall of 12.5 m, the height of the vertical walls are 9 m. The cross-section area is approximately 180 m^2. The total volume of the tunnel is approximately 27 600 m^3. The BLA is designed for approximately 11 500 m^3 of conditioned waste. In the BLA, the waste containers will not be encapsulated in concrete. It is likely that the tunnel will be refilled with sand; hence the containers will be surrounded by sand.

3.2.4 BTF1 and BTF2 deposition tunnels

The waste placed in the BTF tunnels is mainly de-watered low-level ion exchange resin in concrete tanks (as well as some drums with ashes in BTF1). The concrete tanks are placed in two levels; a concrete radiation protection lid is placed on top of the pile. The space between the different tanks is filled with concrete and the space between the tanks and the rock wall will be filled with a concrete backfill. This concrete construction forms the encapsulation of the BTF tunnels. For the space above the encapsulation a sand backfill will be used. The tunnels have a length of 160 m, a width of 15 m and a maximum height in the roof wall of 9.5 m. The height of the vertical walls are 6.5 m. The cross-section area is approximately 130 m^2. The total volume of each tunnel is approx. 19 700 m^3. The BTF tunnels are designed for approx. 7 900 m^3 of waste.

3.2.5 The low permeable plugs in the tunnel system

Before the repository is closed and abandoned, low permeable plugs will be installed at different locations in the tunnel system and all boreholes into the surrounding rock mass will be refilled with low permeable concrete. The purpose of these measures is to limit the groundwater flow in the cavities that make up the tunnels and the boreholes.
The number and locations of the plugs are at present not decided.

In the models of this study we have assumed that low permeable plugs will be installed at the following positions (see Figure 14.1):

- In all access tunnels where these tunnels are in contact with the SILO.
- At both ends of the BMA tunnel.
- At both ends of the BLA tunnel.
- At both ends of each BTF tunnels.
- At two different positions along the main access ramp.

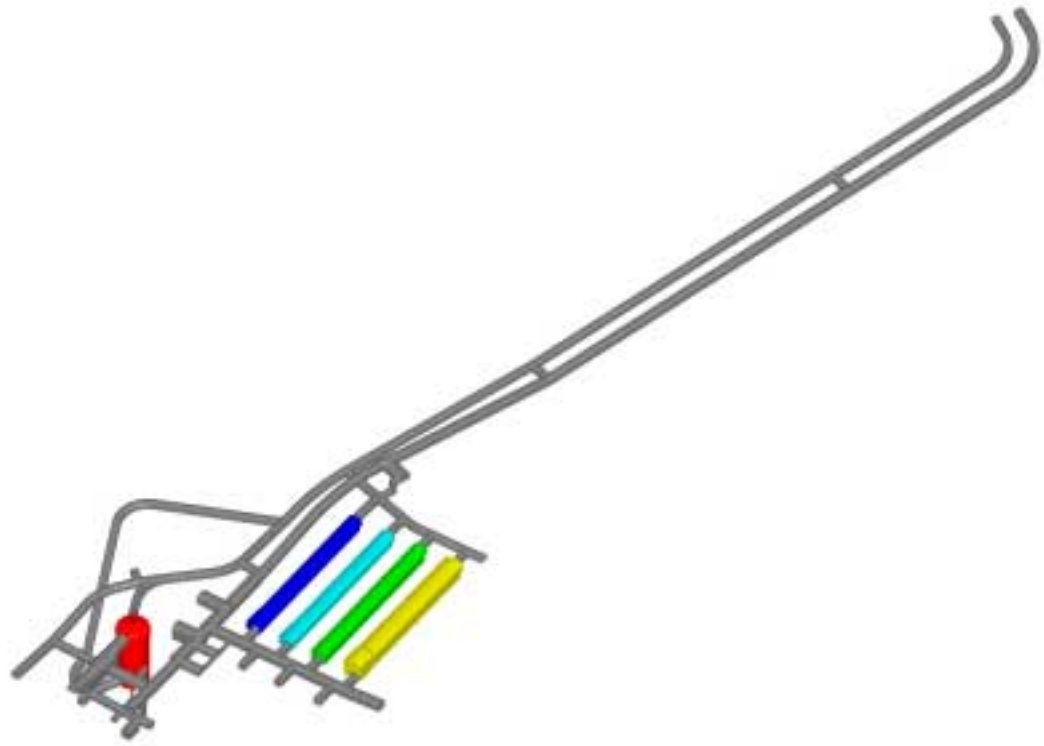

Figure 3.1 *The general layout of the tunnel system at SFR. The grey colour denotes the access tunnels. The red colour denotes the SILO. The dark blue colour denotes the BTF1 and the light blue denotes the BTF2. The green denotes the BLA tunnel. The yellow denotes the BMA tunnel.*

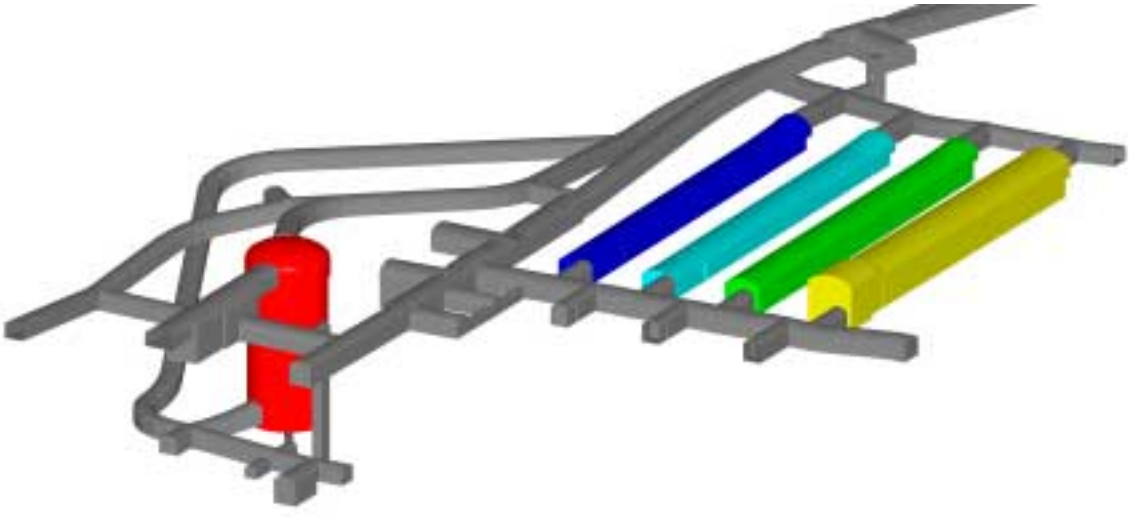

Figure 3.2 *A close-up view of the deposition tunnels and access tunnels at SFR. The grey colour denotes the access tunnels. The red colour denotes the SILO. The dark blue colour denotes the BTF1 and the light blue denotes the BTF2. The green denotes the BLA tunnel. The yellow denotes the BMA tunnel.*

4. Topography and hydro-meteorology

4.1 Topography

4.1.1 Regional topography

On a regional scale, in the surrounding of SFR, the general trend of the topography is a smooth lowering of the topographic elevation, towards Northeast. The regional topography is given in Figure 4.1. The figure presents the topography both above and below the present shoreline.

4.1.2 Local topography and local water divides

On a local scale, the general trend of the topography is the same as the trend of the regional scale; it is a smooth lowering of the topographic elevation, towards Northeast. The local topography at the SFR area is given in Figure 4.2 and the semilocal topography is given in Figure 16.1. The figures present the topography both above and below the present shoreline. The topography of this study does not include piers, embankments and quays of the SFR harbour. Considering the purpose of this study, the presence of these constructions are not very important, furthermore it is possible that the piers and embankments of the SFR harbour will be removed, before the closure of the repository.

A water divide is a theoretical boundary separating waters flowing into different basins (surface water flow) or different discharge areas (groundwater flow). The positions of the water divides are of interest as they indicate boundaries of the flow of surface and ground water. When the land is rising above the sea, a surface water divide is given by the most elevated parts of the topography. A groundwater divide, on the other hand, is a more complicated concept. Groundwater divides occur as three-dimensional surfaces in the flow medium of the groundwater. However, for the groundwater flows close to the ground surface, the groundwater divides are close to the surface water divides. The positions of the local surface water divides are given in Figure 4.2

4.1.3 The topography, the shoreline and the shore level displacement

At the SFR area, the shore level displacement (the land uplift and the sea level change) will cause the shoreline to move towards Northeast. This is illustrated in Figure 2.3. The shoreline will be above the deposition tunnels at about 2800AD. Because of a topographic threshold it is likely that at about 4800 AD a lake (and some smaller lakes and mires) will be established about 1 km North and Northeast of the SFR. The water level of these lakes is somewhat uncertain, but it will probably be close to -15 masl (see Figure 2.2 and Figure 2.3)

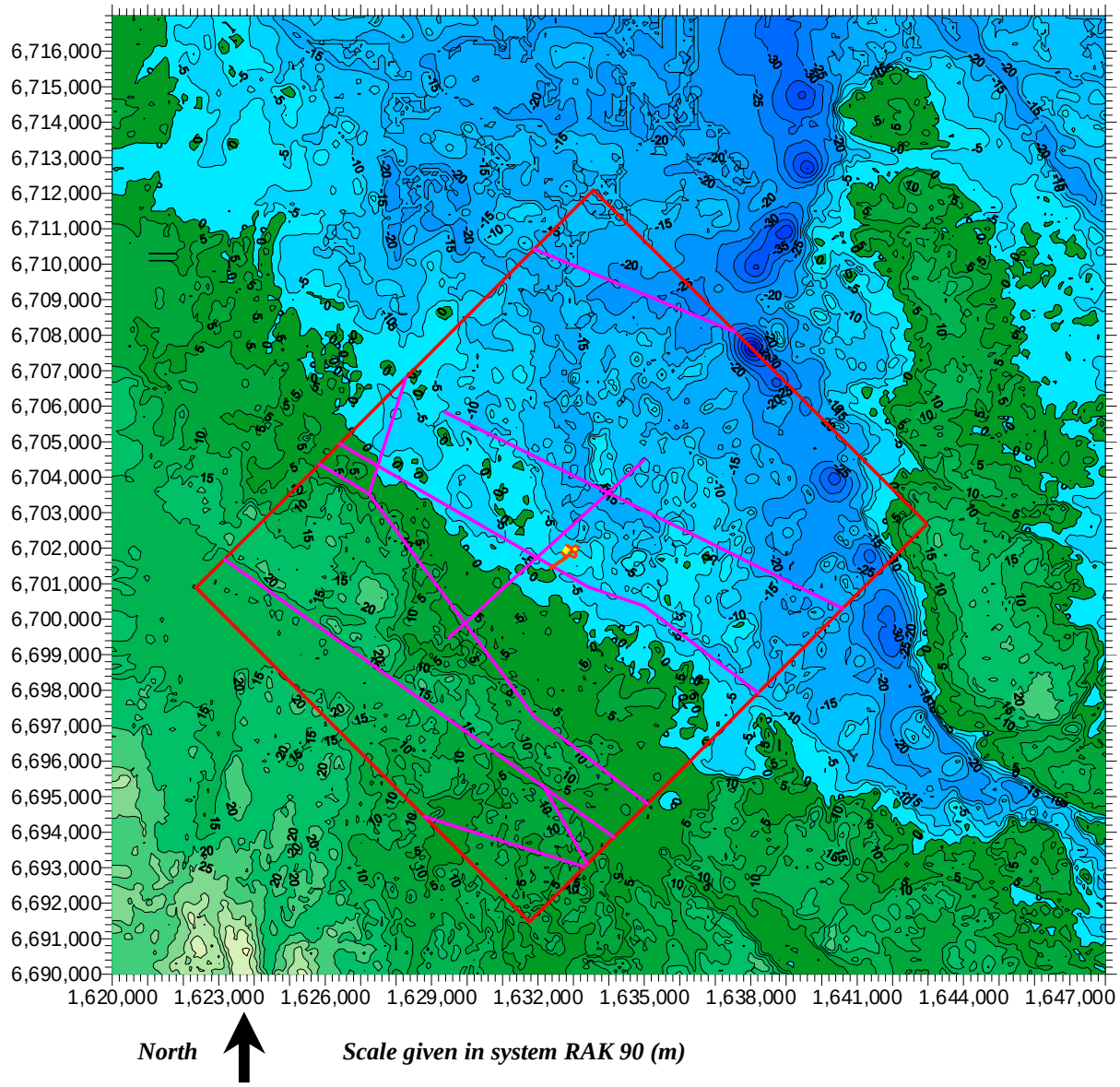

Figure 4.1 *The regional topography, the regional fracture zones, the position of SFR and the horizontal boundaries of the regional model.*

The green colour denotes the topography above the present shoreline. The blue colour denotes the topography below the present shoreline, the ekvidistance between the iso-lines are 5m.

- *The regional fracture zones are denoted by purple lines*
- *The position of SFR is denoted at the center of the figure (red and yellow).*
- *The horizontal boundaries of the regional model (regional scale) is given by the red rectangle.*

4.2 Hydro-meteorology - precipitation and run off

According to Brandt *et al* (1994), for the period 1961-1990, the average precipitation in the Östhammar municipality, which includes the SFR area, is 600-700 mm/year; the average run off is 200-300 mm/year. For the province of Uppland, which includes the SFR area, Figure 4.3 presents the average run off, as measured and estimated by SMHI (1999). The average run off is used in the models as the potential recharge. The average run off at the SFR area is approximately 250 mm/year.

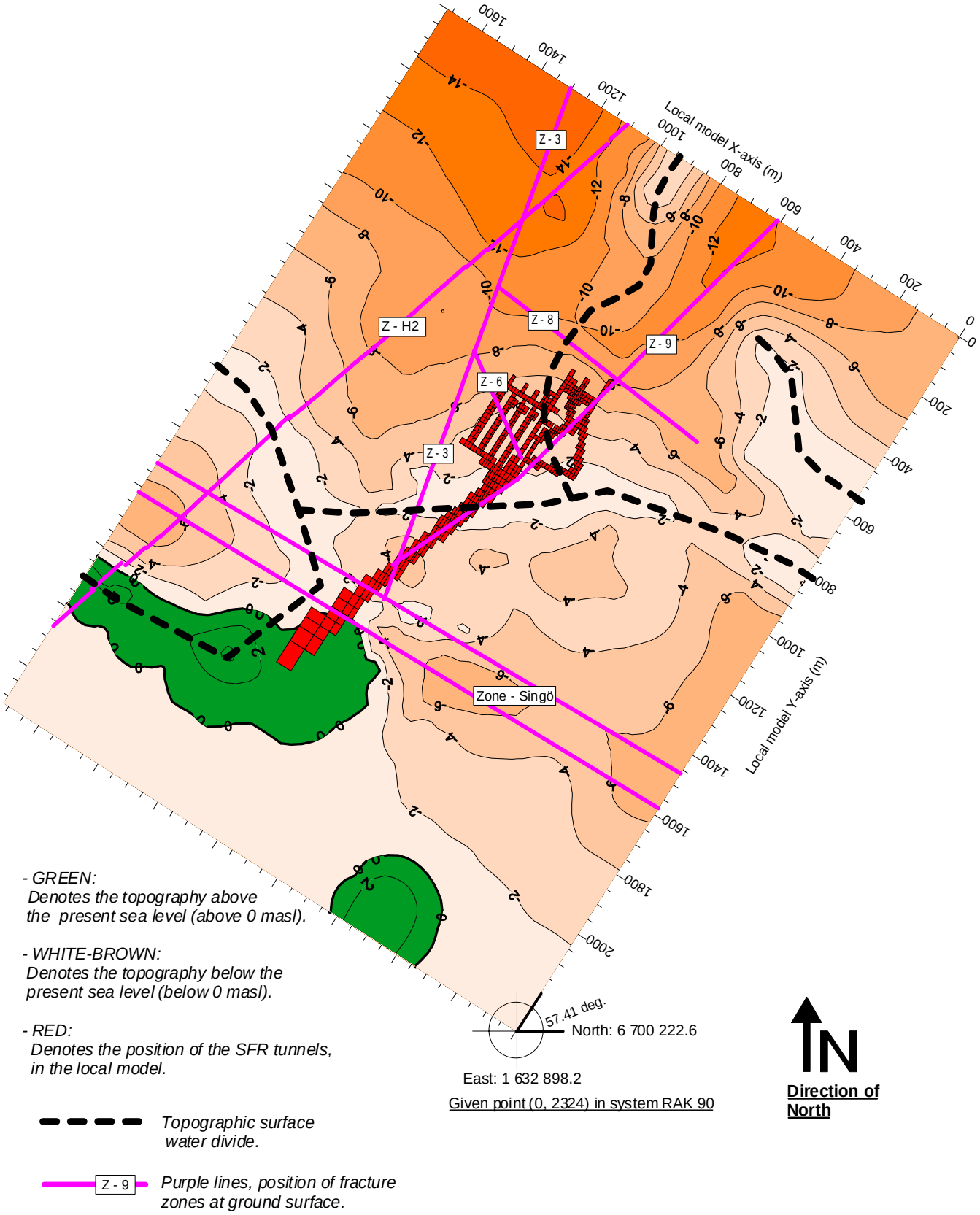

Figure 4.2 *The local topography and the local topographic water divides, as well as the position of the SFR tunnel system and the fracture zones (zones at ground surface).*

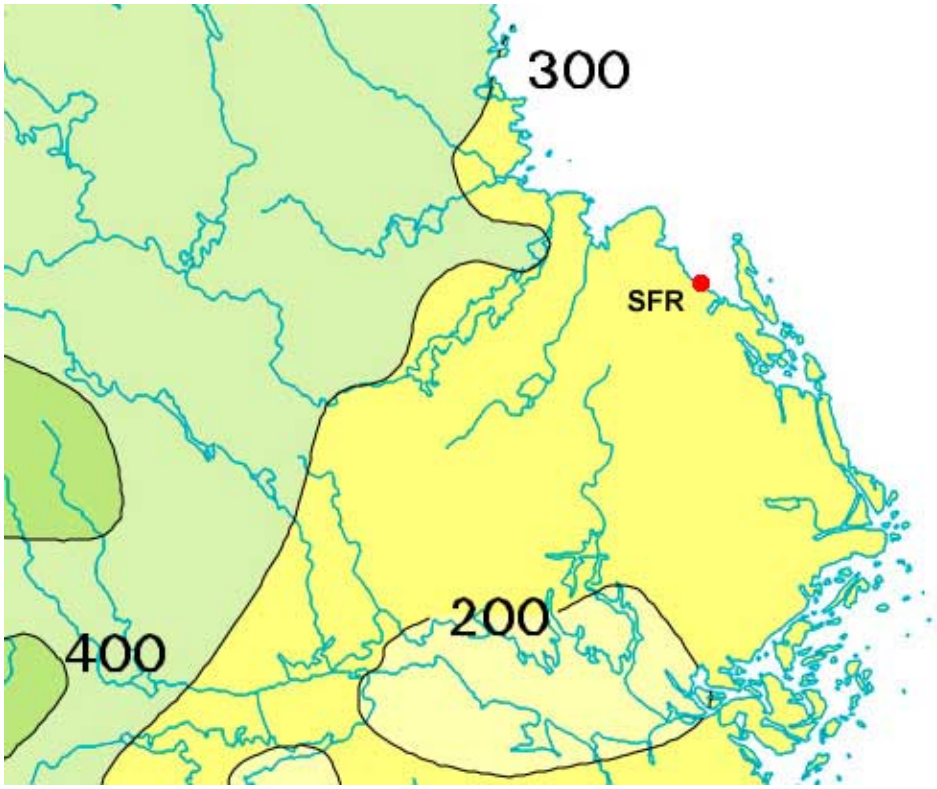

Figure 4.3 *The average run off (the potential recharge) for the province of Uppland, SMHI (1999). The position of SFR is denoted in the figure. The average run off at SFR is approximately 250 mm/year.*

5. Properties of the rock mass

5.1 Structural geological interpretation

5.1.1 Introduction

As a part of the SAFE project Axelsson and Hansen (1997) performed an update of the structural geological interpretation of the rock mass at SFR. For a detailed description of the structural geology at the SFR area, we refer to that study as well as to the studies by Carlsson *et al* (1986) and Christiansson (1986).

5.1.2 Regional scale

The structural geological interpretation proposed by Axelsson and Hansen (1997) concerns mainly the local surrounding of the SFR repository. However, a review of different regional structural geological interpretations is also given in the study. For the regional scale we have based our structural geological interpretation on the work by Axelsson and Hansen (1997), but also on Bergman e*t al* (1996) for horizontal extension of zones, and on SKB (1993) *Slutlig säkerhetsrapport*.

The regional structural geological interpretation consists of 8 large regional fracture zones. Among these zones are the Singö fracture zone and the Forsmark fracture zone. Like the Singö zone all regional zones, except zone H2, are assumed to have a vertical dip. No explicit structural geological information is available for their vertical extension. Two of the zones that occur in the regional scale are also in the local scale, that is the Singö-zone and the sub-horizontal zone H2. Zone H2 is discussed in more detail below. The horizontal extensions at ground surface of the regional fracture zones are shown in Figure 4.1.

5.1.3 Local scale

For the local scale, the structural geological interpretation used in this study is solely based on the updated interpretation by Axelsson and Hansen (1997). The local structural geological interpretation consists of four smaller fracture zones and two large regional fracture zones. The regional zone are the zone H2 and the Singö-zone. The four smaller zones are called: 3, 6, 8 and 9. No explicit structural geological information is available for their vertical extension. The horizontal extensions at ground surface of the fracture zones of the local scale are shown in Figure 4.2.

- Zone H2, is a subhorizontal fracture zone that strikes towards NE and dips about 15 - 20 degrees towards SE. It is a complex zone with varying geological and hydraulic properties. This zone occurs in both the local scale and in the regional scale.

- Zone 3, strikes towards NNE and has an almost vertical dip. It is a composite zone, consisting of several narrower zones and fractures, which diverge and converge, in a complex pattern.

- Zone 6, strikes towards NNW and has an almost vertical dip. It is for most of its length a slightly water bearing gouge-filled joint, occasionally with increased fracturing on one or both sides.

- Zone 8, strikes towards NW and has an almost vertical dip. It is characterised by increased jointing along with the gneissic foliation of the host rock.

- Zone 9, strikes towards ENE and has an almost vertical dip. It is for most of its length a water bearing gouge-filled joint, occasionally with increased fracturing on one or both sides.

The fracture zones of the updated structural geological interpretation and the tunnel system at SFR is given in Figure 5.1 and Figure 5.2. The latter figure gives close-up views of zones H2 and 6, and of the layout of the deposition tunnels of SFR. Zones H2 and 6 are important zones for the groundwater flow in the close vicinity of the deposition tunnels. H2 is a sub-horizontal zone, which intersects the access tunnels below the SILO; Zone 6 is a vertical zone that intersects the deposition tunnels: BTF1, BTF2, BLA and BMA, but not the SILO.

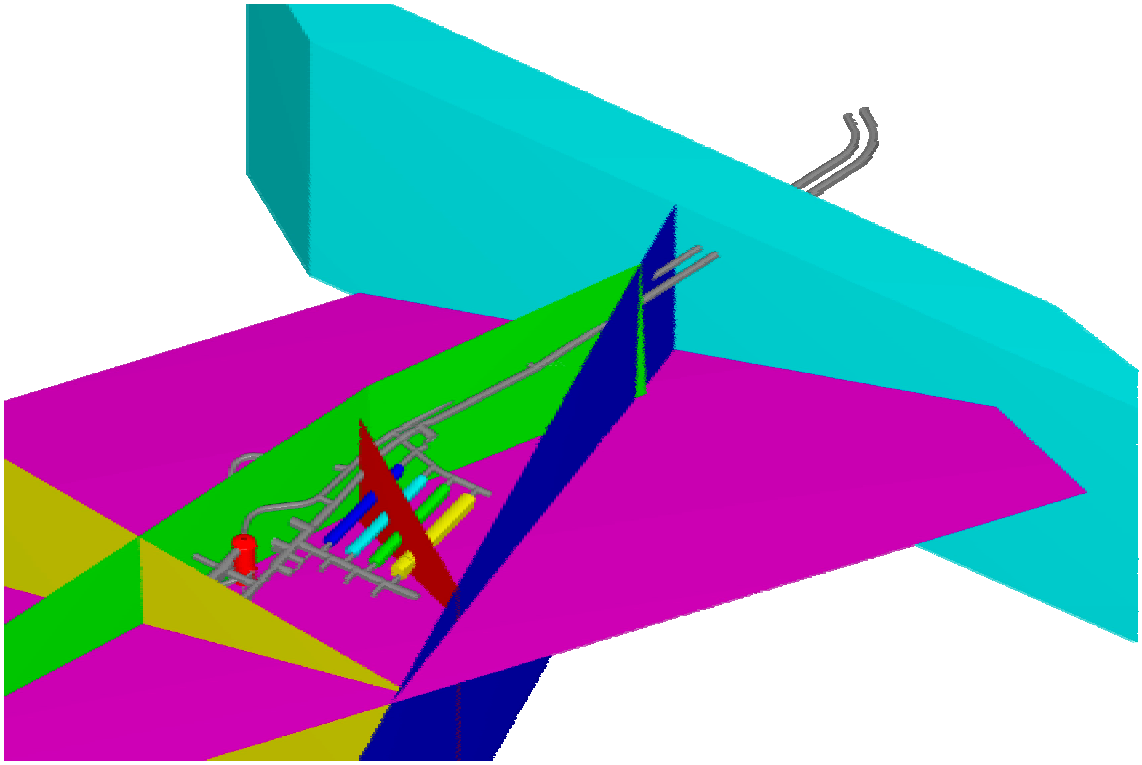

ZONES: Purple= H2. Dark blue= 3. Dark red= 6. Yellow= 8. Green= 9.
TUNNELS: Grey= Access. Red= SILO. Dark blue= BTF1. Light blue= BTF2. Green= BLA Yellow= BMA

Figure 5.1 *The fracture zones of the updated local structural geological interpretation, and the general layout of the tunnel system at SFR.*

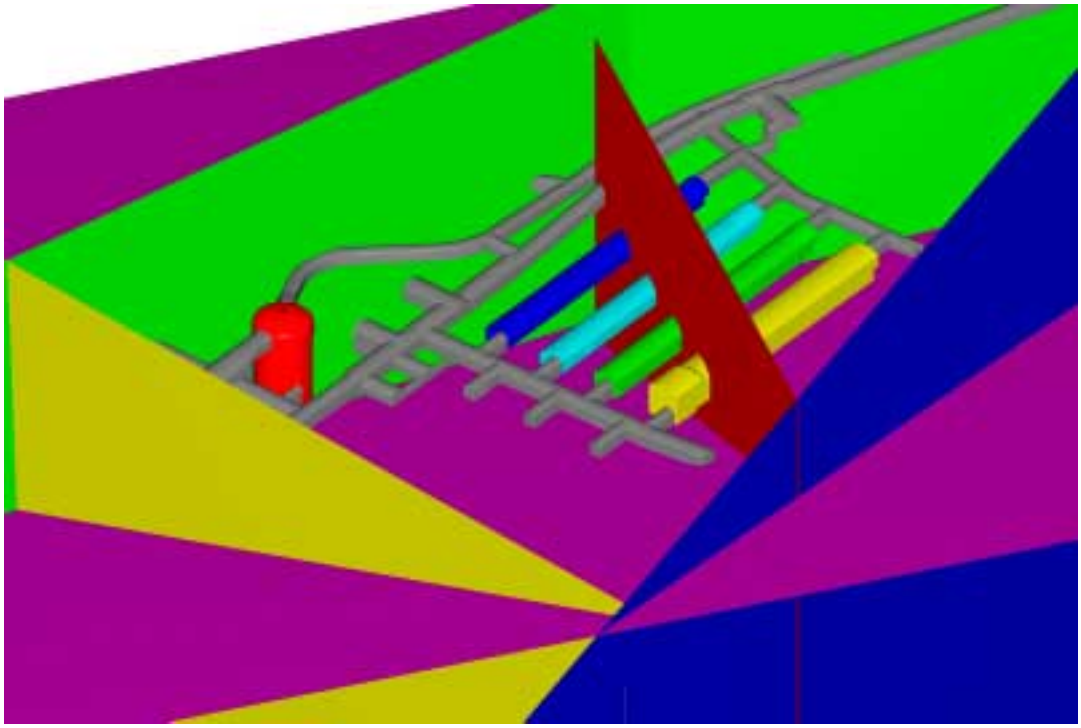

View I. *A close-up view of the fracture zones and the layout of the deposition tunnels at SFR.*
ZONES: *Purple= H2. Dark blue= 3. Dark red= 6. Yellow= 8. Green= 9.*
TUNNELS: *Grey= Access. Red= SILO. Dark blue= BTF1. Light blue= BTF2. Green= BLA. Yellow= BMA*

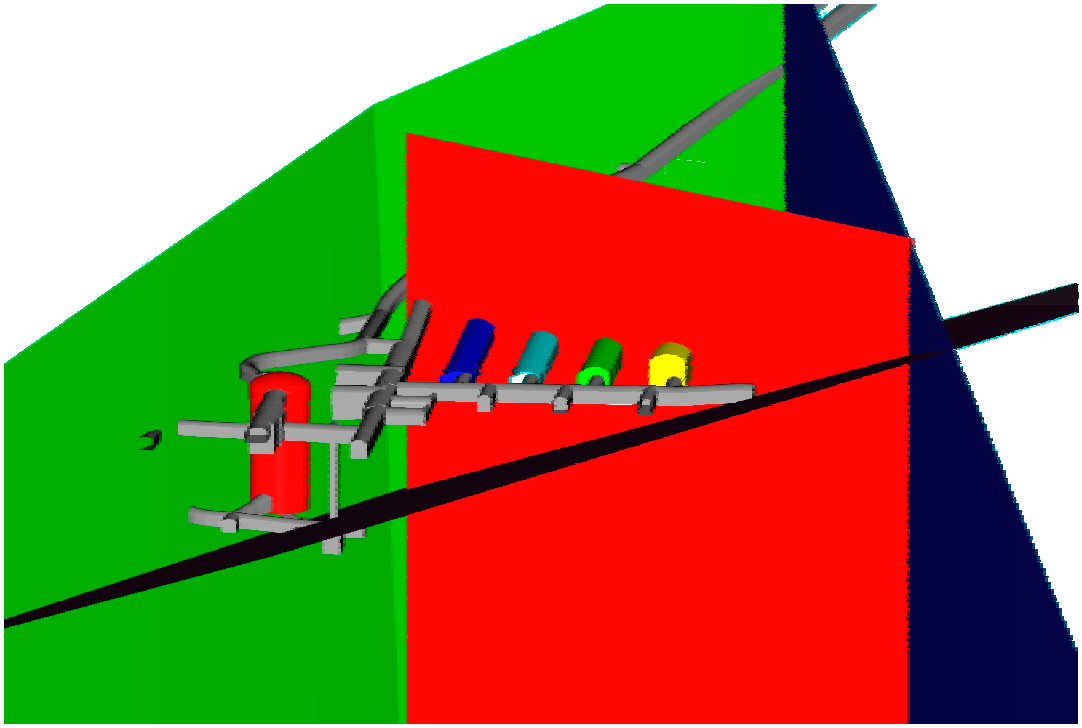

View II. *A close-up view of zones H2 and 6 and the layout of the deposition tunnels. Zone H2 is a sub-horizontal zone, which intersects the access tunnels below the SILO. Zone 6 is a vertical zone that intersects the following deposition tunnels: BTF1, BTF2, BLA and BMA.*
ZONES: *Black= H2. Dark blue= 3. Red= 6. Green= 9.*
TUNNELS: *Grey= Access. Red= SILO. Dark blue= BTF1. Light blue= BTF2. Green= BLA. Yellow= BMA*

Figure 5.2 *Close-up views of the fracture zones of the updated local structural geological interpretation, and the layout of the deposition tunnels at SFR.*

5.1.4 Horizontal and vertical limitations of the fracture zones

The updated structural geological interpretations give no complete information of the vertical and horizontal limitations of the local fractures zones. For the local scale, we have used the information provided in the updated interpretation. However, when no information was available, the local zones have been defined as limited by the size of the local model (see Chapter 6). The regional fracture zones are assumed to be vertical, except zone H2. Their horizontal extension is given by the structural interpretation.

5.1.5 Comparison with the old interpretation at the local scale

The updated interpretation by Axelsson and Hansen (1997) is somewhat different from the old interpretations by Carlsson *et al* (1986) and Christiansson (1986). The main differences are given below

1. In the updated interpretation Zone H2 is extended beyond Zones 3, 6, 8 and 9.
2. In the updated interpretation Zone 9 is extended to Zone 3 in DT tunnel [*].
3. In the updated interpretation Zone 6 terminates between DT and BT tunnel [†].
4. In the updated interpretation Zone 8 is reduced to a third order zone.

This study uses the updated interpretation.

- It is logical to use the latest interpretation, as this interpretation is based on the latest available data.
- In the models the hydraulic properties of the fracture zones will be based on the results of the hydraulic tests conducted at the site and by a calibration procedure. When considering the different structural geological interpretations, we will primarily regard the different geometric interpretations.
- The previous interpretation of the extension of H2, as a small zone bounded by the other local zones, may in a groundwater model cause a somewhat different flow pattern, compared to the updated interpretation in which H2 is much larger. However, it is indicated in the updated interpretation that the large extension of H2 is the most likely interpretation; it is probably also the most conservative interpretation considering the purpose of this study.
- The small change in the geometry of Zone 9 will have no significance, considering the purposes of this study and the layout of the models.
- The small change in the geometry of Zone 6 will have no significance, considering the purposes of this study and the layout of the models.
- The reclassification of Zone 8 will not change the geometric properties of the zone. Consequently, it will be of no major importance.

[*] The SFR access ramp consists of two access tunnels, the DT tunnel is the NW-most of these two tunnels, it is also called the operation tunnel.

[†] The SFR access ramp consists of two access tunnels, the BT tunnel is the SE-most of these two tunnels it is also called the building tunnel.

5.2 Hydraulic tests and hydraulic conductivity

5.2.1 Conductivity and scales – equivalent and effective conductivity

The hydraulic conductivity is a property of the flow medium; it is a measure of the ease with which the groundwater is transported through the medium. The hydraulic conductivity of a fractured rock is given by the ease with which a studied fluid is transported through the fracture system. The conductivity of a volume of fractured rock depends on the properties of the fractures inside the studied volume. The fractures have varying properties; hence the conductivity will vary between different locations of the studied volume and for different directions of flow (a heterogeneous and anisotropic conductivity). As the conductivity of a fractured rock depends on a large number of connected fractures having different properties, the conductivity of fractured rock becomes scale dependent. The scale dependency of the conductivity of fractured rock is documented in several studies; e.g. the scale dependency of the rock at Äspö Hard Rock Laboratory is documented in Gustafson *et al* (1989) and Wikberg *et al* (1991).

Because the studied flow medium is a heterogeneous fractured rock, we will in this study use the concepts of *equivalent conductivity* and *effective conductivity*. By equivalent conductivity we mean a constant hydraulic conductivity tensor representing a heterogeneous flow medium at a given scale and for a given flow direction. The equivalent conductivity will change with scale. A complete equivalence between a heterogeneous medium and a homogeneous representation is impossible hence; the concept of an equivalent conductivity is only applicable under certain conditions. By an effective conductivity we mean an equivalent conductivity taken at such a large scale, that for even larger scales the scale dependency is insignificant. The concept of efficient conductivity is only applicable for a heterogeneous flow medium that fulfils certain conditions, the heterogeneity has to be statistical homogeneous and the average flow direction has to be known; from a theoretical point of view there are certain types of heterogeneity for which there are no effective conductivity.

5.2.2 Hydraulic tests and conductivity of fracture zones

Two different types of tests have been conducted in the local zones of SFR: (i) double packer tests in a single bore hole (packer spacing 3m) and (ii) interference tests between different boreholes. The double packer tests can be interpreted as giving random samples of the conductivity of the tested zone. The interference tests can be interpreted as giving the conductivity of the permeable paths between different boreholes. A summary of the results of the tests is given in Axelsson and Hansen (1997). The arithmetic and the geometric mean of the obtained varying hydraulic conductivity values are given in Table 5.1 and Table 5.2.

Table 5.1 Results of hydraulic tests in the local fracture zones. Results of the double packer tests, with a packer spacing of 3 meters. The underlying data is from Axelsson and Hansen (1997) and SFR 86-03.

Double packer tests					
Zone	Number of Tests	Type of Mean	Width (m)	Transmissivity (m2/s)	Conductivity (m/s)
H2	20	Arithmetic	7.4	9.29E-6	1.87E-6
		Geometric	6.1	1.70E-6	3.36E-7
3	3	Arithmetic	6.4	2.35E-5	3.67E-6
		Geometric	6.2	2.10E-5	2.92E-6
6	2	Arithmetic	2.4	2.58E-6	9.12E-7
		Geometric	2.4	5.05E-7	2.08E-7
8	5	Arithmetic	11.2	1.39E-5	1.14E-6
		Geometric	8.5	4.32E-6	5.14E-7
9	4	Arithmetic	2.9	5.65E-8	2.08E-8
		Geometric	2.7	2.68E-8	9.79E-9

Table 5.2 Results of hydraulic tests in the local fracture zones. Results of the interference tests between different bore holes. The underlying data is from Axelsson and Hansen (1997).

Interference tests			
Zone	Number of Interference tests	Type of Mean	Transmissivity (m2/s)
H2 & 3	20	Arithmetic	2.17E-5
		Geometric	1.41E-5
3 & H2	20	Arithmetic	2.17E-5
		Geometric	1.41E-5
6	0	Arithmetic	-
		Geometric	-
8	3	Arithmetic	6.63E-5
		Geometric	6.19E-5
9	5	Arithmetic	1.68E-7
		Geometric	1.59E-7

5.2.3 Hydraulic tests and conductivity of rock mass

As the conductivity of tested media is heterogeneous and scale dependent it is not possible to derive a representative value of conductivity from the hydraulic tests, without also considering the scale represented by the hydraulic tests. The scale effects have not been fully included in the previous interpretations of the conductivity of the rock mass. An example of an interpretation of the test results is the one by Carlsson *et al*. (1986). For the local scale Carlsson *et al*. give the following conductivity for the upper 40 m of the bedrock at SFR. The lengths of the test sections (in the tested bore holes) were about 30 m. The rock mass is divided into two areas: Area A is bounded by zones 3, 6, 8, 9 and Area B is outside of these fracture zones. For area A and B, the arithmetic mean conductivity were 6.8×10^{-7} m/s and 1.5×10^{-7} m/s, respectively; and the geometric mean were 4.0×10^{-7} m/s and 8.4×10^{-8} m/s, respectively. At SFR the local fracture zones are presumed to be more permeable than the surrounding rock mass. However, in the interpretation by Carlsson *et al*. (1986) the rock mass is assigned

a mean conductivity that is larger than the mean conductivity of some of the fracture zones, tested with double packer tests with a packer spacing of 3m (e.g. zone 9). This is not necessarily wrong, it could be an effect of the heterogeneity of the rock mass and the zones, as well as an effect of the size of the different test-scales (30 m and 3m). It illustrates however, the necessity to consider the support scale of the hydraulic tests and the implications of the heterogeneity of the tested media, when estimating a representative average value of conductivity (an equivalent conductivity).

A representative value of rock mass conductivity can be estimated by studying the measured inflow to the tunnel system. By introducing a number of simplifications, it is possible to calculate the conductivity value of the rock mass that will produce (for the given conditions and simplification) a similar inflow as the measured inflow. The method that we will use for this estimate is based on an analytical solution provided by Thiem (1906), see equation 1 and 2 in Appendix C. We have calculated values of inflow to a drained BMA deposition tunnel, values of inflow that correspond to representative values of rock mass conductivity (i.e. values of the equivalent conductivity for radial flow towards the tunnels). For these calculations we have used Thiem's equation and the following assumptions: (i) a radial two-dimensional flow towards the tunnel, (ii) a steady state condition, (iii) a homogeneous flow medium and (iii) a head difference between the studied tunnel and the sea equal to the difference in elevation between the tunnel roof and the level of the sea. The results are given in Figure 5.3.

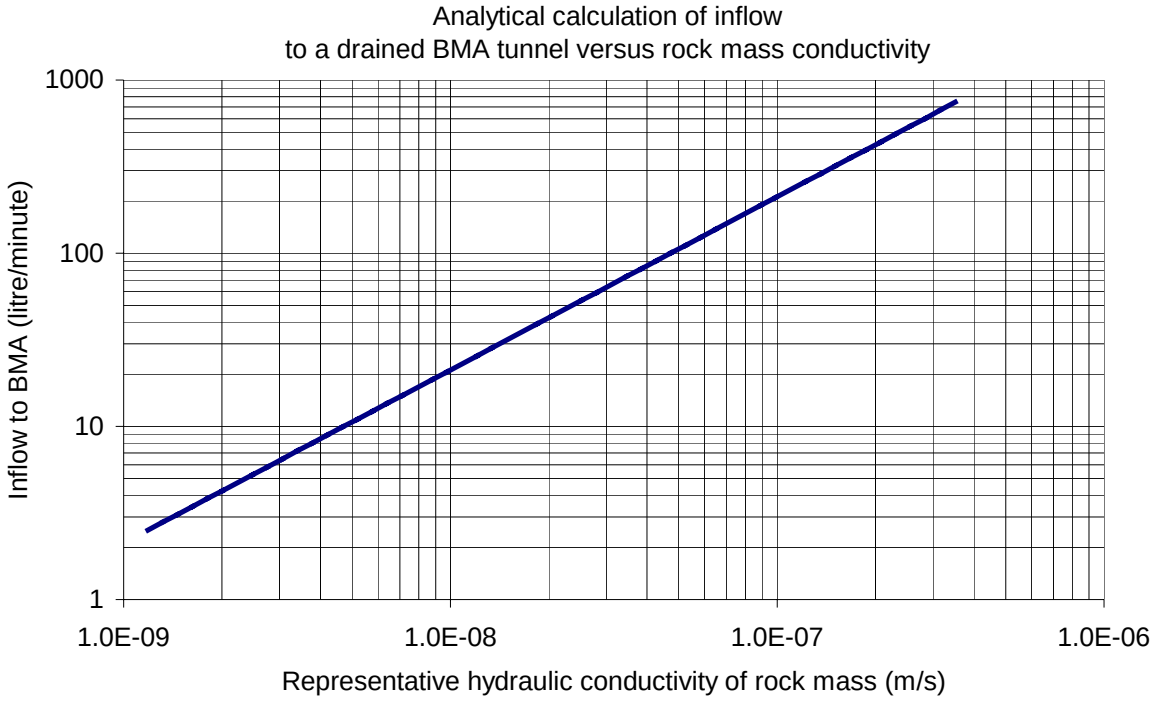

Figure 5.3 *Analytical calculation of inflow to a drained BMA tunnel versus representative hydraulic conductivity of the rock mass.*

The measured inflow to the BMA tunnel is equal to 9.3 litre/minute, which corresponds to a rock mass conductivity of 5×10^{-9} *m/s.*

The measured inflow to the tunnels is discussed in Sec.5.4, below. The calculations above were carried out for the BMA tunnel, because for this tunnel the measured inflow is separated from the inflow to other tunnels. At present the inflows can be assumed to represent a steady state situation; for this situation, the inflow to the BMA deposition tunnel is equal to 9.3 litre/minute. Comparing this measured inflow to the representative values of conductivity as given in Figure 5.3, indicates that the equivalent conductivity for a radial flow towards the tunnels is approximately 5×10^{-9} m/s.

5.3 Porosity, specific yield and storativity

At SFR there have been no direct measurement of porosity, specific yield or storativity. Hence, no such site-specific data is directly available.

5.4 Inflow to the tunnel system at SFR

A compilation of the measured groundwater inflow to the tunnels at SFR is given in Axelsson (1997). Since the regular measurements (four times per year) started in 1992, there has been a decreasing trend in the measured inflow. Between 1992 and 1997 the following changes have occurred:

- The inflow to the entrance tunnels has decreased from 419 to 375 litre/min (11%).
- The inflow to the loading buildings and minor tunnels has decreased from 10.6 to 6.0 litre/min (43%).
- The inflow to the SILO has decreased from 2.1 to 1.6 litre/min (25%).
- The inflow to the BMA decreased from 11.8 to 9.3 litre/min (21%).
- The total inflow to BLA and BTF tunnels as well as to surrounding tunnels has decreased from 98.2 to 83.6 litre/min (15%).

At present the changes are very small, the values of inflow as regards the year 1997 can be assumed as representing a steady-state-like situation. It should, however, be noted that there are uncertainties in connection to the measurements of the inflow.

At present the SILO is used for storage of waste. The SILO consists of a concrete construction (the encapsulation) protected by low permeable flow barriers (bentonite barriers). At present, such barriers are installed below and at the sides of the encapsulation, but above the encapsulation there is an open space for loading of the waste packages. The measured inflow to the SILO is not an inflow to the encapsulation that contains the waste. The measured inflow is (*i*) an inflow to a drainage system, installed between the bentonite barriers and the rock, and (*ii*) the inflow to a water collecting system at the roof of the SILO cavern.

5.5 Quaternary deposits

Investigations of the seabed at SFR have revealed that the fractured rock is mainly covered by a glacial till (morain) of varying thickness with a large amount of boulders and a small amount of fine grained material, Sigurdson (1987). At present, a continuous layer of fine-grained sediments, e.g. clay, does not cover the seabed above the SFR. The

hydraulic conductivity of the glacial till has been estimated by Sigurdson (1987) to be within a range of 1×10^{-5} m/s through 1×10^{-8} m/s. This indicates that on the average, the quaternary deposits have a conductivity that is larger than the average conductivity of the rock mass.

5.6 Excess groundwater head previous to the construction

During the siting investigations for the repository (1980-1981), previous to the construction of the repository, bore holes were drilled from a floating platform at sea. In the bore holes falling head tests were performed and groundwater head was measured. Hagconsult (1982) discusses these tests and the results of the tests.

For the bore holes that intersected the H2 sub-horizontal fractures zone, the results of the head measurements demonstrated, in relation to the mean sea water level, an excess head in the bore holes, which was between +0.11 meters and +0.61 meters (Hagconsult, 1982; Carlsson *et al*, 1987). As previously stated, the boreholes were used for hydraulic tests and it is not obvious how these tests influenced the groundwater head measurements; for example, the measured head values were compensated for the density differences between injected water and the water of the sea. In Carlsson *et al* (1987) different hypotheses have been postulated and examined as regards the reason for the excess head. The following is concluded in that study: “there are reasons to believe that the reported excess head is too high or probably missing due to the measurement and evaluation technique”.

However, considering the shore level displacement and a possible head in the rock mass below the sea (previous to the construction of the repository) from a theoretical point of view, we come to the following conclusion. It is likely that there should be an excess head in the rock mass close to the present shoreline, because the sea water level was previously at higher elevations and a higher sea water level means higher heads in the rock mass below the sea. Hence, previously when the sea level was higher, the head in the rock mass was higher too. The question is; how much of those higher heads remains today? Or in other words, how large is the excess head? The size of the excess head depends on the velocity of the shore level displacement, compared to the velocity of the change of the heads in the rock mass. The velocity of the change of the heads in the rock mass depends on several different factors like. (i) The conductivity and the storage properties of the rock mass, as well as (ii) the conductivity and the extension of previous and present quaternary deposits, and (iii) the effects of the movements of deep groundwater with a high density (fossil salt water) as well as movements of near surface groundwater with a density higher than that of the present seawater. Only if the head change in the rock mass is faster than the movement of the shore level displacement; only then is it possible to have excess head equal to zero (i.e. equal to the sea level).

Thus, from a theoretical point of view it is likely that there should be an excess head in the rock mass at some distance below the sea bottom, however it is difficult to predict the size of the excess head. As discussed above, actual measurements have been performed at the SFR area, previous to the construction of the repository, but the results of these measurements are uncertain. A sensitivity analysis of the importance of the excess head has been performed and is presented in Sec.8.3.

Considering an abandoned tunnel system and a situation for which the sea covers the SFR, it should be noted that if the excess head were equal to zero for such a situation, there would be no flow through the tunnels; except for a very small flow given by temperature and density differences, if such differences occur.

6. Description of local model

6.1 Introduction

The formal models will be established in accordance with the methods presented in Chapter 2. As described in Chapter 2, we will use different models at different scales, representing the studied system (the flow domain). The regional model represents the system on a regional scale; this model will have a regional resolution. The local model represents the system on a local scale; this model will have a local resolution. The local model represents a much smaller volume than the regional model. However, the volume represented by the local model, is in a simplified way also represented at the centre of the regional model. The formal models will be built in the following order. First we will start with the tunnel system and its close surrounding, from there on the models will be built outwards. The local model will be established first, because we have detailed information of the local domain. The local model will be calibrated based on the present flow situation, by use of local boundary conditions representing the present situation. The regional model will be established after the local model. When establishing the regional model, the results of the calibration of the local model will be considered. Figure 2.6 illustrates the order of establishment.

6.2 Size of model

The model represents a rectangular three-dimensional body. The model covers a horizontal area of 1716 m x 2324 m (4.0 km^2) and the depth of the model is 490 m. The upper boundary of the model is the surface topography. The model has vertical sides and a base that is nearly flat. The size and the horizontal position of the local model are given in Figure 6.1.

6.3 Mesh

Three-dimensional cells of different sizes make up the model. The cells form a mesh. The mesh of the local model has 25 layers and contains 80 600 cells. Each cell represents one node in the mathematical model, placed at the centre of the cell. The mesh is primarily optimised to match the layout of the deposition tunnels of the SFR; a secondary optimisation was carried out for the access tunnels. Outside the area where deposition tunnels are defined in the mesh, the size of the cells is increased towards the outer boundaries of the model. The mesh is given in Appendix A.

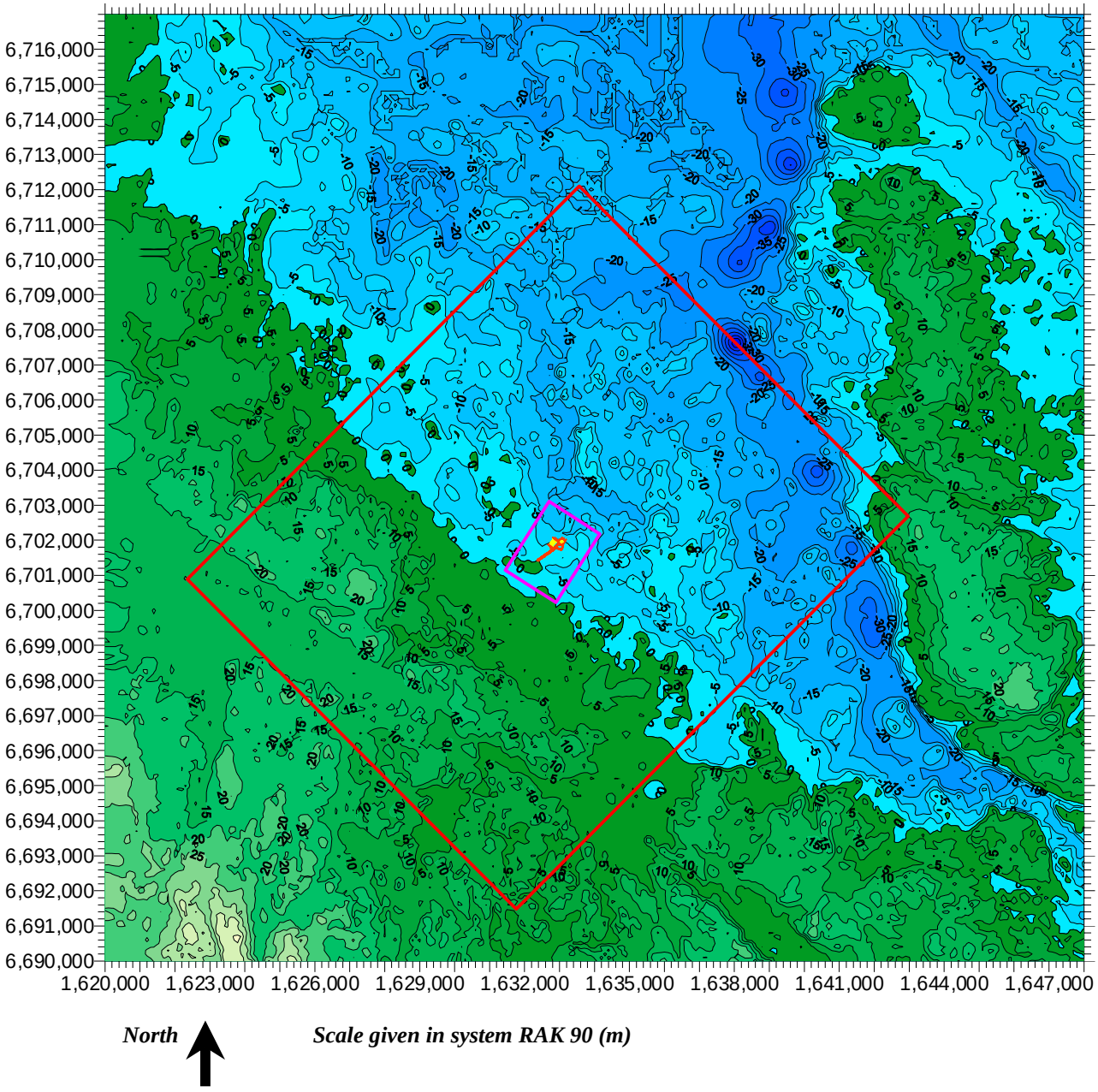

Figure 6.1 *The regional topography, the position of SFR and the horizontal boundaries of the regional model as well as of the local model.*

- *The green colour denotes the topography above the present shoreline. The blue colour denotes the topography below the present shoreline, the ekvidistance between the iso-lines is 5m.*
- *The position of SFR is indicated at the centre of the figure (red and yellow).*
- *The horizontal boundaries of the regional model is given by the red rectangle.*
- *The horizontal boundaries of the local model is given by the purple rectangle.*

6.4 Boundary conditions

The local model will not be used for fully time-dependent simulations. Instead, the local model will be assigned boundary conditions (specified head) that are taken from the regional model (from the time-dependent regional simulation), these conditions represent different moments in time.

Hence, the local model will have the specified head boundary condition at all faces of the model. The actual head values assigned to the boundary nodes of the local model are based on a three-dimensional interpolation between the calculated head values of the nodes of the regional model. The local model has a higher resolution; consequently the surface topography is defined in more detail in the local model. This is considered when the head values are transferred from the surface of the regional model to the surface of the local model. The position of the shoreline and the sea is calculated separately for the local model, considering the more refined topography.

6.5 Representation of tunnel system

6.5.1 Volumes and numerical representation of the tunnel system

The tunnels are defined explicitly in the mesh. Hence, a cell that represents a tunnel represents the tunnel only and no parts of the surrounding rock mass. As previously stated, the mesh is primarily optimised to match the layout of the deposition tunnels of the SFR. The result of this procedure is demonstrated in Figure 6.2. A comparison with the actual shape of the tunnels (see Figure 3.1 and Figure 3.2) demonstrates that the match is acceptable. It is impossible to reach a perfect match, due to practical restrictions in the number of cells that can be used in the model, but also due to the shape of the cells. The actual tunnels have an arch shaped roof, but the cells in the model have a rectangular shape. If we compare the actual volumes of the deposition tunnels with the volumes as defined in the model, we get the volumes given in Table 6.1. It is conservative to make the caverns (deposition tunnels) larger in the model than their actual size, as this will produce an overestimation of the total flow through the caverns. The conductivity of the tunnels is discussed in Section 6.8.

Table 6.1 Volumes of deposition tunnels –actual volumes and volumes in the local model.

Deposition tunnel	Actual volume (m3)	Volume in model (m3)
SILO	47 500	47 400
BMA	47 600	64 600
BLA	27 600	42 800
BTF1	19 700	26 000
BTF2	19 700	26 000

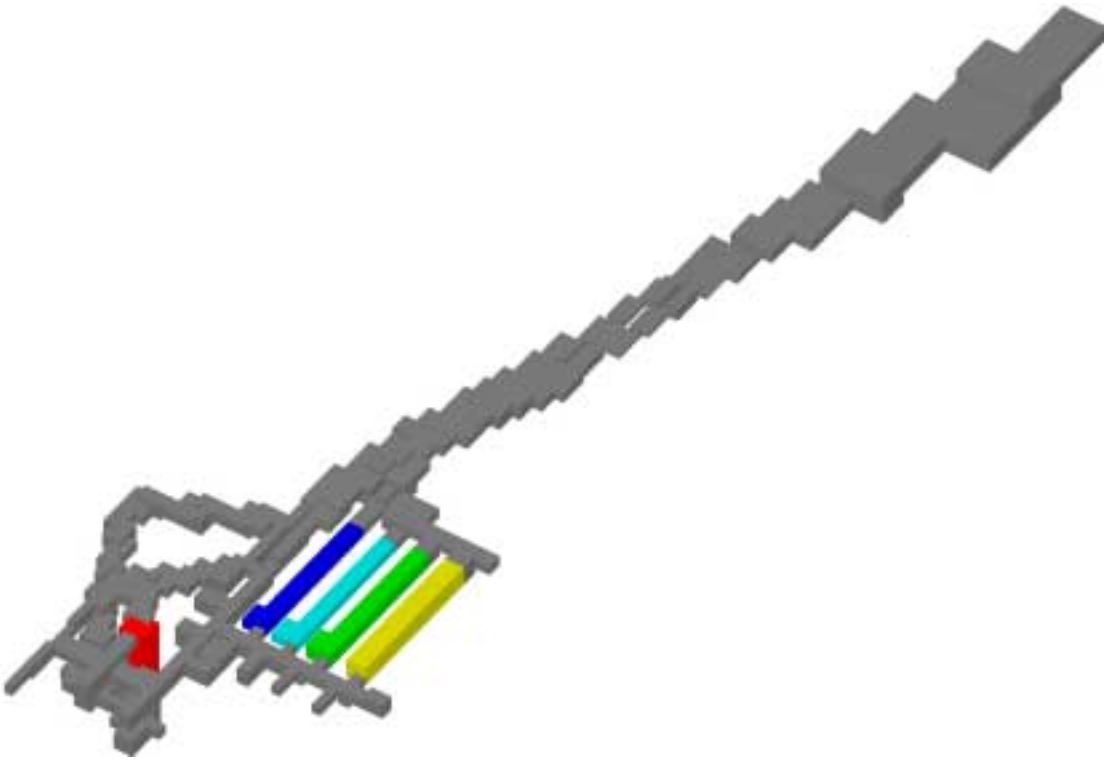

View I. *A close-up view of the deposition and access tunnels at SFR, as defined in local model.*

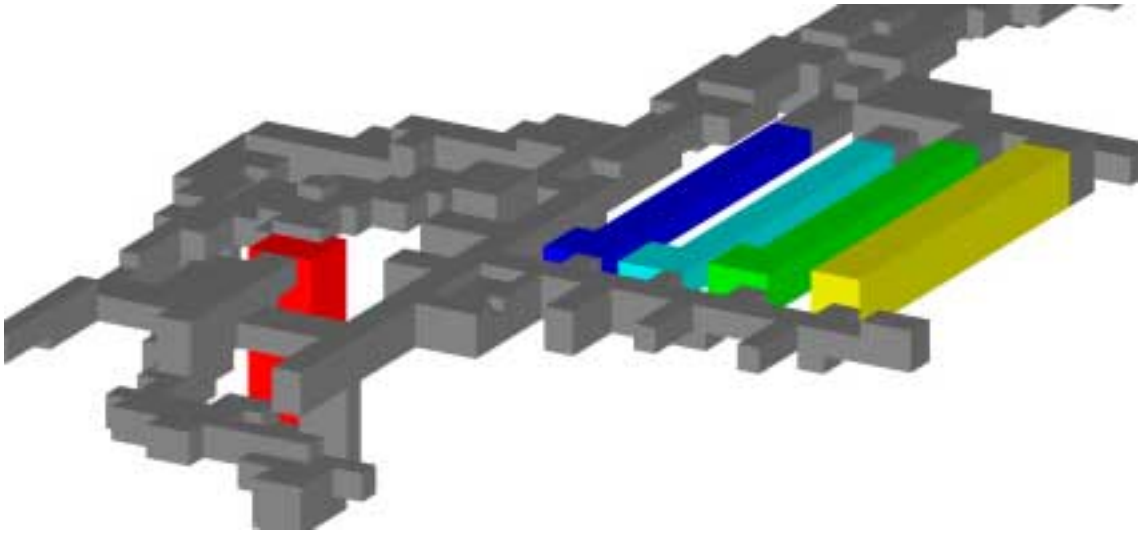

View II. *A close-up view of the deposition and access tunnels at SFR, as defined in local model.*

TUNNELS: *Grey= Access. Red= SILO. Dark blue= BTF1. Light blue= BTF2. Green= BLA Yellow= BMA*

Figure 6.2 *The layout of the tunnel system at SFR, as defined in the local model. The mesh is primarily optimised to match the layout of the deposition tunnels; a secondary optimisation was carried out for the access tunnels.*

6.5.2 Tunnel conductivity

In the local model, all tunnels except the SILO are defined as having a conductivity that is much larger than that of the surrounding rock mass and that of the surrounding fracture zones. If the tunnel is very permeable, compared to surrounding media, the flow in the tunnels will not depend on the permeability of the tunnel, but only on the permeability of the surrounding flow media, see Holmén (1997). Hence, for the conductivity of the tunnels of the model, we have selected a value that is so large that the flow will primarily depend on the surrounding media. However, the value assigned to the models should not be so large that it will cause numerical difficulties and significantly increase the computational demands for numerical convergence. Considering the properties of the system studied we have selected a value equal to, 1.0×10^{-5} m/s.

In the local models, this large value of conductivity has been used for representation of the conductivity in the BMA, BLA, and BTF tunnels. Hence, the local model will predict the flow through highly permeable parts of these tunnels, i.e. the flow through a highly permeable backfill surrounding a concrete construction. As regards the BMA, BLA and BTF runnels, the local models will not predict the flow through a concrete construction installed in the middle of a tunnel, but the flow through a very permeable backfill. The details of the flow through the tunnels will be calculated by use of the detailed model.

6.5.3 Tunnel plugs – representation and resistance

In the calibration procedures, the local model represented the present situation -no plugs were included in the model. In the predictive simulations plugs will be included in the model at the following positions:

- In all access tunnels where these tunnels are in contact with the SILO.
- At both ends of the BMA tunnel.
- At both ends of the BLA tunnel.
- At both ends of each BTF tunnel.
- At two different positions along the main access ramp.

It is possible to define a resistance to groundwater flow, in analogy with the resistance to flow of electricity; the resistance is equal to length divided by conductivity: $R = t / K$ The resistance is denoted as R (dimension: time) the width of the studied domain is denoted as t (dimension: length) and K is the conductivity (dimension: length/time).

The plugs will have a given resistance to flow that is equal to, $2.0 \times 10^{+9}$ seconds. This value of resistance represents the same as, e.g. 1m of a material having conductivity equal to, 5.0×10^{-10} m/s. The advantage of the concept of resistance is that the property of resistance can be defined without considering the geometrical properties of the cells in the mesh.

6.5.4 SILO – representation, conductivity and resistance

6.5.4.1 SILO definition for calibration

The SILO consists of a concrete construction (the encapsulation), in which the waste packages are stored. Low permeable flow barriers (bentonite barriers) protect the encapsulation. At present, such barriers are installed below and at the sides of the encapsulation, but above the encapsulation there is an open space for loading of the waste packages. Before the closure of the repository, a concrete lid and a bentonite barrier will be installed above the encapsulation. At present the groundwater inflow to the SILO cavern is measured. The measured inflow to the SILO is not an inflow to the encapsulation that contains the waste but an inflow to: (i) A drainage system installed between the present bentonite barriers and the rock, and (ii) the inflow to a water collecting system at the roof of the SILO caverns.

During the calibration (see Section 6.8), the SILO is defined as an encapsulation with an open space on top. And during the calibration, the inflow to the open space on top makes up one part of the total inflow to SILO of the model. The rest of the inflow to the SILO of the model comes from the sides and the base of the SILO –an inflow that should pass through the drainage system. For the calibration of the model, the drainage system will cause some problems. Its spatial extension and design is not known in detail, neither is its internal flow resistance or the head inside the drainage system. To represent the limited spatial extension of the drainage system and its internal flow resistance etc, as well as representing a possible skin zone and grouting etc; we have introduced a resistance to inflow, which limits the inflow to the SILO (the definition of resistance is given in Section 6.5.3). Resistance to inflow during the calibration is as follows:

- Inflow at top of SILO (cavern roof) -no inflow resistance
- Inflow at SILO base, inflow through drainage system, resistance = $2.0 \times 10^{+9}$ s
- Inflow at SILO sides, inflow through drainage system, resistance = $2.0 \times 10^{+9}$ s

With an inflow resistance equal to the values specified above, the calibrated model (see Section 6.8) predicts an inflow to the SILO equal to 1.7 litre/min, which is very close to the measured inflow. For the same model, but without inflow resistance, the predicted total inflow to the SILO becomes 3 litre/min. This is less than two times the measured inflow, which, considering the uncertainty in the flow measurement, is not a huge difference.

6.5.4.2 SILO definition for predictive simulations

For the predictive simulations with the local model, the SILO is defined as an encapsulation without the open space on top (it will be refilled) and with low permeable flow barriers on all sides. It is also presumed that the drainage system is no longer in function. Hence in the predictive simulations, the flow through the SILO is the flow through the encapsulation, protected on all sides by low permeable bentonite barriers. It is not the flow through a backfill above the concrete construction. A more detailed description of the SILO is included in the detailed model.

For the predictive simulations, the primary set-up of the SILO of the local model is called "first SILO definition (SD1)". For this set-up, the lateral flow barriers of the encapsulation are defined as low permeable. The definitions are given below:

- Bottom barrier: Resistance = 2.0 x 10^{+9} s (e.g. width=2 m conduc.=1.0 x 10^{-9} m/s).
- Side barrier: Resistance = 2.0 x 10^{+9} s (e.g. width=1 m conduc.=5.0 x 10^{-10} m/s).
- Top barrier: Resistance = 2.0 x 10^{+9} s (e.g. width=1 m conductivity=5.0 x 10^{-10} m/s).
- Concrete encapsulation: having a conductivity equal to 1.0 x 10^{-8} m/s

In addition to the SILO definition above, we have established an alternative set-up of the SILO of the local model, called "second SILO definition (SD2)". For this set-up, the lateral flow barriers of the encapsulation are defined as very low permeable, and also the interior of the SILO (the encapsulation) is defined as low permeable. For the local model this definition is only used as a sensitivity case, however, it is the main alternative for the detailed model (see Chapter 9). The definitions are given below:

- Bottom barrier: Resistance = 2.15 x 10^{+9} s (e.g. width=2 m conduc.=9.3 x 10^{-10} m/s).
- Side barrier: Resistance = 1.82 x 10^{+11} s (e.g. width=2 m conduc.=1.1 x 10^{-11} m/s).
- Top barrier: Resistance = 1.50 x 10^{+9} s (e.g. width=1.5 m conduc.=1.0 x 10^{-9} m/s).
- Concrete encapsulation: having a conductivity equal to 3.5 x 10^{-9}m/s

6.6 Representation of the fracture zones

In the local model, the fracture zones are defined in accordance with the updated structural geological interpretation by Axelsson and Hansen (1997). Planes in space give the locations of the fracture zones. In the models, the fracture zones are defined as separate continuous structures, by use of an implicit formulation as regards the conductivity of the cells intersected by the fracture planes. Hence, a cell that represents a zone will also partly represent the surrounding rock mass. The calculation of the properties of such a cell is based on the condition that the transport capacity of the cell should include both the transport capacity of the zone and that of the surrounding rock mass. If the cell is small its properties will be dominated by the properties of the zone. If the cell is large and the zone is small, the properties of the cell will be dominated by the properties of the rock mass. Cells intersected by a fracture plane will get an anisotropic conductivity formulation, in which some faces of the cells represent the rock mass only, and other faces represent both the zone and the rock mass.

The reason for the implicit formulation is that it is not possible to optimise the mesh for both the tunnels and the zones. The implicit formulation is however a very convenient formulation; e.g. even if the defined fracture planes forms a complicated geometry in three dimension, the mesh can be defined as regular and the geometry of the mesh will not cause numerical difficulties. Additionally, by use of the implicit formulation it is easy to change the location and extension of a zone, without having to change the geometric definition of the mesh.

The updated structural geological interpretations give no complete information of the vertical and horizontal limitations of the local fractures zones. For the local model, we have used the information provided in the updated interpretation. However, when no

information were available, the local zones have been defined as limited by the size of the local model. Hence, the local vertical zones (zones: 3, 6, 8 and 9) will have a vertical extension of about 490 m. Zones H2 and Singö are in both the local and the regional model. The conductivity of the fracture zones is discussed in Section 6.8.

The layout of the tunnel system in the local model and the fracture planes are demonstrated in Figure 6.3. This figure should be compared to Figure 5.1. Such a comparison demonstrates that the intersections between the tunnels and the fracture planes follow closely the local structural geological interpretation.

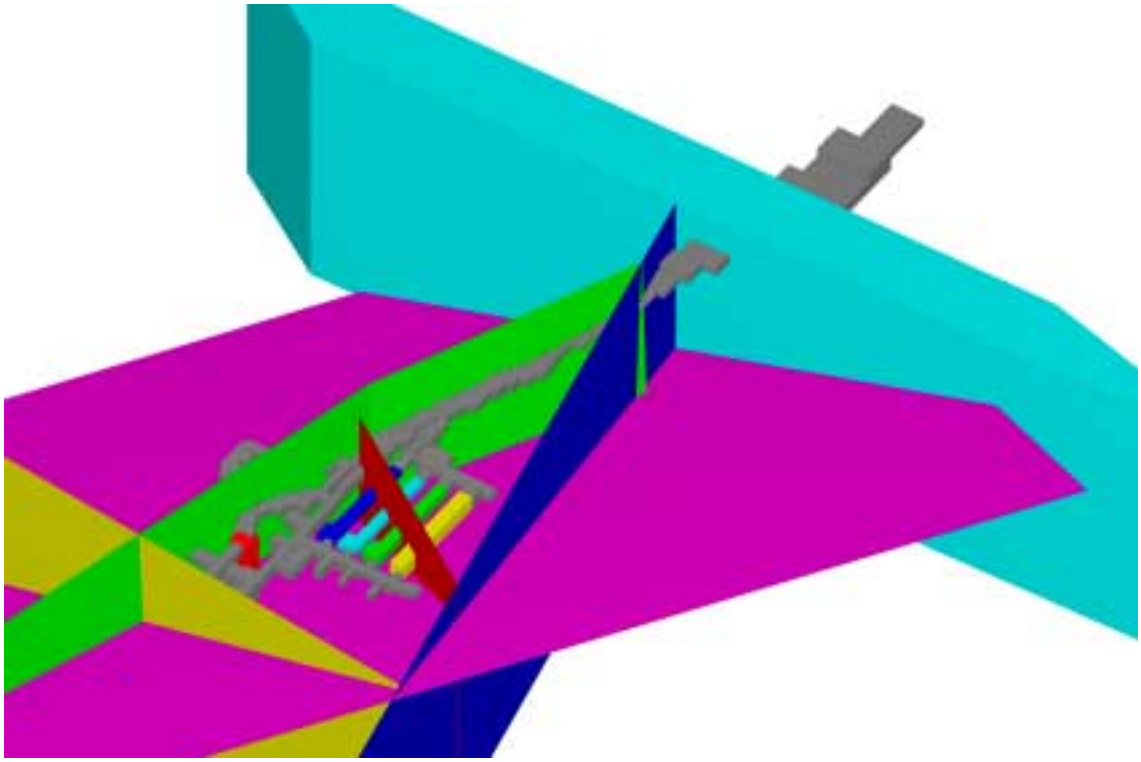

Figure 6.3 *The layout of the tunnel system at SFR as defined in the local model, and the fracture zones of the local model.*

ZONES: Purple= H2. Dark blue= 3. Dark red= 6. Yellow= 8. Green= 9.
TUNNELS: Grey= Access. Red= SILO. Dark blue= BTF1. Light blue= BTF2. Green= BLA Yellow= BMA
In this figure the fracture zones are represented by different 3-dim. planes. In the models the fracture zones are defined as separate continuous structures, by use of an implicit formulation as regards the conductivity of the cells intersected by the planes.

6.7 Representation of quaternary deposits

Quaternary deposits have not been explicitly included in the formal models. At the area studied, a glacial till occurs above the fractured rock with a varying thickness and continuity. We have assumed that on the average this material is more permeable or has approximately the same permeability as the fractured rock. Consequently in the local

model, the quaternary deposits are represented in the models as a part of the fractured rock. At the seabed above SFR, no continuous layer of low permeable sediments, e.g. clay, covers the glacial till. Hence, no such layer is included in the models.

6.8 Calibration of the local model

6.8.1 Introduction

The local model shall represent the properties of the hydraulic system at SFR. For this purpose, the local models have been calibrated in two ways: (*i*) considering the groundwater inflow to the SFR tunnel system, which produces values of the hydraulic conductivity; and (*ii*) considering the break-through times for sea-water to reach two bore holes in the close surrounding of the tunnel system, which produces values of the effective porosity.

6.8.2 Calibration of conductivity - inflow to the tunnel system

6.8.2.1 Objectives of the calibration procedure

The objectives of the calibration were to predict the same inflows to the tunnels in the model, as the inflows measured at SFR, and thereby obtain values of the hydraulic conductivity of the flow medium. For the calibration, the local model was set up in a way that the model represents the present situation. The measured groundwater inflow to the tunnels at SFR is presented in Axelsson (1997) and discussed in Section 5.4. At present the changes are very small, the values of inflow for the year 1997 can be assumed as representing a steady-state-like situation. It should, however, be noted that there are uncertainties in connection to the measurements of the inflow.

6.8.2.2 Boundary conditions of local model during the calibration procedure

The local model has to be assigned boundary conditions for the calibration procedure. At present the tunnels at SFR are kept at atmospheric pressure. During the calibration procedure, the tunnels of the model were also kept at atmospheric pressure, by use of a specified head condition for the cells representing the tunnels. The reader should note the difference between head and pressure; the tunnels are at constant atmospheric pressure, but the head change with depth, because the elevation of the tunnels changes.

For the present situation, the actual head values along the boundaries of the local model are unknown, but we can assume that these values are close to the head of the seawater. We can also assume that the size of the actual variation in head along the boundaries is small, compared to the difference in head between the head in the drained tunnels (at atmospheric pressure) and the head of the seawater level. Consequently, the calibration of the model was carried out under steady state conditions; the outer boundaries of the local model was assigned the specified head boundary condition, with a head equal to

the level of the present seawater table. This is an acceptable simplification, for the calibration procedure, because during the calibration the tunnels are at atmospheric pressure and the general flow pattern will be towards the tunnels.

The applicability of the simplification was verified after the calibration was completed and after the complete chain of predictive simulations was carried through. This was done by re-running the calibration with the head values along the outer boundaries of the model representing the regional flow situation for the year 2000 AD. Such head values were obtained from the regional model Case 4 (see Chapters 7 and 8). The resulting inflows to the drained tunnels were the same as for the original calibration (the divergences were much less than 1%). Hence, the simplification was applicable.

6.8.2.3 Calibration philosophy

To obtain a similar inflow in the local model as the measured inflow, the conductivity of the rock mass and of the zones were changed until the model produced an inflow that was approximately the same as the measured inflow. However, it is important to note that there are an infinite number of combinations of different values of conductivity, which produces the same values of inflow. Hence, there is no unique solution.

The following principles have been followed for the calibration:
- Assumptions must not be multiplied beyond necessity (*the principle of Ockham's razor*, William of Ockham, circa 1300 AD).
- The average conductivity of the rock mass of the local model (the rock between defined fracture zones) should be smaller than the average conductivity of the least conductive fracture zone.
- The average conductivity values of the fracture zones should diverge as little as possible from the geometric average obtained from the hydraulic tests.
- No depth trend will be introduced to the hydraulic conductivity of the flow media. This principle is based on observations at different sites in Sweden, see Walker *et al* (1997).
- The effects of grouting and/or hydraulic skin should be introduced as little as possible.

Two major simplifications of the actual flow medium were also used:
- The rock mass of the local model (the rock between defined fracture zones) is represented in the model as homogeneous and isotropic, by use of a representative average value of conductivity.
- The fracture zones are represented in the models as homogeneous, by use of representative average values of conductivity.

The rationale for representing the local rock mass and the fracture zones as homogeneous is given in Section 2.4.

6.8.2.4 Calibration method

The method to reach the objectives was to change assumed values of conductivity until the model predicted acceptable values of inflow (manual trial-and-error).

6.8.2.5 Results of calibration

During the calibration of the local model, as well as for the present situation at SFR, the groundwater flow is towards the tunnels. This is because the tunnels are at atmospheric pressure and drained. The properties of the flow medium at SFR (the fractured rock) are heterogeneous; hence, the conductivity of the fractured rock will depend on direction of the groundwater flow. The direction of the groundwater flow will not be the same in the predictive simulations as it was during the calibration procedure. Consequently, the conductivity values that the calibration procedure has produced are directly applicable for the simulated situation only (the present situation), and may not be the correct ones for the predictive simulations (the future situation). The conductivity values derived through the calibration can be described as, *an equivalent conductivity for three-dimensional radial flow towards the tunnels* (see Sec.5.2.1).

There exists no unique solution to the calibration procedure and the conductivity values that the calibration procedure has produced may not be the correct ones for the predictive simulations. We should consider this and remember that the calibration procedure will only give us a good estimate of the actual conductivity. The results of the calibration are presented in Table 6.2 and Table 6.3. As can be seen in Table 6.2 the calibration target was reached (the correct prediction of inflow). The divergences are small between measured and predicted inflow.

The main results of the calibration procedure are the hydraulic conductivity values of the calibrated local model. These values are given in Table 6.3. As can be seen in the table, the calibration principles (outlined above) were followed. In the calibrated model, the representative conductivity of the rock mass is smaller than the representative values of conductivity of the different fracture zones. For the fracture zones, except for Zone 6, the divergences are small between the results of the hydraulic tests and the results of the calibration. Considering Zone 6, the difference between the results of the tests and the results of the calibration can be explained by the possible heterogeneity of the zone and/or the presence of grout and skin between Zone 6 and the deposition tunnels. It should also be noted that only two double packer tests have been carried out in Zone 6, which makes the results of the tests, i.e. the geometric mean value, to a very uncertain estimate. As a part of the calibration a reduced conductivity (grouting/skin) was applied at the contact between the BMA tunnel and zone 6, consequently the direct hydraulic connection between Zone 6 and the BMA tunnel is not very effective.

The results of the calibration also demonstrate a good match between the analytical estimate of a representative rock mass conductivity (see Sec5.2.3) and the rock mass conductivity resulting from the calibration. This is not surprising as both the analytical estimate and the calibration were based on the measured inflow to the tunnels.

Table 6.2 Groundwater inflow at SFR –actual measured inflow at 1997 (Axelsson , 1997) and volumes predicted by the calibrated local model.

Studied Tunnel	Measured (litre/min)	Predicted by model (litre/min)
Entrance tunnel	375	363
SILO	1.6	1.7
BMA	9.3	10.7
BLA, BTF and surrounding tunnels	83.6	83.3

Table 6.3 Results of calibration of local model - transmissivity and conductivity. The table gives: (i) the results of the hydraulic tests, geometric mean transmissivity of the single bore hole tests, based on data taken from Axelsson and Hansen (1997); and (ii) the values produced by the calibration procedure.

Studied domain	Test. Geo. Mean Transmissivity (m2/s)	Model Transmissivity (m2/s)	Model Hydraulic width (m)	Model Conductivity (m/s)
Rock mass	-	-	-	6.50E-9
Tunnels	-	-	-	1.00E-5
Zone Singö	-	5.00E-4	2 x 25	1.00E-5
ZoneH2	1.7E-6	1.50E-6	10.6	1.42E-7
Zone 3	2.1E-5	2.05E-5	6.45	3.18E-6
Zone 6	5.0E-7	1.98E-6	1.65	1.20E-6
Zone 8	4.3E-6	3.62E-6	10.5	3.45E-7
Zone 9	2.7E-8	2.09E-8	2.35	8.90E-9
Grouting – Skin between:	Conductivity (m/s)			
Access tunnel & Z-Singö	K_grout = 0.0006 x K_Singö = 6.00E-9			
Access tunnel and Zone 3	K_grout = 0.015 x K_Z3 = 4.77E-8			
BMA tunnel and Zone 6	K_grout = 0.001 x K_Z6 = 1.20E-8			

6.8.3 Estimation of effective porosity

6.8.3.1 Introduction

The effective porosity is defined as “the ratio of the volume of interconnected pore space available for fluid transmission to bulk volume of the solid rock” (Nordic glossary of hydrology, 1984), The effective porosity corresponds to the amount of pores/fractures through which the groundwater flows. Considering a fracture zone, one may also look upon the effective porosity as a measure of the internal properties of that zone e.g. filling material in the zone etc. In a model based on Darcy’s law and for a given flow field, the effective porosity controls the velocity of the groundwater, but not the magnitude of the flow, as this is controlled by the flow field.

6.8.3.2 Flow conditions and measurements at SFR

At present, and for the period during which SFR has existed, the groundwater flow has been towards the tunnels. This is because the tunnels are at atmospheric pressure and drained. Water samples have been taken from different bore holes (sampling points) drilled from the tunnel system and into the surrounding rock mass and fracture zones. These samples have been chemically analysed, some results are presented in Axelsson (1997). It was recommended in Axelsson (1997) that “The chemistry data can be used to calibrate time for breakthrough of Baltic Sea water”. However, some of the interpreted breakthrough times given in Axelsson (1997) were based on erroneous data. The distinct breakthrough of seawater in bore hole HK10 was an artefact of mistaken identity of the sampling points. Starting from a certain time, the identity of sampling points was mixed at SFR. When this error was corrected and the data attributed to the correct sampling points, there was no longer any distinct breakthrough of seawater in HK10, but a very slow change of the chemical properties. It is possible to interpret the smooth change in chemical properties as a result of a complicated heterogeneous flow

medium, in which some flow paths are fast and others are slow. At the sampling points we will have a time-dependent mix of water and not a breakthrough of a distinct front of seawater.

6.8.3.3 Representative values of breakthrough times

The values of effective porosity assigned to the models of this study were derived through simulations by the local model. For these simulations, the local model was set up in a way that the model represents the present situation. The objective of the simulations was to predict breakthrough times for the seawater, in line with the values measured at SFR. Through these simulations we will obtain a range of possible values of the effective porosity. For the simulations we have used the local model that resulted from the previously presented calibration of conductivity values. The same boundary conditions were used (steady state) and the same conductivity values.

As stated above, the used model was set up as a steady state model, representing the present situation. However, the measured change in chemical composition at SFR is the result of the movement of the seawater, from the sea, through fracture zones and rock mass, towards the sampling points; and these flow paths have developed during a time-dependent course, as the construction of SFR was carried out and as the local groundwater situation developed into a steady-state-like situation. Therefore it is likely that for the present situation at SFR (steady-state-like situation), the breakthrough times are shorter than the break though times that are interpreted based on the measured change in chemical composition at SFR.

As no distinct breakthrough of seawater has been measured at the sampling points in the fracture zones that surrounds the SFR, we have estimated a set of representative breakthrough times for the sampling points, which represents the actual smooth change of chemical composition that occurs at these points. As discussed above, we have used a steady state model for the simulations of the breakthrough times, but the actual flow conditions are time-dependent. To compensate for the actual time-dependent flow conditions, we have selected representative values of breakthrough times, which are short, compared to the actual measured times for change in chemical composition.

- The sampling points in Zone 8 (bore holes HK08 and HK11) indicates a first breakthrough of seawater between August 1987 and August 1988, i.e. about 10-22 months after completion of the tunnel system. For the sampling point in Zone 8 we have selected a representative breakthrough time of 10 months.
- The sampling points in Zone 3 (bore hole HK10) indicates no complete breakthrough of seawater after more than 12 years of measurements. But after the first three years of measurements, a significant change in composition has taken place. For the sampling point in Zone 8 we have selected a representative breakthrough time of 30 months.
- Sampling have also been performed in Zone H2 (bore hole HK7a); however the flow conditions in Zone H2 are complicated, and during the construction phase the measured salinity increased in H2, probably due to inflow of deep, more saline, groundwater. After 1989 the salinity at the sampling point in H2 is decreasing very slowly. We have not selected a representative breakthrough time for the sampling point in H2, because of the complicated time-dependent flow conditions in this zone.

6.8.3.4 Simulation of breakthrough times

Simulations in the local model produced breakthrough times for different values of the effective porosity. By a manual trial and error procedure, values of the effective porosity were selected, values that produced the same breakthrough times as the selected representative breakthrough times. The results of these simulations (calibration as regards the effective porosity) are given in Table 6.4.

Table 6.4 Assumed breakthrough of sea water, and predicted breakthrough in the local model; as well as corresponding values of the effective porosity.

Sampling point	Assumed representative breakthrough time (months) Time-dependent course	By local model predicted breakthrough time (months) Steady state conditions.	Effective porosity, as defined in the model for the studied Zone (-)
HK08 in Zone 8	10	9	0.01
HK10 in Zone 3	30	30	0.05

6.8.3.5 Base case and Alternative case

Considering the values of the effective porosity assigned to the model, two different cases have been established, the base case and the alternative case. For the base case, different values of effective porosity were assigned to the model. For the alternative case, the effective porosity was the same for both the rock mass and the fracture zones.

- Base case: The values of effective porosity of the base case were selected based on the simulation of breakthrough times, see Table 6.4. For the rock mass and for the fracture zones in which no sampling have been performed, the selection of values of effective porosity were based on experience from other sites. For the base case, the effective porosity of the local fracture zones is between 1 and 5 percent and that of the rock mass is 0.5 percent. Table 6.5 gives the effective porosity of the base case.

- Alternative case: For the alternative case, the effective porosity of rock mass and fractures zones is set to a constant value of one percent. The alternative case can be used when estimating the breakthrough times for other constant values of the effective porosity, as the breakthrough times predicted by the alternative case are proportional to the value effective porosity.

Table 6.5 The Base case: Values of effective porosity assigned to the model.

Studied domain	Effective porosity (-)
Rock mass	0.005
Zone Singö	0.05
Zone H2	0.025
Zone 3	0.05
Zone 6	0.025
Zone 8	0.01
Zone 9	0.025

7. Description of regional model

7.1 Introduction

The formal models will be established in accordance with the methods presented in Chapter 2. As described in Chapter 2, we will use different models at different scales, representing the studied system (the flow domain). The regional model represents the system on a regional scale; this model will have a regional resolution. The local model represents the system on a local scale; this model will have a local resolution. The regional model will be established after the local model. When establishing the regional model, the results of the calibration of the local model will be considered. Figure 2.6 illustrates the order of establishment.

7.2 Size of model

The model represents a rectangular three-dimensional body. The model covers a horizontal area of, 13 300 m x 15 850 m (210.8 km^2) and the depth of the model is 1000 m. The upper boundary of the model is the surface topography. The model has vertical sides and a base that is nearly flat. The size and the horizontal position of the regional model are given in Figure 6.1.

7.3 Mesh

The mesh of the regional model has 9 layers and contains 81 396 cells of different size. The mesh is given in Appendix A.

7.4 Boundary conditions

7.4.1 Boundary condition along the top of the regional model

The top boundary condition used for the regional model is either: (i) the specified head condition, representing the seawater table or (ii) a non-linear boundary condition, representing the ground surface above the sea and the varying actual groundwater recharge. By use of the non-linear boundary condition we will **not** force a certain value of recharge or head condition upon the model. The model will calculate the actual recharge and the position of the groundwater surface as a part of its solution of the flow field, consequently these properties may vary with time. The extensions and positions of recharge and discharge areas will also be calculated by use of the non-linear boundary condition.

At SFR the precipitation and the evapotranspiration produces a potential recharge that is much larger than the amount of recharge that can, on the average, infiltrate into the bedrock. The actual recharge varies depending on, potential recharge, topography, conductivity and the state of the groundwater system.

For the areas not covered by the sea, the non-linear boundary condition used by the GEOAN model reproduces closely the interaction between, the state of the groundwater system, the potential groundwater recharge and the ground surface topography. The non-linear boundary condition calculates the actual recharge and the position of the groundwater surface by the use of an iterative algorithm.

The iterative algorithm
First step: The model calculates the position of the groundwater surface and compares it to the topography, thereby estimating the extension of recharge and discharge areas.
Second step: The model estimates the actual recharge.

- Discharge areas: the model will use the specified head boundary condition at discharge areas. The head is set equal to the ground elevation and the model calculates the recharge-discharge components. The maximum recharge is equal to the potential recharge. The discharge is larger than zero.
- Recharge areas: the model will use a continuous boundary condition at recharge areas. The recharge is set equal to the potential recharge and the model calculates the head. The maximum head is equal to the ground surface. The discharge is equal to zero.

The steps are repeated.

For the areas covered by the sea, the model will use the specified head boundary condition, representing the seawater table. In the models, the shore level displacement will not be simulated as a raising of the land, but as a lowering of the level of the seawater table, a lowering in relation to a reference co-ordinate system. For each time step taken by the model, the seawater level is lowered, the topography is checked and areas above the new sea level will be assigned the non-linear boundary condition.

As discussed in previous sections (see Sec. 2.6.2 and 4.1.3) lakes will be established about 1 km North and Northeast of the repository at about 4800 AD. In the model this will take place at 4850 AD, and the water level of this lake will be -15 masl. Hence, for the areas defined as these lakes, the model will use the specified head boundary condition, with a head equal to –15 masl.

7.4.2 Boundary conditions along the vertical faces of the regional model

The model has a rectangular three-dimensional shape with four different vertical faces. As far as possible, the boundary conditions of the regional model coincide with the naturally occurring hydraulic boundaries (physical boundaries). The boundary conditions of the models vertical faces are time-independent, but the same for the whole simulation period.

The uppermost cells along the Southwest face, coincides with actual surface water bodies, these lakes will probably be maintained as lakes in the future, consequently, the uppermost cells along the Southeast face have been assigned the specified head boundary condition. Below the surface cells we have used the no-flow condition.

For the Northwest and Southeast faces we have used the no-flow condition. Generally, in the area represented by the regional model, the gradient vector of the topography points towards Northeast. It is likely therefore that the general flow direction of the groundwater is in this direction. The Northwest and Southeast faces are along the general direction of the groundwater flow, hence the boundaries follow approximately a generalised flow path of the groundwater. Therefore, these two boundaries are assigned the no-flow boundary condition. The very large size of the regional model makes these two boundaries of less importance; considering the flow close to SFR, which is mainly dependent on the local topography and the level of the sea. The minimum distance between the SFR and these two boundaries are about 7 km.

We have also used the no-flow boundary condition for the Northeast face. This face is approximately located along the lowest topographic levels in the regional basin (along the bottom of the regional valley). This face is a no-flow boundary, because generally there will be a groundwater flow coming from the opposite side of the basin, which prevents further transport towards Northeast. The uppermost cells along this face will always represent the seawater level, as the studied time period is not long enough for the shore level displacement to completely withdraw the sea from the regional basin.

7.4.3 Boundary condition along the base of the regional model

For the base of the model we have used the no-flow condition. The base of the models is 1000 m below the ground surface. At this great depth, circa 900 m below the SFR, we have presumed that the no-flow boundary condition is an appropriate boundary condition, considering the purpose of the study. The boundary condition at the base of the regional model is time-independent, but the same for the whole simulation period.

7.5 Fracture zones of the regional model

7.5.1 Introduction

In the regional model the fracture zones are defined by use of the implicit method, as described in the presentation of the local model

7.5.2 The local zones

In the regional model, the fracture zones of the local model are defined with the same extension and with the same transport capacity - the same conductivity and same theoretical hydraulic width, as in the local model. However, as the resolution of the regional model is less than the resolution of the local model, these properties will be

included in the large cells of the regional model. Hence, in the regional model the local zones will not be defined with the same degree of detail as in the local model.

7.5.3 The regional zones

The regional structural geological interpretation consists of 8 large regional fracture zones. Among these zones are the Singö fracture zone and the Forsmark fracture zone. Like the Singö zone all regional zones, except zone H2, are assumed to have a vertical dip. No explicit structural geological information is available for their vertical extension. In the regional model, the base of the model limits the vertical extension of the regional zones. Hence, the regional zones will have a vertical extension of about 1000 m. Zones H2 and Singö are in both the local and the regional models. The horizontal extension of the regional zones is given
Figure 4.1

7.6 Correspondence - local and regional properties

7.6.1 Fracture zones

In the models the fracture zones are defined as separate continuos structures. All zones are defined with a given conductivity and a given size (hydraulic width and depth), the conductivity and the size produces a transport capacity for the zone studied. Regardless of the scale and resolution of the models, the fracture zones in the models will always be defined in the same way, having the same transport capacity. However, not all zones are in all models. The regional model includes all zones, but the smaller model includes only the zones that intersect the domain represented by the smaller model.

7.6.2 Rock mass between fracture zones

In a fractured crystalline rock, the groundwater flows in fracture and fracture zones of different sizes. Only fracture zones of a certain size are known explicitly, the transport capacity of all other fractures and fracture zones are represented by the conductivity of the "rock mass" between the known fracture zones. At the local domain in the surrounding of SFR a large number of fracture zones are known, both large zones and small zones; but outside of the local domain only the large regional zones are known. Hence, the rock mass between fracture zones represents different properties inside the local domain and outside of the local domain.

The rock mass of the local model represents the fractured rock between the local and the regional fracture zones that are in the local domain. The conductivity of the rock mass of the local model is a specific value, representing the local properties of the local domain, at a local scale.

For the regional domain (outside of the local domain), only large regional fracture zones are known. Information of small fracture zones is not available *on regional* scale, small fracture zones are known for the local domain only. Therefore, in the regional

model the rock mass conductivity outside of the local domain should be different from the rock mass conductivity of the local model (the local domain), as no local zones are included in the regional model outside of the local domain.

Hence, the average rock mass conductivity in the regional model should be an effective value (effective conductivity), representing the heterogeneous properties at a large scale. While the rock mass conductivity in the local model should be an equivalent value (equivalent conductivity) representing the heterogeneous properties at a local scale. The concept of equivalent and effective conductivity is discussed in Sec.5.2.1.

Generally, the local and regional hydraulic properties represent the same type of fractured crystalline rock. The different values of rock mass conductivity applied in the models reflect different modelling approaches, the different scales studied and the different amount of information available for the regional and the local scale.

7.7 The different cases - uncertainty in regional properties

7.7.1 Introduction

The regional model is not calibrated, as no applicable data is available for calibration at such a scale. From a conceptual point of view, several different modelling approaches are possible for the representation of the rock mass at a regional scale, in which only the very large regional zones are defined separately. This is discussed in Sections 7.6 and 7.7. To investigate the effects of the uncertainties of the regional hydraulic properties of the rock mass several different cases have been tested and the differences in the resulting predictions have been compared –a sensitivity study. In this section we will present the different cases, a summary is given in Table 7.1.

7.7.2 The different methods for estimating the regional conductivity

Two different methods have been used when estimating the effective conductivity of the rock mass on a regional scale.

First method. The conductivity of the rock mass is represented by an effective value. The effective value was selected based on: (*i*) the obtained conductivity of the rock mass of the local model (the local equivalent conductivity for radial flow towards the tunnels as produced by the calibration of the local model); and on (*ii*) an assumed scale dependency, that are in line with the scale dependency at Äspö HRL (see Sec.5.2.1).

Second method. The conductivity of the rock mass is represented by an effective value. The effective value was selected based on a calculation of the equivalent conductivity of the whole of the local model, the equivalent conductivity for flow in a presumed dominating flow direction. For this calculation the no-flow boundary conditions were defined for all faces of the local model except for the Southwest face and the Northeast face, which were assigned a specified head condition. A gradient was defined and the flow through the local model, together with the size of the model, gives the equivalent conductivity of the local model, as regards flow towards Northeast. The equivalent

conductivity becomes, 1.5 x 10^{-8} m/s, this value is half an order of magnitude larger than the local equivalent conductivity for radial flow towards the tunnels, as produced by the calibration of the local model. So it can also be looked upon as an estimation of an effective value, based upon the assumption that the effective value should be approximately half an order of magnitude larger than the local equivalent conductivity for radial flow.

7.7.3 Case 1.

This Case represents a regional rock mass with a large conductivity, but with a limited potential recharge. The heterogeneity of the rock mass between large fracture zones is not represented.

- The rock mass between large fracture zones is defined as homogeneous, but intersected by regional fracture zones, which are also homogeneous.
- The conductivity of the rock mass is represented by an effective value. The effective value was selected based on the obtained conductivity of the rock mass of the local model, and on an assumed scale dependency, that are in line with the scale dependency at Äspö HRL (see Sec.5.2.1). The effective conductivity was defined based on the assumption that the effective value should be approximately one order of magnitude larger than the local equivalent conductivity for radial flow, as produced by the calibration of the local model. This gives an effective value equal to, 6.5 x 10^{-8} m/s.
- The potential groundwater recharge was defined as small, making it to a limiting factor when the model calculates the actual recharge. The potential recharge was set to 5 mm/year. The model will calculate the actual recharge as a part of its solution.

7.7.4 Case 2.

This Case represents a regional rock mass with a conductivity that is not as large as in Case 1, but with a large potential recharge. This case and Case 4 are identical except for the heterogeneity of the rock mass between large fracture zones. For this case, the heterogeneity of the rock mass between large fracture zones is not represented.

- The rock mass between large fracture zones is defined as homogeneous, but intersected by regional fracture zones, which are also homogeneous.
- The conductivity of the rock mass is represented by an effective value. The effective value was selected based on a calculation of the equivalent conductivity of the whole local model, as discussed above (second method). The equivalent conductivity becomes, 1.5 x 10^{-8} m/s, this value is half an order of magnitude larger than the local equivalent conductivity for radial flow towards the tunnels, as produced by the calibration of the local model. So it can also be looked upon as an estimation of an effective value, based upon the assumption that the effective value should be approximately half an order of magnitude larger than the local equivalent conductivity for radial flow.
- The potential groundwater recharge was set equal to the approximate average run-off, which is 250 mm/year. The model will calculate the actual recharge as a part of its solution.

7.7.5 Case 3.

This Case represents a regional rock mass with a large conductivity, and with a large potential recharge. The heterogeneity of the rock mass between large fracture zones is represented by use of the stochastic continuum method.

- The rock mass is defined as heterogeneous and intersected by regional fracture zones, which are homogeneous. The heterogeneity of the rock mass between large fracture zones is represented by the method of stochastic continuum (see Sec.2.4).
- The conductivity of the rock mass varies for different cells, the heterogeneous conductivity of the rock yields an effective value. The effective value is the same as the value used in Case 1. Hence, it is selected based on the obtained equivalent conductivity of the rock mass of the local model, and on an assumed scale dependency, that are in line with the scale dependency at Äspö HRL (see Sec.5.2.1). The used effective value equal is, 6.5×10^{-8} m/s. The rock mass is defined as heterogeneous by use of the stochastic continuum method, The local values of conductivity (the varying conductivity of the cells), were given by probability distributions. These distributions were derived according to the method given by Holmén (1997). This is a method that keeps the effective value of the flow medium constant, regardless of the size of the cells in the mesh. The stochastic conductivity field of the rock mass is not spatially correlated.
- The potential groundwater recharge was set equal to the approximate average run-off, which is 250 mm/year. The model will calculate the actual recharge as a part of its solution.

7.7.6 Case 4.

This Case represents a regional rock mass with a conductivity that is smaller than for Cases 1 and 3, and with a large potential recharge. This case and Case 2 are identical except for the heterogeneity of the rock mass between large fracture zones. For this case, the rock mass between large fracture zones is defined as heterogeneous, by use of the stochastic continuum method.

- The rock mass is defined as heterogeneous and intersected by regional fracture zones, which are homogeneous. The heterogeneity of the rock mass between large fracture zones is represented by the method of stochastic continuum (see Sec.2.4).
- The conductivity of the rock mass varies for different cells, the heterogeneous conductivity of the rock yields an effective value. The effective value is the same as the value used in Case 2. Hence, it is selected based on the obtained equivalent conductivity of the whole of the local model, as discussed above (second method). The used effective value equal is, 1.5×10^{-8} m/s. The rock mass is defined as heterogeneous by use of the stochastic continuum method, The local values of conductivity (the varying conductivity of the cells), were given by probability distributions. These distributions were derived according to the method given by Holmén (1997). This is a method that keeps the effective value of the medium constant, regardless of the size of the cells in the mesh. The stochastic conductivity field of the rock mass is not spatially correlated.
- The potential groundwater recharge was set equal to the approximate average run-off, which is 250 mm/year. The model will calculate the actual recharge as a part of its solution.

7.8 Specific yield and the storativity

At SFR there have been no direct measurement of porosity, specific yield or storativity. Hence, no such site-specific data is directly available. The specific yield and the storativity are properties that should be included in a time-dependent model. The specific yield defines the amount of water that is released/stored in the flow medium when the groundwater surface moves. This property is mainly related to the porosity, we have assumed a value equal to 0.005 (m^3/ m^3), which is the same as 0.5%. The storativity defines the amount of water that is released/stored in the flow medium when the groundwater head changes. This property is related to the rock stresses, we have calculated a value equal to $5 \cdot 10^{-6}$ (1/m), based on the following equation (Carlsson and Gustafsson, 1984).

$S_s = \rho_w \cdot g \cdot (n \cdot \beta_w + \beta_s)$

S_s = Storativity (1/m)
ρ_w = density of water, 1000 kg/m^3
g = acceleration of gravity, 9.81m/s^2
n = porosity 0.5%
β_w = compressibility of water $4 \cdot 10^{-10}$ m^2/N
β_s = compressibility of rock $5 \cdot 10^{-10}$ m^2/N

7.9 Summary - hydraulic properties of regional model

Below is a summary of the hydraulic properties of the regional model.

Table 7.1 The hydraulic properties of the regional model.

Studied domain		Case 1	Case 2	Case 3	Case 4
Rock mass outside of Local model domain Conductivity:		Homogeneous Effective value: 6.5E-8m/s	Homogeneous Effective value: 1.5E-8m/s	Heterogeneous Stochastic Cont. Not correlated K Effective value: 6.5E-8m/s	Heterogeneous Stochastic Cont. Not correlated K Effective value: 1.5E-8m/s
Probability Distribution Parameters (Holmén 1997)	P1:	-	-	1000	1000
	P2:	-	-	2.65	2.65
	P3:	-	-	0.14	0.14
	P4:	-	-	0.04	0.04
Regional zones Hydraulic width (W): Conductivity (K):		W= 50 m K= 1.0E-5m/s	W= 50 m K= 1.0E-5m/s	W= 50 m K= 1.0E-5m/s	W= 50 m K= 1.0E-5m/s
Potential recharge		5 mm/year	250 mm/year	250 mm/year	250 mm/year
Storativity (1/m)		5.0E-6	5.0E-6	5.0E-6	5.0E-6
Specific Yield (-)		0.005	0.005	0.005	0.005
Effective porosity (-)		Not defined	Not defined	Not defined	Not defined
Local fracture zones		As local model	As local model	As local model	As local model
Rock mass inside local model domain		As local model	As local model	As local model	As local model

7.10 Quaternary deposits

Quaternary deposits have not been explicitly included in the regional model. At the area studied, a glacial till occurs above the fractured rock with a varying thickness and continuity. We have assumed that on the average this material is more permeable or has approximately the same hydraulic conductivity as the fractured rock. Consequently, the quaternary deposits are represented in the models as a part of the fractured rock. At the seabed above SFR, no continuous layer of low permeable sediments, e.g. clay, covers the glacial till. Hence, no such layer is included in the models.

7.11 Analytical model

An analytical model has been established. The purpose of the analytical model is to estimate the magnitude of the groundwater flow through the deposition tunnels and thereby check that no fundamental error has been included in the numerical models.

The analytical model is based on a method originally proposed by Carslaw and Jaeger (1959), the method is presented in Holmén (1997). It is an analytical method based on analytical solutions to differential equations.

A tunnel is represented by an ellipsoid analogy. The flow through the ellipsoid-tunnel is calculated based on the following assumptions:

- A deposition tunnel is represented by an ellipsoid, having approximately the same size as the deposition tunnel studied.
- The ellipsoid is homogeneous and isotropic.
- The ellipsoid is placed in an infinite large homogeneous isotropic flow medium
- The flow is at steady state.
- There is a regional flow in the flow medium that tends to a known value at great distance from the ellipsoid

8. Regional model, results of different cases and comparison with local model

8.1 Introduction

The purpose of the regional model is to provide the local model and the semilocal model with time-dependent boundary conditions. Based on the calculated head in the regional model, head values are exported to the specified head boundaries of the local and semilocal models. These head values will not be presented in detail in this study. In this chapter we will present some results of the regional model, as well as a general comparison between the results predicted by the regional and local model for the different cases studied (the cases are defined in Sec.7.7). Based on this comparison, we will select one of the four cases as our main alternative.

8.2 Discretization of the time domain in the regional model

To solve the differential equation with respect to time, we need to divide the time domain into discrete steps – time steps. The larger the number of time steps, the better the representation of the time-dependent course (presuming that the time step is not small enough to cause numerical difficulties). The drawback with a small time step is that the computational demands will be large if the time step is small. The size of the time step has to be balanced between acceptable accuracy and computational demands.

To decide the size of the time step, we have performed a sensitivity analysis. For this analysis, the simulation of the time-dependent course (Case 4) was repeated several times with different time steps being subsequently smaller and smaller. The head distribution in the central domain (SFR area) was checked at time equal to 2000 AD. The optimum size of the time step was found when no significant change in head occurred, in this domain, for subsequently smaller time steps. However, for reproducing the excess head values, which was measured and interpreted at SFR before the construction of the repository (discussed in Sec.5.6), the time step used in the predictive simulations was set somewhat larger than the numerically optimised time step, this is discussed in Sec.8.3. The time step finally selected was used in all simulations with the regional model.

The numerical models are based on the finite difference method, this method replaces the original differential equation with a system of equations (see Sec. 2.2 and 2.3). The method for establishing the system of equations and the method for solving this system will have influence on the necessary size of the time step. The system of equations was established by use of the implicit method (Bear and Verruijt, 1987), the system was solved by use of an iterative solver (Press *et al*, 1992). The selected time step was equal to 20 years, which give 400 steps for a time period of 8000 years.

8.3 Calculated excess head and size of time step

8.3.1 Background

Groundwater heads in the rock mass at SFR were measured previous to the construction of the repository, this is discusses in Section 5.6. For the bore holes that intersected the H2 sub-horizontal fractures zone, the results of the head measurements demonstrated, in relation to the mean sea water level, an excess head level in the bore holes, which was between +0.11 meters and +0.61 meters. From a theoretical point of view it is likely that there should be an excess head, but theoretical assessments gives no exact information of the size of the excess head, and the results of the actual measurements are uncertain. As previously discussed in Sec.5.6, the size of the excess head in the rock mass depends on the velocity of the shore level displacement, compared to the velocity of the change of the heads in the rock mass. The velocity of the change of the heads in the rock mass depends on different factors like. (i) The conductivity and the storage properties of the rock mass, as well as (ii) the conductivity and the extension of previous and present quaternary deposits, and (iii) the effects of the movements of deep groundwater with a high density (fossil salt water) as well as movements of near surface groundwater with a density higher than that of the present seawater.

8.3.2 Sensitivity analysis of size of time step, excess head and tunnel flow

Using the initial condition discussed in Sec.2.6.3 as well as reasonable values of the conductivity and the storage properties of the flow media, the regional model will predict an excess head at the SFR area, which is smaller than the measured and interpreted values (the model predicts an excess head smaller than 0.1 masl). Carlsson *et al* (1987) made similar conclusions based on the results of their model. A large excess head could nevertheless be an actual property of the system studied, as the models are simplified descriptions of the system studied.

The excess head discussed above is a result of the regional groundwater flow, for the flow situation during the time of the measurement (1980-1981 AD), in the model this period is represented by time equal to 2000 AD. As the shore level withdraws from the 2000 AD position, the head in the rock mass will change. With time, as the shore level retreats, the flow pattern of the ground water at the SFR area will be more and more influenced by the local topography and less influenced by the regional flow. Consequently, the uncertainty in the actual value of the excess head will not be very important after approximately 4000 AD (after 3000 AD the shore level has passed the area above the repository).

We have investigated the effects of different values of excess heads, as regards the size of the flow of the deposition tunnels. For this sensitivity analysis we used both the regional model and the local model and the method presented in Sec.2.7. We used the regional model Case 4, but defined without the tunnels. The regional model was set up in a way that the model, for time equal to 2000 AD, produced values of excess head at the SFR area, similar to the actually measured and interpreted values. To achieve this, the size of the time step of the transient calculations was selected somewhat larger than a time step based on strictly numerical considerations. A time step that is larger than the

numerically optimised time step will delay the change of the head values of the model. Consequently for such time steps, large head values will remain at the SFR area for a longer period than for a time step selected based on a strictly numerical consideration.

Two cases were established, Case 4A and Case 4B, for these cases different time steps were selected, larger than a numerically optimised time step. For Case 4A the regional model predicted an excess head of +0.30 masl and for Case 4B the predicted excess head was +0.15 masl (for the rock mass at the SFR area at time equal to 2000 AD). As discussed above, the corresponding actually measured and interpreted excess head was between +0.61 meters and +0.11 meters.

Head values was transferred from the regional model to the boundaries of the local model, and the local model was solved (with tunnels) using these boundary conditions. The flow through the tunnels was calculated by use of the local model. The results are as follows:

- Time equal to 2000 AD, Case 4B will produce a total flow of the deposition tunnels that are ca. 70 percent of the flow predicted by Case 4A.
- Time equal to 3000 AD, Case 4B will produce a total flow of the deposition tunnels that are ca. 80 percent of the flow predicted by Case 4A.
- Time equal to 4000 AD, Case 4B will produce a total flow of the deposition tunnels that are very close to the flow predicted by Case 4A.

Hence, the uncertainty in the measured and interpreted values of excess head, will only have a large influence in predicted flow, for the time period between 2000 AD and 3000 AD. At 2000 AD, the differences between the two cases is approximately equal to 30 percent of the flow of Case 4A, at 4000 AD, the difference between the two cases is insignificant.

8.3.3 Timestep, excess head and tunnel flow -conclusions

Considering the main purpose of this study, which is to predict the flow through the deposition tunnels and the flow paths from the deposition tunnels, it is conservative to set up a model that reproduce a large excess head; because a large excess head will give a larger flow through the tunnels and shorter break-through times than a small excess head. Consequently, we have used the time step of Case 4A, which will produce an excess head, which is large, but in line with the measured and interpreted values. It should be noted that for a situation with an excess head equal to zero, there would be no flow through the tunnels (except for a very small flow given by temperature and density differences, if such differences occur).

Thus, based on the sensitivity analysis regarding corresponding values of excess heads and tunnel-flow, as simulated by the numerical models; we estimate that the uncertainty in the actual value of the excess head produces an uncertainty in the predicted tunnel-flow, which at time equal to 2000 AD is approximately equal to plus/minus 30 percent of the flow predicted. The effects of this uncertainty decreases with time, and at time equal to 4000 AD it is insignificant.

8.4 Calculated recharge in regional model

8.4.1 General

The recharge to the model – the actual recharge, is calculated by the model as a part of its solution of the flow field, based on the potential recharge, the topography and the position of the groundwater surface (see Section 7.4.1). These properties will vary with time and place. When discussing the recharge we will use the following terms:

- *Potential recharge.* It is approximately equal to the difference between the precipitation and the actual evapotranspiration (this difference is also called the *run-off*). The potential recharge is the largest amount of groundwater that can infiltrate in the model, if the local hydrogeological conditions are favourable. It represents the climate and the vegetation. For the simulations presented in this study we have set this value as time-independent. Hence, as regards the potential recharge, we have assumed that the climate will not change during the studied time period.
- *Recharge* (*Actual recharge*). It is the amount of water that infiltrates in the model. This value will vary with time and place. Below we will discuss an average (of the actual recharge) considering the whole of the model. Below the sea, the recharge due to precipitation is zero.

8.4.2 Results

A likely recharge to a crystalline rock mass in Scandinavia is a few percent of the precipitation. For example, Ahokas and Herva (1993) have estimated that about 1-2 percent of the precipitation infiltrates into the bedrock at the Olkiluoto investigation area in Finland; this area is fairly similar to the SFR area. Hence, it is likely that the recharge at the SFR area should be within a range from a few millimetres per year up to about 20 mm/year. As the shoreline retreats in the model, the average actual recharge calculated by the model increases and reaches finally a steady value. The final values of calculated average recharge varies between 4 and 14 mm/year. For all cases studied the results are given in Table 8.1, below.

Table 8.1 The actual recharge as calculated by the regional model.

The case studied	Potential recharge (mm/year)	Actual recharge At 2000 AD (mm/year)	Actual recharge Final value. (mm/year)
Case 1	5	1	4.4
Case 2	250	2	3.9
Case 3	250	6	14.4
Case 4	250	2	4.3

8.5 Agreement between local and regional models, considering average flow

8.5.1 Introduction

The domain represented by the local model is in a simplified way also represented at the centre of the regional model. Hence, both models predict the flow through the local domain. By comparing the flow predicted by the regional and local models we will get information of the correspondence between the two models. Below we will present such a comparison. The comparison is based on results from both the local and the regional models.

8.5.2 Numerical accuracy

The models are based on iterative numerical methods. The local model is solved under steady state condition, but with time-dependent boundary conditions (see Sec.2.7). The divergence in the mass balance (the error) demonstrates the numerical accuracy of the solution. For the local models, the divergences in the global mass balances were less than 0.05 percent. This is a small divergence, which indicates good global solutions and acceptable mass balances for the tunnel system.

8.5.3 Differences between the models

The models will not predict exactly the same flow, as the models are different, but they should predict about the same flow when estimating the average flow that passes through the local domain. If the average flow, predicted by the local and the regional model for the same case are very different (several hundreds of percent), the boundary conditions provided by the regional model for the local models are not the correct ones. The following will cause differences in predicted flow.

- The regional model is a fully time-dependent model, the local models are not.
- The surface topography is not the same. In the local model the surface is defined in more detail.
- The cell sizes are different, the smaller cells in the local model will cause a more detailed model with more heterogeneous properties, compared to the regional model; but the average properties are approximately the same.
- The co-ordinate axis of the meshes of the local and the regional model are not exactly pointing in the same direction (there is a difference of 18degrees). Hence, it is not possible to compare exactly the same domain in both models.

Due to these differences, and especially due to the different cell sizes, we will compare the flow through the local domain between the elevations –450 masl and –50 masl.

8.5.4 Concept of total flow and time dependency

Below we will compare the total flow (dimension: Length^3 / time) that passes through the local domain. The total flow is calculated based on a mass balance taken over the

envelope of the three dimensional body representing the local domain, which is the same thing as a calculation of all flow into and out of the studied body.

The regional model is fully time-dependent, hence, the inflow and the outflow are not equal, unless a steady-state-like situation is reached. The local model is solved under steady state conditions; hence the inflow and the outflow are equal (except for a small error which is a part of the numerical method, see Sec.8.5.2).

For the local model we will present values representing the flow through a local domain for the different times studied, because the local model is solved under steady state conditions the inflow and the outflow are the same. . For the regional model, a time-dependent change in head is caused by the shore level displacement, or as it is represented in the model, by the lowering of the sea water level. The retreat of the shoreline will cause drainage of the rock mass, as the sea water level will be lowered. It follows that for a limited volume of rock mass, such as the studied local domain, the outflow of water will be larger than the inflow, until a steady state situation is reached. A steady state situation is reached at about 5000 AD. For the regional model and for the same domain as in the local model, we will present an average value as regards the transient inflow and outflow of groundwater. For both models results will be presented for a studied time period from 2000 AD and until 8000 AD.

8.5.5 Results of comparisons

Case 1. This Case represents a regional rock mass with conductivity equal to 6.5×10^{-8} m/s and with an actual recharge of approximately 4.4 mm/year (at steady state). The heterogeneity of the rock mass is not represented in the regional model, except for the very large fracture zones, which are defined separately. The flow through the local domain in the regional model is larger than the flow through the local model. The flow of the local model is approximately half of the flow of the regional model; however, after 5000 AD, the difference between the flow predicted by the local and the regional models will be smaller.

Case 2. This Case represents a regional rock mass with conductivity equal to 1.5×10^{-8} m/s and with an actual recharge of approximately 3.9 mm/year (at steady state). The heterogeneity of the rock mass is not represented in the regional model, except for the very large fracture zones, which are defined separately. The flow through the local domain in the regional model is less than the flow through the local model. The largest difference occur at time equal to 3000 AD, at this moment the flow of the local model is approximately 15 percent larger than the flow of the regional model. As the studied course continuous the difference becomes small and at steady-state-like conditions, after year 5000 AD, the flow of the local model is approximately 5 percent larger than the flow of the regional model.

Case 3. This Case represents a regional rock mass with conductivity equal to 6.5×10^{-8} m/s and with an actual recharge of approximately 14.4 mm/year (at steady state). The heterogeneity of the rock mass is represented in the regional model by use of the stochastic continuum method and the very large fracture zones are defined separately. The flow through the local domain in the regional model is larger than the flow through the local model. The flow of the local model is approximately half of the

flow of the regional model. The difference is the same at steady-state-like conditions (after year 5000 AD).

Case 4. This Case represents a regional rock mass with conductivity equal to 1.5×10^{-8} m/s and with an actual recharge of approximately 4.3 mm/year (at steady state). The heterogeneity of the rock mass is represented in the regional model by use of the stochastic continuum method and the very large fracture zones are defined separately. The flow through the local domain in the regional model and the flow through the local model are very close. The largest difference occur at time equal to 2000 AD, at this moment the flow of the local model is approximately 15 percent larger than the flow of the regional model, at 3000 AD the difference is 10 percent. As the studied course continuous the difference becomes small and at steady-state-like conditions, after year 5000 AD, the flow of the local model is approximately 2 percent larger than the flow of the regional model, hence at steady-state-like conditions the difference is negligible. The comparison is given in Figure 8.1, below.

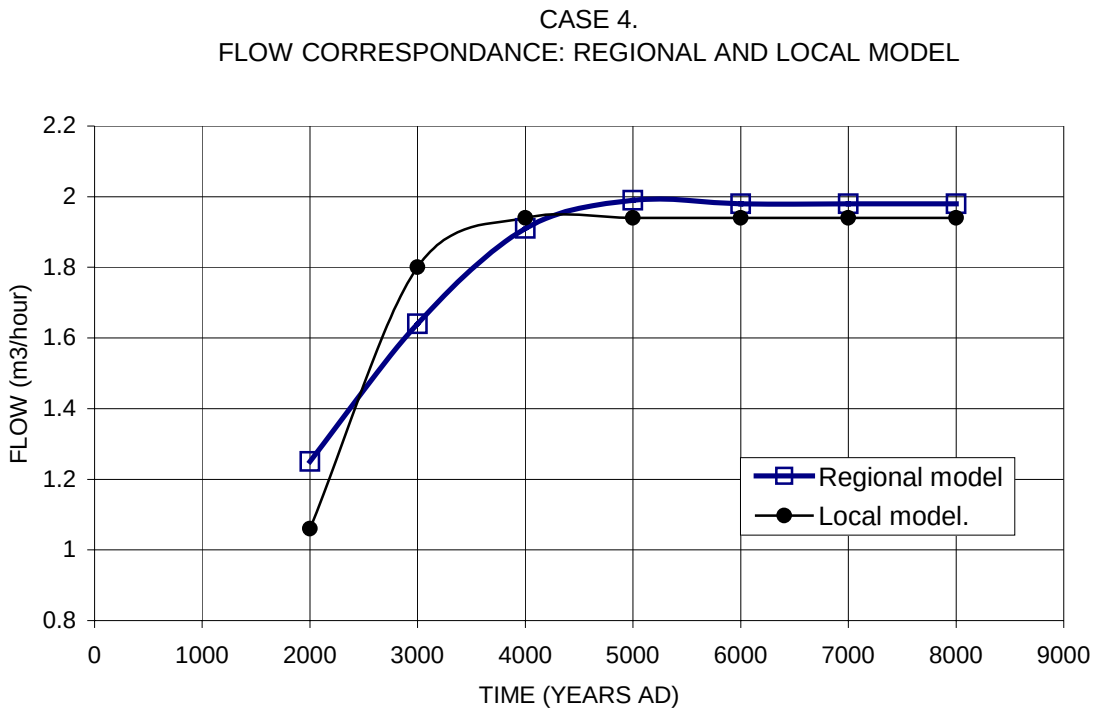

Figure 8.1 *Case 4. Flow correspondence between regional and local model. The figure gives the total flow through a part of the local domain, as it is defined in both models.*

The studied domain is between elevations –450 masl and –50 masl. The flow of the regional model is an average value as regards the transient inflow and outflow of groundwater. Case 4: Regional model: Stochastic continuum, Effective cond.=1.5E-8 m/s, Recharge final=4.3 mm/year.

8.5.6 Agreement between models considering average flow -conclusions

The best match between the flows of the regional and local models is for Case 4, for which the match is very good. However, the local and the regional models are different (as discussed above) and due to these differences we should not completely disregard the other cases. A very good match, as the one for Case 4, might partly be caused by differences between the models that equals out, when comparing the total flow. Another case could actually also be a good representation of the system studied, even if the match is not as good as the one for Case 4.

The good match between regional and local flow in Cases 2 and 4 is probably a result of the method that we used for these two cases, when estimating the effective conductivity of the regional model. The regional model was assigned an effective conductivity that is equal to the equivalent conductivity of the whole of the local model, as regards flow in the direction dominating after approximately 5000 AD. This is also discussed in Sections 7.6 and 7.7. This method will produce a good match considering the correspondence of flow between local and regional models at the boundary of the local model. However, from a conceptual point of view it is not necessarily the best method when deriving the general properties of the regional model. Because by use of this method we presume that the effective conductivity of the regional model is the same as the equivalent conductivity of the local model (the equivalent conductivity at the scale of the local model, for a given flow direction and at a given time). But, the actual properties of the regional domain vary, and the assumption that the general properties of the regional model are well represented by the properties of one local domain is not well founded. Nevertheless, it is a good assumption as regards the properties at the border between the local and the regional model and that is the reason why we will have the good match in regional and local flow in Cases 2 and 4.

Based on the comparisons we conclude: The regional model and the local model seem to be very much in agreement, considering Cases 2 and 4. For Cases 1 and 3 the local model predicts approximately half of the flow in the regional model; this can also be regarded as an acceptable agreement, considering the uncertainties involved in the comparisons of the two different models.

8.6 Comparison between the different cases of the regional model

8.6.1 Introduction

The different cases are defined by different properties in the regional model, the local model is the same for all different cases. The cases are presented in Section 7.7; a summary is given in Table 7.1 and a short summary in Table 8.2 below:

Table 8.2 The different cases as defined in the regional model.

Regional model	Heterogeneity in flow medium	Effective Conductivity.	Potential Recharge	Final actual Recahrge
Case 1	Uniform+Fzones.	6.5E-8 m/s	5 mm/year	4.4 mm/year
Case 2	Uniform+Fzones	1.5E-8 m/s	250 mm/year	3.9 mm/year
Case 3	Stochast+Fzones	6.5E-8 m/s	250 mm/year	14.4 mm/year
Case 4	Stochast+Fzones	1.5E-8 m/s	250 mm/year	4.3 mm/year

Below we will discuss head and flow for the deposition tunnels and for an inner domain. The deposition tunnels include the following tunnels: BMA, BLA, BTF1, BTF2 and the SILO. The inner domain is defined as the volume of rock mass and fracture zones that are in the close surroundings of the deposition tunnels (the tunnels are not included in the rock mass and fracture zones of the inner domain). The average hydraulic head is calculated as a volumetric average considering the size of the different cells in the mesh.

8.6.2 General evolution of the groundwater system

8.6.2.1 A qualitative assessment

A qualitative assessment of the development of the groundwater system is given in Section 2.6. In a generalised way, the models will reproduce this development. Below we will give a short summary.

At present, below the sea and at a moderate depth in the rock mass, the groundwater flow is limited and mainly vertical towards the seabed. The shore level displacement will continue and as a consequence the seawater will be lowered with time. The groundwater heads will change and an increased groundwater flow will take place. Because of the land uplift and the moving shoreline, the groundwater flow will be increased close to the shoreline. Initially, below areas no longer covered by the sea, the main flow direction of the groundwater will be towards the ground surface and towards the retreating shoreline. With time, as the shoreline moves further away, the groundwater flow will develop into a steady-state-like situation, with recharge and discharge areas controlled by the topography. The shoreline will be above the deposition tunnels at about 2800 AD. At about 4800 AD it is likely that lakes and mires will be established about 1 km North and Northeast of the SFR, with water levels close to -15 masl. These lakes will stabilise the local groundwater flow system, as the shoreline continues to retreat further away.

8.6.2.2 Average development at SFR as predicted by models

On the average, the flow pattern is very much the same for all cases studied. It follows the qualitative assessment as outlined above. For the period when SFR is below the sea, the flow will be nearly vertical upward to the seabed. When the shoreline has passed above the SFR, the flow will mainly be directed towards the shoreline; hence, the flow will turn towards a more horizontal flow. When the shoreline has moved far away, the system will develop into a steady-state-like situation (except for Case 1), with the flow directed towards local discharge areas, which means a horizontal flow on the average in

the close surroundings of the deposition tunnels (the inner domain). The flow pattern and the flow paths from the SFR will be discussed in more detail in the next section. The average direction of flow through the rock mass and the fracture zones of the inner domain are presented in Figure 8.2. Locally the flow diverges from these angles; the figure will only give an estimate of the average directions.

8.6.3 Average head in inner domain

Case 1. The average head in the inner domain decreases during the period 2000 AD and until 4000 AD, a decrease of approximately 7 m. From approximately 4000 AD the head continues to decrease, but with a lower rate. For Case 1, the flow system will not reach a steady state situation, after the shoreline has moved away from the SFR, at least not during the studied period. Instead the average hydraulic head will continue to drop in the inner domain and the hydraulic gradient will decrease as well. The head values in the zones are smaller than the head values in the surrounding rock mass, this illustrates that the flow, on the average, is directed from the rock mass towards the fracture zones.

Case 2, Case 3 and Case 4. For all cases, except Case 1, we will have the following development: The average head in the inner domain decreases during the period 2000 AD and until 4000 AD. A decrease of approximately 4 m for the rock mass and approximately 6 m for the fracture zones. From approximately 4000 AD and until 5000 AD the head continues to decrease somewhat in the rock mass, but for the fracture zones the head will not change after approximately 4000 AD. The flow system will reach a steady state situation after approximately 5000 AD. For this situation, the shoreline has moved far away from the SFR and the head values are mainly controlled by the local topography. As the average hydraulic head will not change after approximately 5000 AD we will have a constant hydraulic gradient after 5000 AD. The head values in the zones are smaller than the head values in the surrounding rock mass, this illustrates that the flow, on the average, is directed from the rock mass towards the fracture zones.

8.6.4 Total flow through all deposition tunnels

Representation of the deposition tunnels. Consider the four horizontal deposition tunnels, BMA BLA, BTF1 and BTF2, the predicted total flow that we will discuss below is the flow through highly permeable parts of these tunnels, e.g. the flow through a highly permeable backfill e.g. surrounding a concrete construction (encapsulation). It is not the flow through an encapsulation installed in the middle of a tunnel. The details of the flow inside the tunnels will be studied by use of the detailed model. Consider the SILO, the predicted total flow that we will discuss below is the flow through the encapsulation, protected on all sides by low permeable bentonite barriers. Flow barriers (plugs) are defined at both ends of each horizontal deposition tunnel as well as where access tunnels connects to the SILO.

Case 1. The total flow through the tunnels increases during the period from 2000 AD and until 4000 AD; the flow increases from 50 m^3/year up to 188 m^3/year. Maximum flow occur at about 4000 AD, from this moment the flow starts to decrease. For Case 1, the flow system will not reach a steady-state-like situation, after the shoreline has

moved away from the SFR. Instead the average hydraulic head will continue to drop in the inner domain and the hydraulic gradient will be reduced. As a consequence the flow will continue to decrease during the studied course, from 4000 AD until 8000 AD. See Figure 8.3.

Case 2. The total flow through the tunnels increases during the period from 2000 AD and until 5000 AD. The flow increases from 50 m^3/year up to 193 m^3/year. The flow system will reach a steady-state-like situation after approximately 5000 AD. For this situation, the shoreline has moved far away from the SFR and the head values are mainly controlled by the local topography. See Figure 8.3.

Case 3. The total flow through the tunnels increases during the period from 2000 AD and until ca. 5000 AD. The flow increases from 50 m^3/year up to a maximum of ca. 256 m^3/year. The flow system will reach a steady-state-like situation after approximately 5000 AD. For this situation, the shoreline has moved far away from the SFR and the head values are mainly controlled by the local topography. See Figure 8.3.

Case 4. The total flow through the tunnels increases during the period from 2000 AD and until 5000 AD. The flow increases from 50 m^3/year up to a maximum of 215 m^3/year. The flow system will reach a steady-state-like situation after approximately 5000 AD. For this situation, the shoreline has moved far away from the SFR and the head values are mainly controlled by the local topography. See Figure 8.3.

8.6.5 Conclusions

The behaviour of the flow system depends on the hydraulic properties of the different cases, but mainly on the overall development caused by the shore level displacement.

Case 1 is the only case that significantly differs from the others, considering the behaviour of the flow system after 5000 AD, as no steady-state-like situation will develop. This follows from the small potential recharge and the large conductivity of the regional model. The potential recharge is set to 5 mm/year, which in combination with the large conductivity is too small a value to represent the present climate. We can look upon Case 1 as a representation of a situation in which the climate has changed, in a way that the recharge is very much reduced.

Case 2 represents a likely course. The potential recharge represents the present climate and the calculated actual recharge is likely, the final value is 3.9 mm/year. However, the regional model does not include heterogeneous properties, except for the very large fracture zones, which are defined separately.

Case 3 represents a course in which the conductivity of the regional model is large and the potential recharge represents the present climate. The rock mass in the regional model is defined with heterogeneous properties, as the rock mass between the large fracture zones is represented by use of the stochastic continuum method. The large conductivity of the regional model will give rise to the largest value of actual recharge of the cases studied, the final value is 14 mm/year.

Case 4 is similar to Case 2 except that the regional model is defined with heterogeneous properties, as the rock mass between the large fracture zones is represented by use of the stochastic continuum method. Case 4 represents a likely course. The potential recharge represents the present climate and the calculated actual recharge is likely, the final value is 4.3 mm/year.

For Cases 2 and 4, the effective conductivity of the regional rock mass and the potential recharge is the same, but Case 4 is defined with a heterogeneous rock mass and in Case 2 the rock mass is homogeneous (between the fracture zones). An interesting effect, revealed when comparing Cases 2 and 4, is that case 4 (heterogeneous rock mass in the regional model) produces a somewhat larger flow through the deposition tunnels of the local model, compared to that of Case 2 (homogeneous rock mass in the regional model). The larger flow is a result of larger gradients in the regional model. The larger gradients in Case 4 can have several different explanations. The most obvious is that the larger gradients are caused by a larger actual recharge. In Case 4, the final actual recharge is 4.3 mm/year and in Case 2 the final actual recharge is 3.9 mm/year. The larger recharge can probably be explained by a hydraulic interaction between: (i) the potential recharge, (ii) the large fracture zones and (iii) highly permeable parts of the heterogeneous rock mass. The explanation above can also be stated in the following way: the change in head, which takes place as the shoreline retreats, goes slower in Case 4 than in Case 2, due to the heterogeneity of the rock mass in Case 4 and the larger recharge of Case 4.

For Case 4 we have investigated the effect of a different realisation of the heterogeneity of the conductivity of the rock mass in the regional model. We have performed the complete chain of calculations for an alternative realisation of the conductivity field. Compared to the results of Case 4, no significant change was revealed, that is for the predicted head in the inner domain and for the total flow through the deposition tunnels. No change was revealed, because the local model, which is the same for both realisations, is large enough to cover the effects of small local changes in head along the boundary caused by the different realisations of the regional conductivity field.

The differences between the flow of Case 4 and the flow of the other cases are approximately plus/minus 25 percent. This is a small difference and it reflects uncertainties in the properties of the regional model. The differences are small because the properties of the local model, which are the same for all cases (and better known due to the calibration procedure etc), will tend to even out the changes in flow conditions caused by different properties of the regional model. Thus, considering the objectives of this study, the heterogeneity of the rock mass of the regional domain is not very important.

We have selected Case 4 as the case that we will present in detail. This will also be the case that we will use for more extended investigations.

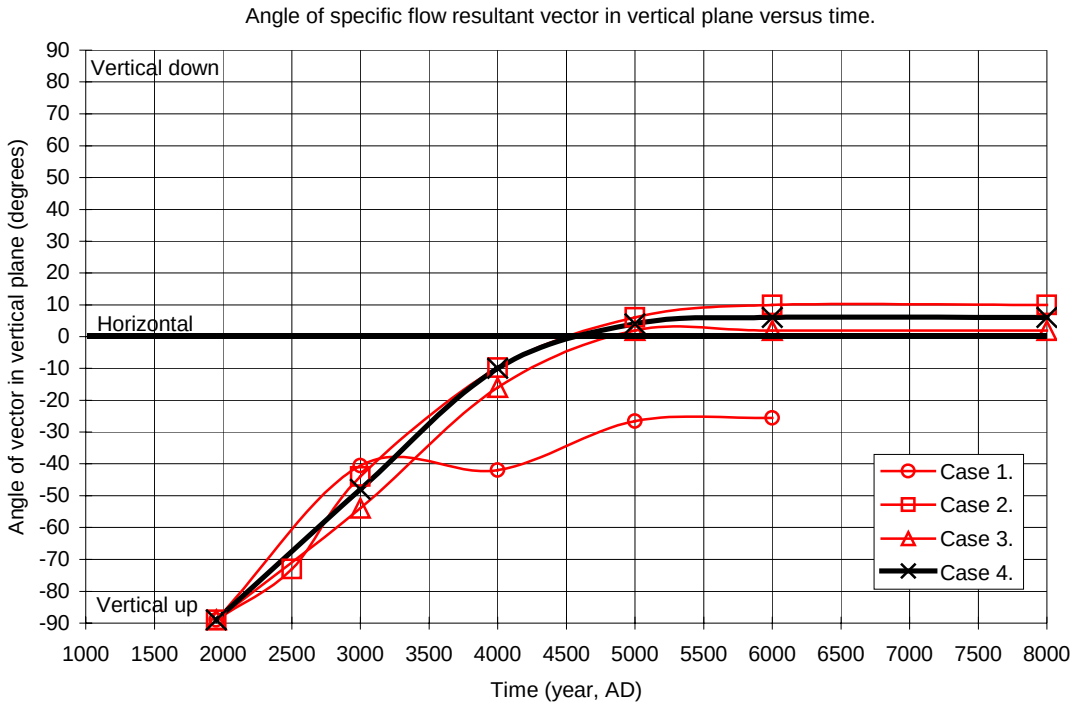

Figure (i) *The vertical component of the specific flow vector.*

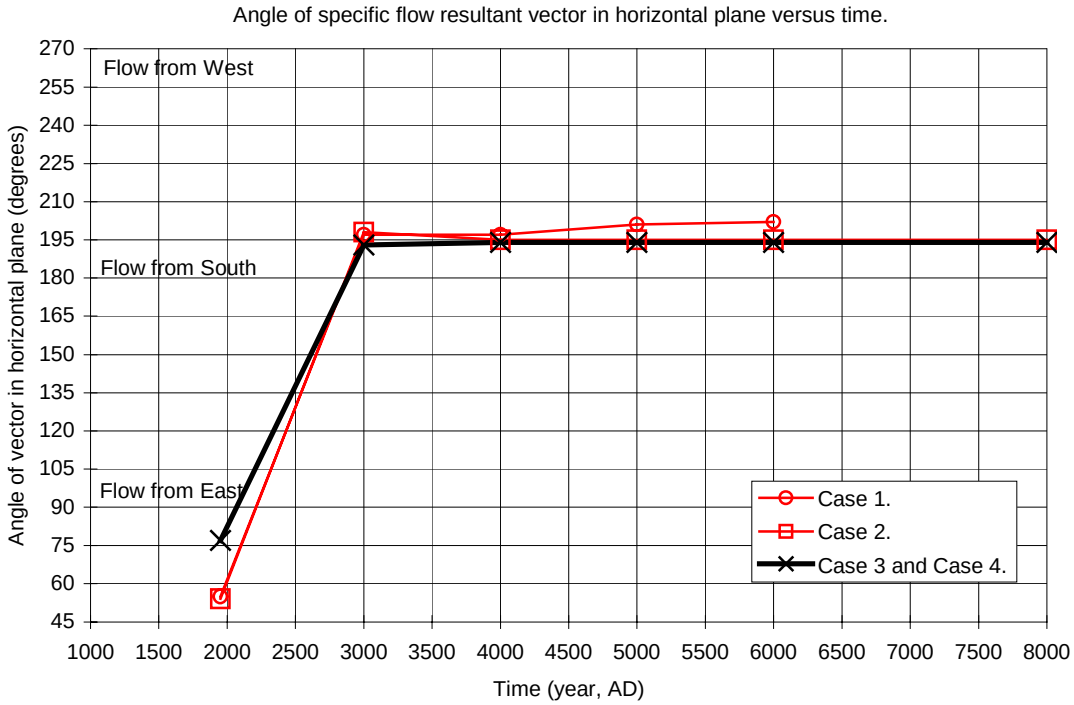

Figure (ii) *The horizontal component of the specific flow vector.*

Figure 8.2 *Average angle of flow through inner domain.*

The figure presents the (i) vertical and (ii) horizontal components of the specific flow vector. The specific flow vector is calculated for the inner domain of the local model without including the flow of the tunnels, the vector is based on the specific flow components at the cells of the mesh and the flow components are weighted based on cell volume.

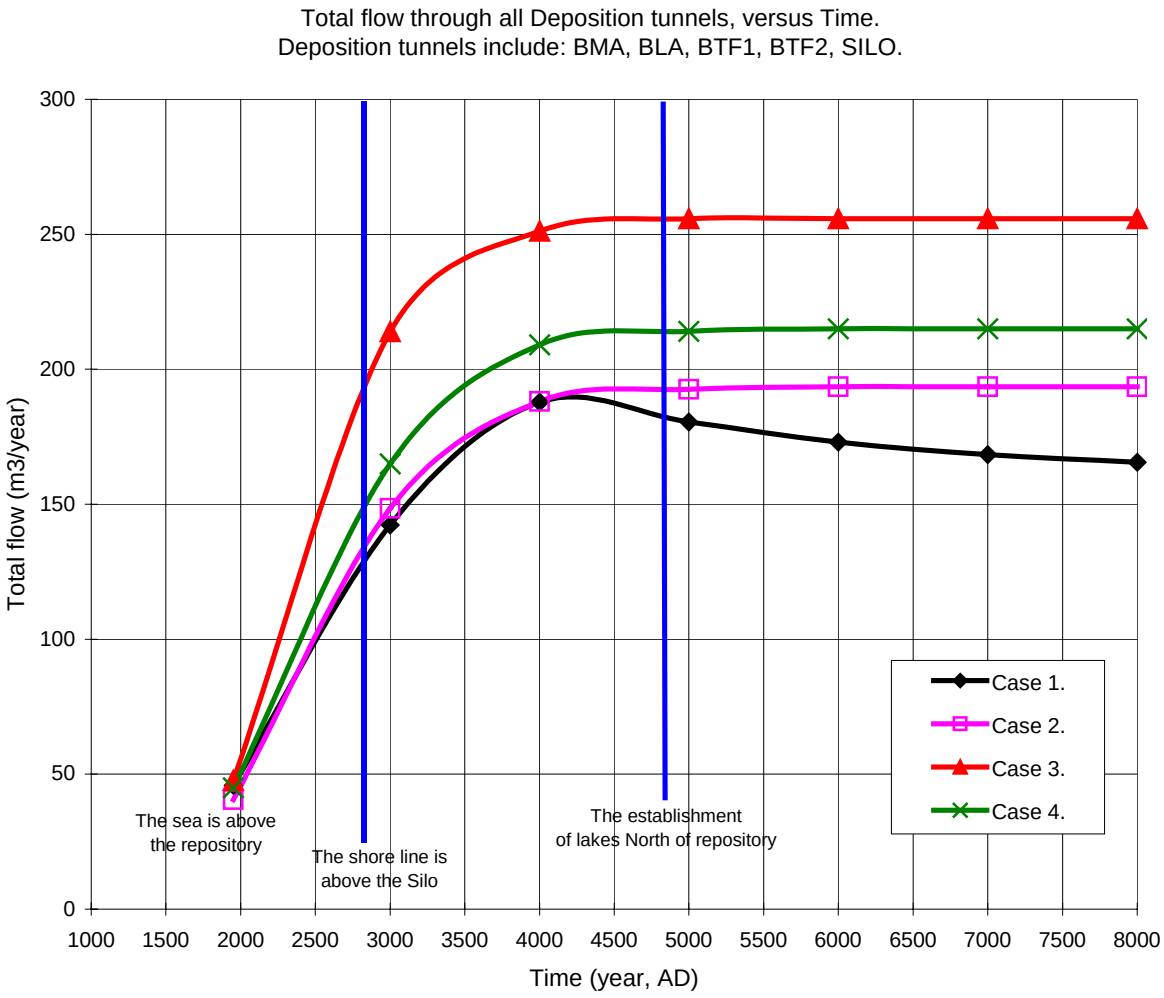

Figure 8.3 *Local model. Total flow through all deposition tunnels for the different cases studied.*

The different cases as defined in the regional model.

Regional model	Heterogeneity in flow medium	Effective Conductivity.	Potential Recharge	Final actual Recahrge
Case 1	Uniform+Fzones	6.5E-8 m/s	5 mm/year	4.4 mm/year
Case 2	Uniform+Fzones	1.5E-8 m/s	250 mm/year	3.9 mm/year
Case 3	Stochast+Fzones	6.5E-8 m/s	250 mm/year	14.4 mm/year
Case 4	Stochast+Fzones	1.5E-8 m/s	250 mm/year	4.3 mm/year

9. Description of detailed model

9.1 Introduction

The purpose of the detailed model is to predict the flow through the deposition tunnels in detail, considering the internal structures of the tunnels, such as flow barriers and encapsulations. The following chapter will not be a repetition of the general presentation of the flow system and the models as given in previous chapters. Below we will only present the detailed model and when necessary compare it to the local model.

9.2 General differences compared to the local model

In the local model all tunnels except the SILO is defined as being homogeneous, hence a tunnel is represented by one value of conductivity only; the SILO is defined with the inclusion of a bentonite barrier surrounding an homogeneous encapsulation. In the local model, the horizontal deposition tunnels (BTF, BLA and BMA) are characterised by their most permeable part, which is the sand volumes that occurs as a backfill e.g. as top filling. Hence, in the local model these tunnels are homogeneous and very permeable

In the detailed model, the different structures that occur inside the deposition tunnels are defined in detail. Both the volumes that occur as backfill at the top of the tunnels and possibly at the sides and base of the tunnels, also the concrete encapsulations are defined in details. The sand backfill of the detailed model is as permeable as that of the local model, but as the detailed model also includes concrete encapsulations etc, and these are much less permeable than the sand, the total resistance to flow inside the tunnels is larger in the detailed model than in the local model. Additionally, in the detailed model, the BTF and the BLA tunnels are defined as having a floor made of low permeable concrete; this floor is not included in the local model, and it will reduce the inflow to these tunnels in the detailed model.

9.3 Size of detailed model and mesh of detailed model

The detailed model is much smaller than the local model, but it is still large enough to include all the deposition tunnels and all access tunnels except the tunnels of the access ramp. Hence, the boundaries of the detailed model are in the rock mass outside of the tunnels. The layout of the tunnel system and the boundaries of the local and detailed models are given in Figure 9.1 and Figure 9.2 .The X and Y axis of the mesh of the detailed model are parallel to the X and Y axis of the local model, and the rows and the columns of the outer boundaries of the detailed model coincide with the position of certain rows and columns in the local model. The detailed model covers an area of 0.21 km^2 and has a vertical extension of 108 m. The mesh contains 73920 cells, it is given in Appendix A.

Figure 9.1 *The horizontal extension of the local model, its topography and the tunnel system of the local model, as well as the outer horizontal boundaries of the detailed model.*

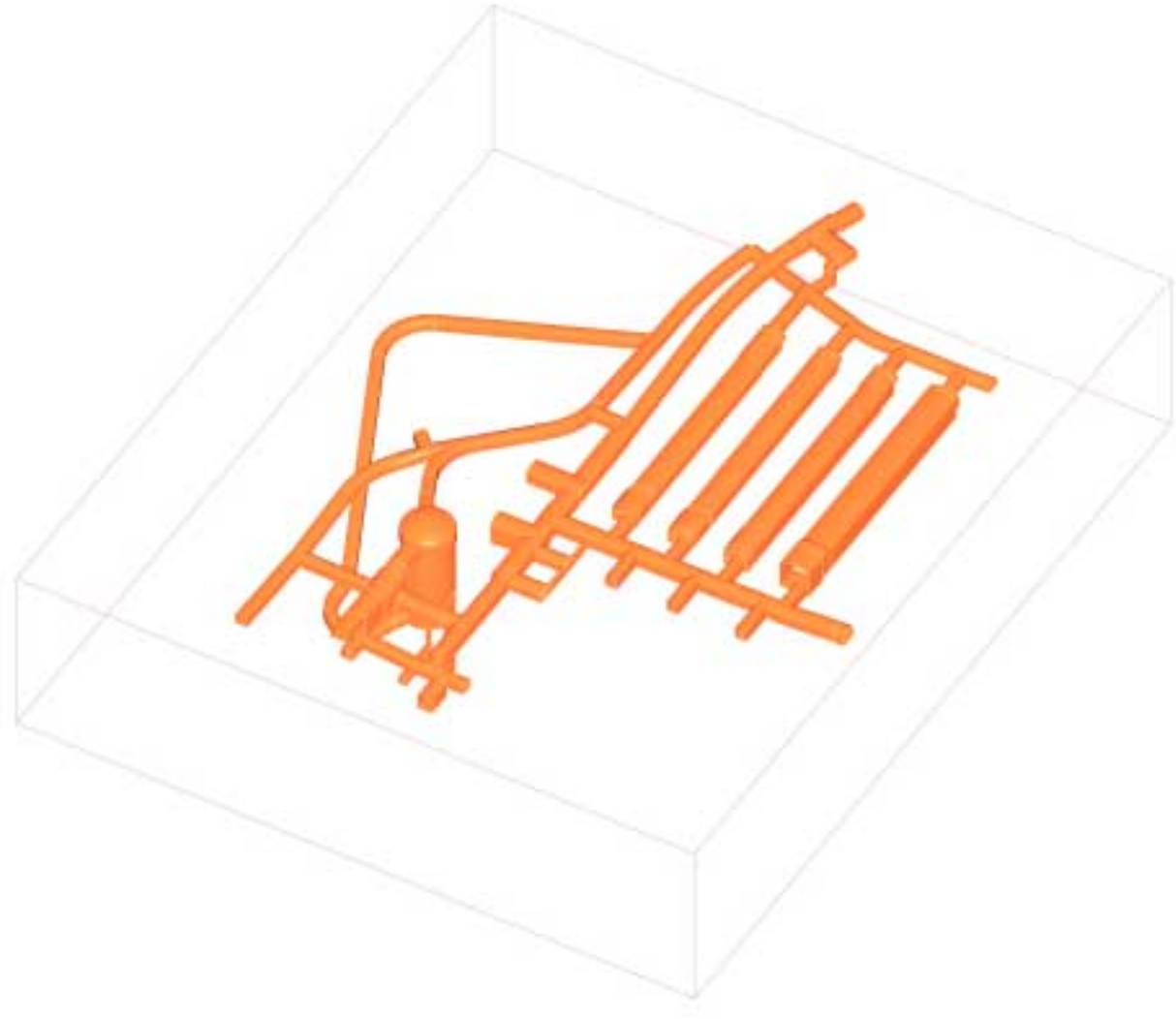

Figure 9.2 *Three dimensional view of the tunnel system at SFR and the outer boundaries of the detailed model.*

9.4 Rock mass, fracture zones and size of tunnels

The rock mass of the detailed model has the same conductivity as in the local model, and the fracture zones of the detailed model have the same transport capacities as well as dips and strikes as in the local model. But, as the detailed model is smaller, it will not include the whole extension of the fracture zones. The tunnels are defined explicitly in the mesh. Hence, a cell that represents a part of a tunnel represents the tunnel only and no parts of the surrounding rock mass. The mesh is primarily optimised to match the layout of the deposition tunnels. It is impossible to reach a perfect match between the actual size and layout of the tunnels and that of the model, due to practical restrictions in the number of cells that can be used in the model, but also due to the shape of the cells. The actual tunnels have an arch shaped roof, but the cells in the model have a rectangular shape. If we compare the actual volumes of the deposition tunnels with the volumes as defined in the local and detailed model, we get the volumes given in

Table 9.1. Due to the different discretizations of the flow domain in the local and detailed models, the tunnels are not of the same sizes in the local and detailed models.

Table 9.1 Volumes of deposition tunnels – actual volumes and volumes in the local and detailed models.

Deposition tunnel	Actual volumes (m3)	Local model. Volumes (m3)	Detailed model. Volumes (m3)
SILO	47 500	47 400	51 456
BMA	47 600	64 600	52 842
BLA	27 600	42 800	29 354
BTF1	19 700	26 000	16 542
BTF2	19 700	26 000	16 542

9.5 Internal layout and conductivity of deposition tunnels

9.5.1 Introduction

Based on the future tunnel layout of a closed repository, and based on the conductivity of the materials that will be inside the tunnels, and also with respect to the layout of the model mesh; values of conductivity have been calculated and these values have been assigned to the model. The results of those calculations are presented in the following sections; the details of the calculations are presented in Appendix B.

9.5.2 Conductivity of tunnel materials

The different materials that will be inside the deposition tunnels have been assigned the following values of hydraulic conductivity.

Table 9.2 Assumed hydraulic conductivity of the different materials inside the tunnels.

MATERIAL		**HYDRAULIC CONDUCTIVITY**		**COMMENTS**
Construction concrete. E.g., walls of encapsulations, concrete moulds, concrete tank walls, etc		8.3E-10 m/s		Non-fractured = 1E-11m/s One penetrating fracture per meter of aperture, 1E-5 m
Concrete backfill		8.3E-9 m/s		In BTF tunnels, in SILO and in BMA alternative layout.
Sand backfill		1E-5 m/s		In all tunnels
Plugs		5E-10 m/s , of length 1 m.		Resistance = 5E10 s
SILO	Sand/Bentonite mix at top of SILO	1E-9 m/s		Only in SILO
	Sand/Bentonite mix at SILO-base	1E-9 m/s		
	Bentonite at SILO-sides, upper part	2E-11 m/s	Average 6E-12 m/s	
	Bentonite at SILO-sides, lower part	2E-12 m/s		
	Concrete lid in SILO	Not considered		Flow channels through lid
Floor:	Concrete layer Sand layer (sand patches)	8.3E-10 m/s (0.2 m) 1.0E-7 m/s (0.2 m)		In BTF and BLA tunnels

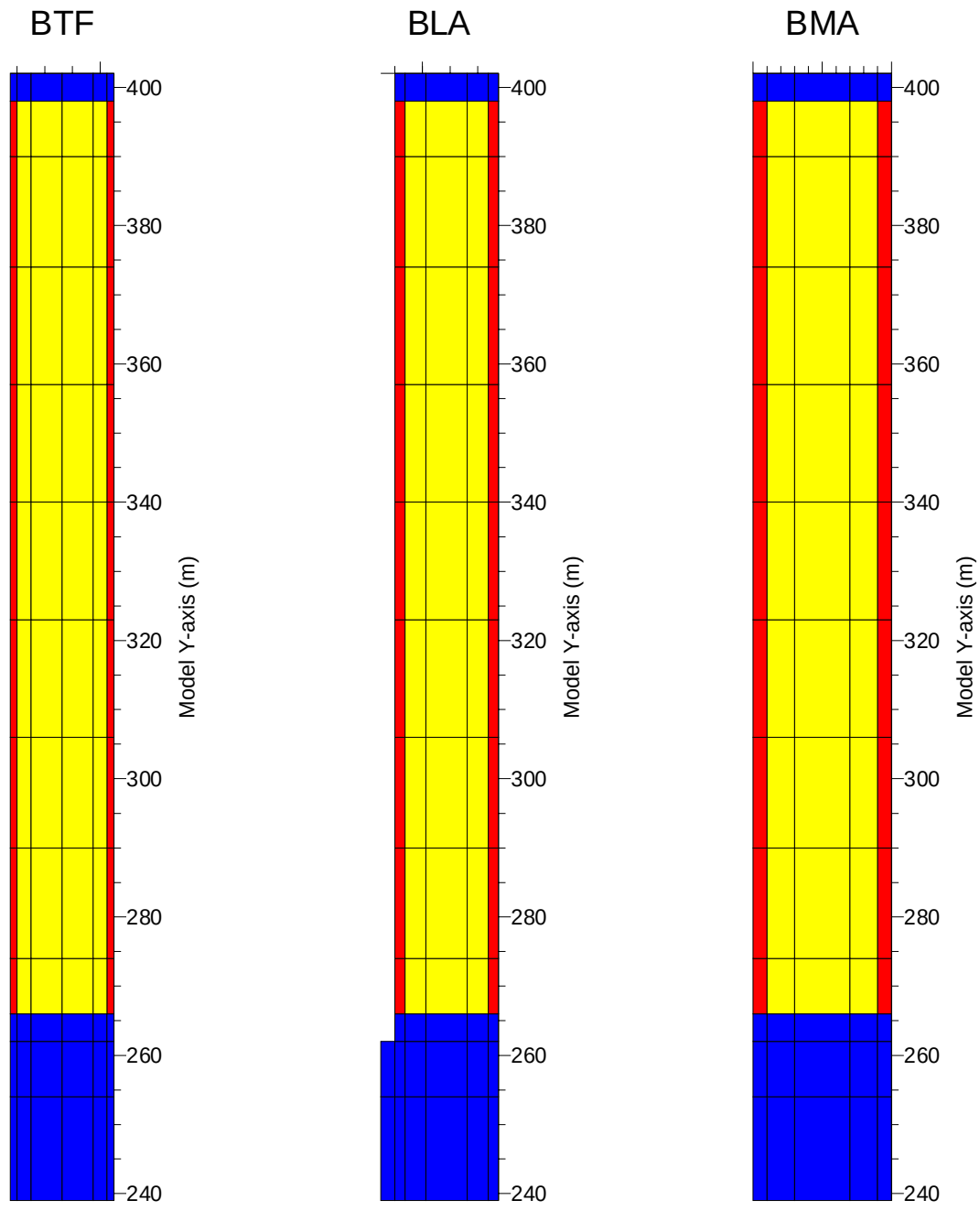

BLUE COLOUR: Denotes loading areas.

RED COLOUR: Denotes barriers (side fill) at sides of waste/encapsulation.

YELLOW COLOUR: Denotes the waste/encapsulation domain.

Figure 9.3 *Three horizontal cross-sections through the horizontal deposition tunnels of the detailed model (BTF, BLA, BMA). The cross-section is taken at an elevation of –82 masl.*

9.5.3 Different structures studied

In the detailed modelling the following structures will be studied separately: (i) the waste/encapsulation, (ii) the top filling, (iii) the filling at sides, (iv) the tunnel floor, (v) the loading and access areas. The "loading areas" are the volumes at both ends of the horizontal deposition tunnels(see Figure 9.3), used for handling of the waste packages. When the sand/gravel backfill is placed in the tunnels it is possible that at the top of the tunnels there will be volumes left, which are not completely filled due to practical difficulties when the filling is placed in the tunnels. Such open volumes are not important for the size of the groundwater flow in the tunnels, as the size of the flow in a highly permeable backfill is determined by the permeability of the surrounding rock mass and not by the permeability of the backfill, it will however influence the distribution of the flow in the backfill.

9.5.4 The BTF deposition tunnels

The waste placed in the BTF is de-watered low-level ion exchange resin in concrete tanks, as well as some drums with ashes (in BTF1). The concrete tanks are placed in two levels, a concrete radiation protection lid is placed on top of the pile. The space between the different tanks is refilled with concrete backfill and the space between the tanks and the rock wall will be filled with concrete backfill. Hence, the waste will be placed in a concrete encapsulation. The space above the radiation protection lid will be filled with sand. The figure and the table below present the layout and the conductivity of the BTF tunnels, as defined in the detailed model (the base case).

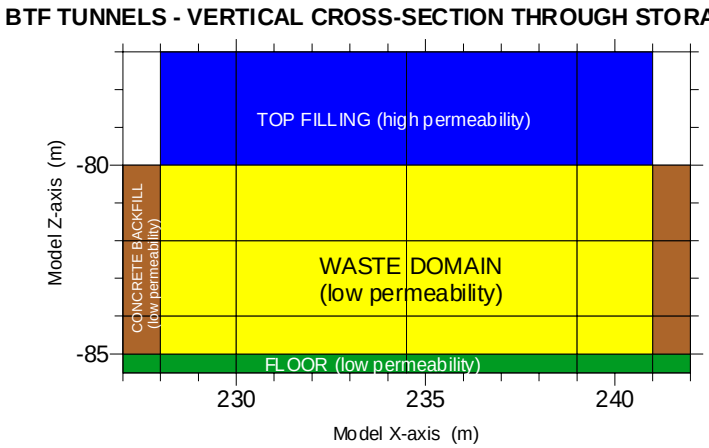

Figure 9.4 *A vertical cross-section through a BTF tunnel, as defined in the detailed model.*

Table 9.3 The conductivity and the volumes of the BTF tunnels, as defined in the base case of the detailed model.

BTF	HYDRAULIC CONDUCTIVITY (m/s) IN FLOW DIRECTIONS			VOLUME (m3)
	X-DIR.	Y-DIR.	Z-DIR.	
Top filling	1E-5	1E-5	1E-5	1 148
Waste domain. Encapsulation.	6.7E-9	3.8E-9	5.3E-9	8 580
Concrete backfill at sides	8.3E-9	8.3E-9	8.3E-9	1 320
Concrete floor with sand patches	4.2E-8	4.2E-8	1.3E-9	990
Loading areas	1E-5	1E-5	1E-5	4 504

9.5.5 The BLA deposition tunnel

The waste deposited in BLA is mainly low level waste placed in standard steel containers. In the BLA, the waste containers will not be encapsulated in concrete. As the tunnels will be refilled with sand, the containers will be surrounded by sand.

The figure and the table below present the layout and the conductivity of the BLA tunnel, as defined in the detailed model (the base case). Note that for the BLA tunnel, the conductivity and the porosity is the same everywhere, except for the tunnel floor. The waste packages will be placed in the storage area and the whole of the tunnel will be refilled with sand. The model will predict the flow through the storage area (storage domain), and not the flow through the waste packages.

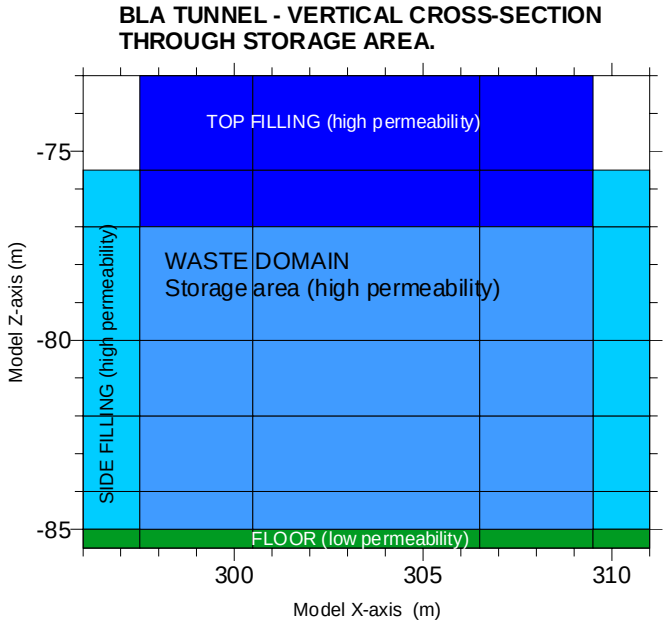

Figure 9.5 *A vertical cross-section through the BLA tunnel, as defined in the detailed model.*

Table 9.4 The conductivity and the volumes of the BLA tunnel, as defined in the base case of the detailed model

BLA	HYDRAULIC CONDUCTIVITY (m/s)			VOLUME (m3)
	IN FLOW DIRECTIONS			
	X-DIR.	Y-DIR.	Z-DIR.	
Top filling.	1E-5	1E-5	1E-5	6 336
Waste domain. Storage area with waste packages.	1E-5	1E-5	1E-5	12 672
Filling at sides.	1E-5	1E-5	1E-5	3 762
Concrete floor with sand patches.	4.2E-8	4.2E-8	1.3E-9	990
Loading areas.	1E-5	1E-5	1E-5	5 594

9.5.6 The BMA deposition tunnel

The radioactivity in the waste that is deposited in the BMA is mainly lower than the activity in the waste intended for the SILO. A concrete construction is installed in the tunnel -an encapsulation; the waste containers will be stored in this encapsulation. On all sides highly permeable flow barriers will protect the encapsulation. Hence, a complete hydraulic cage surrounds the encapsulation of the BMA tunnel.

The figure and the table below present the layout and the conductivity of the BMA tunnel, as defined in the detailed model (the base case). Alternative layouts of the BMA is discussed in Sec. 10.6.8, in which (i) the voids of the encapsulation are backfilled with a low permeable concrete backfill, or (ii) the backfill is assumed to have a larger conductivity than the value below.

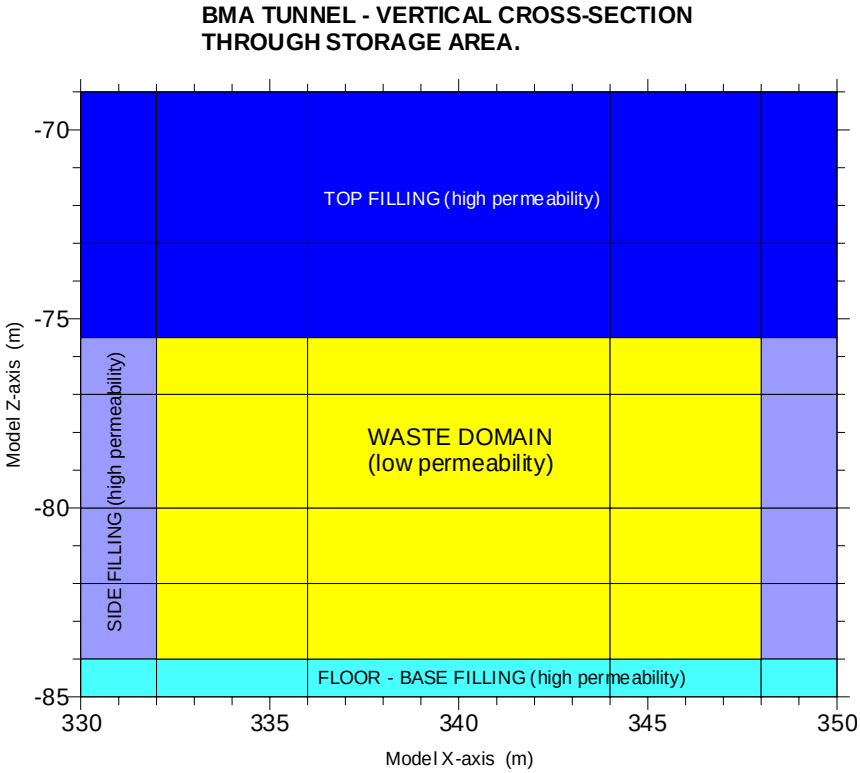

Figure 9.6 *A vertical cross-section through the BMA tunnel, as defined in the detailed model.*

Table 9.5 The conductivity and the volume of the BMA tunnel, as defined in the base case of the detailed model.

BMA	HYDRAULIC CONDUCTIVITY (m/s)			VOLUME (m3)
	IN FLOW DIRECTIONS			
	X-DIR.	Y-DIR.	Z-DIR.	
Top filling (sand/gravel).	1E-5	1E-5	1E-5	17 160
Waste domain. Encapsulation.	1.4E-8	1.7E-8	7.7E-9	17 952
Filling at sides (sand/gravel).	1E-5	1E-5	1E-5	4 480
Filling at base (gravel).	1E-5	1E-5	1E-5	2 640
Loading areas (sand/gravel).	1E-5	1E-5	1E-5	10 610

9.5.7 The SILO deposition tunnel

The main part of the radioactivity of the waste of the SFR repository is to be stored in the SILO. Inside the SILO there is a cylindrical concrete encapsulation, protected on all sides by bentonite barriers. The waste will be stored in vertical shafts in the encapsulation. The figure and the table below present the layout and the conductivity of the SILO, as defined in the detailed model (the base case). In the detailed model, the permeability of the SILO is close to the second SILO definition of the local model (Sec.6.5.4). Note that the scale of the figure depicting the SILO is different from the scale of the previous figures, depicting the other deposition tunnels.

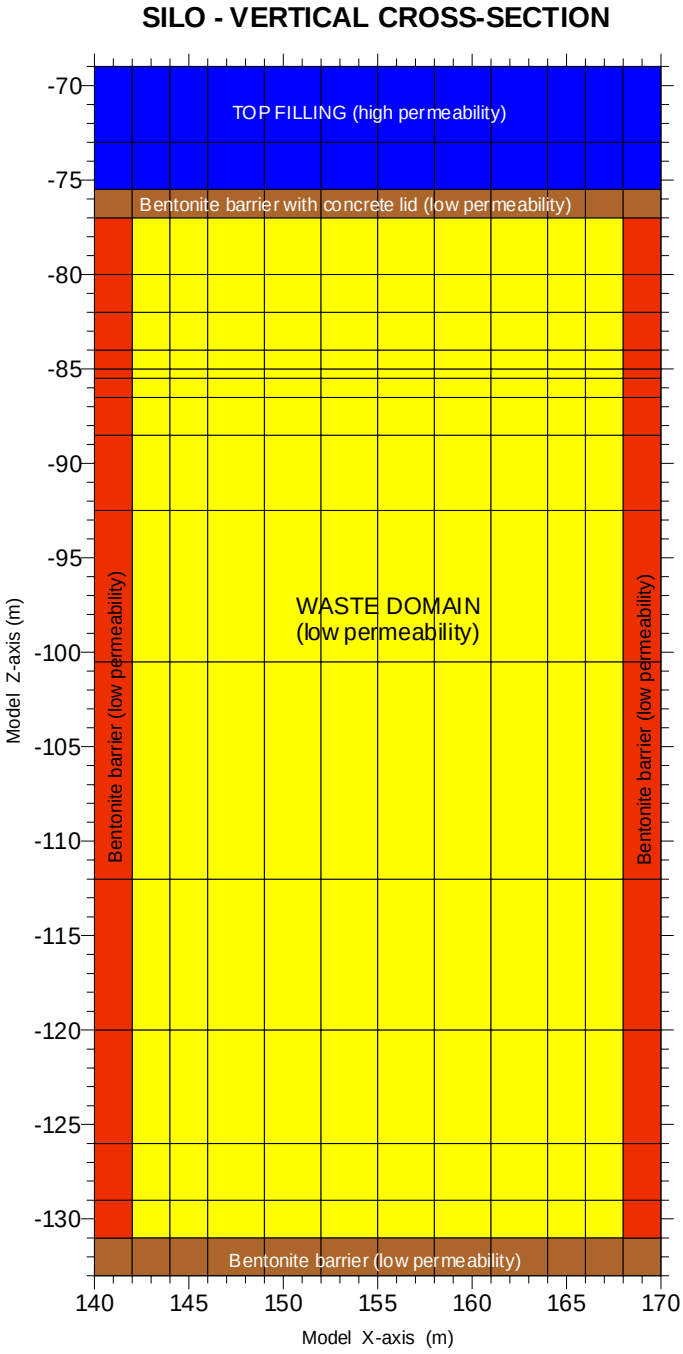

Figure 9.7 *A vertical cross-section through the SILO, as it is defined in the detailed model.*

Table 9.6 The conductivity and volumes of the SILO, as defined in the base case of the detailed model.

SILO	HYDRAULIC CONDUCTIVITY (m/s) IN FLOW DIRECTIONS			VOLUME (m3)
	X-DIR.	Y-DIR.	Z-DIR.	
Top filling.	1E-5	1E-5	1E-5	5 226
Concrete/Bentonite at top.	1E-9	1E-9	1E-9	1 206
Waste domain. Encapsulation.	4.5E-9	4.5E-9	7.4E-9	30 456
Concrete/Bentonite at base.	9.3E-10	9.3E-10	9.2E-10	1 608
Concrete/Bentonite at sides.	1.1E-11	1.1E-11	3.4E-10	12 960

9.6 Methodology - Chain of simulations

9.6.1 Chain of simulations

The chain of simulations is the same as for the local model, but it contains one step further, as the local model will provide the detailed model with boundary conditions. The chain is as follows:

1. Simulation with the regional model. The regional model Case 4 has been used, it provides boundary conditions for the local model. The regional model is run under fully transient conditions. The head field at different moments in time is exported to the local model.

2. Simulation with the local model. The local model will be run under steady state conditions. The heads at the outer limits of the model represents the regional flow situation at different moments in time (2000 AD, 3000 AD, etc).

Step 1 and 2 is the same as in the previously presented chain of simulations regarding the local model (see Chapter 2).

3. Simulation with the detailed model. The detailed model will be run under steady state conditions and the head values at the outer limits of the detailed model are steady as well. These head values are taken from the local model and they represent the local flow situation at different moments in time, as simulated by the local model.

9.6.2 Calibration of detailed model

The detailed model was not calibrated. Considering the rock mass and the fracture zone that occur in the detailed model, these structures have the same values of conductivity (and transport capacity) as in the calibrated local model (see Chapter 6).

9.6.3 Agreement between local and detailed models, considering flow

For the local and regional model it was necessary to investigate the agreement in predicted flow through a common domain, because the conductivity of the rock mass was different in the two models and so was the cells along the boundaries etc (see Sec.7.6). For the local and detailed model, the conductivity of the rock mass and the transport capacity of the fracture zones are the same in both models. Furthermore, the axis of the mesh of the detailed model are parallel to the axis of the local model, and the rows and the columns of the outer boundaries of the detailed model coincide with the position of certain rows and columns in the local model. Hence, the detailed model is a refinement of the local model, with very much the same properties as the local model. Nevertheless, there are differences between the models, primarily in the definitions of the tunnels and a comparison between predicted tunnel flow is given in Section 10.6.9.

10. Predicted tunnel flow

10.1 Introduction

In this chapter we will present the flow through the tunnels as predicted by the local and the detailed models. The local model will predict the flow through tunnels that are defined without internal structures. The detailed model, on the other hand, will predict the flow of the tunnels in detail, including the flow of all the internal structures of the tunnels, such as concrete encapsulations, top and side fillings, floors etc.

10.2 General evolution

Generally, the models predict that as long as the sea covers the ground above the SFR, the regional groundwater flow as well as the flow in the deposition tunnels are small. However, due to the shore level displacement, the shoreline will retreat and at approximately 2800 AD the shoreline will be above the deposition tunnels. Because of the retreating shoreline, the general direction of the groundwater flow at SFR will change, from vertical upward to a more horizontal flow; the size of the groundwater flow will be increased as well. Hence, the predicted regional groundwater flow at SFR and the flow through the deposition tunnels will increase with time, but a steady-state-like situation will be reached at approximately 5000 AD.

10.3 The concept of flow in a tunnel

The concept of flow in a tunnel has previously been discussed (See Sec. 2.8).

- Specific flow, is defined as a flow per unit area [$L^3 / (L^2\ T) = L / T$]. The specific flow gives information about the flow at a local point. The average specific flow of a tunnel or a structure given in this study is a volume weighted average value, considering the specific flow, which varies from cell to cell. The average value is volume weighted as regards the different sizes of the cells in the mesh.
- Total flow, in a tunnel is defined as the flow that enters and/or leaves a tunnel [L^3 / T]. The calculation of total flow is based on a mass balance taken over the envelope of the studied structure (e.g. a tunnel). The total flow gives information about the amount of water that "visits" the tunnel. If the tunnel system is complex, it is possible that water, which previously has been inside the tunnel system, re-enters the tunnel system at some other point downstream. Such water will be added to the total flow every time it enters the tunnel system. The total flow provides no information of the length of the flow paths in the tunnels, a short path or a long path, will both add to the total flow.

10.4 The tunnel definitions in the local and detailed models

Both the local model and the detailed model predict the flow through the tunnels. However, the predictions will not be the same, as the tunnels are not defined in exactly the same way in the two different models.

In the local model all tunnels except the SILO is defined as being homogeneous. The horizontal deposition tunnels (BTF, BLA and BMA), of the local model, are characterised by their most permeable parts, which is the sand volumes that occurs as a backfill e.g. as a top filling. Hence, in the local model these tunnels are homogeneous and very permeable, but in the detailed model the deposition tunnels are not homogeneous, as the internal structures of the tunnels are included, structures which are less permeable than the backfill.

In both the local and the detailed model, the SILO is defined with a bentonite barrier surrounding a concrete encapsulation; but, the sand filled high permeable volume on top of the concrete encapsulation is included in the detailed model, but not in the local model. It is the second SILO definition (SD2) of the local model that corresponds to the SILO definition of the detailed model. But, as the local model has a lower resolution, the conductivity values of the SILO in the local model (SD2) is slightly different compared to the values of the detailed model, the values of the local model being representative average values of the detailed model.

Furthermore, the tunnels are not of the same size in the different models. The horizontal deposition tunnels (BTF, BLA and BMA), of the local model, are defined as larger than the same tunnels in the detailed model. For the SILO it is the opposite, in the local model the SILO is smaller than in the detailed model. In the detailed model the sizes of the deposition tunnels are closer to the actual size of the deposition tunnels at SFR (see Table 9.1), except for the SILO. But, in the detailed model, the shape of the SILO is better than in the local model as it is closer to the cylindrical shape of the actual cavern.

The results of the detailed model are the best predictions of the future groundwater flow through the tunnels of the repository, and these results are to be used in estimations of the release and transport of nuclides.

10.5 Local model – flow through tunnels

10.5.1 Local model - BMA and BLA tunnel

The BMA tunnel is the outermost of the four horizontal deposition tunnels. When the general direction of the groundwater flow changes, from vertical upwards to a more horizontal flow, the flow through BMA increases fast and the BMA tunnel will become the tunnel that carries most flow of all deposition tunnels.

- For the BMA tunnel, the total flow increases from 5 m^3/year at 2000 AD and reaches a maximum total flow of 65 m^3/year, at steady-state-like conditions, at approximately 4000 AD.

- The flow in the BLA tunnel and in the BMA tunnel has a similar trend. For the BLA, the total flow increases from 16 m^3/year at 2000 AD and reaches a maximum total flow of 60 m^3/year, at steady-state-like conditions, at approximately 4000 AD.

10.5.2 Local model - BTF1 and BTF2 tunnels

The BTF1 and the BTF2 tunnels are the innermost tunnels of the four horizontal deposition tunnels; they are surrounded by permeable access tunnels and by the BLA tunnel. The surrounding tunnels will reduce the flow through BTF1 and BTF2, when the general direction of the groundwater flow changes, from vertical towards horizontal, as the surrounding tunnels will act as hydraulic barriers. The flow in the BTF tunnels is smaller than in the BMA and BLA tunnels. The flow in BTF1 is somewhat smaller than in BTF2, as this is the innermost tunnel. The flow of the BTF tunnels has a similar trend.

- For the BTF1, the total flow increases from 12 m^3/year at 2000 AD and reaches a maximum total flow of 41 m^3/year, at steady-state-like conditions, at approximately 5000 AD.
- For the BTF2, the total flow increases from 13 m^3/year at 2000 AD and reaches a maximum total flow of 44 m^3/year, at steady-state-like conditions, at approximately 6000 AD.

10.5.3 Local model - SILO

The SILO is located a short distance from the other four deposition tunnels. It is at three positions connected to access tunnels, but the SILO is mainly a vertical cavern and the surrounding access tunnels will not form an effective hydraulic barrier. No fracture zones intersects the SILO. The flow through the SILO depends primarily on the average flow in the surrounding rock mass, the properties of Zone H2 and on the effect of the flow barriers and plugs that protects the SILO. The flow in the SILO is much smaller than the flow through the other deposition tunnels; however, the general trend of the flow in the SILO is similar to the trends of the flows in the other tunnels. There are two different SILO definitions they are defined in Sec.6.5.4.

For the first SILO definition (SD1), the flow increases from 0.6 m^3/year at 2000 AD and reaches a maximum flow of 4.1 m^3/year at approximately 4000 AD. A steady-state-like flow equal to 3.8 m^3/year is reached at approximately 6000 AD..

For the second SILO definition (SD2), the flow increases from 0.3 m^3/year at 2000 AD and reaches a maximum flow of 1.3 m^3/year at approximately 4000 AD. A steady-state-like flow equal to 1.2 m^3/year is reached at approximately 5000 AD. The flow of the other deposition tunnels (BMA, BLA, BTF) will be approximately the same for the two different SILO definitions.

10.5.4 Local model - Regional specific flow

For Case 4, the model predicts the average regional specific flow in the local model to increase from 3 litre/(m^2 year) at 2000 AD to 7 litre/(m^2 year) at steady-state-like conditions (see Table 10.1). These values are volumetric averages considering the groundwater flow through the cells of the mesh, both the flow in the rock mass and in

the fracture zones, but not the flow through tunnels. The estimation of the average regional flow depends on the type of average used, an arithmetic average will produce a larger regional flow (3 – 9 litre/(m^2 year)) and a geometric average will produce a smaller regional flow (1 – 3 litre/(m^2 year). As the cell sizes are very different a volumetric average (weighting as regards cell size) seems to produce the best estimate. It follows from the discussion above that the concept of average specific flow should be used with care. The changes in total flow in the deposition tunnels are not directly proportional to the change in regional specific flow. The flow in the deposition tunnels depends not only on the size of the regional flow, but also on the direction of the regional flow and on the distribution of flow in fracture zones and rock mass as well as on hydraulic interaction within the tunnel system, etc.

10.5.5 Local model - Summary of total flow and regional flow

Table 10.1 below, provides a summary of the predicted total flow through the deposition tunnels, as well as the average regional specific flow of the local model. For the differences between the two SILO definitions, we refer to Section 6.5.4

Table 10.1 Case 4: Total flow of the deposition tunnels and regional flow of the local model (base case).

(i) *Results considering the deposition tunnels and the first SILO definition.*

	TOTAL FLOW (m3/year)					Regional Flow (litre / (m2 year))
Time AD	SILO (1)	BMA	BLA	BTF2	BTF1	Volumetric mean
2000	0.6	4.8	15	12	13	3
3000	2.3	50	42	33	38	5
4000	4.1	65	61	38	41	7
5000	3.9	65	61	41	43	7
6000	3.8	65	61	41	44	7
8000	3.8	65	61	41	44	7
(1) First SILO definition (SD1).						

(ii) *Results considering the second SILO definition.*

	TOTAL FLOW (m3/year)
Time AD	SILO (1)
2000	0.2
3000	0.7
4000	1.3
5000	1.2
6000	1.2
8000	1.2
(1) Second SILO definition (SD2)	

10.6 Detailed model – flow through tunnels

10.6.1 Introduction

The following section will not be a repetition of the general presentation of the flow system and the models as given in previous chapters. Below we will only present the detailed model and when necessary compare it to the local model. The flow will be predicted for a period starting at present (2000 AD) and continued until steady-state-like conditions prevails, at about 7000 AD.

10.6.2 Different structures studied

In the detailed results presented below, the flow will be given for different structures/domains separately. Considering the BTF, BLA and BMA tunnels, the following structures/domains will be studied: (i) waste/encapsulations, (ii) top fillings, (iii) filling at sides, (iv) concrete floors with sand patches (BTF, BLA) or a sand/gravel floor (BMA), (v) loading areas and (vi) the all-surroundings.

Considering the total flow, two domains need to be discussed. The “Loading areas” are the volumes at both ends of the horizontal deposition tunnels (see Figure 9.3), used for handling of the waste packages etc, when the SFR is closed these volumes are refilled with sand. The loading areas are thus two separate volumes per tunnel; and the total flow for this domain, for a given tunnel, is the sum of the total flow in each of the two separate domains. The “All surroundings” is a volume that includes all the different structures that surrounds the waste/encapsulation i.e. (i) the top filling, (ii) the floor, i.e. the filling at the tunnel base, (iii) the filling at sides and (v) the loading areas. The All-surrounding” represents barriers and materials that surround the encapsulation/waste. The total flow through an object is defined, as the flow through its envelope, and every time a flow passes through the envelope it will be added to the total flow. The waste/encapsulation domain is completely surrounded by the All-surroundings domain. The flow that passes through the waste/encapsulation has first passed through the All-surroundings upstream of the waste/encapsulation, and it will pass through the All-surroundings a second time when it re-enters it downstream of the waste/encapsulation. Hence, the water that passes through the waste/encapsulation will be added to the total flow of the All-surroundings a second time when it re-enters the domain defined as the All-surroundings. This is correct, as that flow enters the All-surrounding domain two times. However, as a description of the amount of flow in the tunnel it is perhaps preferable not to add the flow of the waste/encapsulation an extra time. In the tables presenting the flow, both alternatives are given.

For the SILO, the following structures/domains will be studied: (i) the waste/encapsulation, (ii) the top filling, (iii) the bentonite at top, (iv) the bentonite at base and (v) the bentonite at sides.

10.6.3 Flow in BTF deposition tunnels

Results of the detailed modelling are given in the tables below, the total flow and the specific flow of the different structures inside the BTF tunnels (the base case).

Table 10.2 BTF1 Total flow and average specific flow, as predicted by the detailed model (base case).

BTF1	Total flow (m3/year) Trough different parts of the studied tunnel at different times					
	2000 AD	3000 AD	4000 AD	5000 AD	6000 AD	7000 AD
Top filling	6.6	17.4	24.3	27.4	28.1	28.1
Waste domain Encapsulation	2.4	2.7	6.8	7.8	8.0	8.0
Concrete at sides	0.9	2.7	3.2	3.6	3.7	3.7
Concrete/sand floor	2.4	1.7	6.1	7.0	7.2	7.2
Loading areas	1.2	4.1	9.7	10.8	11.1	11.1
All surroundings	9.9	22.1	33.2	37.5	38.4	38.5
Tunnel flow Qallsurr. – Qwaste	7.5	19.4	26.4	30.7	30.4	30.5

BTF1	Average specific flow (m/s) In different parts of the studied tunnel at different times					
	2000 AD	3000 AD	4000 AD	5000 AD	6000 AD	7000 AD
Top filling	5.4E-10	4.0E-9	6.7E-9	7.0E-9	7.1E-9	6.9E-9
Waste domain. Encap.	3.7E-11	3.9E-11	1.0E-10	1.2E-10	1.2E-10	1.2E-10
Concrete at sides	4.5E-11	6.9E-11	1.3E-10	1.5E-10	1.5E-10	1.5E-10
Concrete/sand floor	7.8E-11	3.4E-10	2.1E-10	2.2E-10	2.3E-10	2.3E-10
Loading areas	9.6E-11	3.7E-10	1.2E-9	1.3E-9	1.4E-9	1.4E-9
All surroundings	2.8E-10	1.9E-9	3.4E-9	3.6E-9	3.6E-9	3.6E-9

Table 10.3 BTF2 Total flow and average specific flow, as predicted by the detailed model (base case).

BTF2	Total flow (m3/year) Trough different parts of the studied tunnel at different times					
	2000 AD	3000 AD	4000 AD	5000 AD	6000 AD	7000 AD
Top filling	5.9	14.2	25.1	26.8	27.2	27.2
Waste domain Encapsulation	2.4	3.0	6.0	6.8	6.9	6.9
Concrete at sides	1.0	3.4	4.1	4.2	4.2	4.2
Concrete/sand floor	2.3	1.4	5.2	6.0	6.2	6.2
Loading areas	1.3	5.1	10.0	10.6	10.7	10.7
All surroundings	9.1	20.6	33.7	36.4	36.8	36.8
Tunnel flow Qallsurr. – Qwaste	6.7	17.6	27.7	29.6	29.9	29.9

BTF2	Average specific flow (m/s) In different parts of the studied tunnel at different times					
	2000 AD	3000 AD	4000 AD	5000 AD	6000 AD	7000 AD
Top filling	7.0E-10	3.9E-9	5.4E-9	5.4E-9	5.4E-9	5.4E-9
Waste domain. Encap.	3.7E-11	4.5E-11	9.0E-11	1.0E-10	1.0E-10	1.0E-10
Concrete at sides	4.9E-11	8.3E-11	1.4E-10	1.5E-10	1.5E-10	1.5E-10
Concrete/sand floor	7.1E-11	2.3E-10	2.8E-10	2.9E-10	2.9E-10	2.9E-10
Loading areas	1.1E-10	3.0E-10	1.1E-9	1.2E-9	1.2E-9	1.2E-9
All surroundings	3.6E-10	1.8E-9	2.8E-9	2.8E-9	2.8E-9	2.8E-9

10.6.4 Flow in BLA deposition tunnel

Results of the detailed modelling are given in the tables below, the total flow and the specific flow of the different structures inside the BLA tunnel (the base case).

Table 10.4 BLA - Total flow and average specific flow, as predicted by the detailed model (base case).

BLA	Total flow (m3/year) Trough different parts of the studied tunnel at different times					
	2000 AD	3000 AD	4000 AD	5000 AD	6000 AD	7000 AD
Top filling	10.1	15.1	32.5	36.5	37.1	37.1
Waste domain Storage area	9.6	19.4	35.0	38.4	38.8	38.8
Filling at sides	10.3	38.1	50.8	53.4	53.6	53.6
Concrete/sand floor	3.2	3.0	7.7	8.7	8.8	8.8
Loading areas	1.0	10.0	12.9	13.4	13.4	13.4
All surroundings	23.2	52.5	85.2	92.6	93.6	93.7
Tunnel flow Qallsurr. – Qwaste	13.6	33.1	50.2	54.2	54.8	54.9

BLA	Average specific flow (m/s) In different parts of the studied tunnel at different times					
	2000 AD	3000 AD	4000 AD	5000 AD	6000 AD	7000 AD
Top filling	3.0E-10	2.4E-9	2.9E-9	2.9E-9	2.9E-9	2.9E-9
Waste domain	1.8E-10	1.5E-9	1.9E-9	1.9E-9	1.9E-9	1.9E-9
Filling at sides	3.4E-10	2.8E-9	3.4E-9	3.4E-9	3.4E-9	3.4E-9
Concrete/sand floor	5.7E-11	1.1E-10	1.9E-10	2.1E-10	2.1E-10	2.1E-10
Loading areas	6.0E-11	5.2E-10	7.6E-10	8.3E-10	8.5E-10	8.5E-10
All surroundings	2.1E-10	1.7E-9	2.1E-9	2.2E-9	2.2E-9	2.2E-9

10.6.5 Flow in BMA deposition tunnel

Results of the detailed modelling are given in the tables below, the total flow and the specific flow of the different structures inside the BMA tunnel (the base case).

Table 10.5 BMA – total flow and average specific flow, as predicted by the detailed model (base case).

BMA	Total flow (m3/year) Trough different parts of the studied tunnel at different times					
	2000 AD	3000 AD	4000 AD	5000 AD	6000 AD	7000 AD
Top filling	5.9	20.6	33.8	35.4	35.5	35.5
Waste domain Encapsulation	0.07	0.13	0.26	0.28	0.28	0.28
Filling at sides	6.8	14.9	27.5	29.5	29.6	29.6
Concrete/sand floor	7.7	12.8	26.4	28.7	28.9	28.9
Loading areas	2.8	22.4	32.2	32.8	32.7	32.7
All surroundings	8.8	36.8	53.0	55.0	55.0	55.0
Tunnel flow Qallsurr. – Qwaste	8.7	36.7	52.7	54.7	54.7	54.7

BMA	Average specific flow (m/s) In different parts of the studied tunnel at different times					
	2000 AD	3000 AD	4000 AD	5000 AD	6000 AD	7000 AD
Top filling	2.2E-10	3.0E-9	4.9E-9	5.1E-9	5.1E-9	5.1E-9
Waste domain. Encap.	9.3E-13	7.5E-12	1.2E-11	1.3E-11	1.3E-11	1.3E-11
Filling at sides	5.2E-10	4.3E-9	7.1E-9	7.3E-9	7.3E-9	7.3E-9
Concrete/sand floor	5.6E-10	4.5E-9	7.4E-9	7.7E-9	7.7E-9	7.7E-9
Loading areas	1.3E-10	6.3E-10	1.0E-9	1.1E-9	1.1E-9	1.1E-9
All surroundings	2.6E-10	2.6E-9	4.2E-9	4.3E-9	4.3E-9	4.3E-9

10.6.6 Flow in the SILO deposition tunnel

Results of the detailed modelling are given in the tables below, the total flow and the specific flow of the different structures inside the SILO (the base case).

Table 10.6 SILO – total flow and average specific flow, as predicted by the detailed model (base case).

SILO	Total flow (m3/year) Trough different parts of the studied tunnel at different times					
	2000 AD	3000 AD	4000 AD	5000 AD	6000 AD	7000 AD
Top filling	0.53	1.4	2.2	2.2	2.2	2.2
Bentonite at top	0.27	0.32	0.21	0.28	0.31	0.31
Waste domain Encapsulation	0.23	0.22	0.16	0.23	0.25	0.25
Bentonite at base	0.24	0.22	0.27	0.33	0.35	0.35
Bentonite at sides	0.023	0.043	0.055	0.054	0.054	0.054

SILO	Average specific flow (m/s) In different parts of the studied tunnel at different times					
	2000 AD	3000 AD	4000 AD	5000 AD	6000 AD	7000 AD
Top filling	2.4E-11	8.5E-11	2.8E-10	2.8E-10	2.8E-10	2.8E-10
Bentonite at top	1.0E-11	1.2E-11	8.4E-12	1.1E-11	1.2E-11	1.2E-11
Waste domain. Encap.	1.3E-11	1.2E-11	6.8E-12	1.1E-11	1.3E-11	1.3E-11
Bentonite at base	1.0E-11	9.4E-12	1.1E-11	1.4E-11	1.4E-11	1.4E-11
Bentonite at sides	8.7E-13	8.1E-13	7.8E-13	9.6E-12	1.0E-12	1.0E-12

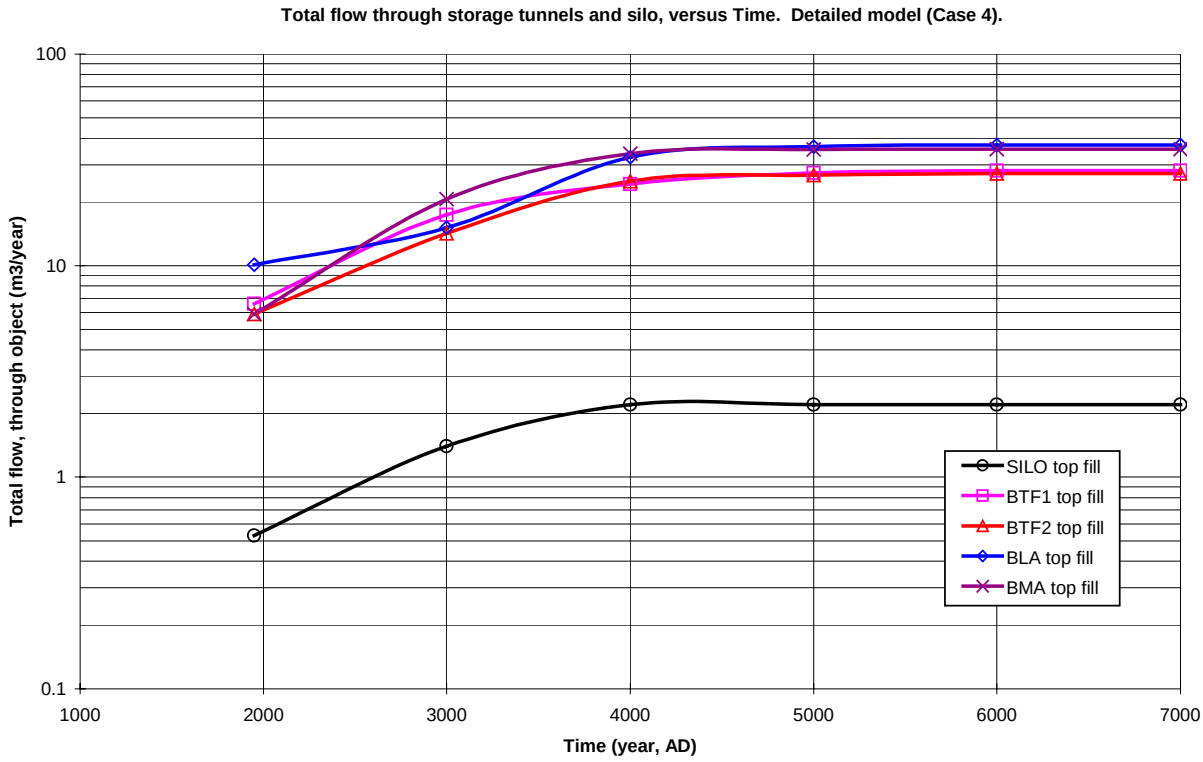

Figure 10.1 *Detailed model - Total flow through the top fill of the deposition tunnels (base case).*

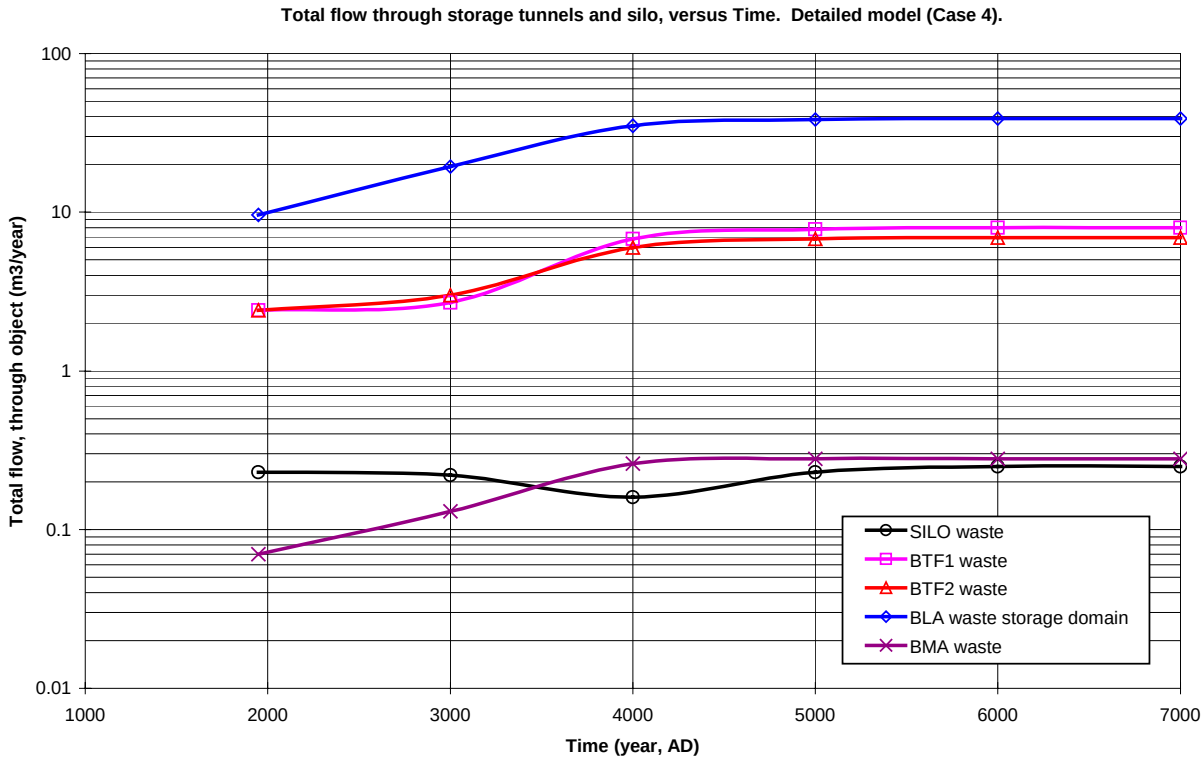

Figure 10.2 *Detailed model - Total flow through the waste encapsulations and waste storage domain (base case).*

10.6.7 General distribution of flow in tunnels

For the encapsulation of the SILO and the BMA tunnel, the models predict very small values of flow. This is a result of the barriers, which surrounds these encapsulations. Barriers having a low permeability (concrete and bentinite) surround the SILO and an efficient hydraulic cage surrounds the BMA. Most of the water that flows in the deposition tunnels will flow in the high permeable parts of the tunnels, e.g. in the top fillings. These high permeable structures will partly act as flow barriers and lead the flow away from the waste encapsulation. However, it is only in the BMA tunnel that high permeable flow barriers surround the encapsulation on all sides; the BMA is the only tunnel at SFR that has a complete hydraulic cage protecting the waste encapsulation. The other deposition tunnel at SFR with an efficient system of flow barriers is the SILO, which is protected by low permeable bentonite flow barriers on all sides. The tunnel with the least barriers is the BLA tunnel, which contains no encapsulation. To demonstrate the distribution of flow in the tunnels, we have compared the total flow of the waste/encapsulation domains to the total flow of the top fillings. The BLA tunnel is not included in this comparison, because in the model it is no difference in conductivity between the two domains of the BLA. The distribution of the total flow changes with time, as the size and direction of the regional flow changes with time. The result of this comparison is given in Figure 10.3.

- BTF, the flow of the waste domain is 15 – 40 % of the flow of the top fillings.
- BMA, the flow of the waste domain is 0.7 – 1 % of the flow of the top filling.
- SILO, the flow of the waste domain is 7 – 40 % of the flow of the top filling.

The most extreme flow distribution occurs for the hydraulic cage of the BMA tunnel. When considering the distribution of the total flow of the SILO, note that the volume of the encapsulation of the SILO is six times larger than that of the top fill of the SILO, and that the flow of the SILO top fill is much smaller than the flow of any other top fill.

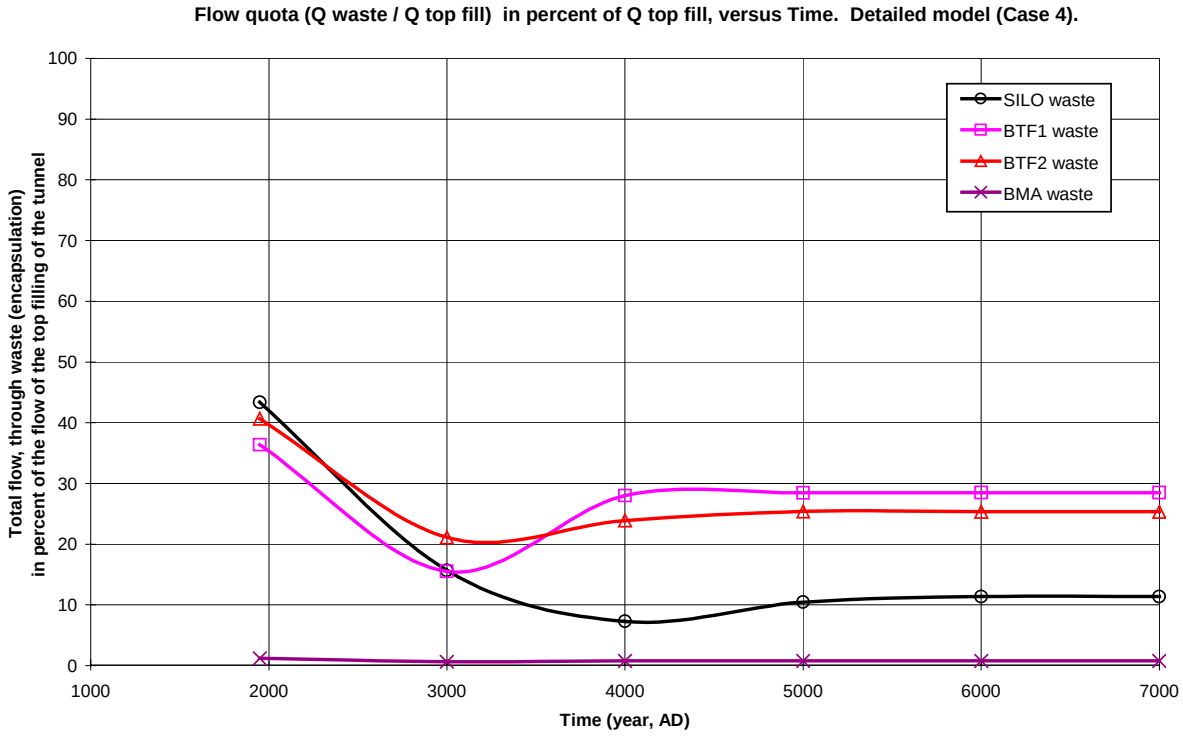

Figure 10.3 *The total flow of the waste/encapsulation domain in relation to the total flow of the top fill (in percent), considering the base case.*

10.6.8 Alternative layout of the BMA tunnel

10.6.8.1 Introduction

The very small values of flow, which are predicted for the BMA encapsulation, are the results of the efficient hydraulic cage that surrounds the encapsulation. The efficiency of the hydraulic cage depends on both: (i) the contrasts in conductivity between the encapsulation and the surrounding flow barriers, as well as (ii) on the extension of the surrounding flow barriers.

10.6.8.2 Flow barrier without a complete coverage of the encapsulation

A hydraulic cage will only work efficiently if it surrounds the encapsulation on all sides; this is discussed in (Holmén 1997). For the present layout of the BMA tunnel, below the encapsulation there is a highly permeable gravel bed. This gravel bed is essential for the function of the hydraulic cage. If for example, the gravel bed is replaced with a concrete floor, similar to the floor that of the BTF and BLA tunnels, the flow through the BMA encapsulation will be about 20-40 times larger than the flow calculated for the present layout.

10.6.8.3 Permeability and flow of barriers and encapsulation

The size of the flow of an encapsulation protected by a highly permeable flow barrier (i.e. a positive flow barrier, a hydraulic cage) is not directly proportional to the size of the flow of the barrier. The size of the flow of a highly permeable flow barrier reaches a maximum value for large values of barrier conductivity, in an asymptotic way; because at large values of barrier conductivity, the flow of the barrier is controlled by the flow through the surrounding rock mass. Hence, for large values of barrier conductivity, the flow of the barrier will only change minimally for different large values of barrier conductivity. However, even if the size of the flow in the barrier does not change much, the flow pattern of the water that flows through the barrier and the encapsulation changes with different large values of the barrier conductivity, this is discussed in (Holmén 1997). As the conductivity of the barrier becomes larger, less water will leave the barrier and pass through the encapsulation; instead more of the flow will stay in the barrier and flow around the encapsulation. Therefore, the efficiency of a positive barrier or a hydraulic cage will be increased, if the conductivity of the barrier is increased. The larger the conductivity contrasts between the encapsulation and the barrier, the smaller the flow through the encapsulation. This goes for all complete barriers having a conductivity that is larger than that of both the rock mass and the encapsulation.

For the BMA tunnel, the conductivity contrast between the encapsulation and the surrounding backfill can be increased by reducing the conductivity of the encapsulation or by increasing the conductivity of the surrounding backfill (or both measures).

First alternative. An alternative layout of the BMA tunnel is that the voids inside the encapsulation -the voids between the waste containers and the concrete walls of the encapsulation, is back filled with a concrete backfill having a low permeability. This is the first alternative layout (BMA Alt.1), the assumed conductivity of the concrete

backfill is given in Table 9.2, and the calculation of the conductivity of the encapsulation is given in Appendix B. The first alternative layout will reduce the permeability of the encapsulation, thereby increase the efficiency of the hydraulic cage that surrounds the encapsulation, and consequently reduce the flow through the encapsulation. For this alternative layout, Table 10.7 below presents the conductivity and the volumes of the BMA tunnel, as defined in the detailed model. Simulations have been carried out with the detailed model using the first alternative layout; results of the detailed modelling, the total flow and the specific flow of the different structures inside the BMA tunnel, are given in Table 10.8. For the first alternative layout, in comparison to the base case layout (results in Table 10.5), the model predicts that the total flow through the encapsulation is reduced to half of the previous flow.

Table 10.7 The conductivity and the available porosity of the BMA tunnel, as defined in the detailed model for the first alternative layout of the BMA tunnel (BMA Alt.1).

BMA	HYDRAULIC CONDUCTIVITY (m/s) IN FLOW DIRECTIONS			INITIAL AVAILABLE POROSITY (-)	VOLUME (m3)
	X-DIR.	Y-DIR.	Z-DIR.		
Top filling (sand/gravel)	1E-5	1E-5	1E-5	0.20	17 160
Waste domain. Encapsulation	5.1E-9	5.3E-9	4.1E-9	0.15	17 952
Filling at sides (sand/gravel)	1E-5	1E-5	1E-5	0.20	4 480
Filling at base (gravel)	1E-5	1E-5	1E-5	0.20	2 640
Loading areas (sand/gravel)	1E-5	1E-5	1E-5	0.20	10 610

Table 10.8 BMA – total flow and average specific flow, as predicted by the detailed model for the first alternative layout (BMA Alt.1).

BMA	Total flow (m3/year) Trough different parts of the studied tunnel at different times					
	2000 AD	3000 AD	4000 AD	5000 AD	6000 AD	7000 AD
Top filling	5.9	20.0	32.8	34.5	34.6	34.6
Waste domain. Encap.	0.03	0.06	0.12	0.13	0.13	0.13
Filling at sides	6.7	14.4	27.0	28.9	29.1	29.1
Filling at base	7.4	12.4	25.6	27.8	28.0	28.0
Loading areas	2.7	22.0	31.7	32.2	32.1	32.1
All surroundings	8.7	36.5	52.4	54.5	54.4	54.4
Tunnel flow Qallsurr. – Qwaste	8.7	36.4	52.3	54.3	54.3	54.3

BMA	Average specific flow (m/s) In different parts of the studied tunnel at different times					
	2000 AD	3000 AD	4000 AD	5000 AD	6000 AD	7000 AD
Top filling	2.0E-10	3.0E-9	4.6E-9	4.8E-9	4.8E-9	4.8E-9
Waste domain. Encap.	4.0E-13	2.5E-12	4.3E-12	4.4E-12	4.4E-12	4.4E-12
Filling at sides	5.1E-10	4.5E-9	7.5E-9	7.7E-9	7.7E-9	7.7E-9
Filling at base	5.5E-10	4.8E-9	7.9E-9	8.1E-9	8.1E-9	8.1E-9
Loading areas	1.3E-10	6.2E-10	1.0E-9	1.1E-9	1.1E-9	1.1E-9
Tunnel flow All surroundings	2.5E-10	2.5E-9	4.2E-9	4.3E-9	4.3E-9	4.3E-9

Second alternative. An alternative layout of the BMA tunnel is a tunnel with backfill conductivity larger than that of the base case. Because it is very likely that the material that will be used as backfill when the repository is closed will be a coarse material having a larger conductivity than that of the base case (the backfill conductivity of the base case is 1×10^{-5} m/s). A larger value of backfill conductivity will only have minimal effect on the size of the flow of the backfill, but it will change the size of the flow of the BMA encapsulation. Hence, the second alternative layout will increase the permeability of the flow barriers (the backfill), thereby increase the efficiency of the hydraulic cage that surrounds the encapsulation, and consequently reduce the flow through the encapsulation. For the second alternative layout (BMA Alt.2) the conductivity of the backfill is set to 1×10^{-4} m/s. Everything else is identical to the base case (see Table 9.5). The results of the second alternative layout are given in Table 10.9.

Table 10.9 BMA – total flow and average specific flow, as predicted by the detailed model for the second alternative layout (BMA Alt.2).

BMA	Total flow (m3/year) Trough different parts of the studied tunnel at different times					
	2000 AD	3000 AD	4000 AD	5000 AD	6000 AD	7000 AD
Top filling	5.9	23.3	38.2	39.7	39.8	39.8
Waste domain. Encap.	0.007	0.01	0.03	0.03	0.03	0.03
Filling at sides	7.0	16.3	29.2	31.1	31.2	31.2
Filling at base	7.9	14.0	28.2	30.5	30.7	30.7
Loading areas	2.8	23.9	35.3	35.9	35.9	35.9
All surroundings	8.8	38.0	55.2	57.3	57.3	57.3
Tunnel flow Qallsurr. – Qwaste	8.8	38.0	55.2	57.3	57.3	57.3

BMA	Average specific flow (m/s) In different parts of the studied tunnel at different times					
	2000 AD	3000 AD	4000 AD	5000 AD	6000 AD	7000 AD
Top filling	2.2E-10	3.7E-9	6.1E-9	6.2E-9	6.3E-9	6.3E-9
Waste domain. Encap.	8.6E-14	6.8E-13	1.1E-12	1.2E-12	1.2E-12	1.2E-12
Filling at sides	4.7E-10	3.9E-9	6.6E-9	6.7E-9	6.8E-9	6.8E-9
Filling at base	5.1E-10	4.1E-9	6.9E-9	7.1E-9	7.1E-9	7.1E-9
Loading areas	1.4E-10	6.8E-10	1.2E-9	1.2E-9	1.2E-9	1.2E-9
All surroundings	2.5E-10	2.9E-9	4.7E-9	4.8E-9	4.9E-9	4.9E-9

Third alternative. It is possible that the conductivity of the backfill is even more permeable than the conductivity value used for the second alternative layout. The third alternative (BMA Alt.3) is identical to the second alternative, except that the conductivity of the backfill is larger; the conductivity of the backfill is set to 1×10^{-3} m/s. Everything else is identical to the base case (see Table 9.5). The results of the third alternative layout are given in Table 10.10.

Conclusion. The alternative layouts will reduce the flow of the BMA encapsulation, compared to the base case. A comparison between the base case and the different alternative layouts is given in Figure 10.4. The figure demonstrates the following. For conductivity contrasts larger than that of the base case, an increase in conductivity contrast will produce an inversely proportional change in encapsulation flow, e.g. an increase of the contrast of one order of magnitude will produce a reduction of

encapsulation flow of about one order of magnitude. However, this conclusion is only valid within the range of applicability of Darcy´s law.

Table 10.10 BMA – total flow and average specific flow, as predicted by the detailed model for the third alternative layout (BMA Alt.3).

BMA	Total flow (m3/year) Trough different parts of the studied tunnel at different times					
	2000 AD	3000 AD	4000 AD	5000 AD	6000 AD	7000 AD
Top filling	6.4	31.3	52.1	53.9	54.7	54.7
Waste domain. Encap.	7E-3	0.002	0.003	0.003	0.004	0.004
Filling at sides	7.1	21.0	37.3	39.7	40.1	40.1
Filling at base	7.9	15.5	30.6	33.0	33.4	33.4
Loading areas	3.1	32.1	49.4	49.8	50.9	50.9
All surroundings	8.8	38.1	55.5	57.5	57.5	57.5
Tunnel flow Qallsurr. – Qwaste	8.8	38.1	55.5	57.5	57.5	57.5

BMA	Average specific flow (m/s) In different parts of the studied tunnel at different times					
	2000 AD	3000 AD	4000 AD	5000 AD	6000 AD	7000 AD
Top filling	3.8E-10	6.2E-9	1.0E-8	1.0E-8	1.0E-8	1.0E-8
Waste domain. Encap.	1.1E-14	1.1E-13	1.9E-13	1.9E-13	1.9E-13	1.9E-13
Filling at sides	5.9E-10	6.4E-9	1.1E-8	1.1E-8	1.1E-8	1.1E-8
Filling at base	6.4E-10	6.6E-9	1.1E-8	1.1E-8	1.1E-8	1.1E-8
Loading areas	1.4E-10	1.2E-9	2.4E-9	2.5E-9	2.6E-9	2.6E-9
All surroundings	3.6E-10	4.8E-9	8.0E-9	8.2E-9	8.3E-9	8.3E-9

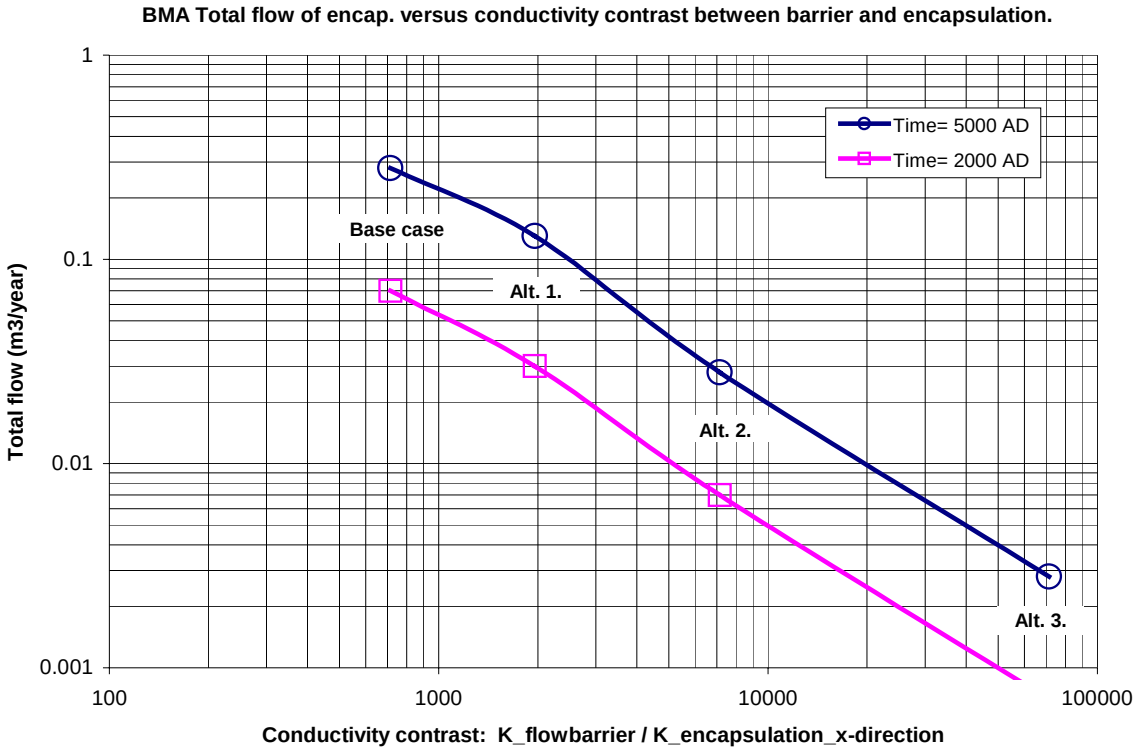

Figure 10.4 *The efficiency of the hydraulic cage of the BMA tunnel as regards conductivity contrasts.*

The conductivity contrast is defined as the quota between the conductivity of the flow barrier and that of the encapsulation (conductivity in model x-direction).

10.6.9 Comparison between detailed and local models

Both the local model and the detailed model predict the flow through the tunnels. However, the predictions will not be the same, as the tunnels are not defined in exactly the same way in the two different models. In the local model all tunnels except the SILO is defined as being homogeneous. The horizontal deposition tunnels (BTF, BLA and BMA), of the local model, are characterised by their most permeable parts, which is the sand volumes that occurs as a backfill e.g. as a top filling. Hence, in the local model these tunnels are homogeneous and very permeable, but in the detailed model the deposition tunnels are not homogeneous, as the internal structures of the tunnels are included, structures which are less permeable than the backfill. In both the local and the detailed model, the SILO is defined with a bentonite barrier surrounding a concrete encapsulation; but, the sand filled high permeable volume on top of the concrete encapsulation is included in the detailed model, but not in the local model. It is the second SILO definition (SD2) of the local model that corresponds to the SILO definition of the detailed model. But, as the local model has a lower resolution, the conductivity values of the SILO in the local model (SD2) is slightly different compared to the values of the detailed model, the values of the local model being representative average values of the detailed model.

Furthermore, the tunnels are not of the same size in the different models. The horizontal deposition tunnels (BTF, BLA and BMA), of the local model, are defined as larger than the same tunnels in the detailed model. For the SILO it is the opposite, in the local model the SILO is smaller than in the detailed model. In the detailed model the sizes of the deposition tunnels are closer to the actual size of the deposition tunnels at SFR (see Table 9.1), except for the SILO. But, in the detailed model, the shape of the SILO is better than in the local model as it is closer to the cylindrical shape of the actual cavern.

A comparison of the predicted flows reveal that the local model predicts values of total flows of the deposition tunnels that are between a few percent and about 40 percent larger than the flow through the whole of the deposition tunnels, as predicted by the detailed model. These differences are reasonable, considering the differences in the description of the tunnels. The detailed model gives the best estimates, as this model includes the internal structures of the deposition tunnels and includes a higher degree of resolution.

10.7 Analytical estimate of tunnel flow

10.7.1 Purpose and methodology

The purpose of the analyticalal model is to estimate the magnitude of the groundwater flow through the deposition tunnels and thereby check that no fundamental error has been included in the numerical models. The methodology of the analytical method is briefly presented in Section 7.11. In short, a deposition tunnel is represented by a homogeneous ellipsoid, having approximately the same size as the deposition tunnel studied. The total flow through the ellipsoid is predicted under steady state conditions.

10.7.2 Results

Considering the regional groundwater flow in the rock mass and the fracture zones that surrounds the tunnels of the repository; at 2000 AD the regional flow is very close to vertical, and after approximately 5000 AD the regional flow is almost horizontal and towards NNE. For the horizontal deposition tunnels (BMA, BLA and BTF) it follows that at 2000 AD the regional flow is along the short axis of an ellipsoid representing a horizontal deposition tunnel; and at 5000 AD, the regional flow is approximately along the main axis of an ellipsoid representing a horizontal deposition tunnel. For the analytical estimates given in this section we have set the ellipsoid-tunnel as perfectly pervious and closed. The length of the tunnel is set to 160 m, as this is the length of the horizontal deposition tunnels, including the loading areas. Analytical estimates of the flow of ellipsoid-tunnels are given below in Figure 10.5. In this figure the total flow is given as a multiple of the regional flow and as a function of tunnel-ellipsoid volume.

To produce an analytical estimate of the tunnel flow, which can be compared to the results of the numerical models, we also need an estimate of the size of the regional specific flow. The numerical model (local model) predicts for Case 4 that due to the shore level displacement, the average regional specific flow in the local model will increase from 3 litre/(m^2 year) at 2000 AD to 7 litre/(m^2 year) at steady-state-like conditions (see Table 10.1). This is a volumetric average considering the flow of both the rock mass and that of the fracture zones, but not the flow of the tunnels. From a theoretical point of view, these values of regional specific flow are not directly applicable in the analytical model. The analytical model presumes a homogeneous flow medium, and the regional flow used in the analytical method should represent a regional flow far away from the ellipsoid, a regional flow that is undisturbed by the ellipsoid. However, the analytical method represents an idealised situation and it will only produce a rough estimate; and it is likely that a representative regional specific flow is within a range of 1 to10 litre/(m^2 year)

Thus, by use of the regional specific flow of the local model, the analytical method predicts values of tunnel flow that can be compared to the values predicted by the local model. The results of the analytical estimations and the corresponding results of the local model are given in Table 10.11. A comparison of the results of the analytical method and of the local model demonstrates that the analytical estimations are fairly close to the predictions of the local model. Hence, no fundamental error has been included in the numerical models.

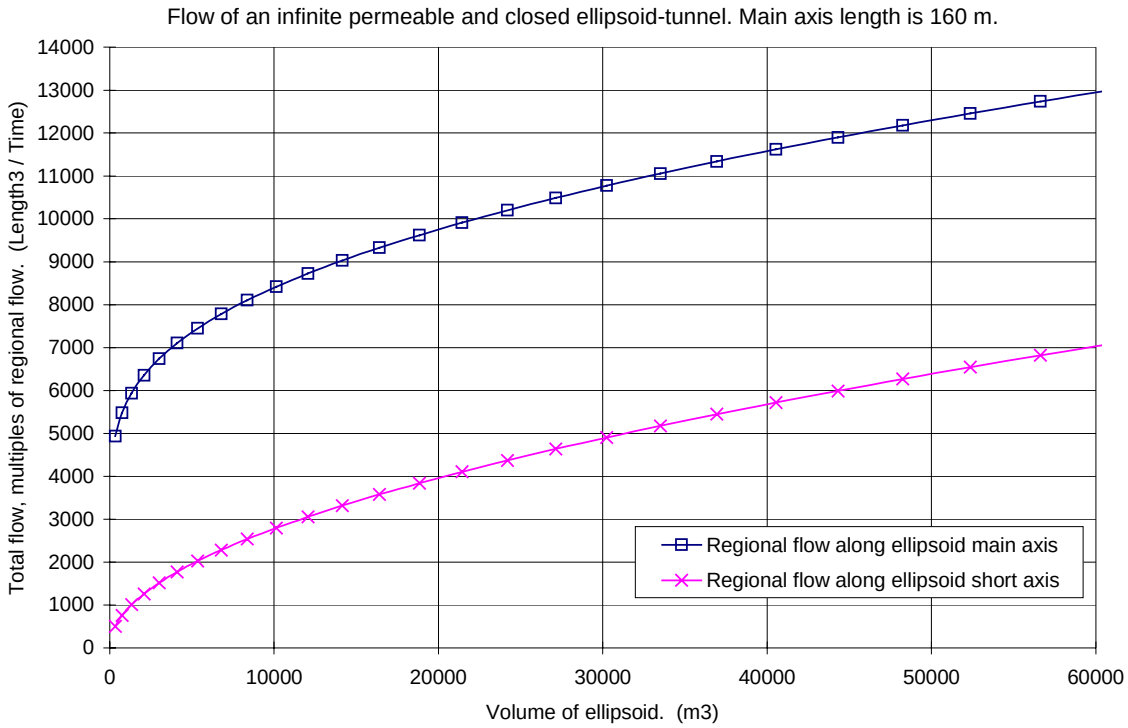

Figure 10.5 *Analytical estimation of total flow through an ellipsoid-tunnel.*

The total flow of the ellipsoid tunnel is estimated as a volume per unit time: Length^3/ Time, and as a multiple of the regional flow. The regional flow should be given as a volume per unit area and time: Length3/(Length2 Time). Hence, for an ellipsoid-tunnel of volume 45 000 m3 and length 160 m and for a regional flow of 1 litre/(m2 year) directed along the main axes of the ellipsoid-tunnel, the analytical method estimates a total flow of 12 000 litre/ year through the ellipsoid-tunnel.

Table 10.11 Analytical and numerical estimates of total flow of deposition tunnels.

Deposition Tunnel	Actual volume (m3)	Analytical Prediction of total flow (m3/year)		Numerical Prediction of total flow (m3/year) Local model. Base case.	
		Time 2000 AD (1)	Time 8000 AD (2)	Time 2000 AD	Time 8000 AD
SILO	47 500	-	-	1	4
BMA	47 600	19	85	5	65
BLA	27 600	14	74	15	61
BTF1	19 700	12	68	13	44
BTF2	19 700	12	68	12	41

(1) Vertical regional flow along ellipsoid short axis. Size of regional flow = 0.003 m3/m2 year
(2) Horizontal regional flow along ellipsoid main axis. Size of regional flow = 0.007 m3/m2 year

10.7.3 Comparison with previous studies

Groundwater flow and transport at SFR have previously been estimated by use of groundwater models.

- As a part of the safety analysis reported in 1987, a groundwater- modelling project was carried out. The work was presented in Carlsson *et al* (1987). The modelling was done in three dimensions. The simulations were carried out on three scales and the method of telescopic mesh refinement was applied. However, due to the computer capacity available at the time, the tunnel system was, even in the small scale, only included in a very simplified way. A single pipe represented all access tunnels, one 10 metres thick horizontal slab represented the deposition tunnels and the SILO was represented as a rectangular block.
- The Swedish Nuclear Power Inspectorate (SKI) analysed and developed the results of the work by Carlsson *et al* (1987), and presented there conclusions in SKI rapport 92:16 (1992).
- Stigsson *et al* (1998) investigated the importance of variable density flow at SFR, by use of a two-dimensional model, representing a large vertical cross-section.

This study predicts much smaller flow values than previous studies. This is partly a consequence of the much more detailed representation of the tunnel system in this modelling study, compared to the coarse representation used in previous studies. The coarse finite element meshes used in the study of Carlsson *et al* (1987) were necessary due to the computer capacities available at the time. A coarse representation of a complicated tunnel system will however have a large influence on the predicted tunnel flow. In a closed and complicated system of tunnels, the flow in the tunnels will vary at different sections of the system, due to the geometry of the tunnel system, the effects of tunnel-intersections and hydraulic cage effects etc. Furthermore, the total flow through a closed tunnel is not linearly proportional to the size of the tunnel (cross-section area, length, volume etc). And the average groundwater velocity and the total flow of a tunnel will not change (scale) in the same way if the size of the tunnel is changed. This is discussed in Holmén (1997). Thus, if a complicated system of small tunnels, like the one at SFR, is represented in a model by only three large structures, the predicted flow through the tunnels of the model will very much depend on the applicability of this simplification.

In the study by Carlsson *et al* (1987), the rock in the near surroundings of the tunnels (which was not defined as fracture zones) was defined with a much larger value of conductivity (see Sec.5.2.3) than the corresponding rock mass of the models of this study. Also a low-permeable skin-zone was introduced in the study by Carlsson *et al* (1987), a skin-zone which surrounded the blocks that represented the tunnels. The skin zone was defined as having a width of 5 m and with a value of conductivity equal to 0.35 times the conductivity of the rock mass. Such a skin-zone will partly reduce the flow through the blocks and thereby, as regards the tunnel flows, compensate for the large rock mass conductivity. No such general skin-zone was introduced in the models of this study; however in this study a skin/grout zone was introduced between the BMA deposition tunnel and Zone 6, see Table 6.3. Considering a drained tunnel system (present situation), the large values of rock conductivity used by Carlsson *et al* (1987) will produce an inflow to the tunnels which is much larger than the measured inflow, even with the skin zones surrounding the tunnels (see Sec.5.2.3 and Figure 5.3). The

coarse representation of the tunnel system and the large values of rock conductivity used by Carlsson *et al* (1987) is the likely explanation to the large values of tunnel flow predicted in that study.

For the BMA tunnel the differences are very large between the predictions by the detailed model of this study and the predictions by Carlsson *et al*. The total flow of the whole of the BMA tunnel, as predicted by the detailed model of this study, is about five percent of the flow predicted by Carlsson *et al*. Furthermore, the study by Carlsson *et al* did not include the internal structures of the deposition tunnels hence, the hydraulic cage that protects the encapsulation of the BMA tunnel were not included in the model established by Carlsson *et al*. As discussed in previous sections (see Sec.10.6.8), the hydraulic cage will significantly reduce the flow of the BMA encapsulation. For the base case of this study, the total flow of the BMA encapsulation, as predicted by the detailed model of this study, is six orders of magnitudes smaller than the flow predicted by Carlsson *et al* for the whole of the BMA tunnel. And as demonstrated by the alternative layouts of the BMA tunnel in the detailed model, a more efficient hydraulic cage can reduce the flow of the encapsulation even further.

Table 10.12 Predicted flow through deposition tunnels, previous estimations and the results of this study.

MODEL AND STRUCTURE	**TOTAL FLOW (m3 / year)** Range of values represents the development of the flow system, from 2000 AD until steady-state-like conditions, at ca. 5000 AD				
	SILO	**BMA**	**BLA**	**BTF1**	**BTF2**
Model by Carlsson et al 1987	7-25	320-1120	230-805	230-805	230-805
Interpretation by SKI 92:16	28	1280	920	920	920
Analytical estimations *(1)*	-	19 - 85	14 - 74	12 - 68	12 – 68
LOCAL MODEL Full tunnel	0.6-3.8 *(2)* 0.2-1.2 *(3)*	5-65	15-61	13-44	12-41
DETAILED MODEL Full tunnel *(4)*		9-55	14-55	7-30	7-30
Waste domain Encapsulation *(5)*	0.2	0.1-0.3	10-39	2-8	2-7
Encap. BMA A1 *(6)*		0.03-0.13			
Encap. BMA A2 *(7)*		0.01-0.03			
Encap. BMA A3 *(8)*		0.001-0.003			

(1) The tunnels are represented by infinite permeable ellipsoids, regional flow from local model, see Sec.10.7.
(2) Local model, SILO defined in accordance to the first SILO definition (SD1), see Section 6.5.4
(3) Local model SILO defined in accordance to the second SILO definition (SD2), see Section 6.5.4
(4) Base case: Total flow of the whole of the tunnel, including loading areas, top fill, encapsulation, etc.
(5) Base case: Total flow of the waste domains.
(6) BMA Alternative layout 1 , less permeable encapsulation (see Sec.10.6.8). Total flow of the waste domain.
(7) BMA Alternative layout 2, more permeable flow barriers (see Sec.10.6.8). Total flow of the waste domain.
(8) BMA Alternative layout 3, more permeable flow barriers (see Sec.10.6.8). Total flow of the waste domain.

11. Flow path analysis

11.1 Methodology

11.1.1 Introduction

As a part of this study we have conducted an extensive flow path analysis. The purpose of this analysis is to investigate the movement of the groundwater in the vicinity of the deposition tunnels. The flow path analysis presented in this chapter is based on simulations with the local model.

11.1.2 Method for calculation of flow paths

The flow pattern of the groundwater can be illustrated by the use of flow paths. The GEOAN model creates flow paths by the use of simulated particles, particles that follow the flow of groundwater through the model. The particle tracking algorithm could also be used for estimation of transportation times, transport processes, etc. For calculation of flow paths the GEOAN model provides the user with both a semi-analytical method (Pollock, 1989) and an iterative numerical method. For all calculations in this study we have used the semi-analytical method.

11.1.3 Method for release of particles

We want to investigate the flow of ground water from the deposition tunnels to the ground surface. The paths should represent the distribution of flow from the deposition tunnels; hence, the release of flow paths (particles) has to be flow dependent. In this study we have used the approach that a single flow path (a single particle) represents a certain amount of flow. Flow paths will be released at the envelope of the studied structures. For each cell having a face along a studied envelope, the model will calculate the flow across the face and release the number of flow paths that represents the flow across the face. The exact location of the start point will be random, but on the face. Hence, the distribution of flow paths will be flow dependent. As this is a discrete method there will be a threshold level, the flow has to be larger than this threshold level to be represented by a single flow path. However, as the calculation of a flow path is not very time-consuming, the threshold level can be set very low. For each studied deposition tunnel and for each studied moment in time we have released approximately 1500 flow paths, which gives a total of approximately 7500 flow paths for each studied moment in time. We have varied the number of released flow paths and found that at this number of flow paths, the calculated statistics of the flow paths are reliable.

11.1.4 Time dependency of flow paths

In the models, flow paths will develop inside a head field that controls the movements of the paths. For a time-independent flow path, the path will develop inside a head field that will not change with time. Hence, the head field is constant during the movement of the simulated particle that gives the flow path. For a time-dependent flow path, the head field will change with time during the movement of the simulated particle that gives the flow path. Theoretically, the actual movement of a particle should take place in a changing head field, because the head field will change while the particle moves through the rock mass. The GEOAN model can simulate both time-dependent and time-independent flow paths. In this study we have primarily generated flow paths that are time-independent. Such flow paths represent the flow field for the studied moment in time.

11.1.5 Dispersion and retardation

Dispersion is the tendency for a solute, dissolved in the groundwater, to spread out from the path that it would be expected to follow according to the advective hydraulics of the flow system. Dispersion is caused by diffusion and mechanical mixing during fluid advection. Additionally, in a mathematical model an unwanted numerical dispersion may also take place, due to the method used for representation of the transport process.

- *Diffusion,* is not included in the established model.
- *The mechanical mixing, called mechanical dispersion,* is caused by the heterogeneous properties of the flow medium. Mechanical dispersion is scale dependent and will occur both at a microscopic scale and at a macroscopic scale. In the models we have not included mechanical dispersion as a tendency for the flow paths to spread out from the advective path. However, the models are defined with some heterogeneous properties (i.e. fracture zones contra rock mass) and there will be a spread of the flow paths caused by the heterogeneity of the flow medium, as the heterogeneity will cause the advective paths to spread out.
- *Numerical dispersion*. If the model uses a fixed mesh and the solution of the advection-dispersion equation for representation of the transport process, numerical dispersion will influence the results. However, the model of this study (GEOAN) uses the approach of tracking of particles and for this approach there is no numerical dispersion. Hence, the established model will not be influenced by unwanted numerical dispersion.
- *Retardation.* No retardation is included in this model.

Thus, in this study we have examined advective transport only, but advective transport through a heterogeneous flow medium.

11.1.6 The not included heterogeneity of the local domain

For some of the results presented in this chapter, the unknown and not included heterogeneity might be of some importance i.e. breakthrough times. This is discussed in Section 17.8. Considering the results of the flow path analysis, the approach used for the local domain, with a homogeneous rock mass between given fracture zones having

different but homogeneous properties, will provide us with good estimates considering average representative results. However, the actual variation of results caused by the local heterogeneity of the rock mass and especially by the heterogeneity inside the fracture zones, is not included in this study. To calculate such a variation also the heterogeneity of the rock mass and the fracture zones need to be included and as such heterogeneity has not been included in this study no such variation is calculated.

11.1.7 Percentiles

The results of the path way analysis are based on a statistical analysis of the properties of each simulated flow path. The properties of the flow paths, e.g. length of paths, form different statistical distributions. The statistical distributions are characterised by percentiles. A percentile is defined as “a value below which a certain percentage of the observations fall”.

11.2 Visualisation

11.2.1 General

To get an impression of the flow conditions and the flow paths at SFR, we have visualised the calculated paths together with the layout of the tunnel system and some of the important fracture zones. The results are given in the following figures of this section.

In these figures the number of released flow paths is selected for the purpose of creating a good visualisation, only the dominating flow routes will be illustrated in the figures. The statistics of the flow paths (presented in the following sections) is based on a much larger number of paths than the paths visualised in the following figures. The release of flow paths is flow dependent, hence the number of released paths depend on the flow across the envelope of the studied tunnel. The number of paths is approximately the same in all figures, but as the flow changes with time, the amount of flow that is represented by a single path is different in the different figures. The actual number of paths, illustrated in a figure, is determined by the flow through the SILO, as this is the object through which the flow is the smallest. Only a small number of paths will illustrate the flow from the SILO, otherwise the number of paths from the BMA, BLA and BTF tunnels will be to many to produce a good visualisation. As the number of paths from the SILO is small, only the very dominating flow routes from the SILO will be illustrated in the figures. The lengths of the paths have also been limited in the figures, the uppermost 20 metres of the paths (the last 20 metres close to the ground surface), are not illustrated.

Generally the flow paths develop in the following way. As long as the sea covers the ground above the SFR, the flow paths are short and nearly vertical from the deposition tunnels to the ground surface. When the general direction of the groundwater flow changes, from vertical to a more horizontal flow in direction towards NNE, the lengths of the paths increases, as the flow pattern becomes more complicated. Deep flow paths will occur, mainly in fracture zone 6.

The models simulate the flow through the repository, as if the repository is closed and abandoned. The illustrated flow paths are time-independent.

11.2.2 Figures

The figures illustrate the flow situation for 4 different moments.

- For time equal to 2000 AD, see Figure 11.1 and Figure 11.2.
- For time equal to 3000 AD, see Figure 11.1 and Figure 11.2.
- For time equal to 4000 AD, see Figure 11.5 and Figure 11.6.
- For time equal to 6000 AD, see Figure 11.7 and Figure 11.8.

Note that only the dominating flow routes will be illustrated in the figures, and that the lengths of the paths have been limited in the figures, the uppermost 20 metres of the paths (the last 20 metres close to the ground surface) are not illustrated.

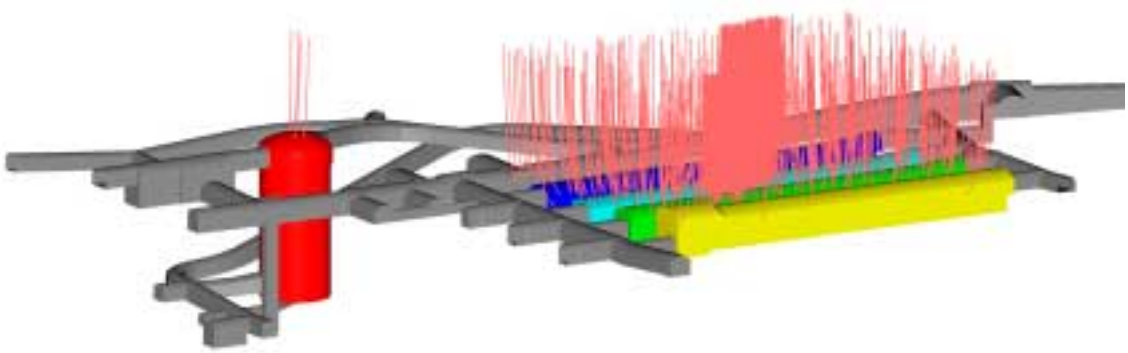

Figure 11.1 *Time: 2000 AD. The tunnel system and the flow paths (base case).*

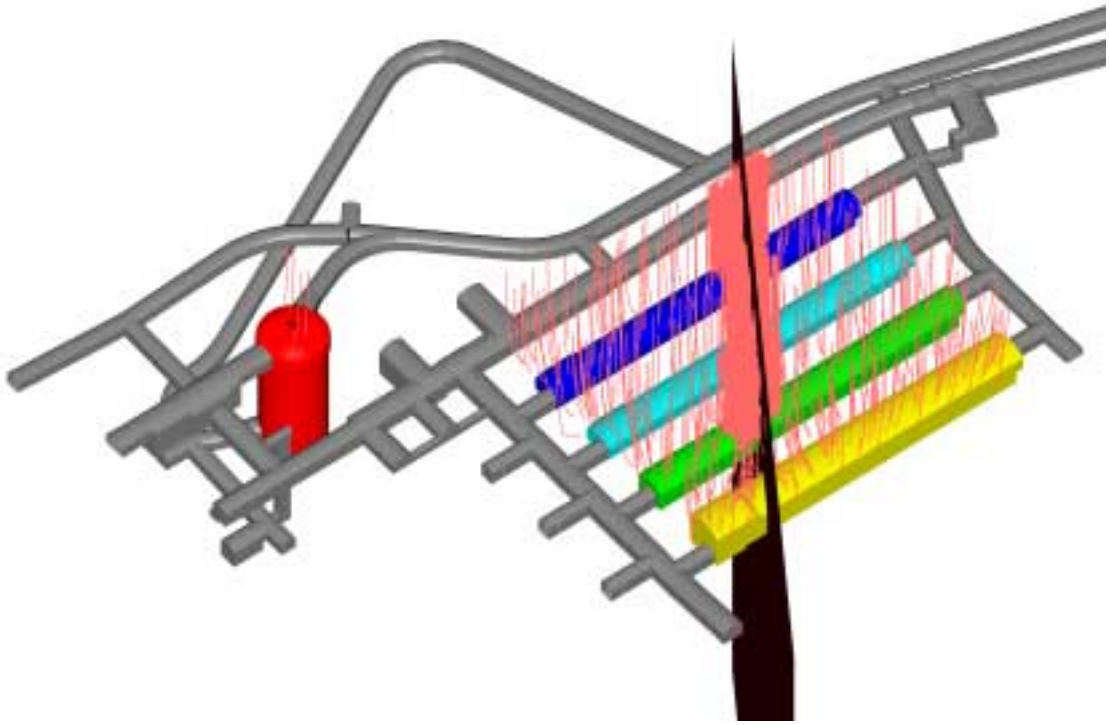

Figure 11.2 *Time: 2000 AD. The tunnel system, the flow paths and the vertical fracture zone 6 (base case).*

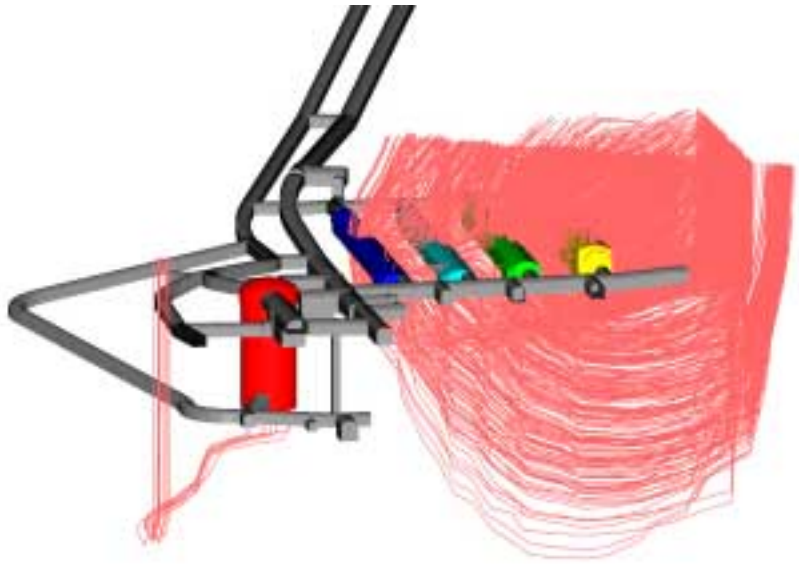

Figure 11.3 *Time: 3000 AD. The tunnel system and the flow paths (base case).*

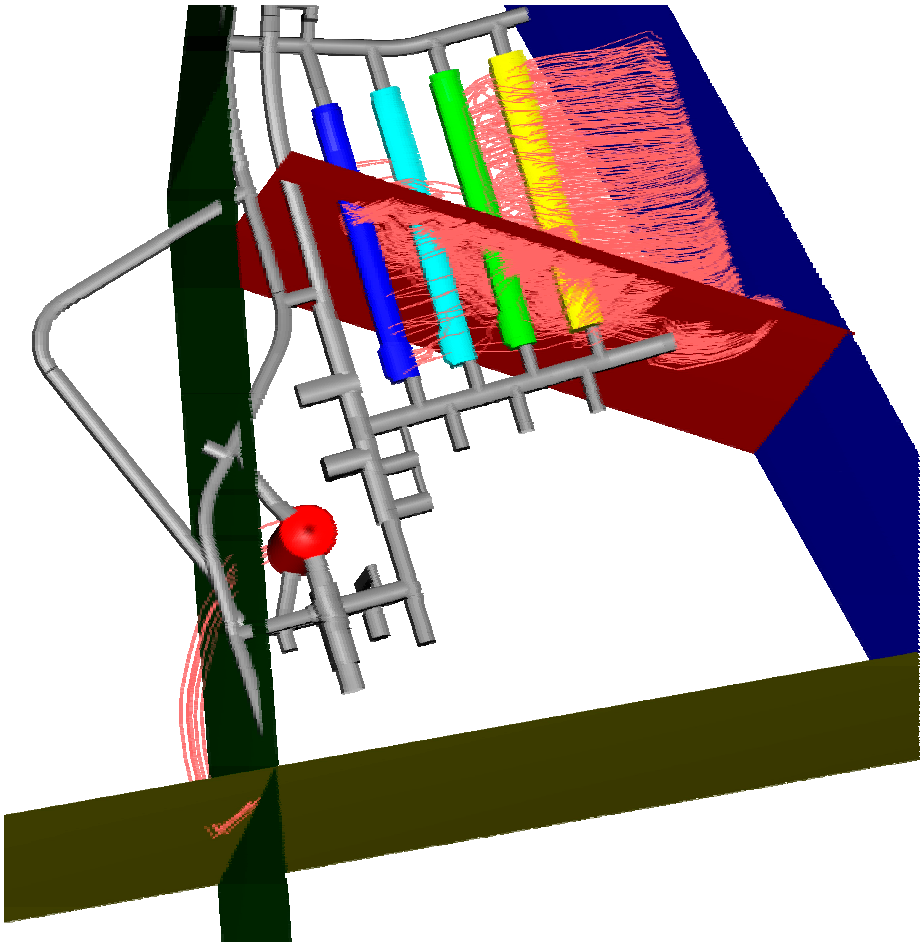

Figure 11.4 *Time: 3000 AD. The tunnel system, the flow paths and the vertical fracture zones (base case).*

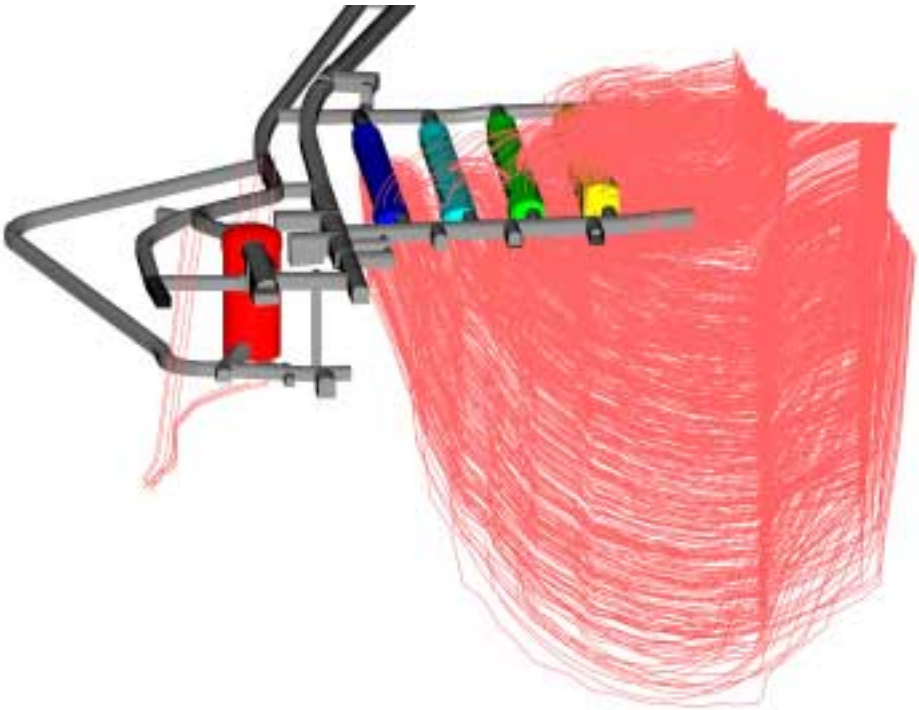

Figure 11.5 *Time: 4000 AD. The tunnel system and the flow paths (base case).*

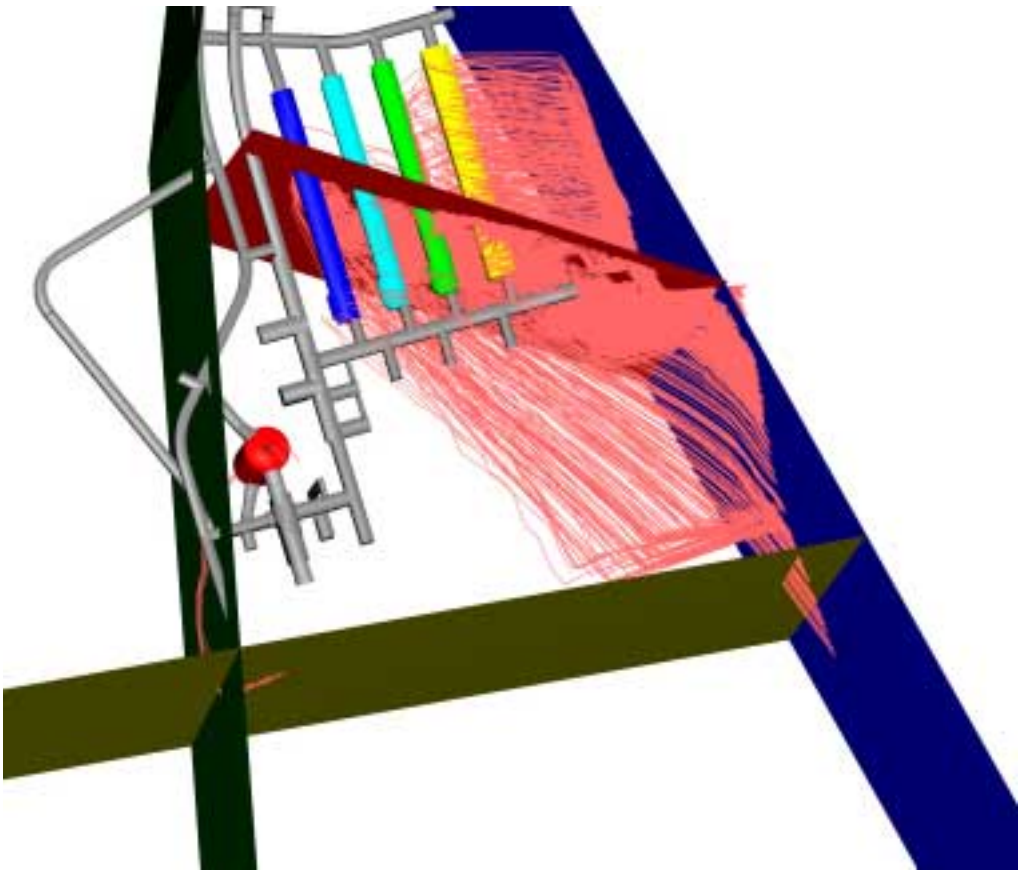

Figure 11.6 *Time: 4000 AD. The tunnel system, the flow paths and the vertical fracture zones (base case).*

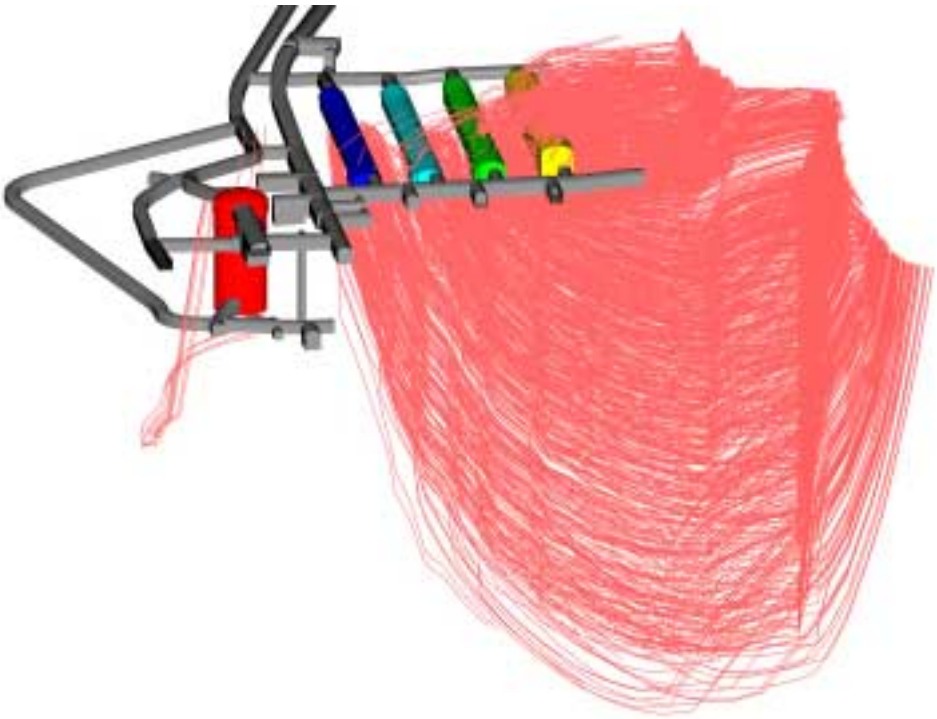

Figure 11.7 *Time: 6000 AD, steady-state-like conditions. The tunnel system and the flow paths (base case).*

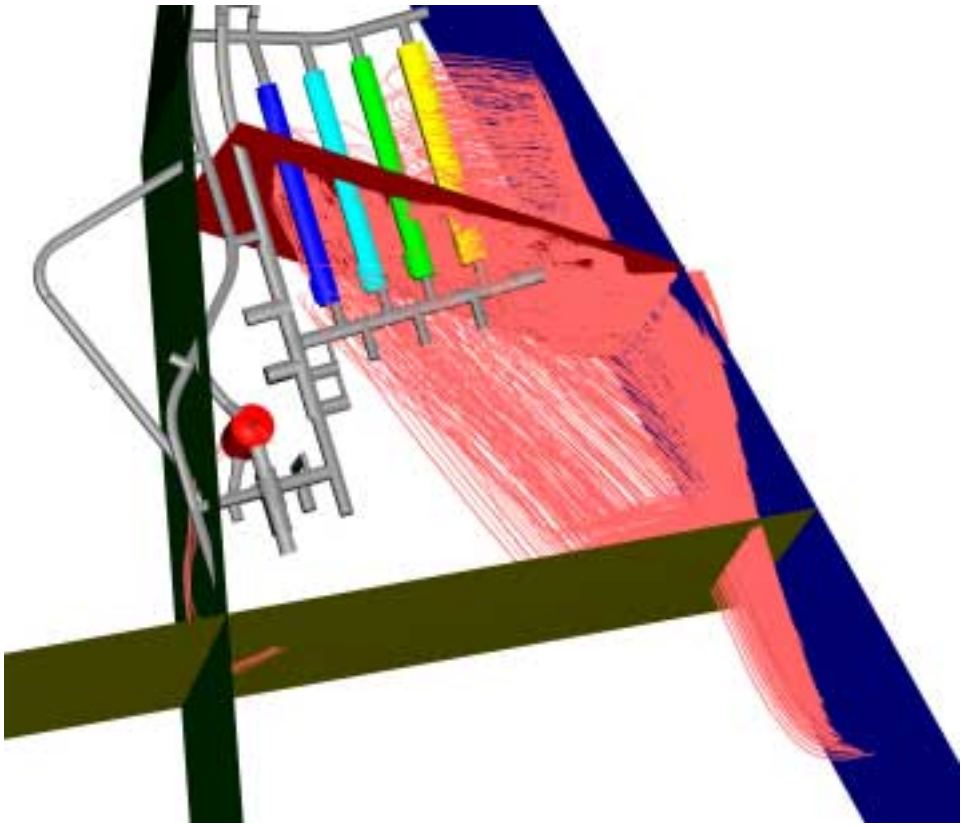

Figure 11.8 *Time: 6000 AD, steady-state-like conditions. The tunnel system, the flow paths and the vertical fracture zones (base case).*

11.3 Length of flow paths

11.3.1 General

The models predict that as long as the sea covers the ground above the SFR, the flow paths are short and nearly vertical from the deposition tunnels to the ground surface. When the general direction of the groundwater flow changes, from vertical to a more horizontal flow, the lengths of the paths increase, as the flow pattern becomes more complicated. For the five different deposition tunnels, the length of the flow paths versus time has been calculated for each tunnel separately. The different lengths of the flow paths form different statistical distributions, the distributions are characterised by percentiles. The results for time-independent flow paths are given in Figure 11.9, as well as in Table 11.1 through Table 11.5. In the tables below results are given for different times. Time equal 2000 AD represents the situation when the sea is above the repository. Time equal 5000 AD represents the situation when the flow field has reached a local steady-state-like situation and is no longer strongly influenced by the shore level displacement. Time equal 7000 AD represents the final situation, for which the flow field is at steady state and the shore level is far away.

11.3.2 BMA and BLA tunnel

Generally, the shortest flow paths are from the BMA and BLA tunnels, as they are closest to the discharge areas.

Table 11.1 Lengths of flow paths from the BMA tunnel (base case).

BMA		Flow path length (m)	
Time AD	10^{th} Percentile	50^{th} Percentile	90^{th} Percentile
2000	66	67	73
3000	77	114	199
4000	96	176	260
5000	112	206	312
6000	114	214	316
7000	115	216	316

Table 11.2 Lengths of flow paths from the BLA tunnel (base case).

BLA		Flow path length (m)	
Time AD	10^{th} Percentile	50^{th} Percentile	90^{th} Percentile
2000	71	71	75
3000	80	89	239
4000	129	308	403
5000	162	375	482
6000	176	387	496
7000	177	387	496

11.3.3 BTF1 and BTF2 tunnels

Generally, the longest flow paths are from the BTF tunnels, as they are furthest away from the discharge areas.

Table 11.3 Lengths of flow paths from the BTF1 tunnel (base case).

BTF1	Flow path length (m)		
Time AD	10th Percentile	50th Percentile	90th Percentile
2000	77	77	78
3000	86	125	459
4000	395	617	735
5000	395	789	930
6000	391	785	934
7000	391	785	934

Table 11.4 Lengths of flow paths from the BTF2 tunnel (base case).

BTF2	Flow path length (m)		
Time AD	10th Percentile	50th Percentile	90th Percentile
2000	77	77	78
3000	84	99	352
4000	366	481	559
5000	416	584	740
6000	418	604	755
7000	418	604	755

11.3.4 SILO

The SILO is located a short distance from the other four deposition tunnels. The flow paths from the SILO are separated from the paths of the other deposition tunnels. For the SILO, the short vertical flow route will be maintained throughout the simulation period.

Table 11.5 Lengths of flow paths from the SILO (base case).

SILO	Flow path length (m)		
Time AD	10th Percentile	50th Percentile	90th Percentile
2000	66	66	131
3000	80	379	425
4000	69	341	384
5000	70	355	395
6000	71	355	395
7000	71	355	395

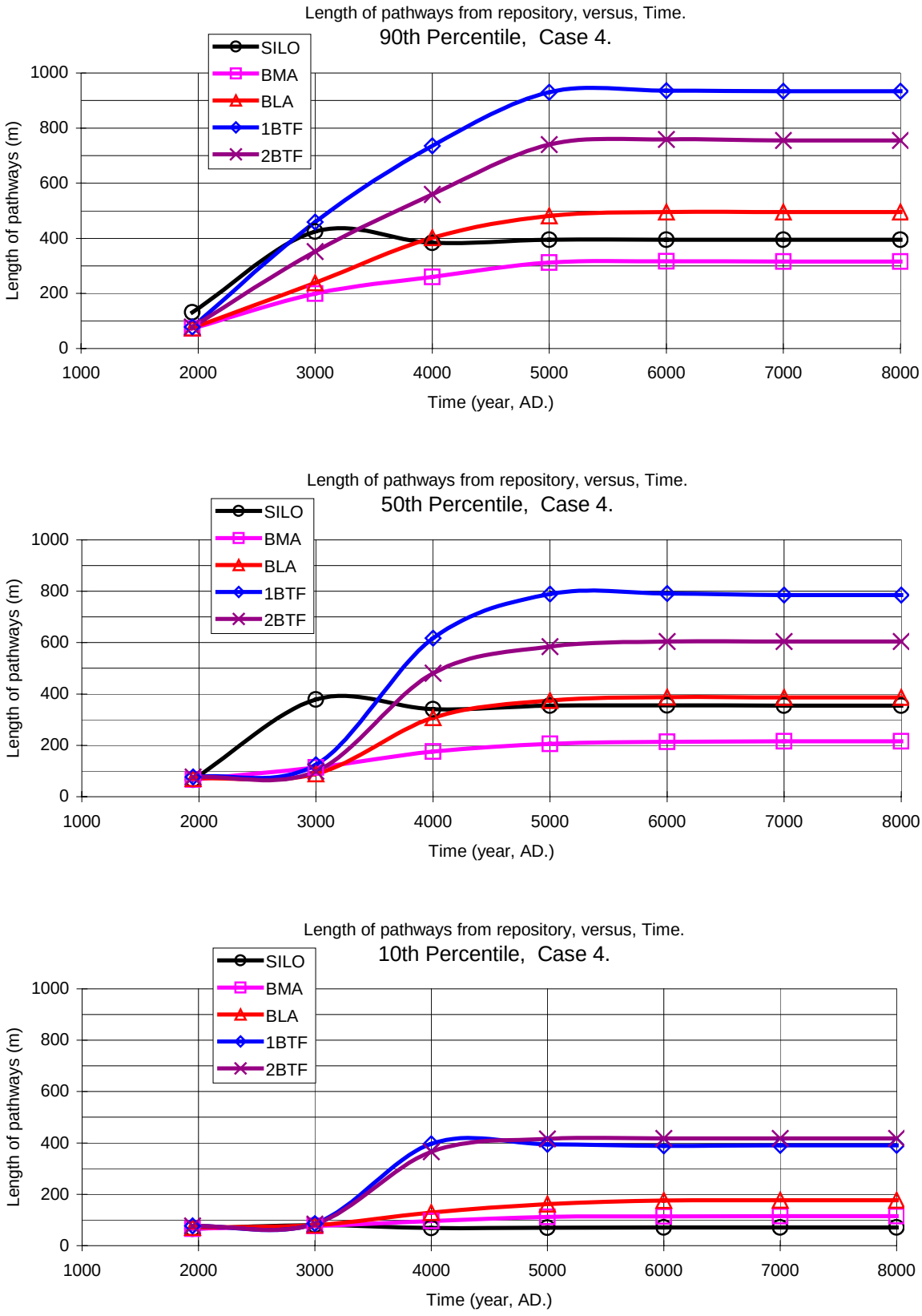

Figure 11.9 *Length of flow paths from the different deposition tunnels (base case). The figures give the length of the paths for three different percentiles, 90, 50 and 10.*

11.4 Breakthrough times

11.4.1 Introduction

In the model the groundwater flow field and the effective porosity govern the velocity of the groundwater; and as the flow field change size and direction due to the shore level progress, the breakthrough times will vary during the studied time period. We have studied two different cases having different values of the effective porosity, the base case and the alternative case.

11.4.2 Different cases

Two different cases have been studied and these cases are presented in Section 6.8.3. For the base case, different values of effective porosity were used in the model, for the alternative case the effective porosity was the same for both the rock mass and the fracture zones.

- Base case: the effective porosity of the local fracture zones is between 1 and 5 percent and the effective porosity of the rock mass is 0.5 percent.
- Alternative case: the effective porosity of rock mass and fractures zones is 1 percent.

The alternative case can be used when estimating the breakthrough times for other values of the effective porosity, as the breakthrough times are proportional to the effective porosity. For example, a constant effective porosity of 0.5 percent as regards fracture zones and rock mass will produce breakthrough times that are close to 0.5 times the values given for the alternative case. However, it should be noted that for some flow paths, the breakthrough times are also dependent on the transport inside the tunnel system, hence for very small values of the effective porosity of the rock mass and the fracture zones, the scaling procedure discussed above is not applicable.

11.4.3 Variables for modelling of radionuclide transport processes

Detailed modelling of nuclide transport processes is not included in this study. If such modelling is based on the results of this study, a variable *C* is of interest; it is defined below:

$$C = \sum \frac{L}{q}$$

Where: L = Length of a section (Length)
q = Specific flow of section (Length / time)

The variable *C* is a cumulative value taken over different sections along the flow paths from the repository to the discharge areas. By use of the studied model it is possible to calculate *C* based on the results of the alternative case, for which the effective porosity is constant and equal to one percent; the calculations are as given below:

$$C = 100 * t_{breakthrough}$$

Where: $t_{breakthrough}$ *= Breakthrough time of alternative case (time)*

Hence, the variable *C* is equal to the breakthrough times of the alternative case multiplied by 100 and is therefore easily deduced from the results of that case.

11.4.4 General results

For the base case, different values of the effective porosity were selected for the rock mass and for the fracture zones, based on the present measured and interpreted movement of seawater from the sea towards the repository; and the same transport as predicted by the model, see Section 6.8.3. Generally for the base case, the models predict that we will have the shortest breakthrough times at approximately 3000 AD, considering flow paths from the BMA, BLA, BTF1 and BTF2, and at 4000 AD for flow paths from the SILO; because during this period we will have a large groundwater flow as well as short flow paths. Earlier, at 2000 AD, the flow paths are short, but the magnitude of the groundwater flow is small too. At 4000-5000 AD and further on, the flow is large but the flow paths are long as well. As the shoreline retreats from the repository area, there is a tendency for the flow paths to more extensively use the fracture zones (see Sec.11.5), compared to the situation when the sea is above the repository. It follows that for the base case, the different values of effective porosity, defined for the rock mass and the zones will influence the breakthrough times.

For the alternative case, one value of effective porosity was used for both the rock mass and the fracture zones. The results of the alternative case are complex and should not be interpreted without considering the constant value of effective porosity used for this case. For the flow paths from the SILO, the breakthrough times decreases with time as the size of the flow increases, a minimum in breakthrough time is reached at about 4000 AD, after which a small increase in breakthrough times take place. For the flow paths from the BMA, the behaviour is similar, except for the 10^{th} percentile which has a minimum at 3000 AD. For the flow paths from the BLA, the breakthrough times has a minimum at 3000 AD. For the flow paths from the BTF1 and BTF2, the breakthrough times has a minimum at 2000 AD for the 10^{th} and 50^{th} percentile, but at 3000 AD for the 90^{th} percentile.

Thus in the model, the breakthrough times depends on both the magnitudes of the groundwater flow and on the lengths of the flow paths; additionally, if different values of the effective porosity are defined for different fracture zones (i.e. the base case), the breakthrough times will also depend on the preferred flow routes, as different flow routes uses different fracture zone and the zones are defined with different values of the effective porosity.

For the flow paths from the five different deposition tunnels, the breakthrough times of the paths versus time has been calculated for each tunnel separately. The different breakthrough times form different statistical distributions and the distributions are characterised by percentiles. The results for time-independent flow paths are given in Figure 11.10 and Figure 11.11, as well as in Table 11.6 through Table 11.15. In the tables below, results are given for different times. Time equal 2000 AD represents the situation when the sea is above the repository. Time equal 3000 AD or 4000 AD represents the situation when the breakthrough times are short and the shoreline is close to the repository. Time equal 7000 AD represents the final situation, for which the flow field is at steady state and the shore level is far away.

11.4.5 BMA and BLA tunnel

Generally, the shortest breakthrough times are for paths from the BMA and BLA tunnels, as they are closest to the discharge areas.

Table 11.6 Base case: Breakthrough times of flow paths from the BMA tunnel.

BMA	Flow paths, breakthrough time (Years)		
Time AD	10th Percentile	50th Percentile	90th Percentile
2000	103	248	319
3000	18	52	91
4000	39	74	106
5000	49	84	127
6000	51	86	132
7000	51	87	132

Table 11.7 Base case: Breakthrough times of flow paths from the BLA tunnel.

BLA	Flow paths, breakthrough time (Years)		
Time AD	10th Percentile	50th Percentile	90th Percentile
2000	32	56	284
3000	12	18	100
4000	31	87	178
5000	55	127	240
6000	58	137	265
7000	58	137	265

Table 11.8 Alternative case: Breakthrough times of flow paths from the BMA tunnel.

BMA	Flow paths, breakthrough time (Years)		
Time AD	10th Percentile	50th Percentile	90th Percentile
2000	68	498	627
3000	15	93	189
4000	22	55	139
5000	26	59	154
6000	27	58	158
7000	27	59	158

Table 11.9 Alternative case: Breakthrough times of flow paths from the BLA tunnel.

BLA	Flow paths, breakthrough time (Years)		
Time AD	10th Percentile	50th Percentile	90th Percentile
2000	13	23	580
3000	9	13	44
4000	13	33	97
5000	22	44	166
6000	24	46	205
7000	23	46	210

11.4.6 BTF1 and BTF2 tunnels

Generally, the longest breakthrough times are for paths from the BTF tunnels, as they are furthest away from the discharge areas.

Table 11.10 Base case: Breakthrough times of flow paths from the BTF1 tunnel.

BTF1	Flow paths, breakthrough time (Years)		
Time AD	10th Percentile	50th Percentile	90th Percentile
2000	46	58	338
3000	35	119	367
4000	238	384	909
5000	262	491	968
6000	262	521	978
7000	262	521	983

Table 11.11 Base case: Breakthrough times of flow paths from the BTF2 tunnel.

BTF2	Flow paths, breakthrough time (Years)		
Time AD	10th Percentile	50th Percentile	90th Percentile
2000	48	56	335
3000	21	44	236
4000	151	214	521
5000	198	286	651
6000	204	297	665
7000	204	303	676

Table 11.12 Alternative case: Breakthrough times of flow paths from the BTF1 tunnel.

BTF1	Flow paths, breakthrough time (Years)		
Time AD	10th Percentile	50th Percentile	90th Percentile
2000	19	23	685
3000	91	157	627
4000	98	399	1610
5000	133	646	1510
6000	129	644	1540
7000	129	644	1540

Table 11.13 Alternative case: Breakthrough times of flow paths from the BTF2 tunnel.

BTF2	Flow paths, breakthrough time (Years)		
Time AD	10th Percentile	50th Percentile	90th Percentile
2000	20	23	691
3000	23	64	247
4000	60	96	875
5000	68	168	1080
6000	72	196	1100
7000	71	192	1080

11.4.7 SILO

The SILO is located a short distance from the other four deposition tunnels. The flow paths from the SILO are separated from the paths of the other deposition tunnels. For the SILO, the short vertical flow route will be maintained throughout the simulation period. Generally for the SILO, the shortest breakthrough times occur at 4000 AD.

Table 11.14 Base case: Breakthrough times of flow paths from the SILO.

SILO	Flow paths, breakthrough time (Years)		
Time AD	10^{th} Percentile	50^{th} Percentile	90^{th} Percentile
2000	300	313	1056
3000	80	379	425
4000	40	121	163
5000	45	129	172
6000	47	131	182
7000	47	131	182

Table 11.15 Alternative case: Breakthrough times of flow paths from the SILO.

SILO	Flow paths, breakthrough time (Years)		
Time AD	10^{th} Percentile	50^{th} Percentile	90^{th} Percentile
2000	590	619	3125
3000	140	344	1608
4000	78	91	266
5000	85	100	264
6000	88	103	268
7000	88	104	268

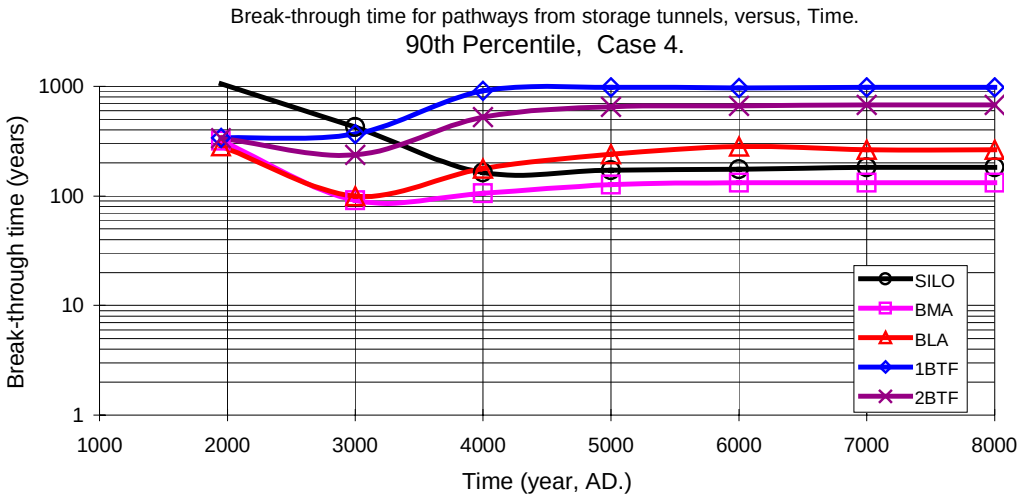

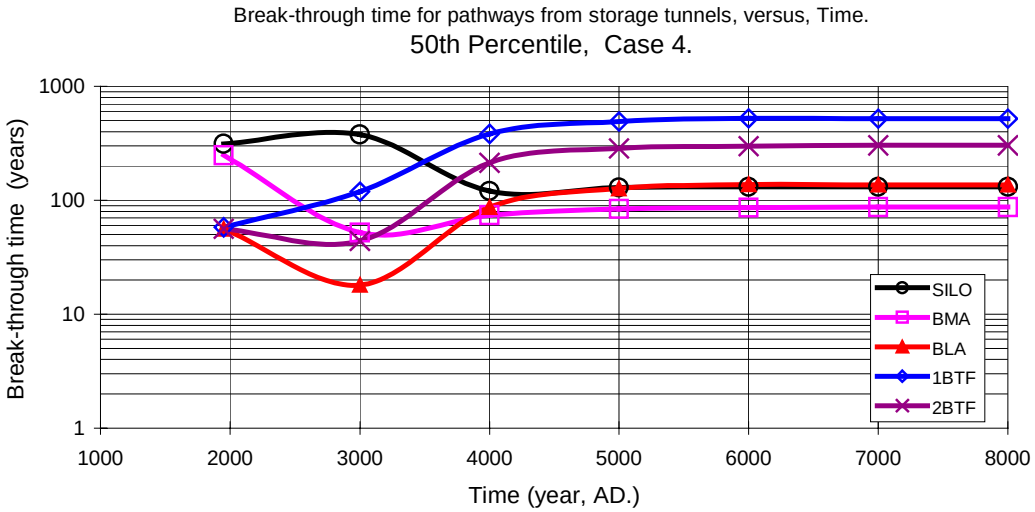

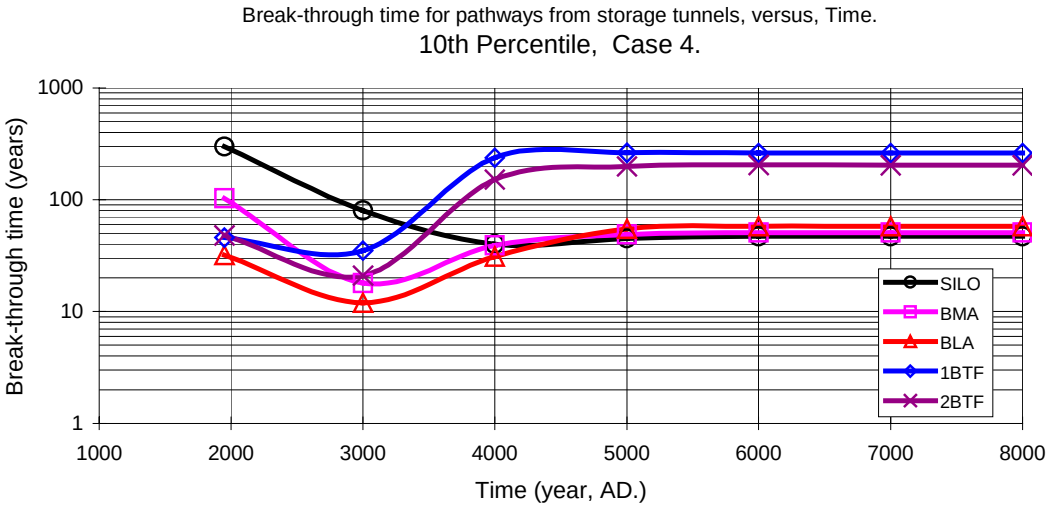

Figure 11.10 *Breakthrough times for the base case. Breakthrough times for flow paths from the different deposition tunnels. The figures give the times for three different percentiles, 10, 50 and 90.*

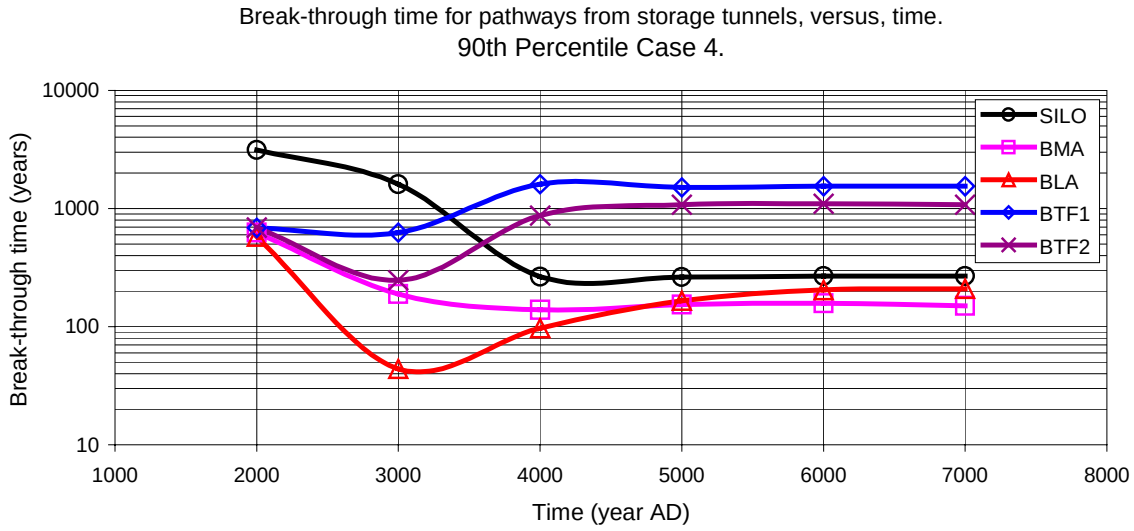

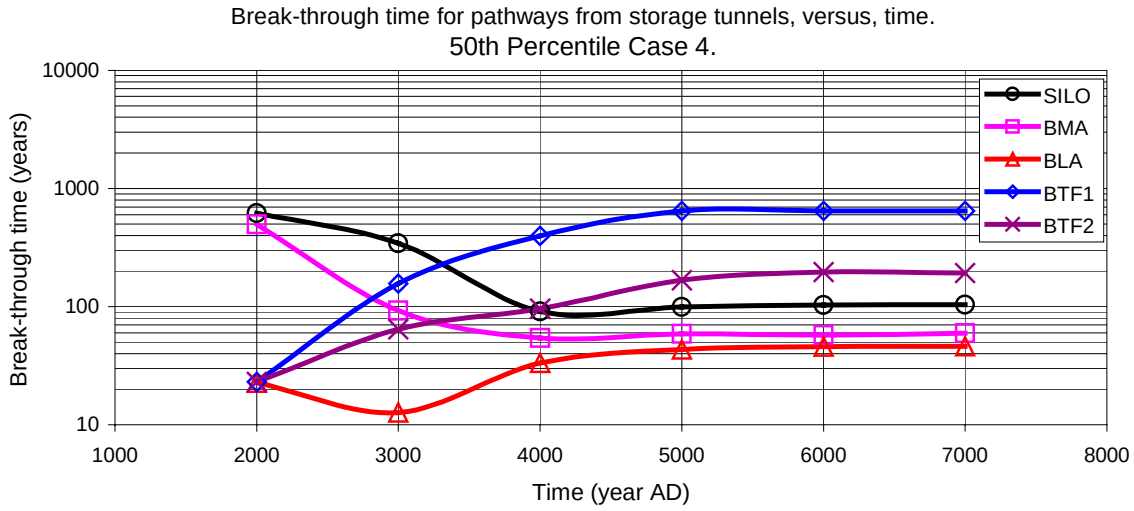

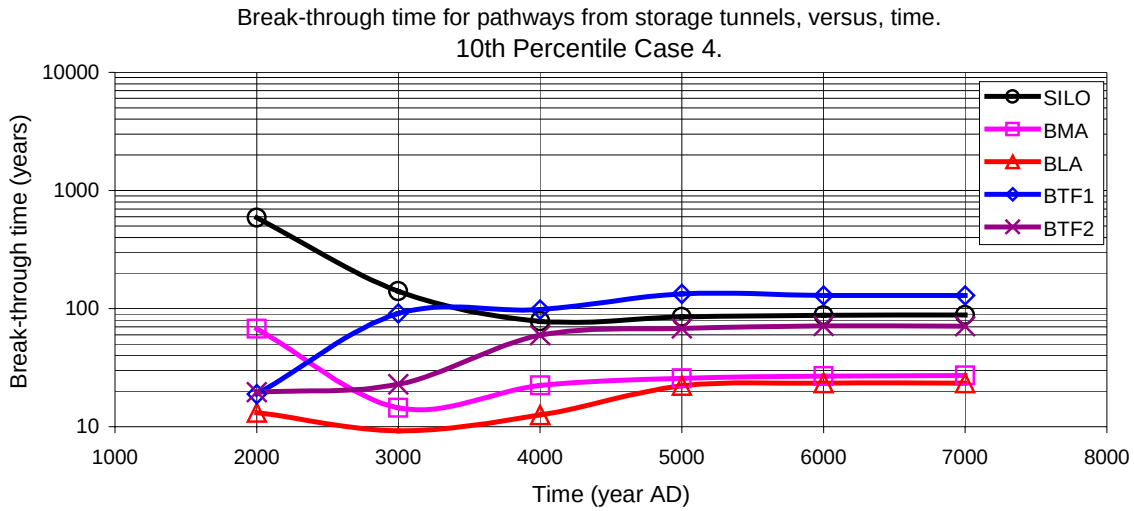

Figure 11.11 *Breakthrough times for the alternative case: Breakthrough times for flow paths from the different deposition tunnels. The figures give the times for three different percentiles, 10, 50 and 90.*

11.5 Importance of Zones as conductors of flow from the deposition tunnels

11.5.1 General

By investigating which fracture zones occur along a flow path, we can estimate the importance of the different zones, as conductors of the flow from the deposition tunnels. To calculate the importance of a zone we will estimate the share of the total flow from a deposition tunnel that passes through the zones (the flow paths were released by use of a flow dependent condition). As the flow paths may use several zones during a single path, the sum of the percentages is not necessarily equal to 100%. The general evolution is that the importance of the zones as conductors of the flow from the deposition tunnels increases with time. At 2000 AD the only important zone is zone 6; at 7000 AD zones H2, 3, 6, 8 and 9 are all involved in the flow pattern of the flow paths from the deposition tunnels. The results for time-independent flow paths are given in Figure 11.12 and Figure 11.13. The figures present the results focusing on the distribution of flow in the different zones. Focusing on the distribution of flow from the deposition tunnels, the detailed results are given in Table 11.16 through Table 11.20. The importance of fracture zones is also discussed in Section 17.3.

11.5.2 BMA tunnel

The percentage of the total flow, from the BMA tunnel, that passes through a fracture zone is given below.

Table 11.16 Important zones for the flow from the BMA tunnel (base case).

	Important Zones (percentage of flow from the tunnel that passes the zone)				
Time AD	Z-H2	Z-3	Z-6	Z-8	Z-9
2000	-	-	24	-	-
3000	28	35	47	-	-
4000	40	62	55	-	-
5000	42	73	61	2	-
7000	45	76	71	2	-

11.5.3 BLA tunnel

The percentage of the total flow, from the BLA tunnel, that passes through a fracture zone is given below.

Table 11.17 Important zones for the flow from the BLA tunnel (base case).

	Important Zones (percentage of flow from the tunnel that passes the zone)				
Time AD	Z-H2	Z-3	Z-6	Z-8	Z-9
2000	-	-	80	-	-
3000	9	13	99	-	-
4000	22	67	96	-	-
5000	24	76	95	7	-
7000	23	77	95	12	-

11.5.4 BTF1 tunnel

The percentage of the total flow, from the BTF1 tunnel, that passes through a fracture zone is given below.

Table 11.18 Important zones for the flow from the BTF1 tunnel (base case).

	Important Zones (percentage of flow from the tunnel that passes the zone)				
Time AD	Z-H2	Z-3	Z-6	Z-8	Z-9
2000	-	-	79	-	-
3000	16	16	93	-	-
4000	39	51	76	47	-
5000	37	74	74	88	-
7000	40	70	73	85	-

11.5.5 BTF2 tunnel

The percentage of the total flow, from the BTF2 tunnel, that passes through a fracture zone is given below.

Table 11.19 Important zones for the flow from the BTF2 tunnel (base case).

	Important Zones (percentage of flow from the tunnel that passes the zone)				
Time AD	Z-H2	Z-3	Z-6	Z-8	Z-9
2000	-	-	79	-	-
3000	17	19	98	-	-
4000	40	84	86	23	-
5000	38	87	84	73	-
7000	41	86	84	87	-

11.5.6 SILO

The percentage of the total flow, from the SILO tunnel, that passes through a fracture zone is given below.

Table 11.20 Important zones for the flow from the SILO tunnel (base case).

	Important Zones (percentage of flow from the tunnel that passes the zone)				
Time AD	Z-H2	Z-3	Z-6	Z-8	Z-9
2000	All flow directly through the rock mass				
3000	83	-	-	75	83
4000	55	-	-	55	55
5000	60	-	-	60	60
7000	61	-	-	61	61

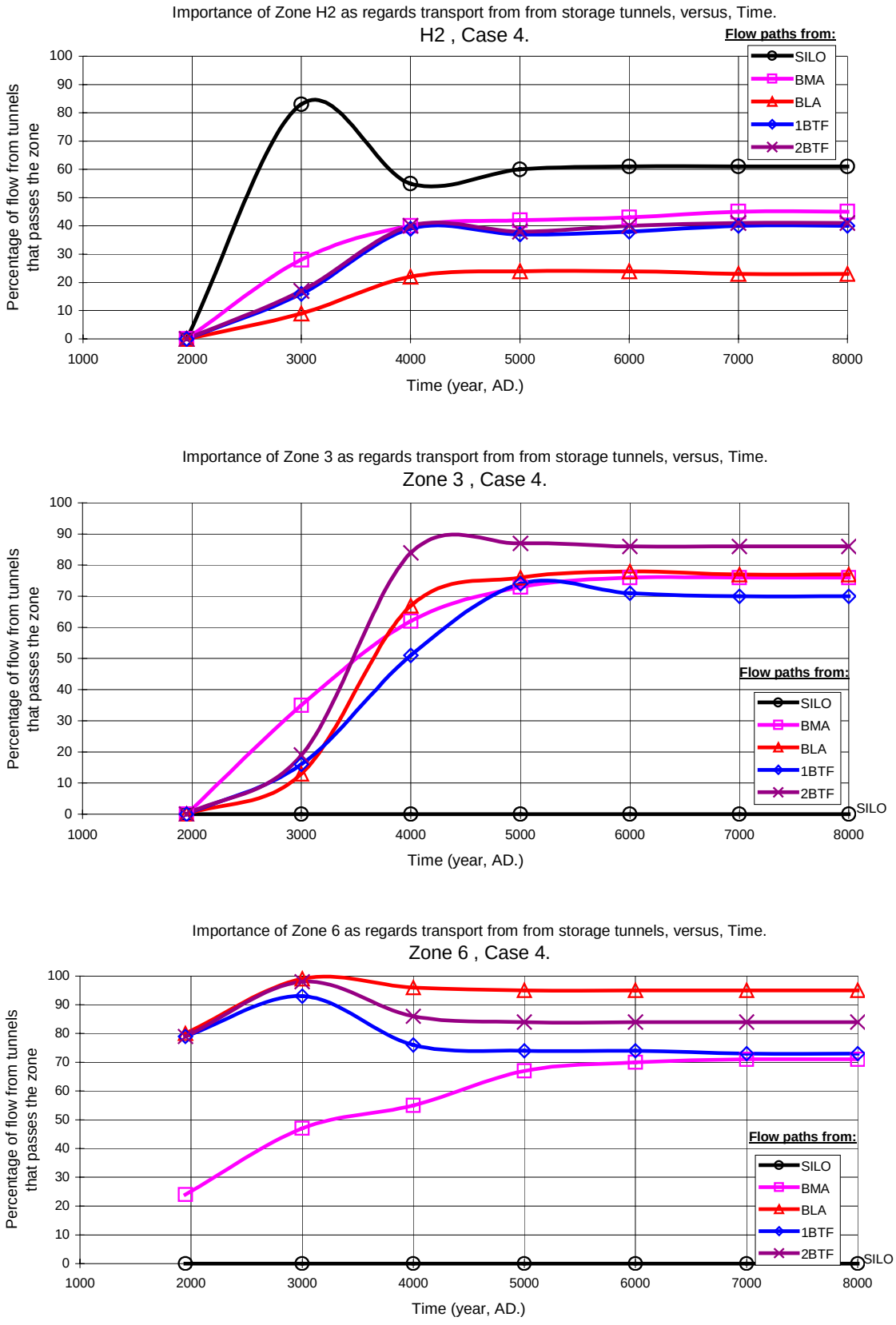

Figure 11.12 *Importance of Zones H2, 3 and 6, as conductors of the transport from the deposition tunnels (base case). The figures give the amount of the flow from a deposition tunnel that passes through a zone (flow dependent release of paths).*

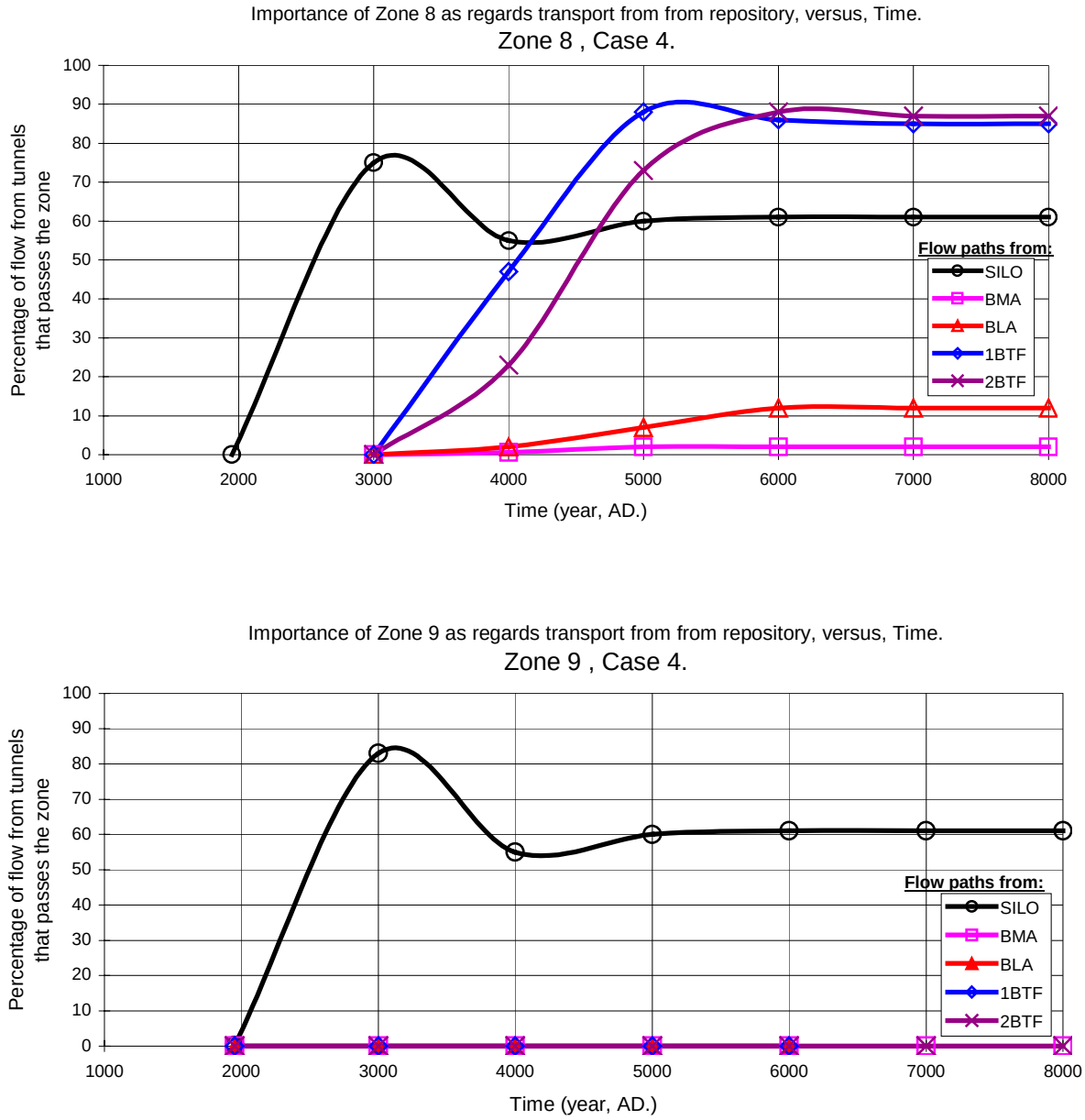

Figure 11.13 *Importance of Zones 8 and 9 as conductors of the transport from deposition tunnels (base case). The figures give the amount of the flow from a deposition tunnel that passes through a zone (flow dependent release of paths).*

11.6 Hydraulic interaction between deposition tunnels

11.6.1 General

By investigating which tunnels occur along a flow path from a deposition tunnel, we can estimate the hydraulic interaction between the different deposition tunnels. We will calculate the share of the total flow from a deposition tunnel that passes through other deposition tunnels (the flow paths were released by use of a flow dependent condition). As the flow paths may use several tunnels during a single path, the sum of the percentages is not necessarily equal to 100%. The general conclusion is that the hydraulic interaction between the deposition tunnels is limited. To a limited extension, flow paths from BTF1 will pass through BTF2, and flow paths from BTF2 and BMA will pass through BLA. The largest interaction takes place between 3000 AD and 4000 AD. However, for the case studied, less than 10 percent of the flow from a deposition tunnel will pass through another deposition tunnel. Considering the BMA and the BTF1 deposition tunnels, the interaction with other deposition tunnels is small, and for the SILO the interaction with other deposition tunnels is negligible.

11.6.2 BLA tunnel

The table below gives the percentage of the total flow from a deposition tunnel that passes through the BLA tunnel.

Table 11.21 Hydraulic interaction between the BLA tunnel and other deposition tunnels (base case).

BLA	Flow from surrounding deposition tunnels (percentage of flow from the surrounding tunnels that passes the BLA)				
Time AD	SILO	BMA	BLA	BTF1	BTF2
2000	-	-	X	-	-
3000	-	6	X	-	5
4000	-	4	X	0.1	8
5000	-	3	X	0.1	4
7000	-	3	X	0.2	4

11.6.3 BTF2 tunnel

The table below gives the percentage of the total flow from a deposition tunnel that passes through the BTF1 tunnel.

Table 11.22 Hydraulic interaction between the BTF2 tunnel and other deposition tunnels (base case).

BTF2	Flow from surrounding deposition tunnels (percentage of flow from the surrounding tunnels that passes the BTF2				
Time AD	SILO	BMA	BLA	BTF1	BTF2
2000	-	-	-	-	X
3000	-	-	-	10	X
4000	-	-	-	4	X
5000	-	-	-	4	X
7000	-	-	-	4	X

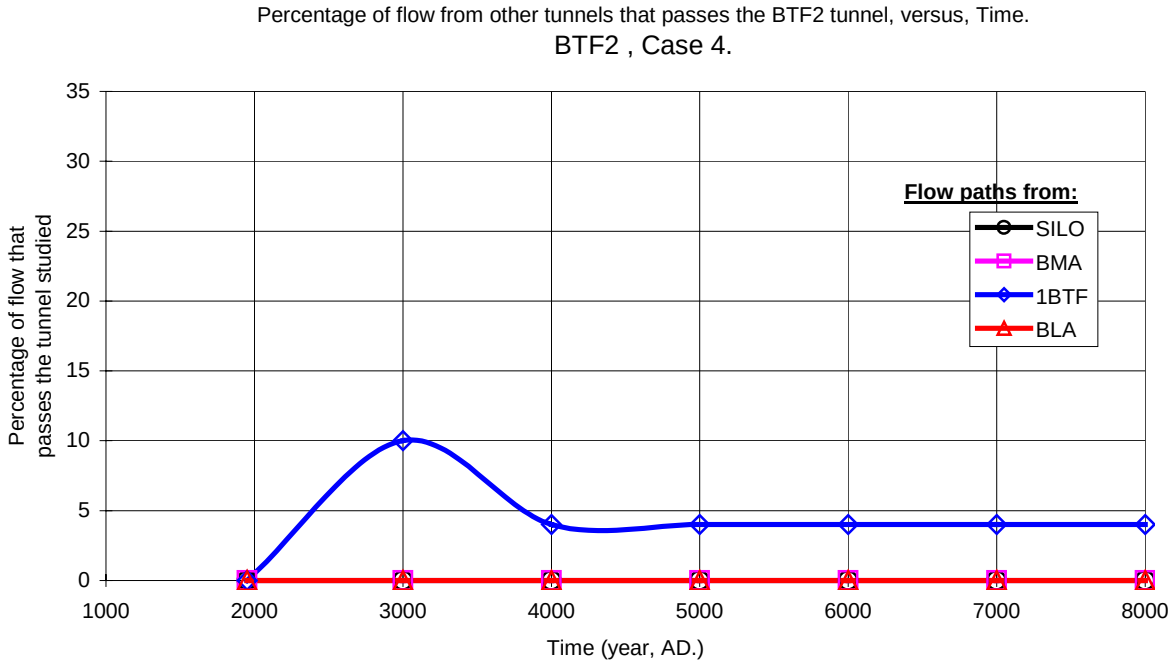

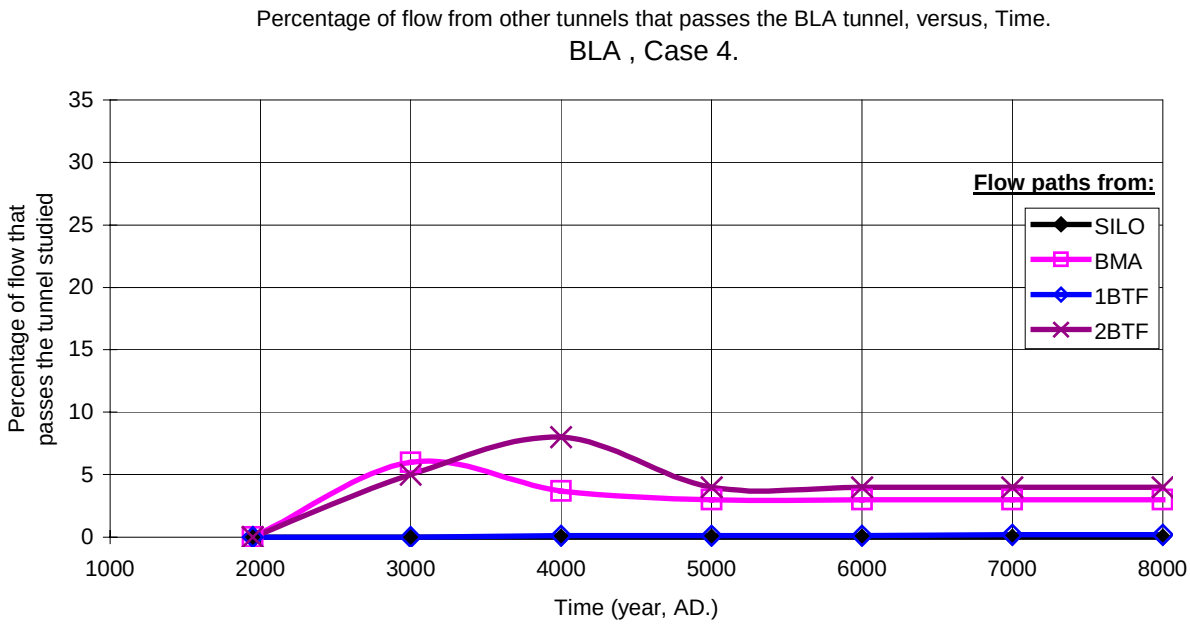

Figure 11.14 *Interaction of flow between different deposition tunnels (base case).*

The figures give an estimation of the amount of flow from a deposition tunnel that passes through the BTF2 and BLA deposition tunnels. Considering the BMA, BTF1 deposition tunnels, the interaction with other deposition tunnels is small, and for the SILO the interaction with other deposition tunnels is negligible.

11.7 Origin of water in deposition tunnels

11.7.1 Purpose

The purpose is to estimate where the groundwater will come from – the groundwater that in the future will flow through the deposition tunnels. This is of interest as the knowledge of the origin of the groundwater, will provide us with some information of the chemical composition (e.g. oxygen and chloride contents etc) of the water that can be expected to reach the tunnels.

11.7.2 Methodology

The groundwater flows through the flow medium (e.g. the rock mass) in different flow paths and discharges at different discharge areas, which is normally at the ground surface, but discharge could also take place at wells and in tunnels that are kept dry. The flow paths of the groundwater are of interest, as they will tell us about the origin of the ground water. For example, the flow paths will reveal the location of the recharge areas of the groundwater and from which depths the groundwater will flow towards the tunnels; and since the tunnels are not drained, the flow paths will continue through the tunnels and finally reach discharge areas. Due to the shore level displacement, the flow pattern of the groundwater will change with time and the analysis of the flow paths has to include the effects of the changing flow pattern.

The depths reached by the flow paths on their way to tunnels are of interests as it will give us information of the type of groundwater that will reach a studied tunnel or well. For example, if all flow paths that reaches a tunnel comes directly from above and also not from the sea, it is very likely that the water that flows through the tunnel is primarily a groundwater that is not very old and does not contain much chloride.

By releasing flow paths in tunnels and wells, flow paths that follow the groundwater upstream, it is possible to investigate the origin of the water in tunnels and wells at SFR. From a mathematical point of view it is not difficult to make a flow path follow the opposite direction of the groundwater flow. The gradients governs the direction of flow and by changing the sign of the gradients, the flow path will develop in an upstream direction. The flow paths will be released at the envelope of the studied structure, by use of a flow dependent release condition. In the following simulations we presume that the repository has been closed and the local groundwater system has recovered from the present drainage of groundwater.

We will simulate both: (i) time-independent (i.e. steady) and (ii) time-dependent (i.e. transient) flow paths. The head field (the distribution of head in the system studied) will change with time as the shore level retreats. It follows from this that steady flow paths, which represent the transport in a specific head field of a studied moment, do not represent the origin of the water that is reaching the tunnels at that moment; as this water is the product of a transport that took place during the previous head fields. A transient path, which develops inside a changing head field, is a better way of exploring

the origin of the water that reaches a tunnel. The steady paths represent the flow system at a given moment, the transient paths represents the actual way a particle has moved during the changes of the flow system as the shore line retreats.

11.7.3 Results

The model predicts the following:

Time: 2000 AD – 2200 AD. As long as the sea covers the repository area, the regional flow in the surroundings of the SFR will be nearly vertical and directed from great depths towards the seabed. During the 200 years, from 2000 AD until approximately 2200 AD, most of the area above the SFR will be below the sea. During this period, nearly all the water that flows through the deposition tunnels comes from below the tunnels and from great depth. However, this all changes when the sea withdraws from the SFR area.

Time: 2200 AD – 2500 AD. From about 2200 AD until about 2500 AD, the water that flows through the tunnels will be a mix of: (i) water coming from great depths and of (ii) surface water coming from recharge areas in the close surroundings. The majority of the water will come from great depth. At 2260 AD about 98 percent and at 2500 AD about 80 percent (transient paths) of the flow through the tunnels comes from below the tunnels (from an elevation lower than -200 masl).

Time: 2500 AD – 2760 AD. An important change in the flow system at SFR takes place during this period. At 2500 AD the shoreline is at the upstream end of Zone 6 and the BMA, BLA, BTF tunnels are below the seabed. The flow in Zone 6 is mainly directed upwards to the seabed above the zone. The water that reaches the deposition tunnels comes mainly from below. However, At 2760 AD the shoreline is at the downstream end of Zone 6 and the BMA, BLA, BTF tunnels are no longer below the sea, but below dry land. At 2760 AD, nearly all the water that reaches the deposition tunnels comes from above and through Zone 6.

Time: 2760 AD – 3000 AD and onwards. At 3000 AD, the sea has withdrawn from most of the area above the SFR, the shoreline is (horizontally) down stream of SFR, and local discharge areas start to develop above the shoreline on the exposed dry land. The general direction of the groundwater flow field in the surrounding of the repository turns from upward to horizontal and finally slightly downward. From about 2760 AD and further on, nearly all the water that flows through the deposition tunnels comes from recharge areas in the close surroundings of SFR. This situation will be maintained as the shoreline continues to retreat.

11.7.4 Conclusions regarding the origin of water in tunnels

During the period from 2200 AD and until 3000 AD, the retreating shoreline will pass above the SFR and as a consequence the groundwater flow pattern will change. Since the flow pattern of the groundwater changes, the origin of the groundwater that reaches the tunnels will change as well. And since the origin of the groundwater changes, the

chemical composition of the groundwater that reaches the deposition tunnels will change.

During the first 750 years of the lifetime of the SFR, the type of groundwater that will reach the deposition tunnels will change, from an old groundwater (e.g. high chloride content, low oxygen content) coming from great depth, to a young groundwater (e.g. no chloride, some oxygen) that comes from recharge areas in the close surroundings of the SFR. The large change in type of water will take place between 2500 AD and 2750 AD.

The situation with local recharge areas providing nearly all the groundwater (i.e. a young groundwater) flowing through the deposition tunnels, will be maintained after 2750 AD, as the sea (the shoreline) continues to withdraw. This will be the final situation as the groundwater flow system evolves into a steady-state-like condition.

Details of the results discussed above are given in Figure 11.15. The results are based on both steady and transient paths.

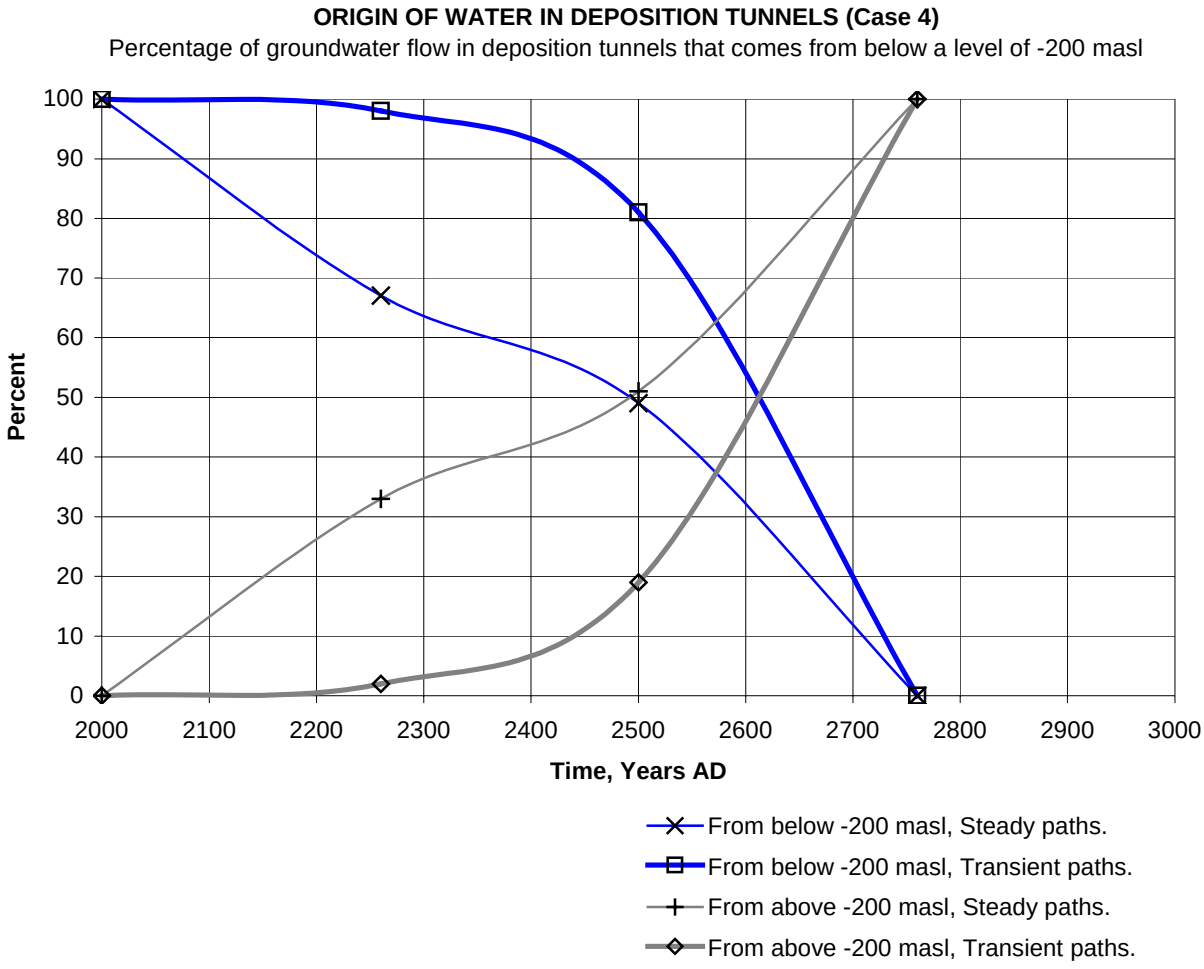

Figure 11.15 *Origin of water in deposition tunnels (base case).*

Percentage of the flow that reaches the deposition tunnels, that has been below or above a depth of –200 masl, on its flow path to the tunnels.

11.8 Local model – Discharge areas

11.8.1 General

For the flow paths from the deposition tunnels, the models predict that the discharge areas change with time. This is because the shore level displacement will change the flow pattern of the groundwater. Most important for the location of the discharge areas are the topography and the position of the shore level. The models predict that most discharge areas occur along low-lying parts of the topography. The largest discharge occurs along permeable fracture zones and especially where permeable fracture zones intersect, at low-lying parts of the topography.

11.8.2 Position of discharge areas at different times

At 2000 AD, the discharge area for the flow that has passed the deposition tunnel is vertically above the tunnels. With time the discharge areas of the flow paths, coming from the BMA, BLA and BTF tunnels, will move North of the repository. The discharge area for the SILO is not the same as the discharge area for the flow of the other deposition tunnels. With time the discharge area of the flow paths, coming from the SILO and some flow paths from the BTF1, will form a separate discharge area Northeast of the SILO. For the SILO there is also a separate discharge area above the SILO.

For the cases presented in this chapter, the base case (calculated by use of the local model), the conductivity and topography of the flow media was the same throughout the period studied, but the position of the shoreline changed with time. The position of the discharge areas will not be the same, as the predictions presented in this chapter, if the topography or the conductivity change with time; such cases have been studied and are presented in Chapter 16.

For the cases presented in this chapter (constant topography and conductivity with time) all discharge will take place within a horizontal distance of approximately 700 m from the deposition tunnels. The results are given in Figure 11.16 and in Figure 11.17.

For the calculation of the discharge areas, a very large number of flow paths were simulated -many thousands for each studied point in time. Each flow path ends at a discharge point on the ground surface. The spatial distribution of the discharge points on the ground surface gives the discharge areas. We have calculated the spatial distribution by use of a kriging routine.

The positions of the discharge areas, for the flow paths coming from the deposition tunnels, are as follows.

- At 2000 AD: The discharge takes place below the sea, more or less straight above the deposition tunnels, mainly along zone 6. See Figure 11.16.
- At 3000 AD: The main discharge takes place close to the shoreline. For BMA, BLA and BTF tunnels, the discharge is along zones 3 and 6, both above and below the sea. As regards the SILO, the discharge will occur above the SILO (close to the shoreline and above the sea), as well as below the sea at the intersection between zones 8 and 9. See Figure 11.16.

- At 4000 AD: Nearly all the discharge takes place above the sea. For the BMA, BLA and BTF tunnels, the discharge takes place along zone 3, mainly at the intersection between zones 3 and 6 as well as at the intersection between zones 3 and 8. As regards the SILO, the discharge will occur above the SILO, as well as at the intersection between zones 8 and 9. See Figure 11.17.
- At 5000 AD and onwards: All the discharge takes place above the sea. For the BMA, BLA and BTF tunnels, the main discharge takes place along zone 3, mainly at the intersection between zones 3 and 8, as well as at the intersection between zones 3 and H2. As regards the SILO, discharge will occur above the SILO, as well as at the intersection between zones 8 and 9. See Figure 11.17. This flow situation represents steady-state-like conditions.

11.8.3 Dilution at discharge areas

The amount of flow from the deposition tunnels that discharges above and below the sea will be different at different times. At 2000 AD all water from the repository discharges below the sea and at 4000 AD all discharge takes place above the sea (this is for the base case in which the topography remains the same in the future). In between, the discharge takes place close to the shoreline.

However, considering the topography of the area in the surrounding of the repository, the groundwater that has passed the deposition tunnels will discharge into two different local drainage basins (see Figure 16.1 and Figure 16.2). The parts of these basins that are above the shoreline will increase in size with time, as the sea withdraws (see Table 16.1). By use of the semilocal model (see Chapter 16), the following flows have been calculated. The total volume of groundwater [‡] that will discharge, above the shoreline and into the two local basins, will increase with time (see Table 16.1). The run-off (see Sec.4.2) times the size of the drainage basins above the shoreline, gives an estimate of the total volumes of surface and ground water that will flow in the drainage basin above the shoreline. The total volumes, in the two drainage basins taken together, increases from ca. 200 000 m^3/year at 3000 AD and up to ca. 667 000 m^3/year at 5000 AD. The groundwater discharge above the shoreline inside the two drainage basins increases from ca. 1800 m^3/year at 3000 AD and up to ca. 34 000 m^3/year at 5000 AD. For comparison, the total flow of the deposition tunnels at 5000 AD is about 200 m^3/year.

Hence, at the discharge areas above the shoreline, where water from the repository will discharge, there will also be a discharge of groundwater that has not passed through the repository. The actual groundwater discharge will be a mix of groundwater from the repository (polluted water) and groundwater that has not been inside the repository (non-polluted water). We have estimated the balance between polluted water and non-polluted water at the discharge areas, and hence estimated the dilution that will take place at the discharge areas. Note that the balance between polluted water and non-polluted water is calculated for the particular discharge areas and not for the whole of the local drainage basins. As the groundwater finally discharge and forms a part of the surface water flows, there will be further mixing and dilution with non-polluted surface water flows.

[‡] In this study, groundwater is defined as the groundwater of the fractured rock; it does not include the near surface groundwater of the quaternary deposits.

The results of the estimate of groundwater dilution demonstrates that water from the deposition tunnels typically comprises only a few percent of the total discharge of groundwater in a discharge area. These results are average values as regards the discharge areas studied, at a local point inside a discharge area the balance is probably different. And in comparison to the runoff of the drainage basins, the groundwater flow from the deposition tunnels is only a small fraction (less than 0.1%).

We have separated the study of discharge areas into two main areas, the discharge areas of the flow from the BMA, BLA and BTF tunnels and the discharge areas of the SILO. The flow from the BMA, BLA and BTF tunnels will discharge above and North of the repository, mainly along Zones 3, 6 and 8. The flow from the SILO will discharge at two separate areas: (i) directly above the SILO and (ii) Northeast of the repository at the intersection of zones 8 and 9, some water from the BTF1 tunnel may also discharge at this area. The results are given in Table 11.23 through Table 11.25, below.

Table 11.23 The SILO - Discharge distribution and dilution at discharge areas (base case). The SILO is defined in accordance with the first SILO definition (SD1).

TIME	FLOW FROM SILO Discharge distribution (%)		GROUNDWATER DISCHARGE Balance between contaminated and non-contaminated water At discharge areas where the water from the Silo (SD1) discharges.			
			Discharge of groundwater (m3/year)		Discharge of groundwater (%)	
	Below sea (%)	Above sea (%)	Not from Silo (non-polluted)	From Silo (polluted)	Not from Silo (non-polluted)	From Silo (polluted)
2000 AD	100	0	-	-	-	-
3000 AD	31 (1)	69 (1)	5.3	1.6	77	23
4000 AD	0	100	190	4.1	98	2
5000 AD Steady state	0	100	139	3.9	97	3
(1) The discharge is close to the shoreline, the distribution below or above the sea is uncertain.						

Table 11.24 The SILO - Discharge distribution and dilution at discharge areas (base case). The SILO is defined in accordance with the second SILO definition (SD2).

TIME	FLOW FROM SILO Discharge distribution (%)		GROUNDWATER DISCHARGE Balance between contaminated and non-contaminated water At discharge areas where the water from the Silo (SD2) discharges.			
			Discharge of groundwater (m3/year)		Discharge of groundwater (%)	
	Below sea (%)	Above sea (%)	Not from Silo (non-polluted)	From Silo (polluted)	Not from Silo (non-polluted)	From Silo (polluted)
2000 AD	100	0	-	-	-	-
3000 AD	31 (1)	69 (1)	6.4	0.5	93	7
4000 AD	0	100	193	1.2	99.4	0.6
5000 AD Steady state	0	100	142	1.2	99.2	0.8
(1) The discharge is close to the shoreline, the distribution below or above the sea is uncertain.						

Table 11.25 The BMA, BLA and BTF tunnels - Discharge distribution and dilution at discharge areas (base case).

TIME	FLOW FROM BMA.BLA, BTF Discharge distribution (%)		GROUNDWATER DISCHARGE Balance between contaminated and non-contaminated water at the discharge areas where the water from the BMA, BLA and BTF tunnels discharges.			
	Below sea (%)	Above sea (%)	Discharge of groundwater (m3/year)		Discharge of groundwater (%)	
			Not from deposition tunnels (non-polluted)	From BMA,BLA,BTF (polluted)	Not from deposition tunnels (non-polluted)	From BMA,BLA,BTF (polluted)
2000 AD	100	0	-	-	-	-
3000 AD	ca. 40 (1)	ca. 60 (1)	- (1)	- (1)	- (1)	- (1)
4000 AD	0	100	4471	205	96	4
5000 AD Steady state	0	100	3903	209	95	5
(1) The discharge is close to the shoreline, the distribution below or above the sea is uncertain.						

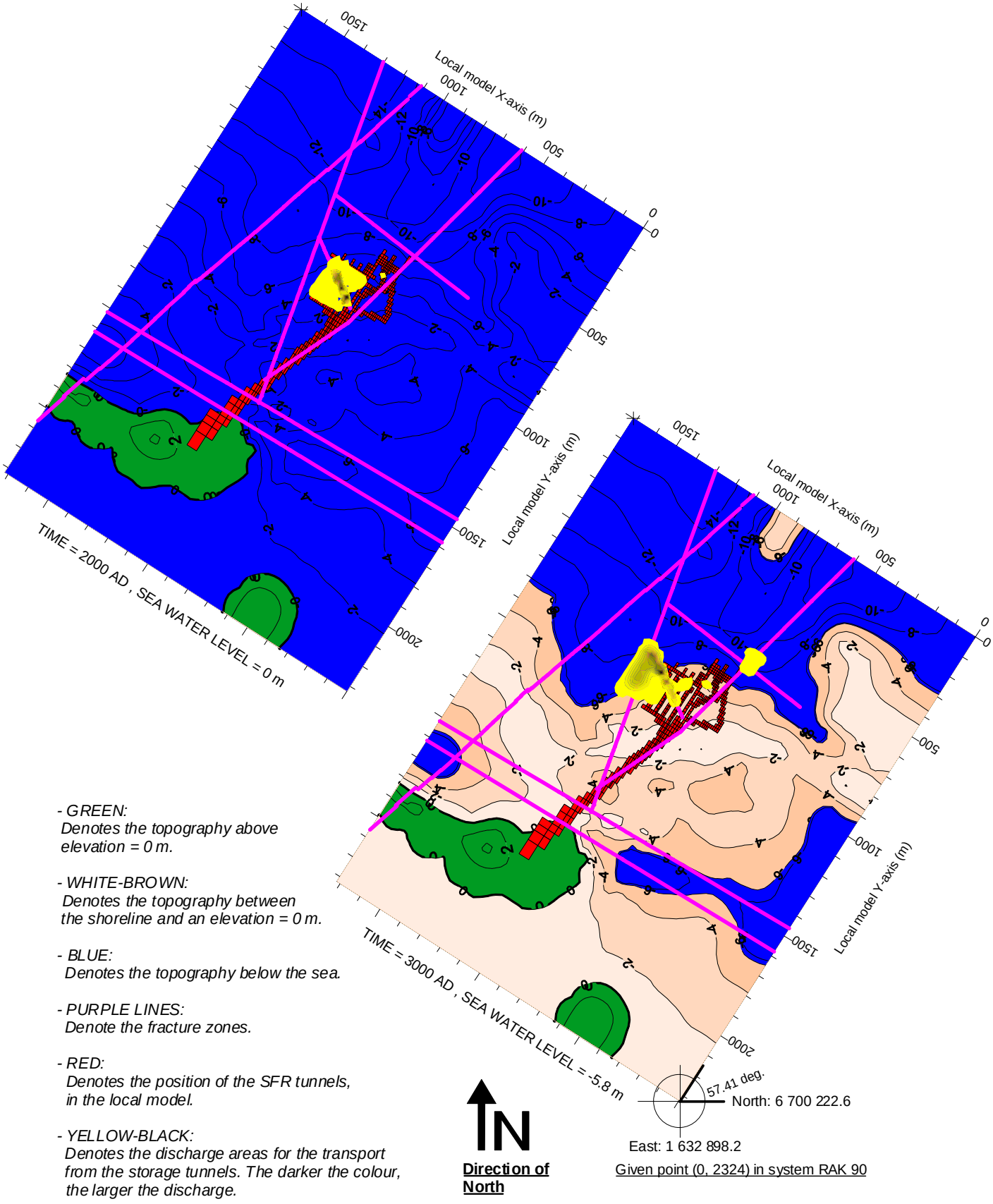

Figure 11.16 *Local model (base case). Discharge areas for the for the flow paths from the deposition tunnels, at time equal to 2000 AD and 3000 AD.*

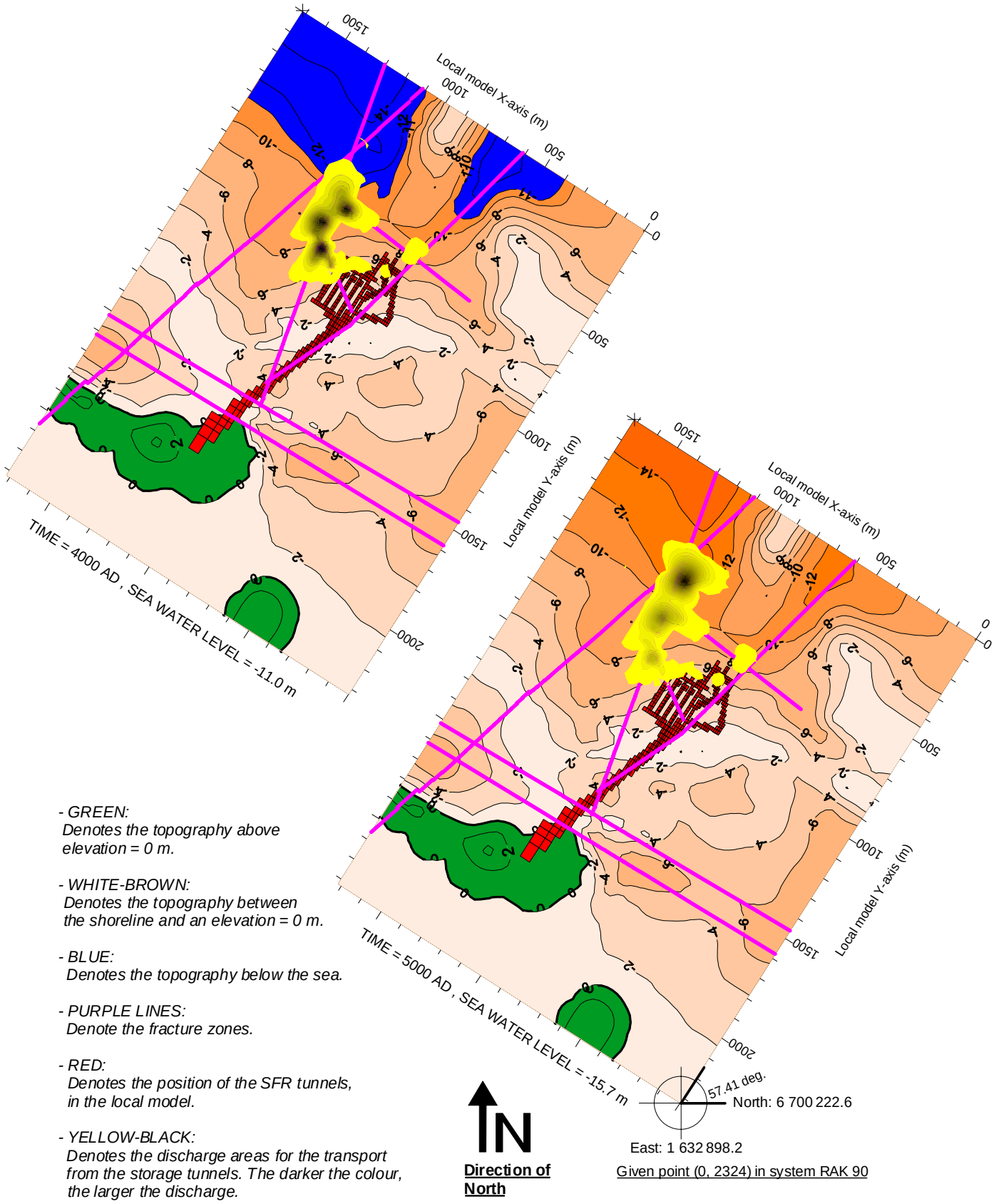

Figure 11.17 *Local model (base case). Discharge areas for the for the flow paths from the deposition tunnels, at time equal to 4000 AD and 5000 AD.*

12. Effect of theoretical wells

12.1 Purpose

As previously discussed, the shoreline will retreat and the present seabed above the repository will in the future be exposed as dry land. It can not be ruled out that in the future, the common knowledge of the repository could be lost. As a consequence of the shoreline retreat and a lost knowledge of the repository location, local wells might be drilled in the close surrounding of the SFR, in connection to settlements above the repository.

The purpose of these well-cases is to study the effects of a small well on the future groundwater flow field in the surrounding of the SFR. The purpose is to estimate: (i) to what amount such a well could form a discharge point for contaminated water from the repository and (ii) to estimate the dilution that will take place in such a well if contaminated water will reach the well.

12.2 Methodology

For these simulations we have used the local model. The chain of simulations was the same as for the previous presented calculations with the local model. The wells will be added to the models, as a local sink of groundwater, inside the mesh representing the flow system studied. The *VF* variable in equation 2.1 represents a well (see Section 2.2). The lowest possible head in a well is equal to atmospheric pressure at the bottom of the well. This is a condition included in the models. Hence, in the models, if a specified well discharge (groundwater sink) causes a pressure lower than atmospheric at a well studied, the specified well discharge is too large to be sustained by the local flow system (the flow medium is not permeable enough to deliver such a flow). If such conditions occur, the models will calculate the maximum possible well discharge at that location.

We have investigated the effects of a well, on the flow pattern of the groundwater, by releasing flow paths that follow the groundwater flow, we have studied flow paths that develops both upstream and downstream from there release locations. Paths have been released both from the well and from the deposition tunnels. The flow paths have been released at the envelope of the studied structure, by use of a flow dependent release condition. In the following simulations we presume that the repository has been closed and the local groundwater system has recovered from the present drainage of groundwater.

12.3 Properties of actual wells at Forsmark

Wells are either drilled, dug or piped wells. A dug or a piped well is a soil well –a well in quaternary deposits. The use of soil wells is decreasing in Sweden, since the quality of near surface groundwater is not always good. Statistics from the Water Well Record Section (well archive) of the Swedish Geological Survey (SGU) indicate that the majority of the new wells in Sweden are hammer drilled in hard rock (Axelsson *et al*, 1991); however, not all soil wells are reported to the SGU. In glacifluvial quaternary deposits, i.e. eskers, soil wells are still commonly used for water supply. In combination with artificial recharge, such wells are used for the water supply of municipalities, e.g. Uppsala municipality. No large glacifluvial deposists have been identified at the SFR area. Consequently, in this study we have investigated wells drilled into fractured hard rock.

In Sweden wells in hard rock, used for fresh water supply, are very rarely drilled to a depth larger than 120 m. At the Forsmark area, the median depth is 55 m; and for the province of Uppland, the median depth is 63 m, see Table 12.1 below.

Statistics of the wells in the province of Uppland and the Forsmark area is given in the table below. These statistics are based on data provided by the Water Well Record Section (well archive) of the Swedish Geological Survey (SGU, 2000).

Table 12.1 Well statistics from the SGU well archive.

Well statistics from SGU well archive. Drilled wells for fresh water supply							
	Size of area (km2)	Number of wells in archive	Number of wells per km2		Mean	Confid.li. (95%)	Median
Forsmark area	1 502	434	0.3	Capacity (l/h)	1 532	186	710
				Depth (m)	57	2.3	55
Uppland province	11 982	15 339	1.3	Capacity (l/h)	1 341	36	600
				Depth (m)	64	0.4	63

12.4 Previous studies

Dilution in wells and effects of wells on the flow field have previously been investigated by use of mathematical models as a part of SKB studies, e.g. Thunvik (1983) and Axelsson *et al* (1991). It was concluded in both these studies that a well discharging 6 m^3/day and placed in a fairly large fracture zone, is not a strong sink, compared to the flow that take place in the fracture zone under natural gradients. Axelsson *et al* (1991) used a two dimensional vertical cross-section representing a fracture zone at the Finnsjön investigation area (Fracture zone 1 at Finnsjön). It was concluded that a well pumping 6 m^3/day at a depth of 60 m, could be as close as 100 m from a discharge area and still not collect contaminated water discharging at that area.

12.5 The well-cases of this study

12.5.1 Effect of shore level displacement

Local wells for fresh water supply will only be installed above the sea. Hence, no fresh water wells will be drilled in the close surrounding of SFR as long as the sea covers the ground above SFR. At 3000 AD, the sea has withdrawn from most of the area above the SFR. The shoreline is however close to the SFR and much of groundwater flow discharges below the sea. At 3000 AD the local groundwater flow is influenced by the retreating shoreline and the local flow field is not at a steady-state-like situation. At 5000 AD, the shoreline is more than a kilometre away from the SFR, and the local flow field is at a steady-state-like situation. The Well-cases of this study are simulated at time equal to both 3000 AD and 5000 AD.

12.5.2 Position of wells

Each Well-case includes one well only. In relation to an undisturbed groundwater flow field without a well; a well at SFR can be placed in three positions: (i) upstream of SFR, (ii) inside SFR and (iii) downstream of SFR. A short description of the wells studied is given in Table 12.3.

Upstream of SFR: A well located upstream of the SFR (in relation to an undisturbed groundwater flow field), can not be below a discharge area for the undisturbed groundwater flow from the repository. Hence for such a well to collect water from the SFR it either has to be a very strong sink, so strong that it changes the general trend of the undisturbed flow, or placed so close to the repository that it may locally change the flow pattern. We have studied wells at three different positions upstream of SFR. One well in fracture Zone 3 (Well A) and two wells in the rock mass, one very close to the an access tunnel and the SILO (Well C) and one a short distance from the repository (Well B), see Figure 12.2. All three wells are studied at both 3000 AD and 5000 AD.

Inside SFR: The SFR is not at a great depth, the main facility is approximately between –60 and –100 masl. Consequently, it is possible that a local well could be drilled directly into the tunnel system, either into an access tunnel or into a deposition tunnel. We have studied wells at two different positions inside SFR. One well in an access tunnel between the SILO and the BTF1 deposition tunnel (Well E) and another well in the BLA deposition tunnel (Well D) see Figure 12.2. Both wells are studied at both 3000 AD and 5000 AD.

Downstream of SFR: A well located downstream of the SFR (in relation to an undisturbed groundwater flow field) can be placed below a discharge area for the undisturbed groundwater flow from the repository. It follows that such a well could collect water from the SFR even if the well is a very weak sink. If the well is located outside of the discharge area it needs to be a strong sink to divert the natural flow field and collect water from SFR. We have studied wells at four different positions downstream of SFR. One well in fracture Zone 3 (Well F), directly below a discharge

area for the water from the BMA, BLA and BTF tunnels. And three wells in Zone 8, one well directly below a discharge area for the water from the SILO (Well I) and two wells below and close to the same discharge area, but outside of it (Well G and Well H), see Figure 12.2. All four wells are studied (in separate cases) at 5000 AD only, because at 3000 AD the wells are below the sea.

12.5.3 Well depth

In Sweden wells in hard rock, used for fresh water supply, are very rarely drilled to a depth larger than 120 m. At the Forsmark area, the median depth is 55 m (see Table 12.1). Along the length of a drilled borehole, water will be extracted from fractures and fracture zones that intersects the borehole. If a well intersects a significant fracture zone, it is very likely that this fracture zone will provide most of the well discharge.

In the model, a simulated well extract all its well discharge from the flow media, along a section of length 5 meters, at an elevation of –77 through –80 masl. The extraction section of a simulated well, represents a section where an actual well intersects a fracture zone (see Figure 12.1, below). In the model, the elevation of the extraction sections corresponds to the elevation of the horizontal deposition tunnels (BMA, BLA and BTF). For the wells that intersects the tunnel system (wells D and E), this means that all of the well discharge will be taken from within the tunnel system.

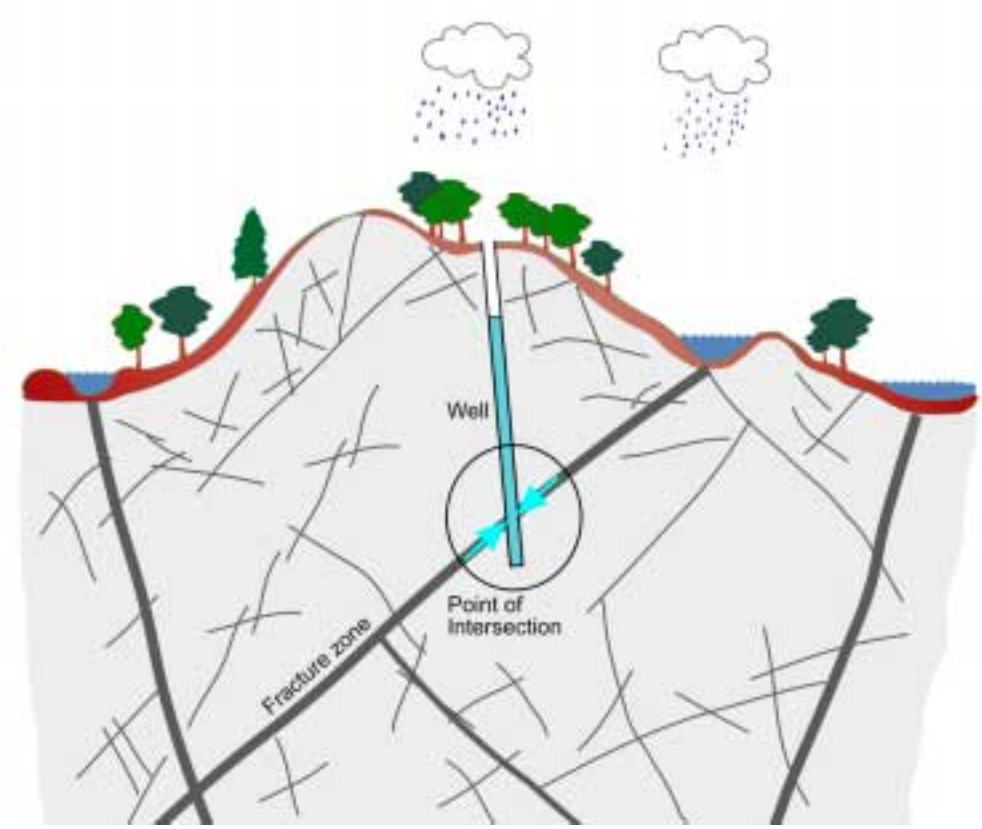

Figure 12.1 *Illustration of well depth and the point of intersection between a well and a fracture zone.*

12.5.4 Well discharge and consumer requirements

The actual discharge of water at fresh water wells varies dependent on type of consumer. A household of four persons consumes about 1 m^3/day, while a small farm might need as mush as 6 m^3/day and a large farm 12 m^3/day or more. The local properties of the groundwater system limits the maximum discharge of a well and it may not be possible to sustain a large steady discharge, such as 6 m^3/day or 12 m^3/day, by just a single well. The fresh water requirements for different consumers are given in

Table ***12.2***, this table is based on a similar table in Axelsson *et al*, (1991), they refer to information provided by Geotec, which is an organisation of well constructors.

Table 12.2 Water requirements for different consumers, from Axelsson et al, (1991).

	Requirements Litres / day	Type of consumer
Household	1000	Complete household, 4 persons
	600	Summer house only
	150 – 200	Per capita and day, no irrigation
	1.5	Per capita and day, for drinking only
Farming	Ca. 6000	Small farm in Uppland, Sweden, 50-80 hektar, 25-30 milk-cows.
	Ca. 12000	Large farm in Uppland, Sweden, 500-800 hektar, ca. 100 milkcows.
	45	Per cattle or horse per day
	75	Per milk-cow

The well discharge used in this study is in line with the well discharge used in the SR97 safety analysis (SKB TR-99-06). Studsvik Eco & Safety AB (2000) gives the rationale for the well discharge used in this study, as below:

- The critical group for which the dose is calculated is a group consisting of 5 - 10 people, living on a small farm. They get their water from a local well drilled into the rock mass. It is assumed that these people drink 1.6 litres of water per day (600 litres/year). In addition to this each person consume 200 litres/day for washing, showering etc. The total consumption for the group studied becomes 1 - 2 m^3/day.
- It is also assumed that the farm has 5 - 10 cows and it is assumed that each cow consumes 65 - 75 litres/day, which gives a total equal to 325 - 750 litres/day.
- Furthermore, the water from the well is used for irrigation of a garden. It is assumed that the garden is irrigated 6 - 14 times per year. The volume of water used at each time is between 0.014 - 0.067 m^3 of water per m^2 of garden. The area of the garden is assumed to be between 150 - 250 m^2. Hence, the total volume used for irrigation will be between 12.6 m^3/year (0.035 m^3/day) and 234.5 m^3/year (0.64 m^3/day)

Thus, the total consumption of water by the small farm is between 1.36 - 3.39 m^3/day. The arithmetic average value of these two numbers is 2.375 m^3/day.

For the wells of this study, we have used a specified discharge of 2.37 m^3/day, which is a flow that represents a small farm. For two of the wells, B and C, which are positioned in the low permeable rock mass and not in a fracture zone, it was not possible to extract this amount, these wells produced a maximum rate of 2.1 m^3/day and 1.1 m^3/day, respectively.

12.5.5 Boundary conditions

We have added the wells to the local model, Case 4, the boundary conditions of the top surface depend on the condition of the flow system and hence are able to adjust to the addition of a well. The average actual recharge of the whole of the regional model varies with time, for Case 4 at 3000 AD it is ca. 3 mm/year and at 5000 AD it is ca. 5 mm/year. However, the potential recharge is 250 mm/year, which is the same as 2.37 m^3/day (the specified well discharge) for a circular area with a radius of 33 m. Hence, the potential groundwater recharge is so large that it is likely that a local well, with a discharge of 2.37 m^3/day and placed in a fracture zone, will only affect the groundwater flow pattern in the near vicinity of the well itself and not influence the flow on a large scale. The results of the simulations demonstrate that for the cases studied, the addition of a well will increase the average actual recharge (compared to a case without the well). The addition of a well with the specified well discharge (2.37 m^3/day) will not cause any significant change of the level of the groundwater surface (since the potential recharge is so large). The vertical and base boundaries are not adjusted for the presence of a well, as the wells studied are placed at the central area of the local model, at a minimum distance of about 500 m from the boundaries, and as the discharge of the wells studied is not very large, compared to the potential recharge and the undisturbed flow through the local model. The wells are at steady state.

Table 12.3 Summary of the wells studied. Each Well-case include one well only.

Well ID.		Well discharge (m3/day)	Extraction at (masl)	Location of well	Studied at Time
Up-stream	**A**	2.37	-77 to –82	Upstream of SFR in Z-3	3000 AD and 5000 AD
	B	2.1	-77 to -82	Upstream of Sfr in rock mass	3000 AD and 5000 AD
	C	1.1	-77 to -82	Close to SILO in rock mass	3000 AD and 5000 AD
Inside	**D**	2.37	-77 to -82	Inside of SFR in BLA tunnel	3000 AD and 5000 AD
	E	2.37	-77 to -82	Inside of SFR in access tunnel	3000 AD and 5000 AD
Down-stream	**F**	2.37	-77 to -82	Downstream of SFR in Z-3	5000 AD
	G	2.37	-77 to -82	Downstream of SILO in Z-8	5000 AD
	H	2.37	-77 to -82	Downstream of SILO in Z-8	5000 AD
	I	2.37	-77 to -82	Downstream of SILO in Z-8	5000 AD

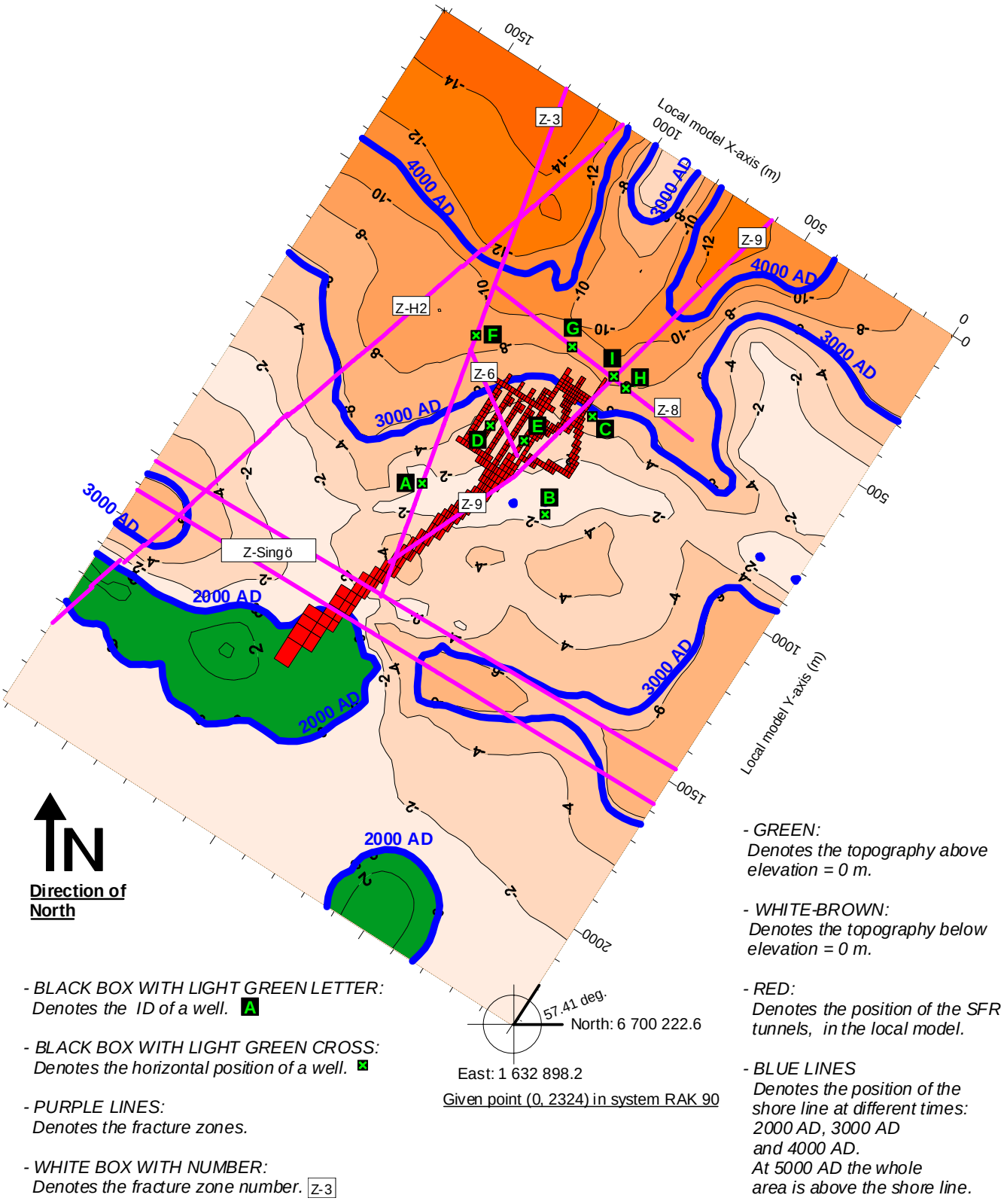

Figure 12.2 *Horizontal positions of the wells studied, the fracture zones and the tunnel system etc.*

12.6 Results of the well-cases

12.6.1 Introduction

The results of the flow path analyses are presented below. The conclusions are given after the presentation of the results. A summary of the results is given in Table 12.14 and Table 12.15. The positions of the wells are given in Figure 12.2.

12.6.2 Wells upstream of SFR

Well-case A. The well is upstream of SFR in fracture zone 3. It will only have a minimal effect on the flow in the SFR tunnel system. No water from the deposition tunnels will reach the well. At 3000 AD, a significant amount of the well discharge will come from great depth, since the zone in which the well is located is vertical and will consequently provide an efficient vertical flow route.

Well-case B. The well is upstream of SFR in the low permeable rock mass. It will have an insignificant effect on the flow in the SFR tunnel system. No water from the deposition tunnels will reach the well.

Well-case C. The well is upstream of SFR in the low permeable rock mass, but the well is placed very close to an access tunnel, and also close to the SILO. The maximum well discharge is 1.1 m^3/day. The well will have an insignificant effect on the flow of the deposition tunnels, except for the flow through the SILO when the shore line is close to the SILO (time equal to 3000 AD). Because when the shore line is close to the SILO, the undisturbed flow in the rock mass close to the SILO (flow without the well) has a significant vertical component. The introduction of the well will increase the size and change the direction of the flow in the rock masses that surrounds the SILO. Even if only a small amount of the flow that passes through the SILO will reach the well, the direction of the flow close to the SILO will change and become more horizontal because of the well. And thereby exposing, to the groundwater flow, a larger area of the SILO, which will increase the total flow that passes through the SILO. The total flow of the SILO, as predicted by the local model for Well-case C at 3000 AD, will be 30 percent larger than the flow for undisturbed conditions. For later time periods, when the shore line has moved further away from the repository, the regional flow in the surrounding of the SILO will become more horizontal due to the new flow situation created by the local topography. It follows that with the changing flow situation after 3000 AD, the well will be of less importance for the flow of the SILO, as the regional flow will be horizontal anyway. For 5000 AD, the total flow of the SILO, as predicted by the local model for Well-case C, is approximately the same as the flow predicted without the well. Both at 3000 AD and at 5000 AD, no water from BMA, BLA or BTF tunnels will reach the well, but 3 percent of the water from the SILO will reach the well. The contribution of water from the deposition tunnels to the total discharge of the well is only 0.02 percent, because the total flow of the SILO is much smaller than the discharge of the well.

12.6.3 Wells inside SFR

Well-case D. The well is placed in the BLA deposition tunnel, it will have a large effect on the groundwater flow in the tunnels. The flow in the tunnels will be increased, most for the tunnels that are closest to the well and especially for the BLA, see Table 12.4.

Table 12.4 Change in predicted total flow of the deposition tunnels for Well-case D.

Well D 2.37m^3/day	CHANGE IN TOTAL FLOW GIVEN AS A FLOW FACTOR- LOCAL MODEL Flow Factor = New Flow / Flow of base case				
Time AD	SILO (1)	BMA	BLA	BTF2	BTF1
3000 AD	Small Changes	1.5	867	2.3	1.1
5000 AD	Small Changes	1.4	867	2.6	1.7
(1) First SILO definition (SD1).					

The well will be a strong sink for the water that flows in the deposition tunnels. The flow paths of the water that flows towards the well forms a complicated pattern, which includes the access tunnels and several fracture zones. For this case (well discharge equal to 2.37 m^3/day) all of the flow of the BLA tunnel will reach the well, and nearly all of the flow from the BMA and BTF tunnels. The SILO is located at some distance from the well and several tunnel plugs protects it, consequently no flow from the SILO will reach the well at this rate of discharge. However, if the well discharge is increased to 6 m^3/day, also some flow from the SILO will reach the well.

Since, the well is placed inside the BLA tunnel, the flow through the BLA will be equal to the well discharge. All of the water that make up the well discharge have passed through the BLA tunnel and have perhaps also passed through other deposition tunnels on its way to the well. Hence, there will be no dilution with non-contaminated water at this well. The total contribution of water from the deposition tunnels to the well discharge, given in percent of the well discharge, is larger than 100 percent, as some of the water has passed through several deposition tunnels. And it increases with time, from 118 percent to 122 percent, because the total flow of the deposition tunnels increases with time.

Table 12.5 Well D. Flow from deposition tunnels to the well (amount of flow that finally reaches a well).

Well D 2.37m^3/day	PERCENTAGE OF TOTAL FLOW OF A DEPOSITION TUNNEL THAT REACHES THE WELL				
Time AD	SILO (1)	BMA	BLA	BTF2	BTF1
3000 AD	0	75	100	100	97
5000 AD	0	75	100	99	67
(1) First SILO definition (SD1).					

Table 12.6 Well D. Contribution of water from deposition tunnels to the well discharge.

Well D 2.37m^3/day	PERCENTAGE OF WELL DISCHARGE THAT COMES FROM A DEPOSITION TUNNEL					
Time AD	SILO (1)	BMA	BLA	BTF2	BTF1	TOTAL
3000 AD	0	4.3	100	9.0	4.5	118
5000 AD	0	3.8	100	12.0	5.6	122
(1) First SILO definition (SD1).						

Well-case E. The well is placed in an access tunnel, it will have a large effect on the groundwater flow in the tunnels. The flow in all tunnels will be increased, most for the tunnels that are closest to the well, see Table 12.7.

Table 12.7 Predicted total flow of the deposition tunnels for Well-case E.

Well E 2.37m^3/day	CHANGE IN TOTAL FLOW GIVEN AS A FLOW FACTOR- LOCAL MODEL Flow Factor = New Flow / Flow of base case				
Time AD	SILO (1)	BMA	BLA	BTF2	BTF1
3000 AD	Small Changes	Small Changes	1.1	1.2	1.4
5000 AD	Small Changes	Small Changes	1.3	1.5	1.8
(1) First SILO definition (SD1).					

The well will be a strong sink for the water that flows through the deposition tunnels. The flow paths of the water that flows towards the well forms a complicated pattern, which includes the access tunnels and several fracture zones. For this case (well discharge equal to 2.37 m^3/day) nearly all of the flow from the BTF1 tunnel will reach the well, but only very small amounts from the BTF2 and the SILO, and from BMA and BLA no flow reaches the well. However, if the well discharge is increased to 6 m^3/day, nearly all of the flow from all deposition tunnels will reach the well.

Since the total flow through all deposition tunnels is much smaller than the well discharge, the total contribution of flow from all deposition tunnels to the well discharge is not more than 5.7 percent at 3000 AD and 6.5 percent at 5000 AD. And as the flow from the deposition tunnels make up only a fraction of the well discharge, a large dilution with non-contaminated water will take place in the well.

Table 12.8 Well E. Flow from deposition tunnels to the well (amount of flow that finally reaches a well).

Well E 2.37m^3/day	PERCENTAGE OF TOTAL FLOW OF A DEPOSITION TUNNEL THAT REACHES THE WELL				
Time AD	SILO (1)	BMA	BLA	BTF2	BTF1
3000 AD	1	0	0	2	99
5000 AD	0	0	0	3	69
(1) First SILO definition (SD1).					

Table 12.9 Well E. Contribution of water from deposition tunnels to the well discharge.

Well E 2.37m^3/day	PERCENTAGE OF WELL DISCHARGE THAT COMES FROM A DEPOSITION TUNNEL					
Time AD	SILO (1)	BMA	BLA	BTF2	BTF1	TOTAL
3000 AD	0.003	0	0	0.09	5.6	5.7
5000 AD	0	3.8	100	0.2	6.3	6.5
(1) First SILO definition (SD1).						

12.6.4 Wells downstream of SFR

Well-cases F, G, H and I are not applicable at time equal to 3000 AD, because the ground above the wells will be below the sea at 3000 AD. The sea will not withdraw from the area above the wells until approximately 3700 AD.

Well-case F. The well is down stream of SFR in fracture zone 3. It will only have a small effect on the size of flow in the SFR deposition tunnels. However, the well will be a strong sink for the water that has passed the deposition tunnels, because the well is placed below the discharge area for the undisturbed flow from the BMA, BLA and BTF tunnels. The well will intercept the flow from these tunnels and a large amount of the water from these tunnels will end up in the well. Since the well is in a fracture zone in which the groundwater flow is directed upwards, the well will not catch much water from above.

For this case, most of the flow from the BMA tunnel and nearly all of the flow from the BLA and BTF tunnels will reach the well, but non-of the flow from the SILO. However, since the total flow through all deposition tunnels is much smaller than the well discharge, the total contribution of flow from all deposition tunnels to the well flow is not more than 19 percent. At the well, the water from the deposition tunnels will be diluted with non-contaminated water. Well-case F is illustrated in Figure 12.5.

Table 12.10 Well F. Flow from deposition tunnels to the well (amount of flow that finally reaches a well).

Well F $2.37 m^3$/day	PERCENTAGE OF TOTAL FLOW OF A DEPOSITION TUNNEL THAT REACHES THE WELL				
Time AD	SILO (1)	BMA	BLA	BTF2	BTF1
3000 AD	-	-	-	-	-
5000 AD	0	53	96	97	76
(1) First SILO definition (SD1).					

Table 12.11 Well F. Contribution of water from deposition tunnels to the well discharge.

Well F $2.37 m^3$/day	PERCENTAGE OF WELL DISCHARGE THAT COMES FROM A DEPOSITION TUNNEL					
Time AD	SILO (1)	BMA	BLA	BTF2	BTF1	TOTAL
3000 AD	-	-	-	-	-	-
5000 AD	0	4.0	6.7	4.6	3.8	19.1
(1) First SILO definition (SD1).						

Well-case G. The well is down stream of SFR in fracture zone 8. It will only have a small effect on the size of flow in the SFR deposition tunnels. The well is placed below and between (i) the large discharge area for the undisturbed flow from the BMA, BLA and BTF tunnels (the well is East of this discharge area) and (ii) the discharge areas for the SILO (the well is West of this discharge area). This case demonstrates that, with the well discharge studied ($2.37\ m^3$/day), the well is not a sink strong enough to change the undisturbed flow pattern in a significant way. And consequently no flow from the deposition tunnels will reach the well. However, if the well discharge is increased to $6\ m^3$/day, the well will intercept about 1 percent of the flow from the BTF2 tunnel, the

flow from the rest of the tunnels will end up at the same discharge areas as without a well.

Well-case H. The well is downstream of the SILO, in fracture zone 8. It will only have a minimal effect on the size of flow in the SFR deposition tunnels. The well is placed below and outside of the discharge area for the undisturbed flow from the SILO (the well is East of the SILO discharge area). However, in the horizontal plane, the well is very close to the discharge area for the undisturbed flow from the SILO. This case demonstrates that, with the well discharge studied (2.37 m^3/day), the well is not a sink strong enough to change the undisturbed flow pattern in a significant way. And even if the well is placed very close to the discharge area, it will not intercept any flow coming from the deposition tunnels. And consequently no flow from the deposition tunnels will reach the well. However, if the well discharge is increased to 6 m^3/day, the well will intercept about 67 percent of the flow from the SILO, the flow from the rest of the tunnels will end up at the same discharge areas as without a well. Well-case H is illustrated in Figure 12.3.

Well-case I. The well is downstream of the SILO, in fracture zone 8, at the intersection between zone 8 and zone 9. It will only have a minimal effect on the size of flow in the SFR deposition tunnels. The well is placed exactly below the discharge areas for the undisturbed flow from the SILO. It follows that the well will intercept the flow from the SILO. However, the well will not catch all the water from the SILO, because the flow from the SILO will spread over a certain volume. And for the well discharge studied (2.37 m^3/day), the well is not strong enough to significantly change the flow pattern of the groundwater in the fracture zone where it is placed in such a way that all flow from the SILO will end up in the well. Well-case I is illustrated in Figure 12.4.

For this case, the majority of the water from the SILO will reach the well (83 percent). However, since the flows from the SILO is only very small compared to the well discharge, the total contribution of flow from the SILO to the well discharge is not more than 0.3 percent. And as the flow from the SILO makes up only 0.3 percent of the well discharge, a large dilution with non-contaminated water will take place in the well.

Table 12.12 Well I Flow from deposition tunnels to the well (amount of flow that finally reaches a well).

Well I 2.37m^3/day	PERCENTAGE OF TOTAL FLOW OF A DEPOSITION TUNNEL THAT REACHES THE WELL				
Time AD	SILO (1)	BMA	BLA	BTF2	BTF1
3000 AD	-	-	-	-	-
5000 AD	83	0	0	0	0
(1) First SILO definition (SD1).					

Table 12.13 Well I. Contribution of water from deposition tunnels to the well discharge.

Well F 2.37m^3/day	PERCENTAGE OF WELL DISCHARGE THAT COMES FROM A DEPOSITION TUNNEL					
Time AD	SILO (1)	BMA	BLA	BTF2	BTF1	TOTAL
3000 AD	-	-	-	-	-	-
5000 AD	0.3	0	0	0	0	0.3
(1) First SILO definition (SD1).						

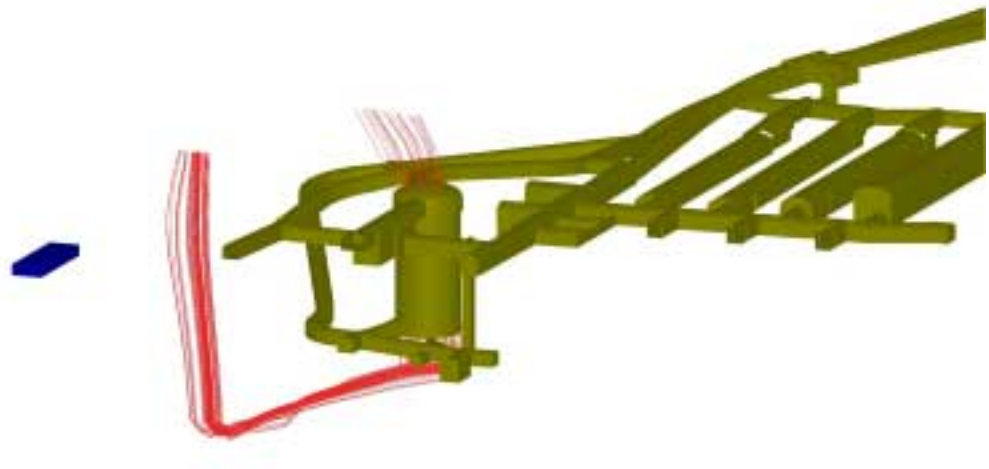

Figure 12.3 *Well-case H. The major flow routes from the SILO, at time equal to 5000 AD. The well is at the centre of the blue box.*

Well H is within Zone 8, but at some distance from the intersection between Zones 8 and 3. The well discharge is extracted at a depth of about 75 meters below the ground. There is no flow from the SILO to the Well. The uppermost 20 m of the flow paths, close to the ground, are not included.

Figure 12.4 *Well-case I. Flow routes.*

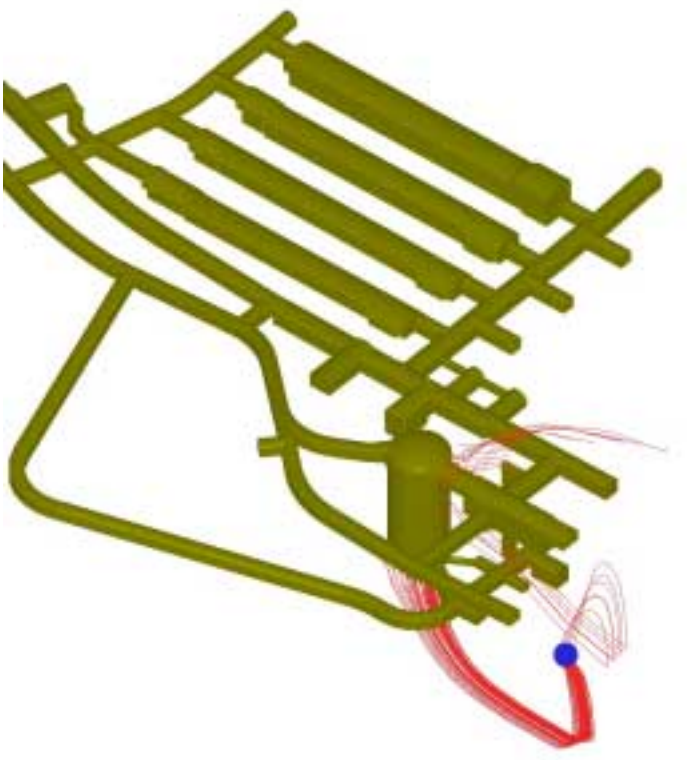

The figure presents flow paths from the SILO to Well I, at time equal to 5000 AD. Well I is located at the intersection between fracture zones 8 and 9. A blue circle denotes the well. The well discharge is extracted at a depth of about 75 meters. The well collects 83 percent of the flow that has passed through the SILO.

Three major flow routes occur:
(i) Lower route, from the SILO base via rock mass to Zone H2, via H2 to Zone 8, via Zone 8 upwards to the well, most of the flow will be conducted by this route.
(ii) Middle route, from the middle part of the SILO via rock mass to Zone 8, via Zone 8 to the well by use of curved flow paths.
(iii) Upper route, from the upper parts of the SILO via rock mass towards the ground, this flow route will not lead to the well.

Even if 83 percent of the flow from the SILO reaches the well, this will only make up 0.2 percent of the total discharge of the well, as the well discharge is much larger than the flow through the SILO. The uppermost 20 m of the flow paths, close to the ground, are not included.

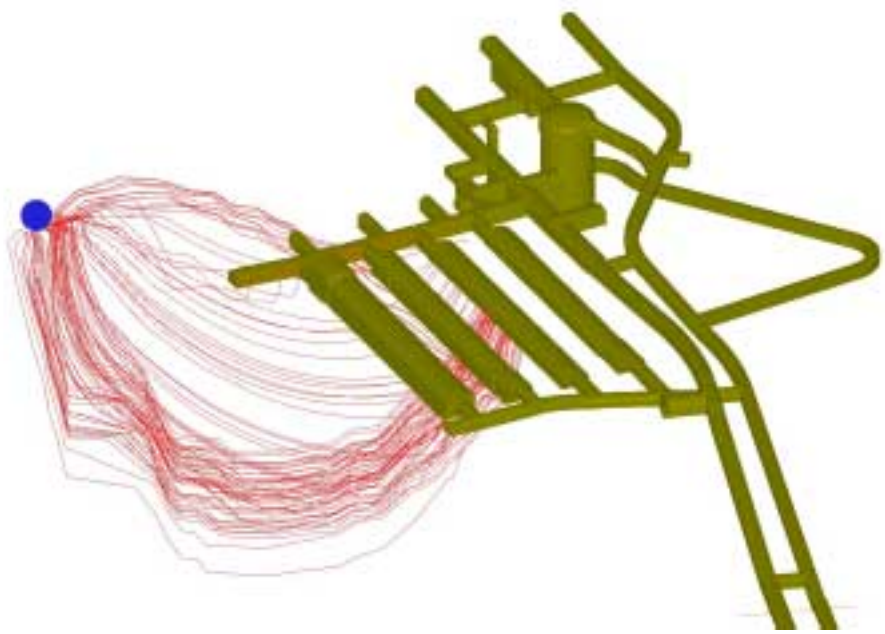

Figure 12.5 *Well-case F. The major flow routes from the BTF2 tunnel, at time equal to 5000 AD. The well is placed at the centre of the blue circle.*

Figure 12.5 presents flow paths from the BTF2 to Well F. The well is located in Zone 3, close to the intersection with Zones 6 and H2 (blue circle). The well discharge is extracted at a depth of about 75 meters below the ground. The well collects 97 percent of the flow that has passed through the BTF2 tunnel. Two major flow routes occur: (i) Lower route, from the base of the BTF2 tunnel via Zone 6 to Zone 3 and finally to the well, this route will conduct most of the flow. (ii) Upper route, from the BTF2 tunnel via access tunnels and/or through the rock mass to Zone H2 and via H2 towards the well.

Even if 97 percent of the flow from the BTF2 tunnel reaches the well, this will only make up 4.6 percent of the total discharge of the well, as the well discharge is much larger than the flow through the BTF2.

12.6.5 Discussion of the results of the Well-cases

12.6.5.1 Depths of flow paths to wells and effects of regional flow direction

A well is a sink in the groundwater system. In the surroundings of a well, the well will divert and intercept the groundwater flow. A well will collect water from all directions, but most water from the flow routes with the smallest resistance. A flow path analyses of the flow routs to the wells demonstrate that even if a well is placed in a flow field, which is dominated by local recharge and discharge areas and by a local flow cell, the well will still collect a certain amount of groundwater from great depth. How much groundwater that will be collected from great depth depends on the regional flow field. Two examples are given below:

- At 3000 AD, the flow situation is in a transient phase, the shoreline has recently passed over the SFR and on the average, the regional flow in the close surrounding of the SFR is directed towards the ground surface at a vertical angle of about 45 degrees (see Sec. 8.6.2). Considering the wells upstream of SFR, on the average, 15 percent of the well discharge comes from below –200 masl. For the wells inside

of SFR, on the average, 21 percent of the well discharge comes from below –200 masl. The wells downstream of SFR are not applicable at 3000 AD.

- At 5000 AD, the local flow is at a steady-state-like situation, the shoreline is far away from SFR and on the average, the regional flow in the close surrounding of the SFR is horizontally directed (see Sec. 8.6.2). Considering the wells upstream and inside of SFR, on the average, 6 percent of the well discharge comes from below –200 masl. For the wells downstream of SFR, on the average, 28 percent of the well discharge comes from below –200 masl.

12.6.5.2 Flow of water from deposition tunnels to a well upstream of SFR

For a well placed upstream of SFR, the possibility to collect contaminated water from SFR is very small. To collect contaminated water, the well either needs to be an extremely strong sink or to be placed extremely close to the tunnel system.

If the well is not placed very close to the tunnel system, if the well is placed at least about 100 m upstream of SFR. For such a well to create a sink, so strong that it will turn around the natural groundwater flow pattern, is probably not possible. At least not by a single well. Because:

- The potential groundwater recharge is large (unless the climate will change) and a large recharge will limit the influence radius of a well.
- If the well is placed in a rock mass and does not intersect a fracture zone, the conductivity of the rock mass is not large enough to sustain a well discharge of the size necessary to turn around the natural flow pattern. Additionally, the maximum sustainable discharge at such a well is probably too small for the needs of a farm.
- If the well is placed in a fracture zone i.e. fracture zone 3, the large conductivity of the zone and the connection between zone 3 and the Singö zone, together with the large potential groundwater recharge, will tend to direct the influence radius upstream, away from SFR. And thereby limit the possibility of the wells influence radius to extend downstream, all the way to the SFR.

Well-cases A and B demonstrate the conclusions above.

However, if the well is placed very close to the tunnel system, it is possible that the well may collect some water from the deposition tunnels, but as the well is upstream of the natural flow pattern, it is likely that it will only be a limited amount. Well-case C demonstrates this.

12.6.5.3 Flow of water from deposition tunnels to a well inside of SFR

A single well that intersects the tunnel system will probably collect a large amount of the contaminated water that flows through the deposition tunnels, but not necessarily all the flow, as the spatial distribution of the deposition tunnels will lead to a spread of the contaminated water. Well D exemplifies this; it is placed inside the BLA tunnel and takes all its water from this tunnel. However, via the BLA tunnel, the well will also collect most of the flow from the BMA and BTF tunnels, but at a discharge rate of 2.37 m^3/day no flow from the SILO will reach the well.

A well within the tunnel system will also give rise to an increase in the flow passing through the deposition tunnels. For example, without a well the total flow through all deposition tunnels might be about 0.7 m^3/day, but a likely well discharge is perhaps 1 m^3/day to 6 m^3/day. Hence, a well inside a deposition tunnel means an increase of flow. For example, Well D intersects the BLA tunnel, this generates an increase of flow through the tunnel of about 21 times at 3000 AD and 14 times at 5000 AD, compared to the situation without Well D.

If a well intersects the tunnel system of SFR, it can either intersect an access tunnel or a deposition tunnel. The deposition tunnels are separated from the other tunnels by low permeable plugs at both ends of the tunnels. An interesting effect of the tunnel plugs is that a flow path from deposition tunnels through access tunnels to a well, will have to pass at least two low-permeable plugs if the well is in a deposition tunnel; but only one plug if the well is in an access tunnel. This could, for some well locations in access tunnels and some well discharge rates, make a well in an access to a stronger sink than a well inside a deposition tunnel, as regards the flow from other deposition tunnels.

12.6.5.4 Flow of water from deposition tunnels to a well downstream of SFR

A well located downstream of the SFR (in relation to an undisturbed groundwater flow field) can be placed below a discharge area for the undisturbed groundwater flow from the repository and/or along a flow route from the repository. It follows that such a well could intercept and collect contaminated water from the SFR even if the well is a very weak sink. However, if the well is located outside of the flow routes from the repository and/or outside of the discharge areas for the undisturbed flow coming from the repository, the well needs to be a strong sink to divert the natural flow field and collect water from SFR (Well-cases G and H demonstrates this).

For the base case of this study we have assumed that the topography remains the same in the future. For such a situation it is not possible by a single well, downstream of SFR, to collect all the contaminated water from the SFR, because the flow paths from the deposition tunnels will spread over a large domain. For the undisturbed flow paths from the repository, the maximum distance between discharge areas is about 700 m. For the base case, the discharge of flow paths from the repository will mainly take place at two different areas, the discharge area for the BMA, BLA and BTF tunnels along zone 3, and the discharge area for the SILO along and close to the intersection of zones 8 and 9 (see Chapter 11.8).

- It is possible to collect most of the flow coming from BMA, BLA and BTF in a single well. If that well is placed below the discharge area for the undisturbed flow from these tunnels or along the flow routs from these tunnels; but such a well will not collect anything from the SILO (Well-case F demonstrates this).
- It is possible to collect most of the flow from the SILO in a single well. If that well is placed below the discharge area for the undisturbed flow from the SILO or along the flow routs from the SILO; but such a well will not collect anything from the BMA, BLA and BTF tunnels (Well-case I demonstrates this).

However, the topography may change in the future, e.g. because of erosion and sedimentation, if the topography changes the flow pattern of the groundwater will change as well. For such a situation it is possible that all flow paths from the repository

will discharge at the same area, this is discussed in Chapter 16, e.g. Figure 16.5. If all flow paths from the repository discharge at the same area, and the extension of that discharge area is limited; for such a situation it is possible for a single well to collect most of the flow from the repository, if the well is located in the near vicinity of that discharge area.

12.6.5.5 Dilution of contaminated water in a well

Since the total flow through deposition tunnels is normally much smaller than the well discharge, the contribution of contaminated water to the total well discharge becomes small. Except if a well intersects a deposition tunnel and the well collects all its water from this tunnel, for such a situation all of the well discharge will be contaminated water, and no dilution will take place in the well. However, this is the only situation for which no dilution will take place in the well; normally the contaminated water coming from the deposition tunnels will be diluted in the well by non-contaminated water.

The dilution in a well is function of the size of the well discharge and the size of the flow of contaminated water. Generally, a large discharge at a well will result in a large dilution, giving a small amount of contaminated water (low dose) to a large number of consumers, while a small discharge will result in less dilution and give a large amount of contaminated water (high dose) to a few consumer,

Considering the well studied, which intercept flow from the deposition tunnels (Well-cases C, D, E, F and I), the dilution at these wells of water coming from the repository varied between zero dilution, i.e. 100% of well discharge coming from deposition tunnels (Well D), and a dilution equal to 5000 times, i.e. 0.02% of well discharge coming from deposition tunnels (Well C). The contribution of contaminated water from the deposition tunnels to the total discharge in a well is given in Table 12.15.

12.6.6 Effects of an abandoned well that intersects a tunnel

By use of Well D we have studied the effects of an abandoned well that intersects a deposition tunnel. We have studied a well that is no longer in use, but connects the surface water system with the BLA deposition tunnel, via an open borehole. Presuming that the water level of Well D is equal to the level of the ground surface, the borehole will cause an increased flow through the BLA tunnel. At 3000 AD the flow of BLA will be increased 3 times, and at 5000 AD the flow of BLA will be increased 7 times, in comparison to the flow without the open borehole. For the above given conditions, the borehole will be a source of water; hence groundwater will flow through the borehole, into the BLA tunnel and further on, e.g. via zone 6. It is likely that any abandoned and open borehole that intersects the tunnel system will be a source of water and not a sink, as long as the water level of the borehole is equal to the level of the ground surface. However, for such a borehole to remain filled with water, there has to be an inflow of water into the borehole, and that flow is not negligible. For the case discussed above (Well D), the inflow of water has to be equal to 126 m^3/year (14 litre/hour) at 3000 AD, and equal to 406 m^3/year (46 litre/hour) at 5000 AD. It is not unlikely that these amounts of flow are available during rainy and wet seasons (spring and autumn), but not necessarily during summer and winter. Hence, it is likely that for the situation studied the flow through the intersected tunnel will drop during dry periods.

12.7 Estimation of probability of well contamination

12.7.1 Introduction

In a simplified way we will below estimate the probability for a well, in the surrounding of the SFR repository, to be placed in a such a way that it may collect contaminated water coming from the repository or intersect a deposition tunnel (BMA, BLA BTF and SILO). No well will be drilled into the rock mass, for the purpose of fresh water supply, as long as the sea covers the studied area. Hence, the conclusions given below correspond to a situation when the sea has withdrawn from the area studied.

12.7.2 Size of risk area considering contamination of well discharge

Based on the discharge areas of the undisturbed flow from the repository and the lay out of the tunnel system at SFR, it is possible to outline a risk area. The risk area is an area limited by the following condition. There is a significant probability that a well located within the risk area will intercept contaminated water coming from the deposition tunnels of the SFR repository. However, this risk area does not include wells drilled directly into the tunnel system The size of the risk area changes with time, as the discharge areas changes with time, see Chapter 11.8. In the following analysis we have used a conservative approach and the risk area corresponds to a time when the discharge areas are at there largest extension, this corresponds to the steady-state-like conditions at 5000 AD. This risk area is indicated in Figure 12.6; the size of the area is approximately 0.2 km^2, and this area is called Risk Area 1.

12.7.3 Size of risk area considering a well drilled into a deposition tunnel

Below we will estimate the size of the risk area, within which a borehole of a well may directly intersect a deposition tunnel, and thereby become contaminated.

- Presuming that the borehole is vertical, the risk area corresponds to the horizontal extension of the deposition tunnels. Put together, the total horizontal area of these tunnels is 2 400 m^2, we will call this area Risk Area 2; and it is the risk area for a vertical borehole into a deposition tunnel. A vertical borehole within this risk area will intersect a deposition tunnel, if the length of the borehole is larger that ca. 60 m.
- Presuming that the borehole studied is inclined with an unknown angle, between zero and 45 degrees, the risk area becomes much larger. We have estimated the size of such a risk area based on the following condition: It is a significant probability that an inclined borehole located within this risk area will intersect a deposition tunnel. We will call it Risk Area 3 and the size of this area is ca. 140 000 m^2.

Hence there is an important difference between the two risk areas (Risk Area 2 and Risk Area 3). Considering Risk Area 2, the probability for a vertical borehole, from this area, intersecting a deposition tunnel is 100 percent; if the borehole is long enough (larger than ca. 60 m). Considering Risk Area 3, the probability for an inclined borehole, from this area, intersecting a deposition tunnel is much less than 100 percent, regardless of borehole length.

12.7.4 Area studied and localisation of a well

Consider a circular area surrounding the SFR repository (centre at SFR), we will call this area “the area studied”. We also presume that a well is to be placed within this area. For the localisation of the well it is assumed that the well is placed within the circular area in a uniform random way (unconditioned). An example of such an area is given in Figure 12.6. Considering the time domain, no wells will be drilled into the rock mass, for the purpose of fresh water supply, as long as the sea covers the studied area. This condition limits the size of the area studied, dependent on time.

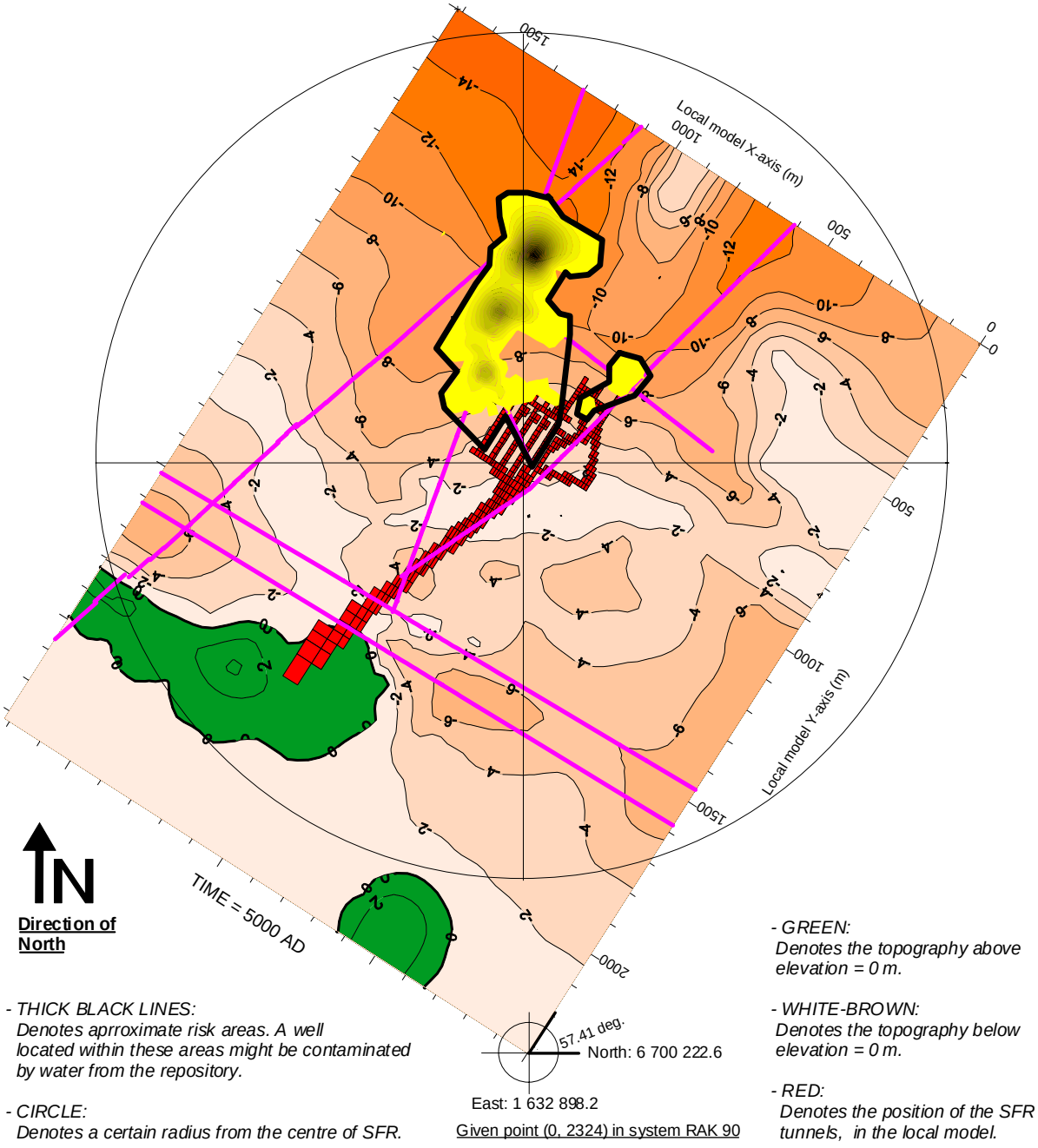

Figure 12.6 *The risk area within which a well might become contaminated by water from the repository (Risk Area 1). The size of the denoted risk area is approximately 0.2 km^2. The figure also gives an example of an area studied, denoted by a circle*

12.7.5 Results - estimation of probability

12.7.5.1 Risk Area compared to an area of a given size

Based on a simple comparison between (i) the size of a risk area and (ii) the size of an area studied, it is possible to estimate the probability of placing a well within a risk area, for different areas studied. Or in other words, presuming that a risk area is within an area studied and that a well is placed in a uniform random way within the area studied; the size of a risk area expressed in percent of the area studied, correspond to the probability, expressed in percent, for placing a well within the risk area. The results of such a comparison is given in Figure 12.7. This figure presents the size of the risk area in percent of a circular area defined by a radius from SFR, as a function of the radius from SFR. The following conclusions can be made based on Figure 12.7.

Considering Risk Area 1: Contamination of well discharge.

- The larger the radius of the circular area studied the smaller the probability that a well within this area will also be within the risk area.
- If the radius of the circular area studied is larger than 1 km (the radius from the SFR is larger than 1 km), the probability that the well will be within the risk area is less than 7 percent.
- If the radius of the circular domain studied is larger than 5 km (the radius from the SFR is larger than 5 km), the probability that the well will be within the risk area is less than 0.3 percent.

Considering Risk Area 2 and 3: A borehole intersecting a deposition tunnel.

- The larger the radius of the circular area studied the smaller the probability that a well within this area will also be within the risk area.
- If the radius of the circular area studied is larger than 1 km (the radius from the SFR is larger than 1 km) we get the following results. The probability that the well will be within the risk area is less than 0.08 percent considering Risk Area 2 (vertical borehole) and less than 4.5 percent considering Risk Area 3 (inclined borehole).
- If the radius of the circular domain studied is larger than 5 km (the radius from the SFR is larger than 5 km) we get the following results. The probability that the well will be within the risk area is less than 0.003 percent considering Risk Area 2 (vertical borehole) and less than 0.18 percent considering Risk Area 3 (inclined borehole).

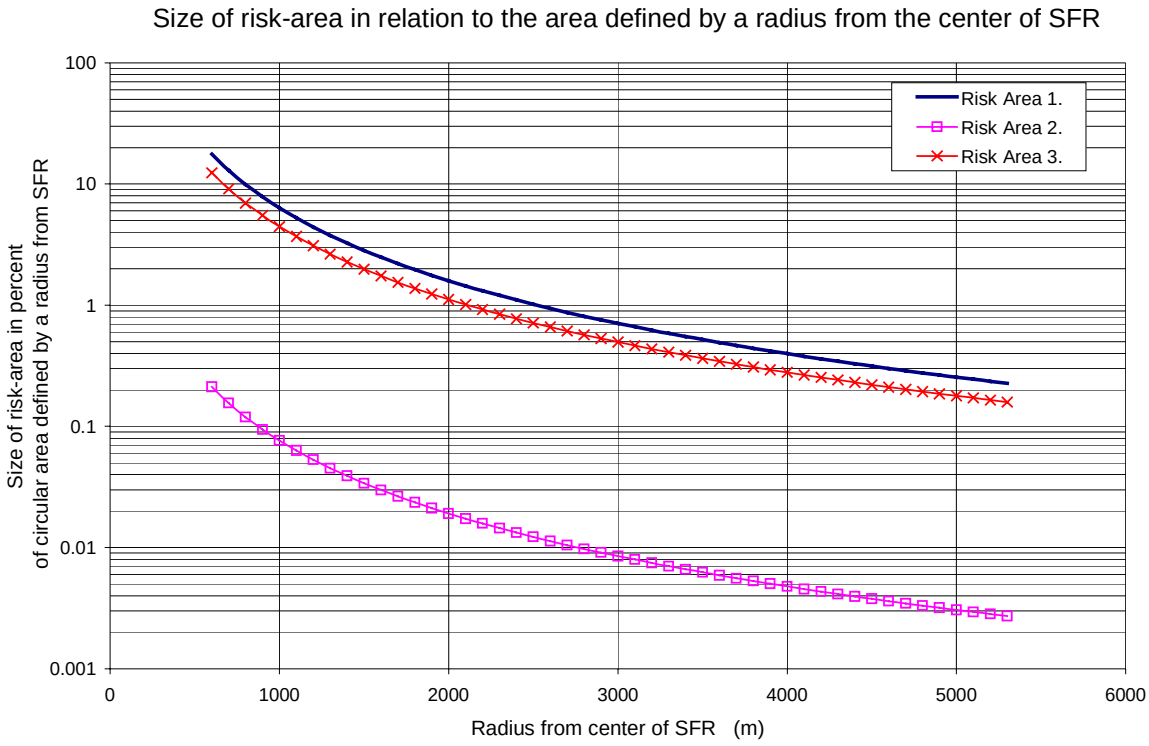

Figure 12.7 *Size of risk areas in relation to the area defined by a radius from the centre of the SFR.*

12.7.5.2 Risk Areas compared to present well density

It possible to estimate the probability of a future well being within the risk areas by studying the number of wells that at present is within the Forsmark area (well density as provided by the SGU well archive). By knowing the well density and by presuming that, (i) in the future the wells will be located in a uniform random way and (ii) the well density will be the same in the future; it is possible to estimate the probability of a well being within the risk areas.

Such a comparison will however not consider the aspect of time. As the sea withdraws new land will be exposed, initially the well density of this new land is zero. Hence, the estimates given below correspond to a situation when the sea has withdrawn from the areas surrounding repository, humans have developed the new land, and the well density of the new land has increased from zero to the present value.

A small value of well density will produce a small probability of a future well being within the risk areas, and a large value of well density will produce a large probability. Considering the well density (given in Table 12.1) which for the Forsmark area is estimated to 0.3 wells per square kilometre, the following results are obtained (calculated as, size of risk areas times the well density).

Considering Risk Area 1: Contamination of well discharge.

- The resulting probability is 0.06, which is the same thing as 6 percent.

Considering Risk Area 2 and 3: A borehole intersecting a deposition tunnel.

- Risk Area 2 (vertical borehole): The resulting probability is 7×10^{-4}, which is the same thing as a probability of 0.07 percent.
- Risk Area 3 (inclined borehole): The resulting probability is 0.04, which is the same thing as a probability of 4 percent.

It is important to remember that the values of probability given above correspond to the probability of a well being within a certain risk area. Hence it is not the same thing as the probability of a well discharge being contaminated (Risk Area 1) or that of a well intersecting a deposition tunnel (Risk areas 2 and 3).

Risk Area 1 represents an area for which it is a significant probability that a well located within this area will intercept contaminated water. It is however perfectly possible that a well within this area is not contaminated. This is demonstrated by well-cases H, I and G, they are all within the Risk Area 1, but with a discharge rate of 2.37 m^3/day, it is only case I that will produce contaminated water (see Figure 12.3 and Figure 12.4). Thus, the probability of a well discharge being contaminated is smaller than the probability of a well being within Risk area 1.

We may look upon Risk Areas 2 and 3 as estimations of upper and lower bounds for the probability of a well intersecting a deposition tunnel. Considering the well density of the Forsmark area we estimate that the probability for a well intersecting the deposition tunnels is between 0.07 percent and 4 percent.

Table 12.14 Percentages of the total flow of a deposition tunnel that reaches a well.

The wells studied are in the in the surroundings of the SFR and have a depth of about 80 meters. The discharge of a well is assumed to represent the water requirements of a small farm.

Time, And Case.	Well ID.		Well Discharge (m3/day) (1)	Percentages of the total flow of a Deposition tunnel that reaches a well.(2)					Location of well
				SILO (3)	BMA	BLA	BTF2	BTF1	
Time: **3000 AD** Case 4B Plus Wells	Upstream	**A** (w1)	2.37	0	0	0	0	0	Upstream of SFR in Z-3
		B (w0)	2.1	0	0	0	0	0	Upstream of Sfr, in rock mass
		C (w7)	1.1	3	0	0	0	0	Close to SILO in rock mass
	Inside	**D** (w3)	2.37	0	75	100	100	97	Inside of SFR in BLA tunnel
		E (w2)	2.37	1	0	0	2	99	Inside of SFR in access tunnel
	Downstream	**F** (w4)	Below sea	-	-	-	-	-	Downstream of SFR in Z-3
		G (w8)	Below sea	-	-	-	-	-	Downstream of SILO in Z-8
		H (w5)	Below sea	-	-	-	-	-	Downstream of SILO in Z-8
		I (w11	Below sea	-	-	-	-	-	Downstream of SILO in Z-8
Time: **5000 AD** Case 4B Plus Wells	Upstream	**A** (w1)	2.37	0	0	0	0	0	Upstream of SFR in Z-3
		B (w0)	2.1	0	0	0	0	0	Upstream of Sfr, in rock mass
		C (w7)	1.1	3	0	0	0	0	Close to SILO in rock mass
	Inside	**D** (w3)	2.37	0	75	100	99	67	Inside of SFR in BLA tunnel
		E (w2)	2.37	0	0	0	3	69	Inside of SFR in access tunnel
	Downstream	**F** (w4)	2.37	0	53	96	97	76	Downstream of SFR in Z-3
		G (w8)	2.37	0	0	0	0	0	Downstream of SILO in Z-8
		H (w5)	2.37	0	0	0	0	0	Downstream of SILO in Z-8
		I (w11	2.37	83	0	0	0	0	Downstream of SILO in Z-8

(1) For Well B and C, the largest possible discharge is < 2.37 m3/day, due to the low permeable rock mass. For all wells, the water is discharged along a section length of about 5 m, at an elevation of ca. –80 masl.
(2) The total flow of a tunnel is defined in Section 2.8 it is given in m3/seconds.
(3) First SILO definition , Local model.

Table 12.15 Contribution of water from the deposition tunnels to the well discharge.

Expressed in percent of the discharge, the contribution demonstrates the dilution that will take place in a well. Dilution in a well occurs because the discharge of the well studied is larger than the flow of contaminated water. Hence, in the wells studied, the contaminated water from the deposition tunnels will mix with non-contaminated water. The well discharge represents the water requirements of a small farm

Time, And Case.	Well ID.		Well discharge (m3/day) (1)	**Contribution of water from the deposition tunnels to the total well discharge. In percent of the total well discharge. (2)**						Location of well
				SILO (4)	BMA	BLA	BTF2	BTF1	Total	
Time: **3000 AD** Case 4B Plus Wells	Upstream	**A** (w1)	2.37	0	0	0	0	0	0	Upstream of SFR in Z-3
		B (w0)	2.1	0	0	0	0	0	0	Upstream of Sfr, in rock mass
		C (w7)	1.1	0.02	0	0	0	0	0.02	Close to SILO in rock mass
	Inside	**D** (w3)	2.37	0	4.3	100	9.0	4.5	117.9 (3)	Inside of SFR in BLA tunnel
		E (w2)	2.37	0.003	0	0	0.09	5.6	5.7	Inside of SFR in access tunnel
	Downstream	**F** (w4)	Below sea	-	-	-	-	-	-	Downstream of SFR in Z-3
		G (w8)	Below sea	-	-	-	-	-	-	Downstream of SILO in Z-8
		H (w5)	Below sea	-	-	-	-	-	-	Downstream of SILO in Z-8
		I (w11	Below sea	-	-	-	-	-	-	Downstream of SILO in Z-8
Time: **5000 AD** Case 4B Plus Wells	Upstream	**A** (w1)	2.37	0	0	0	0	0	0	Upstream of SFR in Z-3
		B (w0)	2.1	0	0	0	0	0	0	Upstream of Sfr, in rock mass
		C (w7)	1.1	0.02	0	0	0	0	0.02	Close to SILO in rock mass
	Inside	**D** (w3)	2.37	0	4.3	100	12.0	5.6	121.9	Inside of SFR in BLA tunnel
		E (w2)	2.37	0	0	0	0.2	6.3	6.5	Inside of SFR in access tunnel
	Downstream	**F** (w4)	2.37	0	4.0	6.7	4.6	3.8	19.1	Downstream of SFR in Z-3
		G (w8)	2.37	0	0	0	0	0	0	Downstream of SILO in Z-8
		H (w5)	2.37	0	0	0	0	0	0	Downstream of SILO in Z-8
		I (w11	2.37	0.2	0	0	0	0	0.2	Downstream of SILO in Z-8

(1) For Well B and C, the largest possible discharge is < 2.37 m3/day, due to the low permeable rock mass. For all wells, the water is discharged along a section length of about 5 m, at an elevation of ca. –80 masl.
(2) The contribution in % is calculated as: Contribution% = (Q_from_tunnel / Q_total_discharge) * 100
(3) The total percentage is larger than 100, because the flow has passed through several deposition tunnels.
(4) First SILO definition, Local model.

13. Extended tunnel system at SFR

13.1 Introduction and purpose

SFR is designed for the final disposal of low and intermediate level nuclear waste from the Swedish nuclear power plants and from the CLAB (central interim storage for spent nuclear fuel) as well as from other industries, research and medical care. In total the present layout of the SFR is intended for 90000 m^3 of waste. There are plans for expansion of the SFR to make place for the disposal of radioactive waste from the decommissioning of the nuclear power plants. The original planned extension of SFR will make room for an additional 127 000 m^3 of waste.

The purpose of the model study that we will present below is to estimate the future flow through the extended repository. The estimate is based on simulations with mathematical models.

13.2 The extended SFR and the models representing it

13.2.1 Layout of the extended tunnel system

In the following modelling study we will use the originally planned extension of SFR as defined in the original drawings of SFR (SKB - SFR drawings). The planned extension of SFR includes a new SILO and six new horizontal deposition tunnels, as well as access tunnels. The new SILO is placed close to the old SILO, but the new SILO will not have the same vertical extension as the old SILO, the new SILO will be shorter. The six new horizontal deposition tunnels includes two tunnels of BMA-type, called BMA2 and BMA3; as well as four new tunnels of BLA-type, called BLA 2 through BLA5. The horizontal deposition tunnels are in approximately the same horizontal plane as the old horizontal deposition tunnels, but placed North and North-East of the old tunnels.

The localisation and layout of the new tunnel system is given in Figure 13.1 and Figure 13.2.

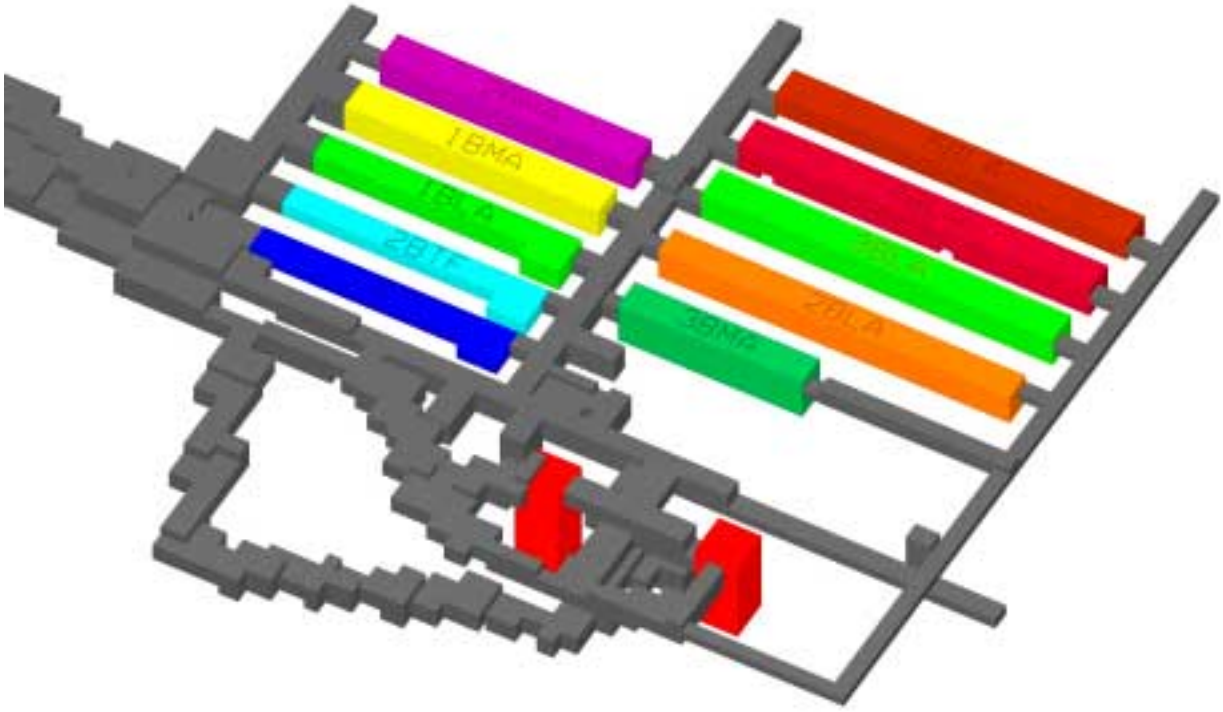

Figure 13.1 *The extended tunnel system of SFR, as defined in the model, 3D- view.*

Note that the new tunnel BMA2 (purple) is parallel to the old tunnel BMA1 and in the same row of tunnels as all the old deposition tunnels. All other new tunnels are placed in a new row of deposition tunnels. The new SILO is placed close to the old SILO.

NEW DEPOSITION TUNNELS:
BMA2 (last in old row)= Purple. *BMA3 (first in new row)= Dark green.*
BLA2 (second in new row)= Orange. *BLA3 (third in new row)= Light green.*
BLA4 (fourth in new row)= Red. *BLA5 (last in new row)= Brown.*
New SILO (close to the old SILO) = Light red.

13.2.2 Size of extended model

The new local model that represents the extended tunnel system is somewhat larger than the old local model representing the old tunnel system. The new model extends about 200 m further towards North-East and about 100 meters further towards North-West. The model covers a horizontal area of, 1834 m x 2481 m (4.5 km^2). The depth of the model is the same as for the old local model (490 m). The upper boundary of the model is the surface topography. The model has vertical sides and a base that is nearly flat. The horizontal size of the extended local model is given in Figure 13.2.

13.2.3 Mesh

Three-dimensional cells of different sizes make up the model. The cells form a mesh. The mesh of local model representing the extended tunnel system and surrounding rock masses has 25 layers and contains 108 800 cells. Each cell represents one node in the mathematical model, placed at the center of the cell. The mesh is primarily optimized to match the layout of the deposition tunnels of the SFR; a secondary optimization was carried out for the access tunnels. Outside of the area where deposition tunnels are defined in the mesh, the size of the cells is increased towards the outer boundaries of the model. The mesh is given in Appendix A.

13.2.4 Methodology, chain of simulations and boundary conditions

For the local model representing the extended tunnel system, we will use exactly the same methodology and the same chain of simulations as for the local model representing the old tunnels. The only difference between the new model and the old model is:

(i) the size of the models (the new model is somewhat larger),
(ii) the extension of the tunnel system and
(iii) the discretisation of the mesh (more cells in the new model).

Hence, as for the old local model, the new local model representing the extended tunnel system will not be used for fully time-dependent simulations. Instead, this model will be assigned boundary conditions (specified head) that are taken from the regional model (from the time-dependent regional simulation), these conditions represents different moments in time. This is exactly the same method as the method used for the old model.

Hence, the local models will have the specified head boundary condition at all faces of the model. The actual head values assigned to the boundary nodes of the local models are based on a three-dimensional interpolation between the calculated head values of the nodes of the regional model.

13.2.5 The studied case - the regional properties

The extended local model represents the same case as the previously presented Case 4.

13.2.6 Calibration of extended model

The extended model was not calibrated; its flow properties (e.g. conductivity) are the same as for the calibrated local model, which includes the present tunnel system (see Chapter 6).

13.2.7 Discretisation of the tunnel system and volumes of deposition tunnels

As in the local model with the present tunnel system (the old tunnels), the new tunnels are defined explicitly in the mesh. Hence, a cell that represents a tunnel represents the tunnel only and no parts of the surrounding rock mass. As previously stated, the mesh is primarily optimized to match the layout of the deposition tunnels of the SFR. The result of this procedure is demonstrated in Figure 13.1. It is impossible to reach a perfect

match between the planned shape of the tunnels and there representation in the model, due to practical restrictions in the number of cells that can be used in the model, but also due to the shape of the cells. The actual tunnels have an arch shaped roof, but the cells in the model have a rectangular shape. If we compare the actual volumes (old tunnels) and the planned volumes (new tunnels) of the deposition tunnels, with the volumes as defined in the model, we get the volumes given in Table 13.1. It is conservative to make the tunnels larger in the model than their actual size, as this will produce an overestimation of the total flow through the tunnels.

Table 13.1 Volumes of SILO and deposition tunnels in the extended repository – actual and planned volumes, compared to the volumes of the model (note, this is not the waste volumes).

OLD DEPOSITION TUNNELS		
Deposition tunnel	Actual volume (m3)	Volume in model (m3)
SILO1	47 500	47 400
BMA1	47 600	64 600
BLA1	27 600	42 800
BTF1	19 700	26 000
BTF2	19 700	26 000

NEW DEPOSITION TUNNELS		
Deposition tunnel	Actual volume (m3)	Volume in model (m3)
SILO2	Not available	37 860
BMA2	Not available	64 680
BMA3	Not available	59 580
BLA2	Not available	80 510
BLA3	Not available	89 460
BLA4	Not available	89 460
BLA5	Not available	68 160

13.2.8 The extended tunnel system and the local fracture zones

The horizontal extension of the extended tunnel system and the fracture zones are given in Figure 13.2. A three-dimensional perspective of the tunnels and the fracture zones is given in Figure 13.3.

The local fracture zones, as known today, are all in the close surroundings of the SFR. In the model, the position of the fracture zones is according to the updated structural geological model (Axelsson and Hansen 1997). The knowledge of these zones is based on information from exploratory drillings and information gathered during the construction of the repository. Hence, the local structural geological model is based on information gathered in the close surroundings of the present repository. And it needs to be stated that outside of this area we have no information of other fracture zones, because no detailed investigation have been carried out outside of the close surroundings of the present repository. For example, it is very likely that several more fracture zones occur close to the repository, but outside of the known local fracture zones that are indicated in Figure 13.2 and Figure 13.3. However, zones that we have no indications of can not be explicitly included in the present model. It is likely that before new tunnels are constructed more field investigations (exploratory drillings etc) will be carried out and thereby more information will become available. Nevertheless, for the present model of the extended tunnel system, we have to rely on the present knowledge of the local fracture zones.

In the modelling study presented below, the extended tunnel system are according to the originally planned extension of SFR, as defined in the original drawings of SFR (SKB - SFR drawings). However, during the design and construction of the SFR repository, when the original layout of the extended tunnel system was decided, the presence and extension of the local fracture zones were not known to the same degree as they are today. Therefore the layout of the extended tunnel system was not designed to avoid the local fracture zones.

Consequently, from a hydrogeological point of view, the layout of the new horizontal deposition tunnels is not the best possible and can probably be improved. For the new horizontal deposition tunnels all tunnels, except one, are intersected by at least one fracture zone, and they are all located in the very near vicinity of a future discharge area. It follows that the groundwater flow through the new tunnels will be larger than for the old tunnels, and the flow paths from the new tunnels to the ground surface will also be shorter than for the old tunnels. For the new SILO the situation is different, no fracture zones intersect it.

The following zones intersect the new horizontal deposition tunnels:

- BMA2: Intersected by Zone 6 (possible intersection with H2, but not in model).
- BMA3: Not intersected.
- BLA2: Intersected by Zones H2 and 8
- BLA3: Intersected by Zones H2 and 8
- BLA4: Intersected by Zones H2 and 8
- BLA5: Intersected by Zones H2, 3, 6 and 8.

Zones H2 and 8 will intersect nearly all of the new tunnels. Tunnel BLA5 has an especially unlucky position, it is intersected by four different fracture zones and is straight below the final discharge area.

In comparison to the old SILO, the new SILO is placed closer to Zone 8 and also closer to the discharge area formed by the intersection between Zones 8 and 9, however no fracture zones intersect it. The new SILO will not have the same vertical extension as the old SILO, the new SILO will be shorter because it is on purpose not extended down to the sub-horizontal zone H2.

Three-dimensional perspectives of the most important fracture zones and the tunnel system are given in Figure 13.4 and Figure 13.5. The first of these two figures presents the tunnel system and Zones H2 and 3, the second figure presents the tunnel system and Zones 6 and 8.

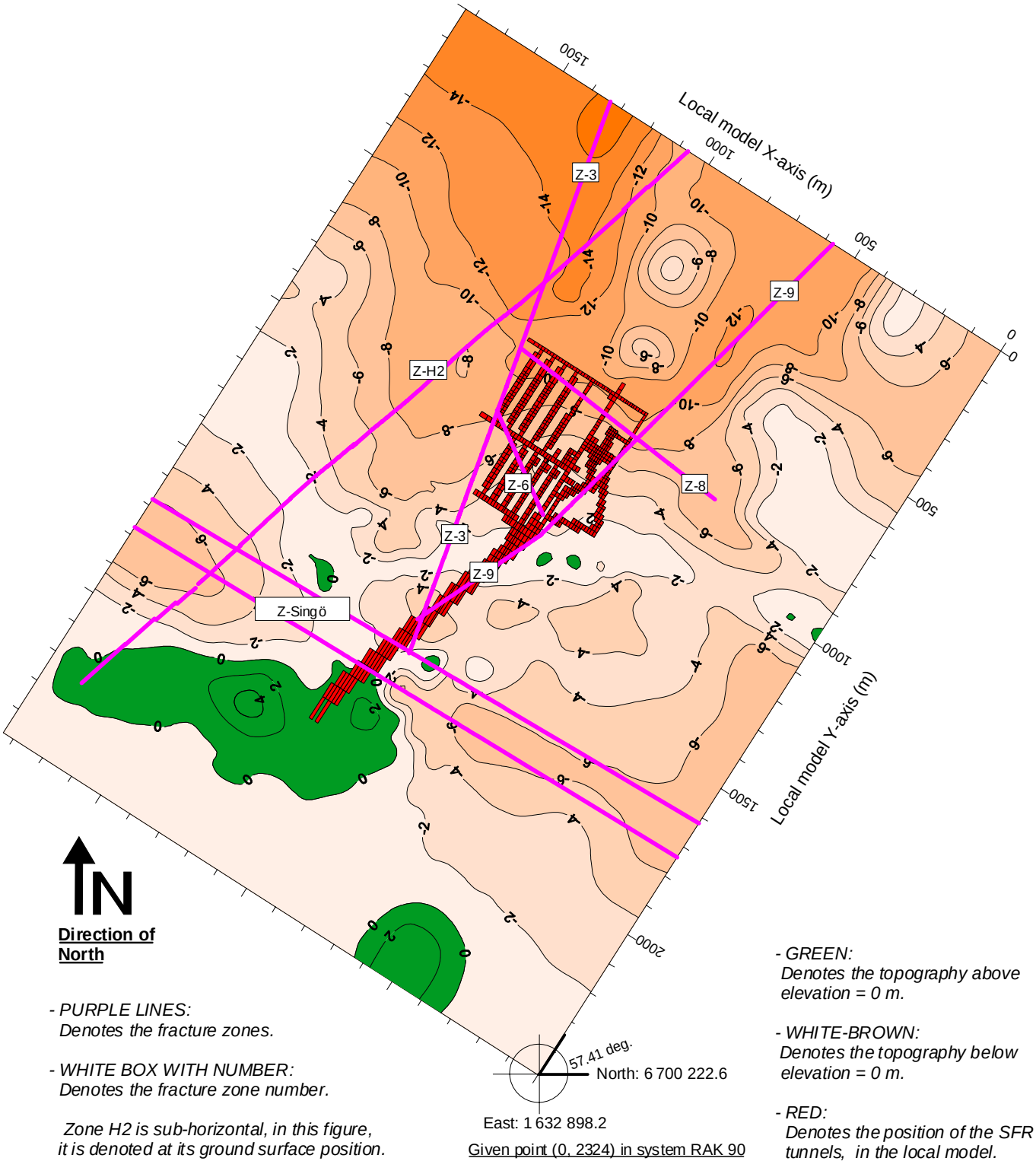

Figure 13.2 *Extended repository, horizontal position of the fracture zones and the tunnel system as well as the topography of the ground surface/seabed.*

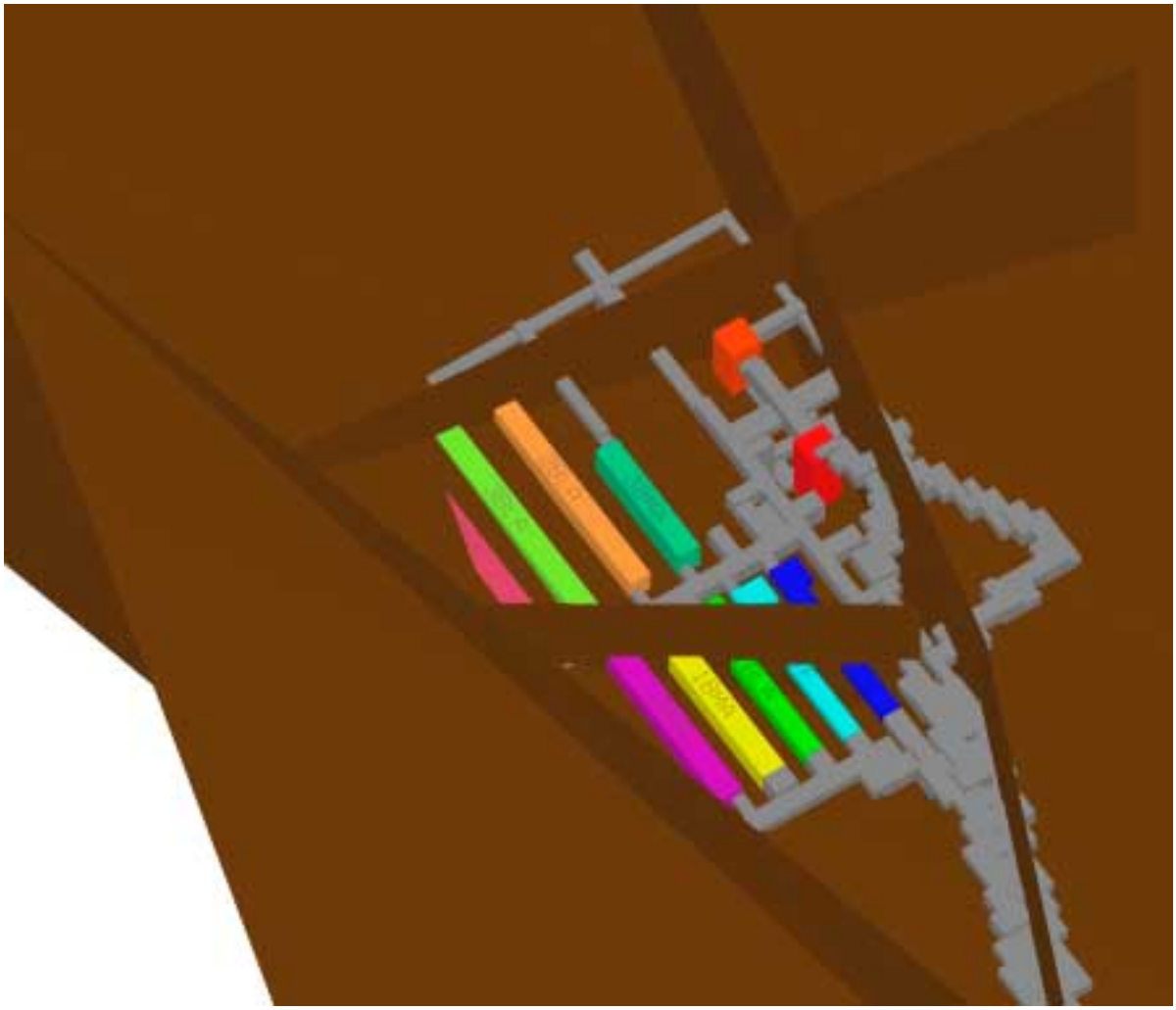

Figure 13.3 *The extended tunnel system of SFR and the local fracture zones, 3D-view.*

Not all of the new tunnels (e.g. BLA5) are visible in this figure, as zone H2 hides some of the tunnels.
Zone 6 will intersect all the old tunnels as well as two of the new tunnels, BMA2 and BLA5.
Zone 8 will intersect tunnels BLA2 through BLA5.
Zone H2 will intersect BLA2 through BLA5.
Zone 3 will intersect BLA5.

The BLA5 tunnel will be at the intersection of Zones H2, 6, 3 and 8.
The new SILO will be very close to both Zone H2 and Zone 8, but will not be intersected by them.

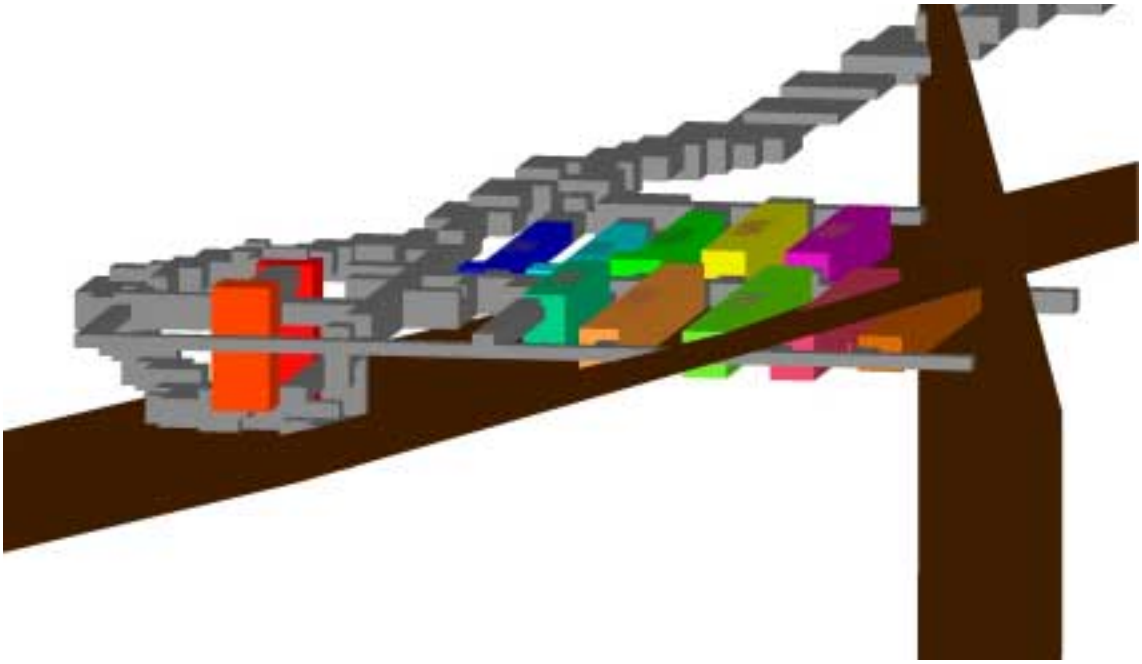

Figure 13.4 *The extended tunnel system of SFR and the local fracture zones H2 and 3.*

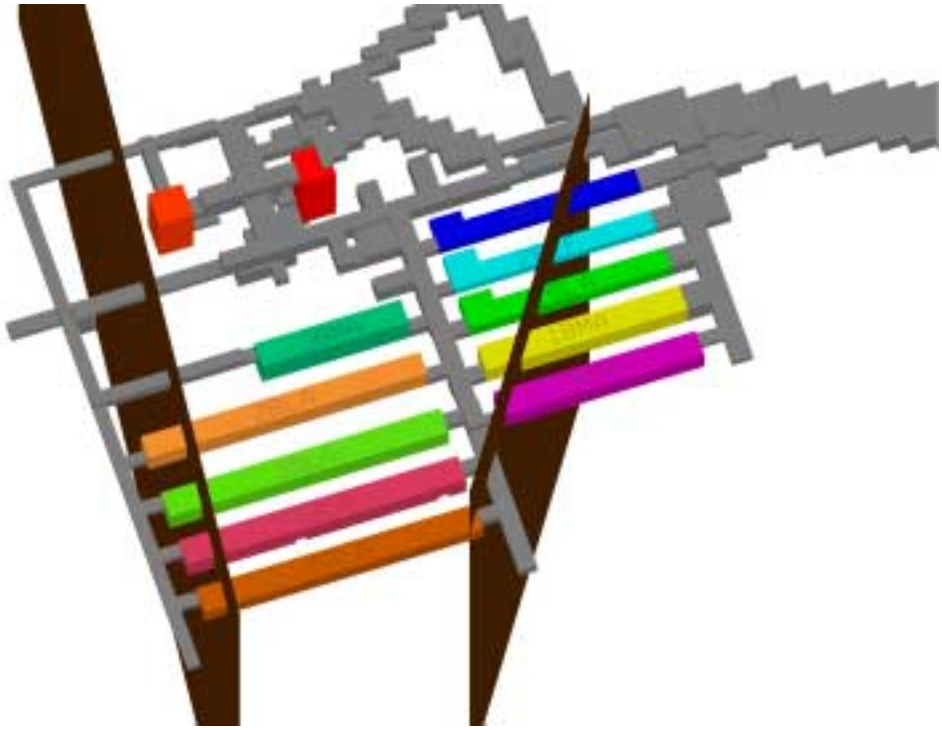

Figure 13.5 *The extended tunnel system of SFR and the local fracture zones 6 and 8.*

13.3 Results of local model representing the extended SFR

13.3.1 Predicted total flow through deposition tunnels

13.3.1.1 General trend

The general trend of the flow is the same as for the model representing the present tunnel system. The extended model predicts that as long as the sea covers the ground above the SFR, the regional groundwater flow as well as the flow in the deposition tunnels are small. However, due to the land-rise the sea-level will be lowered and the shore-line will retreat, at approximately 2800 AD the shore-line will be above the old deposition tunnels. As a consequence of the retreating shore-line, the general direction of the groundwater flow at SFR will change, from vertical upward to a more horizontal flow; the size of the groundwater flow will be increased as well. Hence, the predicted regional groundwater flow at SFR and the flow through the deposition tunnels will increase with time, but a steady-state-like situation will be reached at approximately 5000 AD-6000 AD. For the different deposition tunnels, the total flow versus time has been calculated for each tunnel separately, the results are given in Table 13.2.

It should be noted that the presence of the new tunnels will influence the flow in the old tunnels and the model with the extended tunnels system will not predict the same flow in the old tunnels as was predicted by the previously presented local model.

13.3.1.2 Representation of the deposition tunnels and the tunnel flow

Generally, the representation of the tunnels of the extended model is similar to those of the previous local model. Considering the horizontal deposition tunnels, BMA BLA and BTF, the predicted total flow that we will discuss below, is the flow through highly permeable parts of these tunnels, e.g. the flow through a highly permeable backfill surrounding a concrete construction. It is not the flow through a concrete construction installed in the middle of a tunnel. Considering the SILOs, the predicted total flow that we will discuss below, is the flow through the encapsulation, protected on all sides by low permeable bentonite barriers. It is not the flow through a backfill above the encapsulation. The permeability of the two SILOs are in accordance to the first SILO definition (SD1), as given in Sec.6.5.4. Flow barriers (plugs) are included at both ends of each horizontal deposition tunnel. Flow barriers (plugs) are also included where access tunnels connects to the SILO.

The flow for the different tunnels will be given as a total flow, that is the flow that enters the tunnels through the envelope surface of the tunnels (length^3/time). As the simulations presume steady state conditions and that no sinks occur in the tunnels, the same amount of flow will leave the tunnels through the envelope surface. However, the tunnels interact with the surrounding rock mass and other tunnels, so the lengths of the flow paths through the tunnels will vary.

13.3.1.3 BMA tunnels

The model of the extended tunnel system will not predict the flow of the encapsulations of the BMA tunnels, but the flow through a highly permeable backfill that surrounds the encapsulations. In the old model the BMA tunnel was the tunnel that carried most flow. The presence of the new tunnels will lead to a reduced flow in this tunnel (BMA1), compared to the old situation without the new tunnels. The new BMA2 tunnel is located outside of the old BMA1 and this tunnel will for the new situation carry even more flow than BMA1 used to do. However, the new BLA tunnels will carry even more flow than the new BMA tunnels.

- BMA1 (old tunnel): The flow increases from 8 m3/year at 2000 AD and reaches a steady-state-like flow equal to 40 m3/year at approx. 6000 AD.
- BMA2 (new tunnel): The flow increases from 15 m3/year at 2000 AD and reaches a steady-state-like flow equal to 103 m3/year at approx. 6000 AD.
- BMA3 (new short tunnel): The flow increases from 18 m3/year at 2000 AD and reaches a steady-state-like flow equal to 47 m3/year at approx. 6000 AD.

13.3.1.4 BLA tunnels

The new BLA tunnels are the tunnels located closest to the discharge areas and are also the tunnels that are most intersected by fracture zones. Consequently, the model predicts that these tunnels will carry most flow of all the deposition tunnels. Especially the BLA5 tunnel has an unlucky position in relation to the fracture zones and the discharge areas, BLA5 is intersected by four different fracture zones and is located below a large discharge area. The flow predicted for BLA5 is about two times the flow that is predicted for all the old tunnels put together. And the flow predicted for BLA4 is 50% through 80% of the flow predicted for all the old tunnels put together.

- BLA1 (old tunnel): The flow increases from 15 m3/year at 2000 AD and reaches a steady-state-like flow equal to 79 m3/year at approx. 6000 AD.
- BLA2 (new tunnel): The flow increases from 30 m3/year at 2000 AD and reaches a steady-state-like flow equal to 147 m3/year at approx. 6000 AD.
- BLA3 (new tunnel): The flow increases from 30 m3/year at 2000 AD and reaches a steady-state-like flow equal to 187 m3/year at approx. 6000 AD.
- BLA4 (new tunnel): The flow increases from 28 m3/year at 2000 AD and reaches a steady-state-like flow equal to 215 m3/year is reached at approx. 6000 AD.
- BLA5 (new tunnel): The flow increases from 91 m3/year at 2000 AD and reaches a steady-state-like flow equal to 590 m3/year is reached at approx. 6000 AD.

13.3.1.5 BTF tunnels

The BTF1 and the BTF2 tunnels are old tunnels, they are the innermost tunnels of the system of horizontal deposition tunnels and they are surrounded by permeable access tunnels and by other deposition tunnels. In comparison to the other deposition tunnels, the surrounding tunnels will limit the flow through BTF1 and BTF2, when the general direction of the groundwater flow changes, from vertical towards horizontal, as the surrounding tunnels will acts as hydraulic barriers. The flow in the BTF tunnels is smaller than in the BMA and BLA tunnels.

- BTF1 (old tunnel): The flow increases from 11 m3/year at 2000 AD and reaches a steady-state-like flow equal to 72 m3/year at approx. 6000 AD.
- BTF2 (old tunnel): The flow increases from 10 m3/year at 2000 AD and reaches a steady-state-like flow equal to 60 m3/year at approx. 6000 AD.

13.3.1.6 SILOs

The two SILOs are located a short distance from the other deposition tunnels. The SILOs are at several different positions connected to access tunnels, but the SILOs are primarily vertical structures and the surrounding access tunnels will not form effective hydraulic barriers. No fracture zones intersects the SILOs. For the extended model, the permeability of both SILOs are defined in accordance to the first SILO definition (SD1), as given in Sec.6.5.4. The first SILO definition represents a more permeable SILO than the second definition (SD2); hence, the predicted flows will be larger for the first SILO definition than if the SILOs were defined in accordance to the second SILO definition.

The flow through the SILOs depends primarily on the average flow in the surrounding rock mass and on the effect of the flow barriers and plugs that protects the SILOs. The flow in the SILOs is much smaller than the flow through the other deposition tunnels, but the general trend of the flow in the SILOs is similar to the trends of the flow of the other tunnels.

The new SILO will be smaller than the old SILO. The new SILO will be shorter because it is on purpose not extended down to the sub-horizontal zone H2. Nevertheless, the flow through the new SILO will be larger than the flow through the old SILO. This is partly because the new SILO is placed closer to Zone 8 and also closer to the discharge area formed by the intersection between Zones 8 and 9, and the average flow in the rock mass increases close to discharge areas.
- SILO1 (old SILO, permeability according to SD1): The flow increases from 0.6 m3/year at 2000 AD and reaches a steady-state-like flow equal to 3.3 m3/year at approx. 5000 AD.
- SILO2 (new SILO, permeability according to SD1): The flow increases from 0.6 m3/year at 2000 AD and reaches a steady-state-like flow equal to 6.7 m3/year at approx. 6000 AD.

13.3.2 Predicted total flow – summary

The table below provides a summary of the predicted total flow through the deposition tunnels of the extended repository.

Table 13.2 Case 4 extended repository: Total flow of the deposition tunnels. SILO permeability in accordance to the first SILO definition (SD1).

(i)

	OLD DEPOSITION TUNNELS				
	TOTAL FLOW (m3/year)				
Time AD	SILO1 (SD1)	BMA1	BLA1	BTF2	BTF1
2000	0.6	8	15	10	11
3000	2.8	25	34	25	29
4000	3.2	38	73	56	68
5000	3.3	40	79	60	72
6000	3.3	40	79	60	72
8000	3.3	40	79	60	72

(ii)

	NEW DEPOSITION TUNNELS						
	TOTAL FLOW (m3/year)						
Time AD	SILO2 (SD1)	BMA2	BMA3	BLA2	BLA3	BLA4	BLA5
2000	0.6	15	18	30	30	28	91
3000	3.9	63	25	72	79	63	203
4000	6.7	99	45	158	208	222	559
5000	6.7	102	46	146	187	215	590
6000	6.7	103	47	147	187	215	591
8000	6.7	103	47	147	187	215	591

(iii)

	OLD AND NEW DEPOSITION TUNNELS		
	TOTAL FLOW (m3/year)		
Time AD	ALL OLD TUNNELS	ALL NEW TUNNELS	ALL TUNNELS OLD AND NEW
2000	45	213	257
3000	116	509	625
4000	238	1298	1536
5000	254	1293	1547
6000	254	1297	1551
8000	254	1297	1551

14. Sensitivity case - failure of barriers

14.1 Introduction

As a part of this study we have included some sensitivity cases, which demonstrates the effect of failing flow barriers. The purpose is not to investigate the causes for such failures, but to demonstrate the effects of failing flow barriers as regards the flow of the tunnel system. In this chapter we have studied the following cases:

- Tunnel flow and degradation of tunnel plugs.
- Flow of a failed SILO encapsulation.
- Flow of a failed section of the BMA tunnel.
- Flow of a failed section of the BTF1 tunnel.

Another section of this study also concerns failing barriers, that is Section 10.6.8, which discusses the permeability of the barriers of the BMA tunnel, considering the efficiency of the hydraulic cage that surrounds the BMA encapsulation.

14.2 Tunnel flow and degradation of tunnel plugs

14.2.1 Introduction and purpose

The purpose is to estimate the flow in the horizontal deposition tunnels (BMA, BLA, BTF) and in the SILO, as regards an increased permeability of the plugs that separate these deposition tunnels from the access tunnels. The increase in permeability represents an assumed degradation of the plugs.

14.2.2 Location of plugs

Before the repository is closed and abandoned, low permeable plugs will be installed at different locations in the tunnel system, and all bore holes into the surrounding rock mass will be refilled with low permeable concrete. The purpose of these measures is to limit the groundwater flow in the tunnels and to create a physical obstacle between the deposited waste and the surroundings. The final number and locations of the plugs are at present not decided.

In the models of this study we have assumed that low permeable plugs will be installed at the following positions (see Figure 14.1):

- In all access tunnels where these tunnels are in contact with the SILO.
- At both ends of the BMA tunnel.
- At both ends of the BLA tunnel.
- At both ends of each BTF tunnels.
- At two different positions along the main access ramp.

14.2.3 Location of local water divides

A water divide is a theoretical boundary separating waters flowing into different basins (surface water flow) or different discharge areas (groundwater flow). The positions of the water divides are of interest as they indicate the boundaries of the flow of surface and ground water. When the land uplifts above the sea, a surface water divide is given by the most elevated parts of the topography. A groundwater divide, on the other hand, is a more complicated concept. Groundwater divides occur as three-dimensional surfaces in the flow medium of the groundwater. However, for the groundwater flows close to the ground surface, the groundwater divides are close to the surface water divides (presuming that the area studied is above the sea). The positions of the local water divides are given in Figure 4.2 and Figure 14.1. The latter figure also gives the position of the groundwater divide in the access ramp at 5000 AD.

At present (2000 AD), the depth of the sea is about 2 - 6 meters at the area where the SFR deposition tunnels are located, and the deposition tunnels are about 600 meters off the shore line. In relation to the period studied (ca. 5000 years into the future) the seabed above the repository will rise above the sea in the near future. As the shore level retreats from the present position, the first part of the seabed that will rise above the sea is the ridge above the Northeast part of the access ramp; at present a pier is located along this ridge. Already at 2250 AD, when the sea water level is 1.5 m lower than the present level, with or without the pier this part of the seabed has risen above the sea and formed a small island. This “new land” will influence the groundwater flow pattern and after some time create a groundwater divide in the access ramp, as more land uplifts above the sea this divide is more firmly established. The status of the plugs in the ramp is not very important for the position of this groundwater divide; with or without the plugs there will be a groundwater divide in the access ramp.

14.2.4 Importance of groundwater divide in access ramp

A consequence of the groundwater divide in the access ramp is that the plugs in the access ramp are of little importance as regards the groundwater flow in the ramp. Because as stated above, with or without the plugs in the ramp, there will be a water divide in the access ramp, and the groundwater flow is not reduced because of the plugs, but because of the water divide.

Hence, with or without plugs in the access ramp, the groundwater flow through the rest of the tunnel system is close to the same. Because of the groundwater divide in the access ramp, the large regional fracture zone intersecting the access ramp (the Singö zone) will not have a large impact on the flow of the SFR tunnel system. Because even without plugs in the access ramp there will be a groundwater divide in the ramp positioned between the Singö zone and the lower parts of the repository (see Figure 14.1) and no groundwater will pass the groundwater divide.

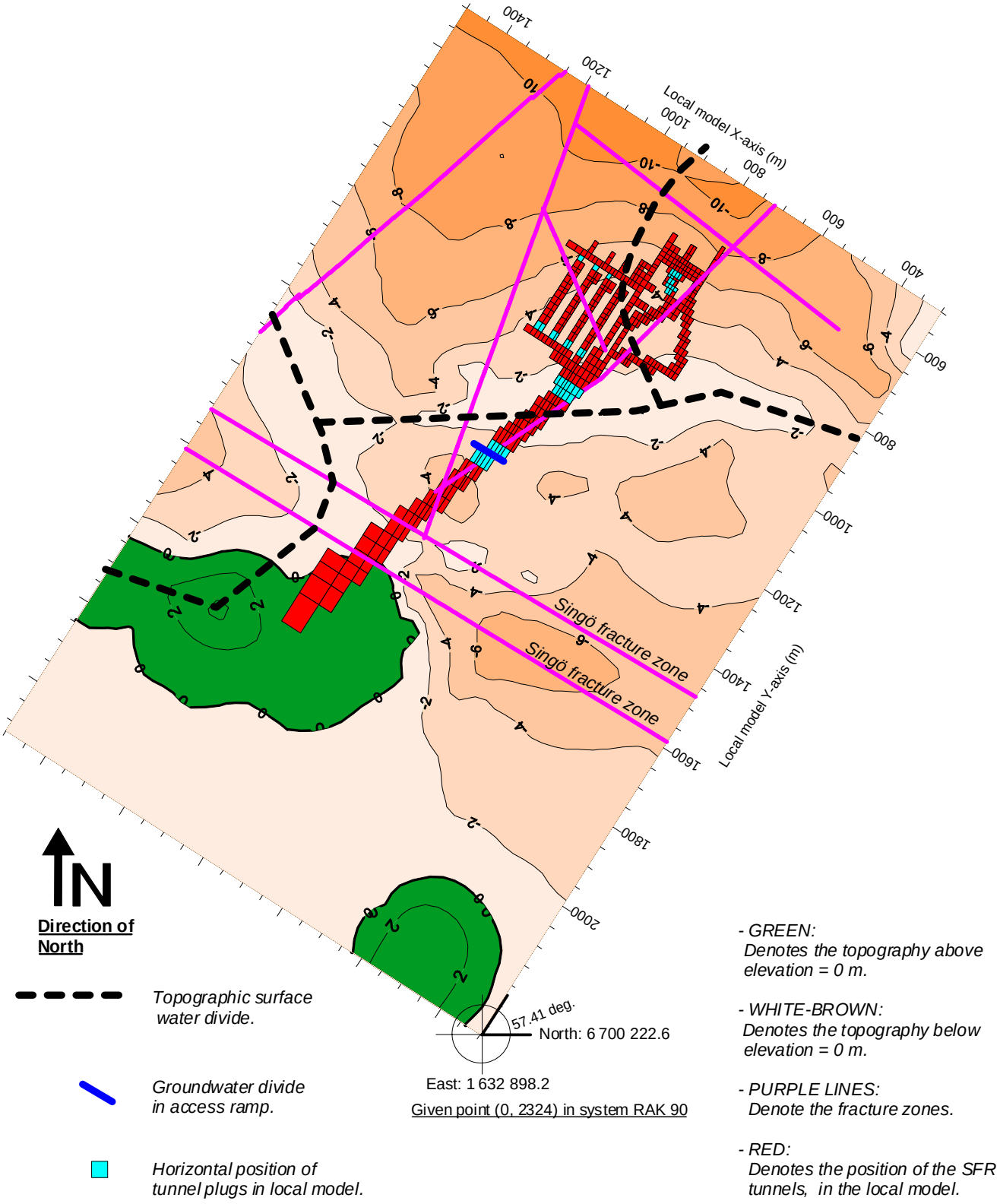

Figure 14.1 *Location of tunnel plugs as defined in the local model and water divides in the close vicinity of the SFR repository, as well as the groundwater divide in the access ramp at 5000 AD.*

14.2.5 Assumed degradation

14.2.5.1 Resistance and conductivity of plugs

The plugs could consist of different layers of materials having different thickness e.g. bentonite and concrete, which together produces one value of resistance. For these calculations we have assumed that some plugs will slowly degrade and finally carry no resistance to flow at all. In the model, the non-degraded (intact) plugs are defined as structures having a resistance to flow equal to $2 \times 10^{+9}$ s, which is the same thing as a plug of thickness one meter having a conductivity of 5×10^{-10} m/s. The tunnels will be backfilled with a highly permeable sand. In these simulations we have assumed a conductivity of the backfill that is equal to 1×10^{-5} m/s. A plug that has a conductivity that is equal to this value, or larger, will not reduce the flow in the tunnels. Hence a completely degraded plug will in these simulations have a conductivity that is equal to 1×10^{-5} m/s. The difference in conductivity between a non-degraded plug and a completely degraded plug is four and a half orders of magnitude. Two different cases have been established. D1 and D2, which represent assumed courses of plug degradation. For both case D1 and D2, all the plugs in the SFR repository are assumed to degrade.

14.2.5.2 Case D1

Case D1 is an assumed situation, for which the conductivity and the resistance of the plugs will degrade two order of magnitudes over a period of 3000 years (see Figure 14.2). The final conductivity of the degraded plugs is 5×10^{-8} m/s (final resistance is $2 \times 10^{+7}$ s). The degrading plugs were added to the local model, Case4.

14.2.5.3 Case D2

Case D2 is an assumed situation, for which the conductivity and the resistance of the plugs will degrade completely over a period of 3000 years (see Figure 14.2). The final conductivity of the plugs is 1×10^{-5} m/s (final resistance is $1 \times 10^{+5}$ s). The degrading plugs were added to the local model, Case 4.

14.2.5.4 Case D3

Case D3 is an assumed situation, for which the plugs carry a negligible resistance to flow. This case (D3) represents a situation for which, from a fluid mechanical point of view, no plugs occur in the tunnel system. As previously discussed, the presence of a plug in the access ramp is of very little importance from a fluid mechanical point of view. The conductivity of the plugs is set equal to 1×10^{-5} m/s (see Figure 14.2), which is the same as the conductivity of the assumed back fill. This case was evaluated by use of the detailed model; plugs with negligible resistance were added to the base case of the detailed model.

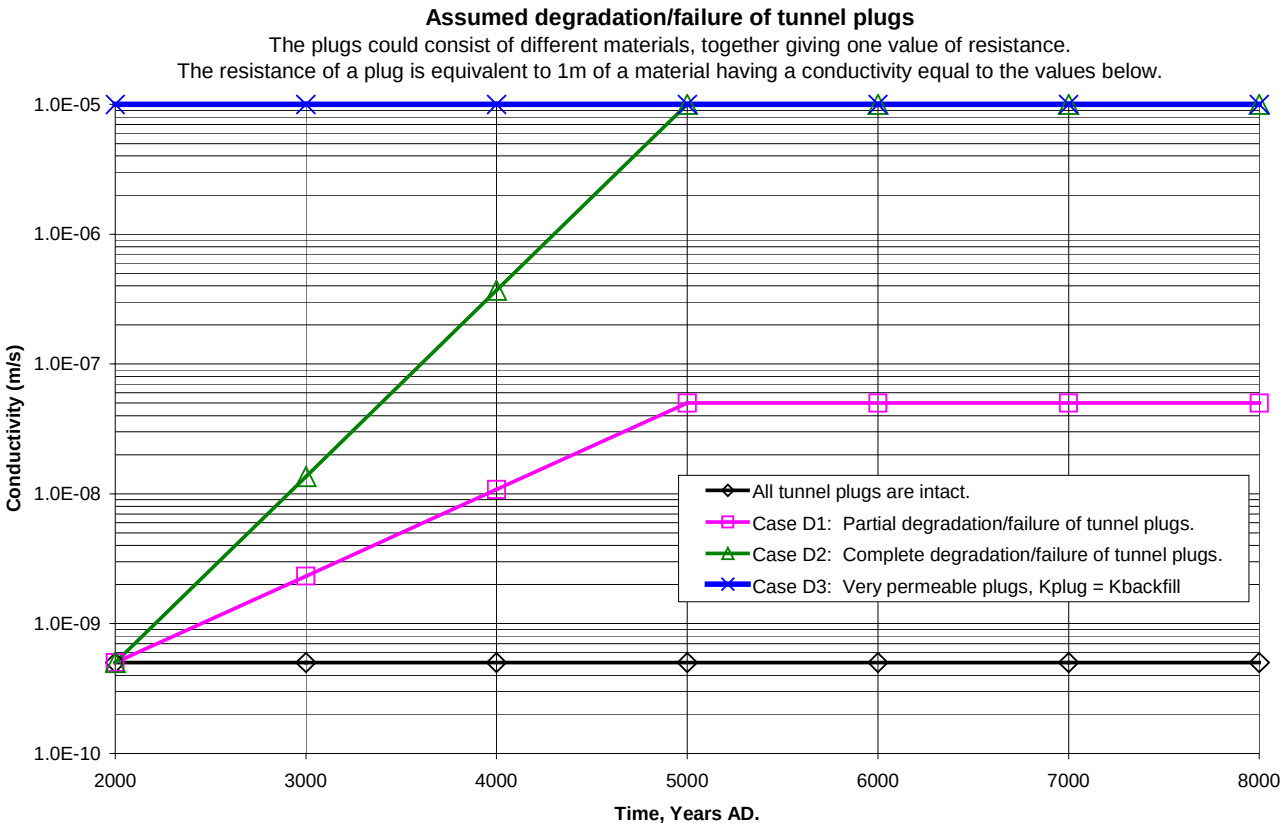

Figure 14.2 *Assumed courses of degradation. For Case D1, the conductivity of the plugs will degrade two order of magnitudes over a period of 3000 years. For Case D2, the conductivity of the plugs will degrade completely over a period of 3000 years. For Case D3, the plugs are set as highly permeable from the start; the plug conductivity is set equal to the back fill conductivity.*

14.2.6 Methodology

For these simulations we have used the local model for Cases D1 and D2 and the detailed model for Case D3. The chain of simulations was the same as for the previous presented calculations with the local and detailed models. For Cases D1 and D2, the degrading plugs were added to the local model and for each moment, represented by the local model, new values of plug resistance was calculated and assigned to the local model. For Case D3, the highly permeable plugs were added to the base case of the detailed model, the same value of plug conductivity was uses for all moments.

14.2.7 Results of Case D1 – partly degrading plugs – local model

Case D1 is an assumed situation, for which the conductivity and the resistance of the plugs will degrade two orders of magnitudes over a period of 3000 years. During the period of degradation, the total flow in the deposition tunnels will increase due to the development of the regional groundwater flow pattern, which is discussed in previous sections. In addition to this, the degradation of the plugs will produce a further increase in total flow. The local model predicts that after 5000 AD, when the plugs are assumed to have degraded two orders of magnitudes, the total flows of the BMA, BLA and BTF

tunnels are ca.1.8 times the total flow of the same tunnels having intact plugs (before 5000 AD the differences are less). As this case is defined in the local model, details of flow inside the BMA, BLA BTF and SILO tunnels are not calculated, such results will be given for Case D3.

14.2.8 Results of Case D2 – fully degrading plugs – local model

Case D2 is an assumed situation, for which the plugs will completely degrade over a period of 3000 years. After 5000 AD, the plugs will not reduce the flow in the tunnels at all. During the period of degradation, the total flow in the deposition tunnels will increase due to the development of the regional groundwater flow pattern, which is discussed in previous sections. In addition to this, the degradation of the plugs will produce a further increase in total flow. This is demonstrated in Figure 14.3, which gives the total flow of the deposition tunnels (local model) with completely degrading plugs, in relation to the total flow of the deposition tunnels with intact plugs (local model).

The model predicts that the complete degradation of the plugs produces a total flow in these tunnels, which is as follows:

- For the BMA and BLA tunnels, the final total flow will be 2.7 times the total flow of the same tunnels having intact plugs (local model).
- For the BTF2 tunnels, the final total flow will be 3.2 times the total flow of the same tunnels having intact plugs (local model).
- For the BTF1 tunnels, the final total flow will be 4.2 times the total flow of the same tunnels having intact plugs (local model).

As this case is defined in the local model, details of flow inside the BMA, BLA BTF and SILO tunnels are not calculated, such results will be given for Case D3.

14.2.9 The new flow pattern inside the tunnel system

With intact plugs, much of the flow in the BMA, BLA and BTF tunnels used zone 6 as a part of the flow route to the discharge areas, because the connections to the rest of the tunnel system was blocked by the plugs. Without the plugs or with very permeable plugs, much of the flow of the deposition tunnels will not use zone 6 in the same way. A new major flow route is through the tunnel system towards the part of the tunnel system closest to the discharge area (the Northwest end of the access tunnel located North of the BMA, BLA and BTF tunnels) and further on via Zones H2 and 6 towards the discharge areas.

Without the plugs or with very permeable plugs, the interaction of flow between the deposition tunnels is reduced, less water is flowing from BTF1 to BTF2, and from the BTF tunnels to the BLA tunnel.

Without the protection of the plugs, the flow of the BMA, BLA and BTF tunnels will be increased. This is because much of the water which use to flow around these tunnels, in the access tunnels and in zones H2, 6 and 9, will now take a flow route with a smaller resistance, and that is a flow route through the unprotected horizontal deposition tunnels. The large increase of flow for the BTF tunnels, and especially for the BTF1

tunnel, is probably because these tunnels are closest to the large access tunnels, e.g. the access ramp, and closest to zone 9.

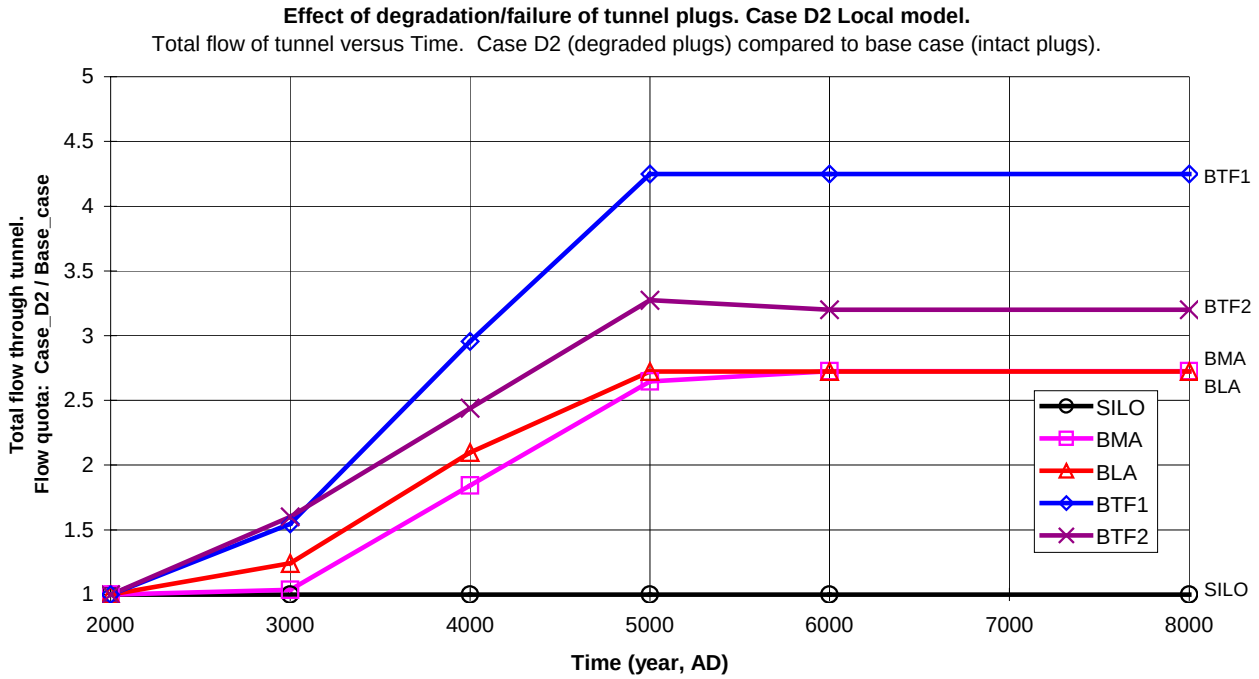

Figure 14.3 *Case D2 – completely degrading plugs in local model. Flow of deposition tunnels with degrading plugs, as a multiple of the flow of deposition tunnels with intact plugs. The plugs are assumed to be fully degraded after 5000 AD.*

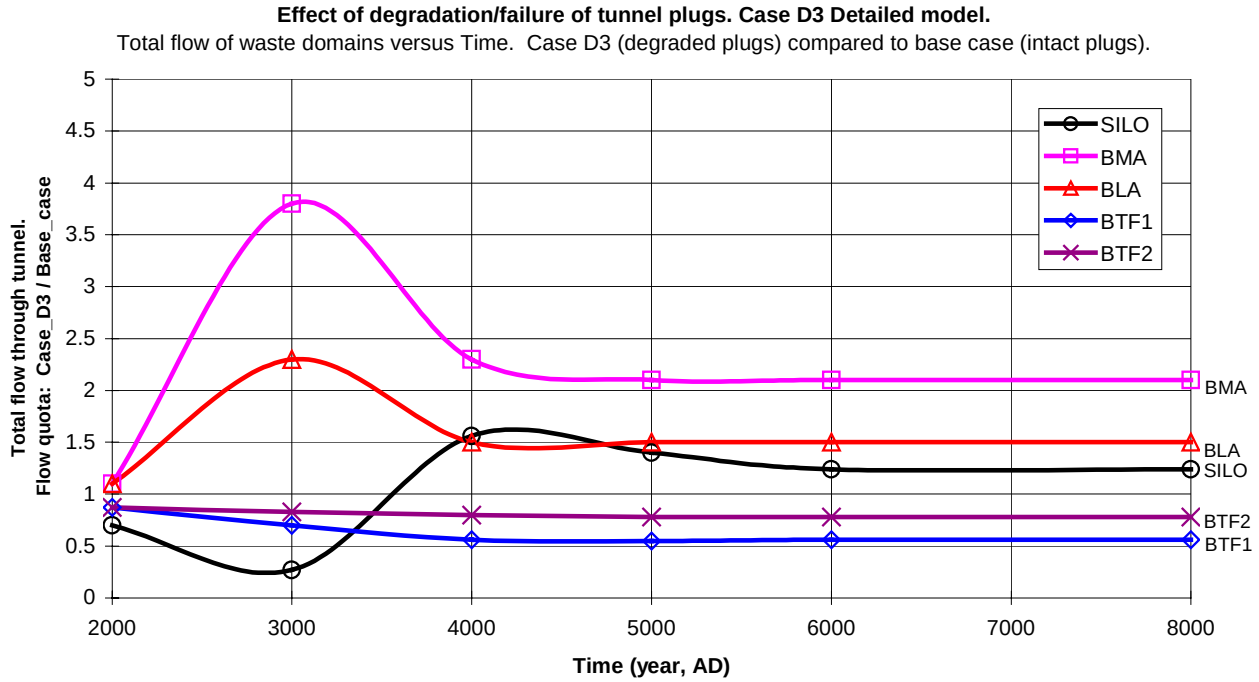

Figure 14.4 *Case D3 – completely degraded plugs in detailed model. Flow of waste domains in deposition tunnels without any plugs, as a multiple of the flow of the waste domain with intact plugs. The plugs are assumed to be fully degraded from the start (2000 AD.)*

14.2.10 Results of Case D3 – fully degraded plugs – detailed model

Case D3 is an assumed situation defined in the detailed model, for which no plugs, or plugs with a negligible resistance to flow, takes place in the tunnel system. Results of the detailed modelling of this situation are given in the subsections and the tables below, but also in Figure 14.4 (above). The tables below give the total flow of the different structures inside the deposition tunnels. Considering the flow through the tunnel and the flow through the waste domains, the results are compared to the results of the case with intact plugs (detailed model, see Sec.10.6). When comparing the predicted total flow of the waste domains of the tunnels, for the situations with and without plugs, an interesting aspect of the results is that for the situation with no plugs, also the direction of the flow through the tunnels will change. And that change in direction will influence the size of the predicted total flow of the waste domains. If one compares the results of the detailed models, to the results of the local model, it is important to note the differences between the two models (see Sec.10.6.9).

14.2.10.1 BTF tunnels

The detailed results are especially interesting for the BTF tunnels. With no plugs, the total flow through the BTF tunnel increases in comparison to the situation with intact plugs. The largest increase of flow, as predicted by the detailed model is 2.1 times in the BTF1 tunnel and it takes place after 4000 AD, for the BTF2 tunnel the largest increase is 1.7 times and it takes place after 5000 AD.

However, for the situation with no plugs, the total flow through the waste domains of the BTF tunnels is less than for the situation with plugs. With no plugs, the flows of the waste domains are between 0.6 and 0.9 times the flow with intact plugs. This may at first look strange, especially as the flow through the whole of the tunnel increases, but it is not an erroneous result, what has changed is the direction of the flow through the waste domain. To understand how this affects the total flow, it is necessary to remember the definition of the total flow of a tunnel (see Sec.2.8): *The calculation of total flow is based on a mass balance taken over the envelope of the studied structure. The total flow provides no information of the length of the flow paths in the tunnels, a short path or a long path, will both add to the total flow.* For the new situation with no plugs, on the average the flow in the tunnel has changed direction, to a new direction that has a larger horizontal component than for the situation with intact plugs. A comparison between the old situation with intact plugs and the new situation with no plugs reveals the following. For the new situation with no plugs, more water flows through the top filling, but less water flows through the waste domain, and the flow paths through the waste domain are longer than for the situation with intact plugs. For the old situation with intact plugs, more water went through the waste domain, but the flow paths through this domain were shorter. The waste domains of the BTF tunnels have a low permeability and no complete hydraulic cage surrounds them. From a general point of view, as regards direction of the regional flow, the total flow of such structures will vary in the following way. If the conductivity of the structure is small compared to the conductivity of the rock mass, maximum total flow will occur when a large area of the studied structure is exposed to the regional flow (regional flow along short axis of the structure) and minimum total flow will occur when a small area is exposed (regional flow along main axis of the structure).

Table 14.1 BTF1 Total flow, as predicted by the detailed model for the base case with no plugs (D3).

BTF1 No plugs	Total flow (m3/year) Trough different parts of the studied tunnel at different times					
	2000 AD	3000 AD	4000 AD	5000 AD	6000 AD	7000 AD
Top filling	8.6	21.2	51.5	57.2	58.2	58.2
Waste domain. Encap.	2.1	1.9	3.8	4.3	4.5	4.5
Concrete at sides	0.8	1.8	1.5	1.6	1.6	1.6
Concrete/sand floor	2.2	1.4	4.0	4.7	4.8	4.8
Loading areas	5.5	20.7	51.9	58.3	59.9	60.0
All surroundings	12.6	25.8	60.6	68.1	70.0	70.1
Tunnel flow Qallsurr. – Qwaste	10.5	23.9	56.8	63.8	65.5	65.6
Waste Flow Factor Q_Fac = Q2 / Q1 Q2 =Qwaste_no plugs Q1 =Qwaste_basecase	0.87	0.70	0.56	0.55	0.56	0.56
Tunnel Flow Factor Q_Fac = Q2 / Q1 Q2=Qtunnel_no plugs Q1=Qtunnel_basecase	1.4	1.2	2.1	2.1	2.1	2.1

Table 14.2 BTF2. Total flow, as predicted by the detailed model for the base case with no plugs (D3).

BTF2 No plugs	Total flow (m3/year) Trough different parts of the studied tunnel at different times					
	2000 AD	3000 AD	4000 AD	5000 AD	6000 AD	7000 AD
Top filling	7.6	22.7	41.7	45.7	46.4	46.5
Waste domain. Encap.	2.1	2.5	4.8	5.3	5.4	5.4
Concrete at sides	0.9	2.3	3.1	3.2	3.2	3.2
Concrete/sand floor	2.1	1.6	4.4	5.0	5.1	5.1
Loading areas	5.0	21.8	43.7	46.3	47.1	47.2
All surroundings	11.4	27.3	49.9	55.3	56.7	56.8
Tunnel flow Qallsurr. – Qwaste	9.3	24.8	45.1	50.0	51.3	51.4
Waste Flow Factor Q_Fac = Q2 / Q1 Q2 =Qwaste_no plugs Q1 =Qwaste_basecase	0.87	0.83	0.80	0.78	0.78	0.78
Tunnel Flow Factor Q_Fac = Q2 / Q1 Q2=Qtunnel_no plugs Q1=Qtunnel_basecase	1.4	1.4	1.6	1.7	1.7	1.7

14.2.10.2 BLA tunnel

With no plugs, the total flow through the BLA tunnel is larger than for the situation with intact plugs. The largest increase of flow, as predicted by the detailed model is 2.5 times and it takes place at 3000 AD, after 3000 AD the increase is 1.6 times. In the models, there are no conductivity differences inside the BLA tunnel; it follows that the increase of flow for the waste domain (storage area) of the BLA tunnel is nearly the same as for the whole of the tunnel.

Table 14.3 BLA - Total flow, as predicted by the detailed model for the base case with no plugs (D3).

BLA No plugs	Total flow (m3/year) Trough different parts of the studied tunnel at different times					
	2000 AD	**3000 AD**	**4000 AD**	**5000 AD**	**6000 AD**	**7000 AD**
Top filling	11.1	46.3	44.1	51.1	52.7	52.7
Waste storage area	10.2	44.1	51.6	57.2	58.4	58.5
Filling at sides	10.2	49	52.3	54.7	54.9	54.9
Concrete/sand floor	3.1	5.0	8.2	8.9	8.9	8.9
Loading areas	4.9	77.1	81.2	88	90.0	90.1
All surroundings	26.1	126.4	129.3	142.7	145.5	145.6
Tunnel flow Qallsurr. – Qwaste	15.9	82.3	77.7	85.5	87.1	87.1
Waste Flow Factor Q_Fac = Q2 / Q1 Q2 =Qwaste_no plugs Q1 =Qwaste_basecase	1.1	2.3	1.5	1.5	1.5	1.5
Tunnel Flow Factor Q_Fac = Q2 / Q1 Q2=Qtunnel_no plugs Q1=Qtunnel_basecase	1.2	2.5	1.6	1.6	1.6	1.6

14.2.10.3 BMA tunnel

With no plugs, the total flow through the BMA tunnel is larger than that of the situation with intact plugs. The largest increase of flow, as predicted by the detailed model is 3.3 times and it takes place at 3000 AD, after 3000 AD the increase is 2.5 times. For the situation with no plugs, the total flow of the waste encapsulation of the BMA tunnel is larger than for the situation with intact plugs. The maximum increase of flow, as predicted by the detailed model is 3.8 times and it takes place at 3000 AD, after 5000 AD the increase is 2.1 times.

Table 14.4 BMA – total flow, as predicted by the detailed model for the base case with no plugs (D3).

BMA No plugs	Total flow (m3/year) Trough different parts of the studied tunnel at different times					
	2000 AD	**3000 AD**	**4000 AD**	**5000 AD**	**6000 AD**	**7000 AD**
Top filling	7.0	55.7	69.2	72.2	72.9	73.0
Waste domain. Encap.	0.08	0.46	0.59	0.60	0.60	0.60
Filling at sides	8.2	46.1	57.4	58.9	58.6	58.6
Concrete/sand floor	9.1	51	61.7	62.3	61.4	61.3
Loading areas	7.9	117.8	138.8	144.3	146.1	146.2
All surroundings	12.3	120.3	133.4	135.7	135.8	135.8
Tunnel flow Qallsurr. – Qwaste	12.2	119.8	132.8	135.1	135.2	135.2
Waste Flow Factor Q_Fac = Q2 / Q1 Q2 =Qwaste_no plugs Q1 =Qwaste_basecase	1.1	3.8	2.3	2.1	2.1	2.1
Tunnel Flow Factor Q_Fac = Q2 / Q1 Q2=Qtunnel_no plugs Q1=Qtunnel_basecase	1.4	3.3	2.5	2.5	2.5	2.5

14.2.10.4 SILO tunnel

With no plugs, the total flow through the top fill of the SILO is much larger than for the situation with intact plugs. The largest increase of flow, as predicted by the detailed model is 30 times and it takes place after 6000 AD, between 2000 AD and 3000 AD the increase is 14 times. This large increase of flow for the situation with no plugs takes place because with no plugs an efficient flow route will be created for the groundwater flow in the access tunnels, a flow route that uses the top filling of the SILO.

The situation with no plugs will create a large increase of flow through the top filling. It will however not create a large increase in the flow of the SILO encapsulation. Because the SILO encapsulation is protected from the flow of the top filling by low permeable bentonite barriers, and the flow of the top filling prefers to flow in the high permeable access tunnels and not in the less permeable SILO encapsulation.

With no plugs, the total flow through the SILO encapsulation is either somewhat smaller or somewhat larger than for the situation with intact plugs, dependent the period studied. At 2000 AD the flow of the encapsulation is reduced 0.7 times, and at 3000 AD the flow of the encapsulation is reduced 0.3 times, in relation to the flow of the situation with intact plugs. At 4000 AD the flow of the encapsulation is increased 1.6 times, and after 5000 AD the flow of the encapsulation is increased 1.2 times, in relation the flow of the situation with intact plugs. The reason why the total flow of the encapsulation for the situation with no plugs, is smaller than that of the situation with intact plugs for the period 2000 AD through 3000 AD, and larger than that of the situation with intact plugs for the period after 3000 AD, is the complicated interplay between (i) the direction of the regional flow, (ii) the influence of Zone H2 and (iii) the flow routes provided by the access tunnels, with and without the tunnel plugs.

Table 14.5 SILO – total flow, as predicted by the detailed model for the base case with no plugs (D3).

SILO No plugs	**Total flow (m3/year) Trough different parts of the studied tunnel at different times**					
	2000 AD	**3000 AD**	**4000 AD**	**5000 AD**	**6000 AD**	**7000 AD**
Top filling	7.7	19.9	58.1	64.1	66.4	66.5
Bentonite at top	0.15	0.04	0.3	0.34	0.36	0.36
Waste domain. Encap.	0.16	0.06	0.25	0.30	0.31	0.31
Bentonite at base	0.20	0.12	0.33	0.39	0.40	0.41
Bentonite at sides	0.02	0.02	0.04	0.04	0.04	0.04
Waste Flow Factor Q_Fac = Q2 / Q1 Q2 =Qwaste_no plugs Q1 =Qwaste_basecase	0.70	0.27	1.56	1.30	1.24	1.24
Top fill Flow Factor Q_Fac = Q2 / Q1 Q2=Qtopfill_no plugs Q1=Qtopfill_basecase	14.5	14.2	26.4	29.1	30.2	30.2

14.3 Flow of a failed silo encapsulation

14.3.1 Introduction and purpose

As a sensitivity case we have studied the flow through a failed SILO encapsulation. This case represents a situation for which the concrete barriers and the bentonite barriers of the SILO encapsulation are breached. A motivation of the case is a theoretical collapse of the concrete walls of the encapsulation, and the following collapse of the bentonite barriers. This case has been studied for two different assumptions regarding the plugs that separate the access tunnels from the SILO deposition tunnel: (i) all tunnel plugs are intact, and (ii) no tunnel plugs occur in the tunnel system. All simulations of a failed SILO encapsulation were carried out with the detailed model.

14.3.2 Assumed properties of a failed SILO encapsulation

As stated above this case represents a situation for which the concrete barriers and the bentonite barriers of the SILO encapsulation are breached, and the tunnel plugs are either intact or absent. For this case, the assumed properties of the SILO are given in Table 14.6. All other parts of the model have the same properties as in the previous discussed detailed model (the base case). The difference compared to the previous definition of the detailed model is that the low permeable barriers of the SILO encapsulation and the inside of the SILO encapsulation, are defined as having the same conductivity, equal to 1×10^{-8} m/s, in all directions.

The conductivity value of the SILO encapsulation (1×10^{-8} m/s) used in these simulations is an assumed value, which represents the permeability of the SILO encapsulation after a theoretical crack/collapse of its concrete walls. It is however likely that much of the bentonite will remain in the barriers, even if the concrete walls are cracked/failed. And inside the encapsulation there will probably be both cracked and intact concrete containers. Hence, even if the concrete walls of the SILO collapses, the SILO will still carry a significant resistance to flow.

Table 14.6 Conductivity and volumes of the failed SILO encapsulation, a sensitivity case of the detailed model.

SILO	HYDRAULIC CONDUCTIVITY (m/s)			VOLUME (m3)
	IN FLOW DIRECTIONS			
	X-DIR.	Y-DIR.	Z-DIR.	
Top filling	1E-5	1E-5	1E-5	5 226
Concrete/Bentonite at top	1E-8	1E-8	1E-8	1 206
Waste and encapsulation	1E-8	1E-8	1E-8	30 456
Concrete/Bentonite at base	1E-8	1E-8	1E-8	1 608
Concrete/Bentonite at sides	1E-8	1E-8	1E-8	12 960

14.3.3 Results – detailed model

The groundwater flow through a failed SILO encapsulation is much larger than the flow through an intact encapsulation. But as the SILO after the collapse still carries a certain resistance to flow, the flow through the failed SILO will not be the same as the flow through a completely empty SILO cavern.

Results of the detailed modelling of this sensitivity case are given in the Table 14.7 and Table 14.8; the tables give the total flow and the specific flow of the different structures inside the SILO. As can be seen in the tables, the total flow of the SILO will increase due to the development of the regional groundwater flow pattern, which is the same behaviour as for the base case, discussed in previous sections. The table also gives the total flow of the waste domain of a failed SILO (the studied case), in relation to the total flow of an intact SILO (the base case).

The model predicts that a failed SILO, having a conductivity equal to 1×10^{-8} m/s, produces a total flow in the waste domain of the SILO, between 3 and 10 times the total flow of the waste domain of an intact SILO, depending on the shore level progress. The largest differences occur at time 3000 AD, as this is the situation for which the regional flow is close to horizontal, which will produce a primarily horizontal flow through a failed SILO. With intact barriers the flow through the SILO is primarily vertical, even at 3000 AD.

As demonstrated in previous sections, the flow in the top filling depends strongly on the properties of the plugs that separate the access tunnels from the SILO deposition tunnel. Without plugs, the flow of the top filling is much larger than if low permeable plugs are present. The large flow of the top filling, which is the result of a tunnel system without plugs, will not have a large effect on the flow of the failed SILO. Because in the model studied, the failed SILO carries a certain resistance to flow, and the flow of the top filling prefers to flow in the high permeable access tunnels and not in the less permeable failed SILO.

As regards the flow through the other deposition tunnels, the change in flow due to a failed SILO is very small if the other parts of the tunnel system are intact.

Table 14.7 Failed SILO encapsulation and intact tunnel plugs– total flow as predicted by the detailed model.

Failed SILO Intact tunnel plugs	**Total flow (m3/year) Trough different parts of the studied tunnel at different times**					
	2000 AD	**3000 AD**	**4000 AD**	**5000 AD**	**6000 AD**	**7000 AD**
Top filling	0.81	1.82	2.64	2.46	2.44	2.44
Bentonite at top	0.72	1.32	0.98	0.89	0.91	0.91
Waste domain. Encap. Q2	0.66	1.08	1.47	1.54	1.58	1.58
Bentonite at base	0.51	0.34	0.84	1.00	1.04	1.04
Bentonite at sides	0.82	1.69	2.71	2.89	2.95	2.95
Waste Flow Factor Q_Factor = Q2 / Q1 Q2 =Qwaste_failed Q1 =Qwaste_base case	2.9	4.9	9.2	6.7	6.3	6.3

Table 14.8 Failed SILO encapsulation and no tunnel plugs –total flow as predicted by the detailed model.

Failed SILO No tunnel plugs	Total flow (m3/year) Trough different parts of the studied tunnel at different times					
	2000 AD	3000 AD	4000 AD	5000 AD	6000 AD	7000 AD
Top filling	7.69	19.98	58.19	64.12	66.43	66.58
Bentonite at top	0.29	0.25	1.15	1.18	1.19	1.19
Waste domain. Encap. Q2	0.62	0.74	1.53	1.64	1.66	1.66
Bentonite at base	0.68	0.42	1.16	1.34	1.37	1.37
Bentonite at sides	0.89	1.29	2.46	2.57	2.6	2.6
Waste Flow Factor Q_Factor = Q2 / Q1 Q2 =Qwaste_failed Q1 =Qwaste_base case	2.7	3.7	9.6	7.1	6.6	6.6

14.4 Flow of a breached section of the BMA encapsulation

14.4.1 Introduction and purpose

The BMA encapsulation is divided into different sections separated by concrete walls. As a sensitivity case we have studied the flow through an assumed failed or breached section. This case represents a situation for which a limited part of the BMA encapsulation has a much larger permeability than the surrounding intact parts of the encapsulation. A motivation of the case is a theoretical large fracture intersecting the concrete walls of the encapsulation or a local collapse of the concrete walls. All simulations of a breached section of the BMA encapsulation were carried out with the detailed model.

14.4.2 Assumed properties of a breached section of the BMA encapsulation

This sensitivity case represents a situation for which the concrete walls of a section of the BMA encapsulation are breached. As stated above, the actual BMA encapsulation is divided into different sections, these sections have a length of 10.3 meters along the tunnel. Due to numerical reasons, the section studied in the detailed model is of length 16 meters, and corresponds to one and a half of the actual sections of the BMA encapsulation. The studied section corresponds to the whole of the actual section No.12 (Fack 12) and half of the actual section No.11 (Fack 11).

Compared to the base case of the detailed model, the difference is that a limited part of the encapsulation, located close to Zone 6, is defined as having the same conductivity, equal to 1×10^{-5} m/s, in all directions. This is also the conductivity of the surrounding back fill. All other parts of the model have the same properties as in the previous discussed detailed model (the base case).

The conductivity value of the breached section (1 x 10^{-5} m/s) used in these simulations is an assumed value that represents the permeability of a completely failed section of the BMA encapsulation or a section intersected by large fractures. Such a large conductivity value represents an encapsulation for which the voids inside the encapsulation are not back filled with a low permeable filling; hence it is a collapse of the base case, not a collapse of the first alternative BMA layout. The breached section is located where Zone 6 intersects the tunnel; this is a conservative assumption as this the part of the BMA where the flow is the largest.

The assumed properties of the breached section are given in Table 14.9. The position of the assumed breached section is given in Figure 14.5.

Table 14.9 Conductivity and size of the failed section of the BMA encapsulation, a sensitivity case of the detailed model.

BMA ASSUMED BREACHED SECTION OF ENCAPSULATION	**HYDRAULIC CONDUCTIVITY (m/s) IN FLOW DIRECTIONS**			**SIZE OF SECTION**
	X-DIR.	**Y-DIR.**	**Z-DIR.**	
Waste domain and encapsulation (1)	1E-5	1E-5	1E-5	- Length along tunnel: 16 m. - Volume of section: 2176 m3
(1) Note, that these properties are applied to a limited section of the encapsulation only, the rest of the BMA encapsulation is assumed to have intact properties (see Table 9.5).				

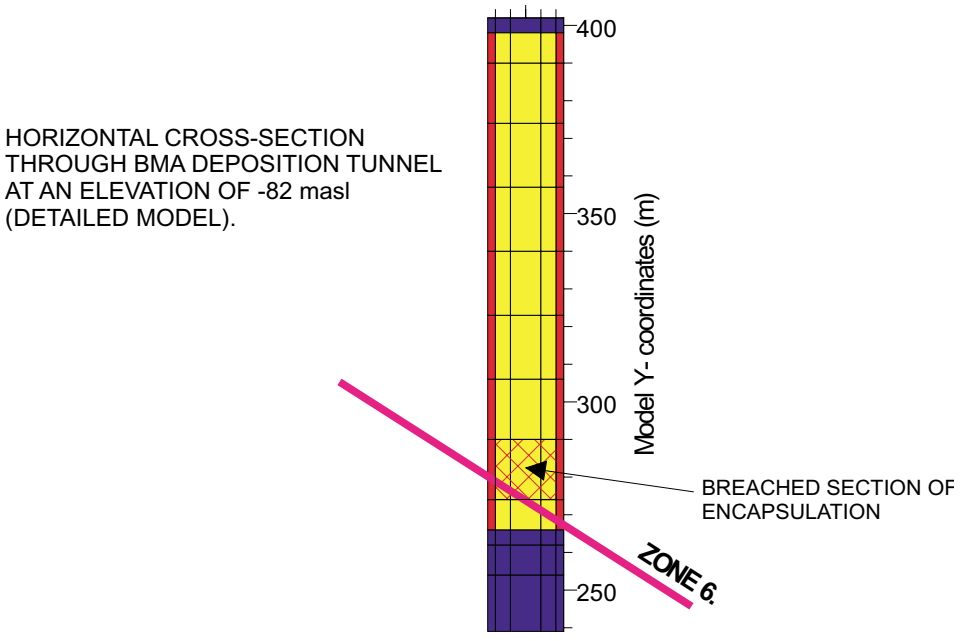

Figure 14.5 *Position of assumed breached section in the BMA encapsulation. As defined in a sensitivity case of the detailed model.*

14.4.3 Results – breached section in BMA – detailed model

The groundwater flow through a failed or breached section of the BMA encapsulation is larger than the flow of the same section with intact concrete walls, because a certain amount of the flow in the surrounding barriers will be redirected through the breached section. However, as the intact parts of the encapsulation remains low permeable (separated by intact concrete walls), the size of the flow through the intact parts of the encapsulation will only change very little. Hence, the change in flow will primarily take place at the breached section.

Results of the detailed modelling of this sensitivity case are given in Table 14.10 below; the table gives the total flow of the different structures inside the BMA. As can be seen in the table, the flow of the BMA will increase due to the development of the regional groundwater flow pattern, which is the same behaviour as for the base case, discussed in previous sections. The flow is given separately, for both the breached and the intact parts of the encapsulation. The flow of the intact parts of the encapsulation is close to the same as the flow of the encapsulation of the base case. Considering the flow of the whole of the encapsulation (including both breached and intact parts) the total flow of the encapsulation increases from 2.4 m^3/year and reaches a steady value of 10.5 m^3/year at about 6000 AD. The total flow of the breached parts makes up about 97 percent of the total flow of the encapsulation.

The table also gives the total flow of the whole of the breached encapsulation (the sum of the flow in breached and intact parts), in relation to the total flow of the encapsulation with intact properties (the base case). The model predicts that a breached section, having conductivity equal to 1×10^{-5} m/s, produces a total flow of the encapsulation, which is between 30 and 37 times the total flow of an intact encapsulation (the base case).

As discussed above, the breached section of the detailed model is of length 16 meters, and corresponds in size to one and a half of the actual sections of the BMA encapsulation. However, the flow of the breached section depends not only of its size but also of its permeability. The breached section studied in the detailed model has the correct permeability, equal to an assumed representative value, which is much larger than the permeability of the intact parts. Therefore, the results obtained from the detailed model, i.e. the flow of the breached section of the detailed model, can be looked upon as a conservative estimate of the flow of one of the actual sections.

Considering the flow values calculated for other parts of the BMA tunnel e.g. top fill, side fill etc, in comparison to the flow values of the base case, the change in flow values are small, because the properties of the surrounding materials are not changed. The effect of the breached section is mainly to redirect some of the flow that occurs in the backfill and hence provide a short cut through the encapsulation. Considering the predicted flow of other deposition tunnels, the values predicted for this case are the same as the values predicted for the base case.

Table 14.10 Flow of BMA tunnel with a breached encapsulation. The table gives the total flow as predicted by the detailed model.

BMA With breached encap.	Total flow (m3/year) Trough different parts of the studied section at different times					
	2000 AD	3000 AD	4000 AD	5000 AD	6000 AD	7000 AD
Top filling	5.9	21.4	35.1	36.6	36.6	36.6
Intact parts of encapsulat.	0.04	0.16	0.29	0.30	0.30	0.30
Breached part of encapsulat.	2.4	3.7	9.2	10.1	10.2	10.2
All of encapsulation	2.4	3.86	9.5	10.4	10.5	10.5
Flow of breached part in relation to that of all encap.	>99%	96%	97%	97%	97%	97%
Filling at sides	4.7	14.4	23.2	24.2	24.2	24.2
Filling at base	7.5	12.7	26.0	28.2	28.4	28.4
Loading areas	2.4	22.1	31.8	32.3	32.2	32.2
All surroundings	11.1	40.4	62.0	64.9	65.0	65.0
Tunnel flow Qallsurr. – Qwaste	8.7	36.6	52.6	54.6	54.6	54.6
Waste Flow Factor Q_Factor = Q2 / Q1 Q2 =Qencap_breached Q1 =Qencap_base case	34.8	30.0	36.5	37.1	37.5	37.5
Tunnel Flow Factor Q_Factor = Q2 / Q1 Q2 =Qtunnel_breached Q1 =Qtunnel_base case	1.0	1.0	1.0	1.0	1.0	1.0

14.5 Flow of a breached section of the BTF1 tunnel

14.5.1 Introduction and purpose

As a sensitivity case we have studied the flow through an assumed breached or failed section of the BTF1 tunnel. This case represents a situation for which a limited part of the BTF1 tunnel has a much larger permeability than the surroundings. A motivation of the case is a theoretical large fracture intersecting the concrete walls of the encapsulation and/or floor and side fillings, or a local collapse of concrete walls. All simulations of a breached section of the BTF1 tunnel were carried out with the detailed model.

14.5.2 Assumed properties of a breached section of the BTF1 tunnel

In the model, the BTF1 tunnel is divided into different horizontal sections. We have selected one of these horizontal sections as the breached section. The selected section has a length of 17 metres and it is located where Zone 6 intersects the tunnel; this is a conservative assumption as this is the part of the tunnel where the flow is the largest. We have studied two different alternatives considering to what extension the different barriers are breached, see Figure 14.6

- Alternative 1. Only the waste domain (encapsulation) of the section studied is breached; the floor and the side fillings (concrete) are intact. This case represent a situation for which the fracture or the collapse of the concrete walls only takes place in the encapsulation and not in the surrounding barriers and floor.

- Alternative 2. All parts of the tunnel, at the section studied, are breached or failed, including the floor and the side fillings.

Compared to the base case of the detailed model, the difference is that a limited part of the tunnel, located close to Zone 6, is defined as having the same conductivity, equal to 1 x 10^{-5} m/s, in all directions, see Table 14.11. This is also the conductivity of the top fill of the tunnel. All other parts of the model have the same properties as in the previous discussed detailed model (the base case). The conductivity value of the breached section used in these simulations is an assumed value that represents the permeability of large fractures or that of completely failed barriers and encapsulations.

Table 14.11 Conductivity and size of the failed section of the BTF1 tunnel, a sensitivity case of the detailed model.

BTF1 ASSUMED BREACHED SECTION	**HYDRAULIC CONDUCTIVITY (m/s) IN FLOW DIRECTIONS**			**SIZE OF SECTION**
	X-DIR.	**Y-DIR.**	**Z-DIR.**	
Alternative 1. Only encapsulation (waste) (1)	1E-5	1E-5	1E-5	Length along tunnel: 17 m. Volume, breached part: 1 105 m3
Alternative 2. Encapsulation, fillings and floor (1)	1E-5	1E-5	1E-5	Length along tunnel: 17 m. Volume, breached parts: 1 402 m3
(1) Note, that these properties are applied to a limited section of the tunnel only, the rest of the BTF1 tunnel is assumed to have intact properties (see Table 9.3).				

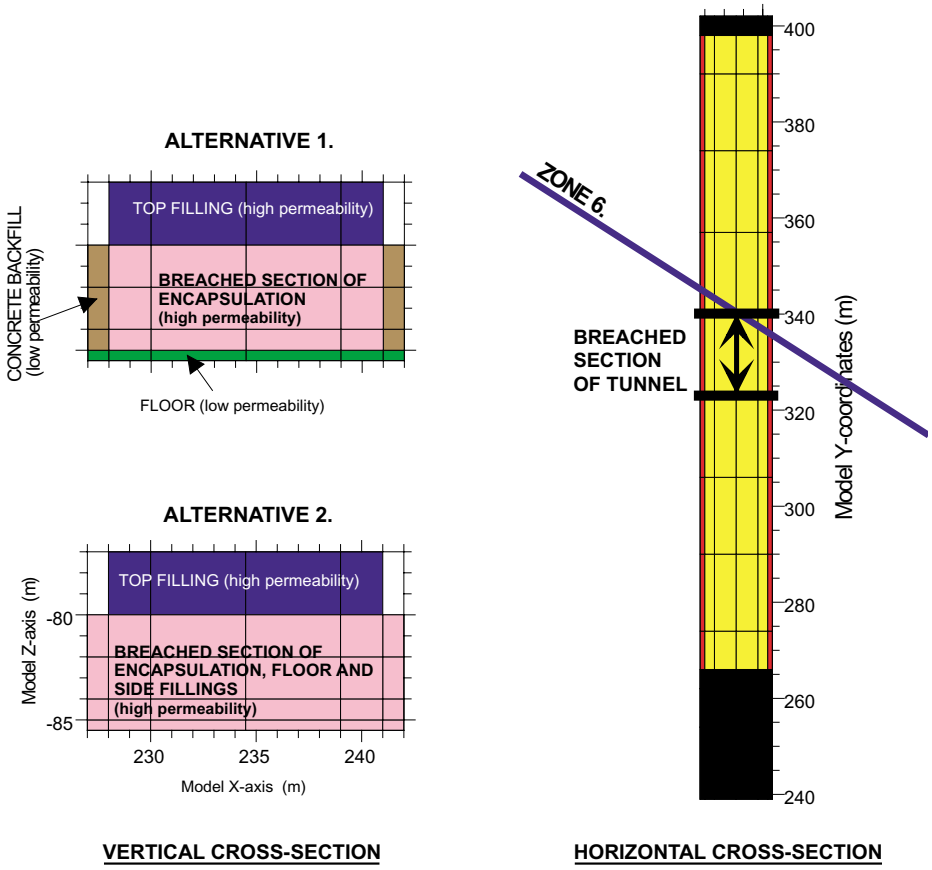

Figure 14.6 *Position and extension of assumed breached section in the BTF1 tunnel. As defined in a sensitivity case of the detailed model.*

14.5.3 Results – breached section in BTF1 – detailed model

The groundwater flow through a failed or breached section of the BTF1 tunnel is larger than the flow of the same section being intact, because a certain amount of the flow in the surroundings will be redirected through the breached section. However, as the intact parts of the encapsulation remains low permeable, the size of the flow through the intact parts of the encapsulation will not increase.

As previously discussed, we have studied two different alternatives considering to what extension the different barriers are breached, see Figure 14.6. Results of the detailed modelling of these two alternatives are given in Table 14.12 and Table 14.13 below; the tables gives the total flow of the different structures inside the BTF1. As can be seen in the tables, the flow of the BTF1 will increase due to the development of the regional groundwater flow pattern, which is the same behaviour as for the base case, discussed in previous sections. The flow is given separately, for both the breached and the intact parts of the encapsulation.

- Considering Alternative 1, the total flow of the whole of the encapsulation (including both breached and intact parts) increases from 4.2 m^3/year and reaches a steady value of 12.6 m^3/year at about 6000 AD. The total flow of the breached parts makes up about 60 percent of the total flow of the encapsulation. In comparison to a completely intact encapsulation (the base case), the flow of the breached encapsulation is about 1.6 times larger (at 3000 AD the flow is 2.3 times larger).
- Considering Alternative 2, the total flow of the whole of the encapsulation (including both breached and intact parts) increases from 13.2 m^3/year and reaches a steady value of 40.8 m^3/year at about 6000 AD. The total flow of the breached parts makes up about 90 percent of the total flow of the encapsulation. In comparison to a completely intact encapsulation (the base case), the flow of the breached encapsulation is about 5 times larger (at 3000 AD the flow is 6.3 times larger).

Considering the predicted flow of other deposition tunnels (SILO, BMA, BLA, BTF2), the values predicted for this sensitivity case are very close to the values predicted for the base case.

Table 14.12 Flow of BTF1 tunnel with a breached encapsulation (Alternative 1). The table gives the total flow as predicted by the detailed model.

BTF1 Alt 1. Breached Encap.	Total flow (m3/year) Trough different parts of the studied section at different times					
	2000 AD	3000 AD	4000 AD	5000 AD	6000 AD	7000 AD
Intact parts of encapsulat.	1.7	2.1	5.3	6.1	6.3	6.3
Breached part of encapsulat.	2.6	4.3	5.8	6.3	6.5	6.5
All of encapsulation	4.2	6.3	11.0	12.3	12.6	12.6
Flow of breached part in relation to that of all encap.	61%	67%	53%	51%	51%	51%
Waste Flow Factor Q_Factor = Q2 / Q1 Q2 =Qencap_breached Q1 =Qencap_base case	1.8	2.3	1.6	1.6	1.6	1.6
Tunnel flow (Qallsurr. – Qwaste)	8.2	19.8	28.5	31.3	32.1	32.1
Tunnel Flow Factor Q_Factor = Q2 / Q1 Q2 =Qtunnel_breached Q1 =Qtunnel_base case	1.09	1.02	1.08	1.02	1.05	1.05

Table 14.13 Flow of BTF1 tunnel with a breached section, including breached encapsulation, breached floor and breached side fillings, (Alternative 2). The table gives the total flow as predicted by the detailed model.

BTF1 Alt 2. Breached Encap, Floor and Side-fillings	Total flow (m3/year) Trough different parts of the studied section at different times					
	2000 AD	3000 AD	4000 AD	5000 AD	6000 AD	7000 AD
Intact parts of encapsulat.	1.2	1.9	4.0	4.7	4.9	4.8
Breached part of encapsulat.	12.0	15.1	30.7	33.9	34.5	36.1
All of encapsulation	13.2	17.0	34.7	38.6	39.3	40.8
Flow of breached part in relation to that of all encap.	91%	879%	88%	88%	88%	88%
Waste Flow Factor Q_Factor = Q2 / Q1 Q2 =Qencap_breached Q1 =Qencap_base case	5.5	6.3	5.1	4.9	4.9	4.9
Tunnel flow (Qall_structures)	14.5	24.1	45.0	50.2	51.2	51.2
Tunnel Flow Factor Q_Factor = Q2 / Q1 Q2 =Qtunnel_breached Q1 =Qtunnel_base case	1.94	1.24	1.71	1.64	1.69	1.68

15. Groundwater saturation of SFR

15.1 Introduction

At present the tunnel system at SFR is kept dry, all the water that leaks into the tunnels are pumped to the ground surface. In the close surroundings of the tunnels the groundwater flow is directed towards the empty tunnels. However, in the future the repository will be closed and abandoned and the tunnels will not be kept dry. Due to the inflow of groundwater, the groundwater head will rise in the tunnels and in the surrounding rock mass, after some time the tunnels will be filled with water (saturated with groundwater). The groundwater system will after some time reach a new equilibrium, in which most of the tunnels will act as permeable conductors of the groundwater flow. There will be a transition period when the tunnels are being filled with water and the local groundwater situation develops into a steady-state-like situation (with respect to the flow in the tunnels). This steady-state-like situation and local equilibrium should not be confused with the slow change in flow conditions caused by the shore level displacement.

15.2 Purpose of simulations – studied course

In this chapter we will study the transition period after the tunnels are abandoned and no longer kept dry; the transition period during which the groundwater leaks in to the tunnels and the head in the tunnels will rise. The purposes of these simulations are to predict the length of the time period during which the saturation will take place, and the spatial distribution of the saturation process versus time. We will call the time period during which the inflow takes place “the saturation period”.

15.3 General assumptions and simplifications

A prerequisite for this study of the saturation process is that the repository will be abandoned as a dry tunnel system. An alternative is to abandon the repository after the tunnel system has been artificially re-filled with water i.e. water is pumped into the tunnels from the surface. If the repository is abandoned in that way, the repository will be saturated with water before or in conjunction with its closing, hence for such a situation there will be no saturation period that depends on the natural inflow of groundwater.

In all of the following discussions and calculations, it is assumed that the air/gas inside a studied tunnel (e.g. the SILO) can escape out of the tunnel, as the tunnel becomes filled with water, without influencing the inflow of groundwater or change the pressure inside the tunnel studied. This is a simplification of the actual system, which makes it possible

to handle the course of saturation as a problem concerning one phase only i.e. the groundwater. If the gas phase would have been included in the calculations, it is likely that the predicted length of the saturation period would have been somewhat longer.

To reduce the complexity of the studied problem and since the capillary properties of the material inside the tunnels (concrete constructions, waste etc) are not known, the mathematical models presented below will not include the capillary forces of unsaturated volumes, e.g. an unsaturated backfill or an unsaturated concrete encapsulation. In the models presented in this section, the local pressure of an unsaturated domain is always equal to atmospheric.

The numerical models of this study include, in a simplified way, a groundwater flow inside the unsaturated domain –an unsaturated flow. Such a flow is defined as a vertical movement (not horizontal) of the water that flows into the unsaturated domain of a tunnel, a movement to the lowest part of the unsaturated domain, where the water is stored. When the unsaturated vertical flow is calculated, the model will use a value of conductivity equal to the conductivity for fully saturated flow. When a part of a tunnel (a cell representing a part of a tunnel) has reached full saturation, the cell will no longer be a part of the unsaturated domain, instead it will be part of the saturated domain. In the saturated domain there will be a saturated flow, in all dimensions. For the numerical model, the degree of saturation of the unsaturated domain in a tunnel is calculated based on the cell sizes of the model mesh, the inflow of water and the available porosity.

For the studied course, the regional flow pattern of the groundwater system represents the present flow situation for which the sea covers the repository, hence the situation representing the year 2000 AD (See Chapters 8 through 11.8). A compilation of the measured groundwater inflow to the tunnels at SFR is given in Axelsson (1997). At present the changes are very small, the values of inflow as regards the year 1997 can be assumed as representing a steady-state-like situation. It should, however, be noted that there are uncertainties in connection to the measurements of the inflow. For the SILO the present measured inflow represents the inflow to a drainage system of a partly unknown design and resistance. In the future, when the SILO is abandoned, the possible function of this drainage system is unknown, we have assumed that it is no longer working. The inflow to the SILO, which the models will predict for the saturation period, is not the inflow to the drainage system, but the inflow to the SILO itself –the inflow to barriers or the inflow to the waste inside of the barriers etc.

15.4 Analytical estimate based on the present inflow

15.4.1 Methodology

An estimate of the length of the time period that is needed to fully saturate a tunnel of the repository can be based on the present inflow to the repository. The present values of inflow can be assumed to represent a steady-state-like situation. The steady state assumption implies that the values of inflow will be the same for the whole period during which the saturation takes place.

However, during the saturation period, the actual inflows are not constant but changes with time due to three different processes. (i) If the tunnel studied contains a backfill giving a flow resistance, for such a tunnel the actual inflow to an unsaturated volume inside the tunnel will decrease with time as the boundary area of the unsaturated volume decreases in size. (ii) The actual inflow to a tunnel, which remains not saturated, may during a limited time period increase with time as other tunnels become saturated and the groundwater flow will be redirected to the remaining unsaturated tunnel. (iii) The boundaries of the regional groundwater flow may change during the saturation period. Process number (iii) will not be important at the SFR repository, because during the time period studied, the sea will always be above the tunnels and at an approximately constant level. And the shore level progress will not influence the process of repository saturation, as the saturation of the repository will only take a few decades. Consequently, estimates of the length of the saturation period based on the steady state inflow could be underestimates as well as overestimates of the actual times. However, the range within which the time for saturation may vary, can generally be studied based upon such estimates

To use the steady state inflow approximation for the estimation of the length of the saturation period we need to know: (i) the volume of the tunnels, (ii) the initial available porosity of the tunnels and (iii) the steady state inflow. The initial available porosity of the tunnels is given by the porosity of the material stored in the tunnels and the initial saturation of that material. If a tunnel in a model contains and represents several different materials, the available porosity should be an average value representing the different materials. For the analytical estimates and in the local model, each tunnel is defined with one value of available porosity only; hence the values of available porosity are average values representing the different materials that occur in the tunnels, e.g. encapsulation and backfill. In the detailed model, different values of porosity are used for the different materials that takes place inside the tunnels.

15.4.2 Results

The estimates will be based on the properties of the local model i.e. the volumes of the tunnels as defined in the local model and the steady state inflow to the tunnels as predicted by the calibrated local model.

These properties of the local model are given in Table 15.1 below.

Table 15.1 Local calibrated model, volumes of the tunnels and the steady state inflow to the tunnels.

Tunnel	Volume in local model (m3)	Inflow to model (litre/minute)
BMA	64 600	11
BLA	42 800	25
BTF1	26 000	19
BTF2	26 000	17
SILO SD1 (1)	47 400	1.7
SILO SD2 (2)	47 400	0.52
(1) First SILO definition (SD1), see Section 6.5.4 (2) Second SILO definition (SD2), see Section 6.5.4		

The lengths of the periods for the complete saturation of the deposition tunnels as a function of the initial available porosity and the steady state inflow of the tunnels are given in Figure 15.1. Based on the results given in the figure, the following conclusions are made:

- **SILO.** Considering the first SILO definition (SD1), the time period for the complete saturation of the SILO is about 6 years, and for the second SILO definition (SD2), the time period is about 17 years; if the initial available porosity of the SILO is 10%
- **BMA.** The time period for the complete saturation of the BMA tunnel is about 2 years if the initial available porosity is 20%
- **BLA, BTF.** The time period for the complete saturation of the BLA and BTF tunnels is about 1 year if the initial available porosity is 20%

The numerical calculations, presented in later sections, will demonstrate that the results given above (and in Figure 15.1), are underestimates of the lengths of the periods for the complete saturation of the deposition tunnels.

The final layout within the tunnels will not be homogeneous. Inside the tunnels there will be different barriers as well as a concrete constructions (encapsulations) in which the waste will be stored. Hence, to make a better estimate of the length of the saturation period, we need to use a numerical model that includes the heterogeneity of the actual tunnel layout.

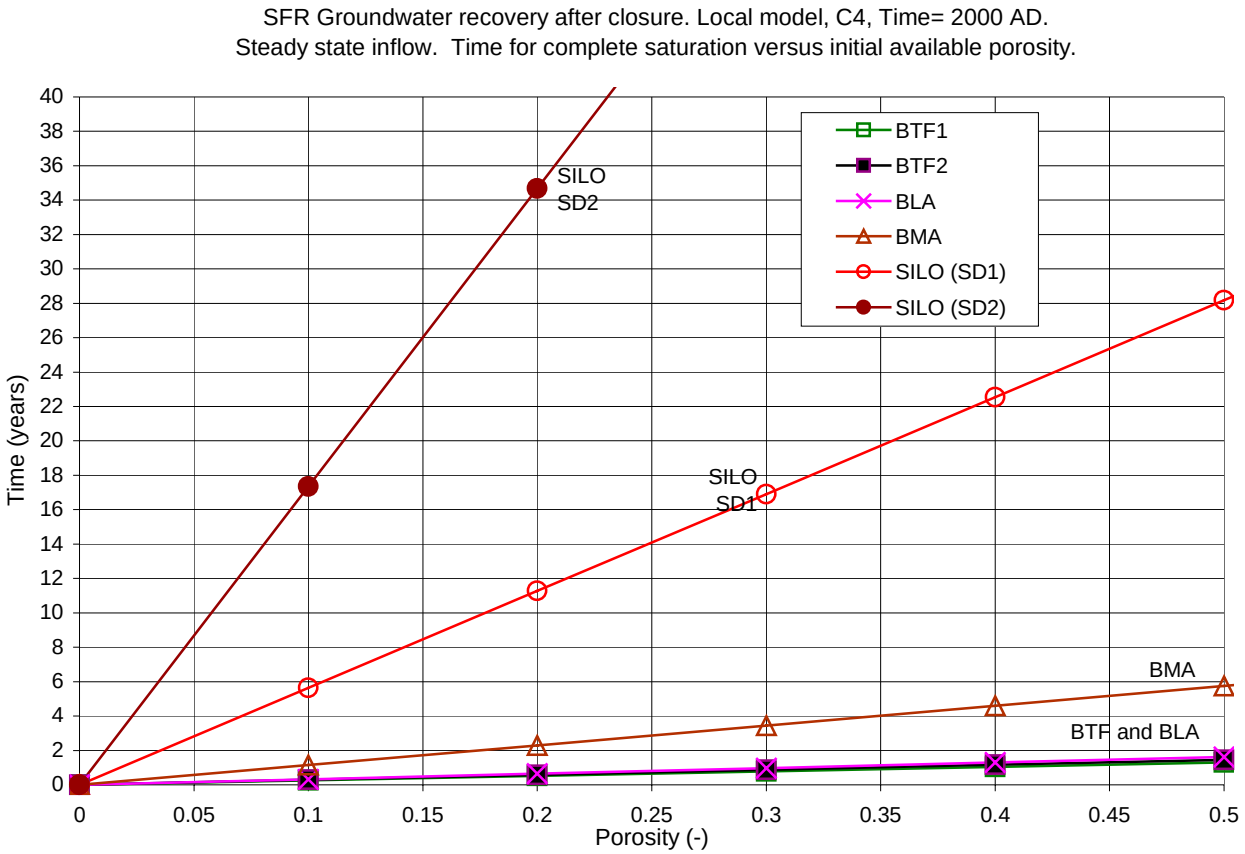

Figure 15.1 *Time period for complete saturation of the deposition tunnels, estimated by use of the steady state inflow of the calibrated local model, for different values of the available initial porosity.*

15.5 Transient simulations - Methodology

15.5.1 Introduction

For these simulations we have used the calibrated models representing the present tunnel system at SFR and not the extended tunnel system. We have used the complete chain of models of different sizes, including the regional model, the local model and the detailed model. The differences between the previously used models and the models used in these simulations are the boundary conditions of the cells representing the tunnel system in the local and detailed models. The regional model was the same as for the previous simulations.

15.5.2 Mathematical description of the saturation process

A transient simulation of groundwater recovery and saturation of a system of drained tunnels is not as straightforward as one might first suppose. Constantly drained tunnels is not a problem to simulate, as the drained water can be considered to leave the tunnel system immediately and therefore a steady head will be maintained at the tunnel walls. However, when simulating the saturation process we need to consider what happens to the water that leaks into the tunnels, and consider how this water will change the head and the degree of saturation of the tunnels.

The tunnels can be empty or re-filled with a backfilling. If the tunnels are empty, the water that has leaked into the tunnels will flow, as a surface flow, at the base of the tunnels, following the topographic gradient of the tunnels and accumulate at different positions. However, tunnel plugs etc will interrupt surface flows inside a tunnel; so there will be no continuous surface flow of water inside the access tunnels, all the way from the top of the tunnel system to the lowest parts of the tunnel system. If the tunnels are re-filled with a backfilling, the water that leaks into the tunnels will flow as an unsaturated or as a saturated groundwater flow, inside the tunnels, towards lower groundwater head. As groundwater flows into the tunnels and accumulates in the tunnels, the degree of saturation will increase in the tunnel. When a tunnel is fully saturated, no more water will be stored in that tunnel (except for a negligible amount dependent on the specific storage).

The actual final layout of the tunnels, at the closure of the repository, is at present not decided; all tunnels may contain some backfill or backfill may only be used in parts of the tunnel system. For these simulations we have assumed that the saturation process of the tunnel system studied, can be represented as the saturation process of a tunnel system that contains a backfilling. This is an acceptable simplification, as the tunnels that we are primarily interested in -the deposition tunnels, will probably contain a backfill.

In the model, the tunnels are divided into small volumes (tunnel-cells). The saturation process is described for each of these tunnel-cells separately. At the start of the simulation it is assumed that all tunnel-cells contain a certain amount of empty space, that space is given by the bulk porosity, the size of the tunnel-cell and the volume of water inside the cell (initial saturation). The product of the bulk porosity and the initial saturation is the available porosity of the tunnel-cell studied. Hence, the volume of a

tunnel-cell available for storage of fluid, is equal to the product of the available porosity and the size of the tunnel cell. For a tunnel without any backfill, the whole tunnel volume is considered as an empty volume.

The hydraulic head is the sum of the pressure (in meters) and the elevation. At the start of the transient simulation (the initial condition), the head of a tunnel-cell is given by the elevation of the cell and by a pressure set as atmospheric. Hence, the head values will be different for cells at different elevations. During each time step of the transient simulation, the model calculates the groundwater inflow to the unsaturated tunnel-cells. The model will also calculate new head values and these are given by the volume of inflow and the available empty space (available porosity) of the tunnel cells. The head in a tunnel cell will increase with the size of the inflow, until it is equal to the top elevation of the cell, at that moment the tunnel cell turns from an unsaturated to a saturated cell.

15.5.3 Chain of simulations

The chain of simulations is as follows:

1. Simulation with the regional model. The regional model Case 4 has been used, it provides boundary conditions for the local model. The regional flow situation at the year 2000 AD is exported to the local model.

2. Local model, initial condition. The initial condition is the flow situation of the calibrated local model with specified head values at the outer limits of the model taken from the regional model. The head values at the outer limits represents the flow situation at 2000 AD. All tunnels are drained. The predicted inflow is the same as for the calibrated local model.

3. Simulation with the local model, transient conditions. The local model will be run under transient conditions. The heads at the outer limits of the model represents the regional flow situation at 2000 AD. The head values at the boundary are steady, as the local flow situation at SFR will not change the regional flow situation, and the transient process of shore level displacement is much to slow to influence the studied course (saturation of the tunnel system). The tunnels are not kept dry; the groundwater will leak into the tunnels and the head in the tunnels will rise.

4. Detailed model, initial condition. The initial condition is the flow situation of the detailed model at steady state with completely drained tunnels. The specified head values at the outer limits of the detailed model taken are from the local model. The head values represents the flow situation at 2000 AD.

5. Simulation with the detailed model, transient conditions. The detailed model will be run under transient conditions. The head values at the outer limits of the detailed model are transient as well. These changing head values are taken from the local model. The head values represents the transient flow situation as simulated by the local model. The tunnels are not kept dry; the groundwater will leak in to the tunnels and the head in the tunnels will rise. The purpose of the detailed model is to predict the saturation process in more detail than the local model.

As stated above, the local and detailed models will have the specified head boundary condition at all faces of the models. The actual head values assigned to the boundary nodes of these models are based on a three-dimensional interpolation between the calculated head values of the nodes of the larger models.

15.5.4 Conductivity

The values of conductivity used in these simulations are identical to those previously used for the local and detailed models, as presented in previous sections.

15.5.5 Yield, storativity and available porosity

The local and detailed models have to be assigned properties that imitate the transient behaviour of the system studied. Such properties are the specific yield and the storativity (specific storage) of the rock mass and the fracture zones as well as the available porosity of the closed tunnels. The specific yield defines the amount of water that is released/stored in the flow medium when the groundwater surface moves. This property is mainly related to the porosity. The storativity defines the amount of water that is released/stored in the flow medium when the groundwater head changes. This property is related to the rock stresses. At SFR there have been no direct measurement of porosity or storativity. Hence, no such site-specific data is available.

For the rock mass and fracture zones of the local and detailed models, the values of specific yield and storativity are the same as the values of the regional model. However, as the groundwater surface will not move in the simulations (the sea is above the repository), the specific yield is never used in the calculations. The storativity is set equal to $5 \cdot 10^{-6}$ m^{-1}. The dominating process during the saturation period is the storage of fluid inside the empty space of the tunnels; and compared to this storage, the storage of fluid inside the rock mass, due to the storativity, is not very important.

A certain content of water (moisture) will always occur in backfill and in other materials of the tunnels, even if the tunnels are kept dry from visible water. The initial available porosity of the closed tunnels is given by the bulk porosity of the material stored in the tunnels and the initial saturation of that material (the initial amount of moisture of the material). If a tunnel-cell represents several different materials, the available porosity should be an average value representing the different materials. In the local model, each type of tunnel has one value of available porosity only; hence the values of available porosity are average values representing the different materials that occur in the tunnels, e.g. encapsulation and backfill. In the detailed models the different materials are defined separately within each tunnel, hence, in the detailed model there are different values of available porosity within each tunnel. The assumed initial available porosity for different materials is given in Table 15.2

The initial available porosity of the local model is given below in Table 15.3. For the detailed model the initial available porosity is given in Table 15.4. The available porosity of the local model is volume weighted average values of the different values representing the different materials, as defined in the detailed model.

Table 15.2 Assumed porosity of different materials inside the tunnels.

Material	Bulk porosity (void) %t	Initial available porosity %
Construction concrete	7.5	1
Porous concrete	15	5
Concrete floor with sand patches	7.5	1
Concrete backfill	15	5
Sand backfill	25	20
Plugs	<1	1
SILO: Sand/Bentonite mix at SILO top	25	1
SILO: Sand/Bentonite mix at SILO base	25	1
SILO: Bentonite at SILO sides, upper part	50	1
SILO: Bentonite at SILO sides, lower part	50	1
SILO: Concrete lid in SILO	Not considered	Not considered
SILO: Void to saturate in compartment	20	10
BMA: Void to saturate in compartment	30	15
BTF: Void to saturate in waste block	30	25

Table 15.3 Local model - Initial available porosity of the tunnels.

Tunnel	Initial available porosity	Percent
Access tunnels	0.5	Empty tunnels, 50% available (1)
BMA	0.17	17
BLA	0.19	19
BTF1	0.20	20
BTF2	0.20	20
SILO	0.083	8.3
(1) Tunnel volume is reduced because of the excessive size of the access tunnels in the numerical models.		

Table 15.4 Detailed model initial available porosity of different structures of the tunnel system.

Material in Tunnel	Initial available porosity	Percent
Access tunnels	0.5	Empty tunnels, 50% available (1)
Sand backfill	0.2	20
Bentonite backfill	0.01	1
Porous concrete	0.05	5
Concrete (encapsulation, floor)	0.01	1
Waste SILO	0.10	10
Waste BTF	0.25	25
Waste BLA	0.20	20
Waste BMA	0.15	15
(1) Tunnel volume is reduced because of the excessive size of the access tunnels in the numerical models.		

15.5.6 Discretization of the time domain

To solve the governing differential equation with respect to time, we need to divide the time domain into discrete steps – time steps. The larger the number of time steps, the better the representation of the time-dependent course (presuming that the time step is

not small enough to cause numerical difficulties). The drawback with a small time step is that the computational demands will be large if the time step is small. The size of the time step has to be balanced between acceptable accuracy and computational demands.

To decide the size of the time step, we have performed a sensitivity analysis. For this analysis, the simulation of the saturation period was repeated several times with different time steps being subsequently smaller and smaller. The different calculated lengths of the saturation period were compared. The right size of the time step was found when no significant change in length of saturation period occurred, for subsequently smaller time steps. This time step was then used for all simulations.

The numerical models are based on the finite difference method; this method replaces the original differential equation with a system of algebraic equations. The method for establishing the system of equations and the method for solving this system will have influence on the necessary size of the time step. The system of equations was established by use of the implicit method (Bear and Verruijt, 1987), the system was solved by use of an iterative solver (Press *et al*, 1992). The implicit method of establishing the system of equations makes it possible to use a large time step.

The selected time step was equal to 1 week (7 days), which give 1560 steps for a time period of 30 years.

15.6 Results of transient modelling

15.6.1 Local and detailed model, differences in tunnel definitions

Both the local and numerical models were used for transient simulations, but the results are not the same, since the models are slightly different.

The sizes of the tunnels are different in the local and in the detailed model (see Table 9.1), however, it is not the size alone, but the size times the available porosity that gives the void of the tunnel.

In the local model all tunnels except the SILO is defined as being homogeneous, hence a tunnel is represented by one value of conductivity only; the SILO is defined with the inclusion of a bentonite barrier surrounding the inside of the SILO, and the inside is defined as homogeneous. Additionally in the local model, the horizontal deposition tunnels (BTF, BLA ans BMA) are characterised by there most permeable part, which is the sand volumes that occurs as a backfill e.g. as top filling. Hence, in the local model these tunnels are homogeneous and very permeable (1×10^{-5} m/s).

In the detailed model, the different structures that occur inside the deposition tunnels are defined in detail (see Sec.9). Both the volumes that occur as backfill at the top and at the sides, as well as the concrete encapsulation are defined in details. The backfill of the detailed model is as permeable as that of the local model, but as the detailed model also includes concrete encapsulations etc, and these are less permeable than the backfill, the total resistance to flow inside the tunnels is larger in the detailed model than in the local

model. Additionally, in the detailed model, the BTF and the BLA tunnels are defined as having a floor made of low permeable concrete; this floor will further reduce the inflow to the tunnel. Thus, as the flow resistance inside the tunnels is larger in the detailed model than in the local model; it follows that if the void of the tunnels are the same, the saturation period will be longer in the detailed model than in the local model.

15.6.2 Local model - Saturation of the deposition tunnels

The results of the local model demonstrate that the BTF and BLA tunnels will be fully saturated in less than a year. The BMA tunnel will need about two and a half years to reach the same condition, and the SILO will need either six and a half years considering the first SILO definition, or 21 years considering the second SILO definition. Detailed results are given in the table below.

Table 15.5 Local model – Length of saturation period for the different deposition tunnels.

DEPOSITION TUNNELS	LENGTH OF SATURATION PERIOD Saturation of initial available porosity.	
	50% saturation	100% saturation
BTF1	3 month	7 month
BTF2	3 month	5 months
BLA	3 month	8 months
BMA	6 months	2 years and 4 months
SILO (SD1)	2 years and 1 months	6 years and 6 months
SILO (SD2)	7 years	21 years

15.6.3 Detailed model - Saturation of the deposition tunnels

In the BTF tunnels, the waste is stored inside a concrete encapsulation below a top fill made up of highly permeable sand. The whole of the BTF1 will be fully saturated within one year and five months and the whole of the BTF2 will be fully saturated within one year and two months. The last part to be fully saturated in the BTF tunnels is the waste encapsulation containing the waste boxes. See Table 15.6 and Table 15.7, as well as Figure 15.2.

In the BLA tunnel the waste is not stored inside a concrete encapsulation, but placed at the centre of the tunnel and the whole of the tunnel is backfilled with a backfill (sand). The BLA tunnel will be fully saturated within two years and four months; the last part to be fully saturated is the top filling. The waste will be stored in the central part of the tunnel below the top filling, for this part of the tunnel it will take one year and one month to reach full saturation. See Table 15.8, as well as Figure 15.3.

In the BMA tunnel, the waste is stored inside a concrete encapsulation. Above the encapsulation there is a top fill and on both sides of the encapsulation there are side barriers, all of these fillings/barriers are made up of highly permeable sand. The whole of the BMA will be fully saturated within two year and four months. The last part to be fully saturated in the BMA tunnels is the top filling. For the encapsulation, containing the waste, it will take one year and six months to reach full saturation. See Table 15.9, as well as Figure 15.4.

In the SILO, the waste is stored inside a concrete encapsulation. Above the encapsulation there is a horizontal bentonite barrier and above the bentonite there is concrete lid. The lid is assumed to have a negligible resistance to flow as the lid is penetrated with flow channels. Above the concrete lid there is a top filling of sand. Below the encapsulation there is a horizontal bentonite barrier, and at the sides of the encapsulation, surrounding the encapsulation, there is vertical bentonite barrier. Note that for the detailed model the values of permeability are defined in a way similar to the second SILO definition (SD2) of the local model, see Sec.6.5.4.

The first part of the SILO to become saturated is the bentonite at the base; it will be fully saturated within half a year. Next comes the bentonite above the encapsulation; it will be fully saturated within two years. The top filling will be fully saturated within about 4 years. The vertical bentonite barriers at the sides of the SILO are fully saturated within 13 to 16 years. The last part of the SILO to become fully saturated is the encapsulation; it will take about 23 years for the encapsulation to reach full saturation. See Table 15.10, as well as Figure 15.5.

As discussed in Section 15.3, the numerical models include an unsaturated flow inside all unsaturated domains; the general tendency of the unsaturated flow is to transport water, inside the unsaturated domain, downward to the lowest part of the unsaturated domain, where it will be stored. The saturation of the SILO encapsulation is partly correlated to the saturation of the vertical bentonite barriers at the sides of the SILO. Both these structures are mainly saturated from the base and upwards. But the degree of saturation of the vertical bentonite barrier demonstrates also a spatial distribution, which is dependent on the presence of access tunnels etc. The encapsulation is however steadily saturated from the base and upward (see Figure 15.6).

Table 15.6 BTF1: Detailed model - Length of saturation period.

BTF1	LENGTH OF SATURATION PERIOD Saturation of initial available porosity	
Part of tunnel	50% saturation	100% saturation
Tunnel floor (concrete)	< 1 month	< 1 month
Porous concrete at sides	1 month	6 months
Top fill (sand)	1 month	5 months
Waste domain, encapsulation	5 months	1 year and 5 months

Table 15.7 BTF2: Detailed model - Length of saturation period.

BTF2	LENGTH OF SATURATION PERIOD Saturation of initial available porosity	
Part of tunnel	50% saturation (1)	100% saturation
Tunnel floor (concrete)	< 1 month	< 1 month
Porous concrete at sides	1 month	4 months
Top fill (sand)	1 month	4 months
Waste domain, encapsulation	5 months	1 year and 2 months

Table 15.8 BLA: Detailed model - Length of saturation period.

BLA	LENGTH OF SATURATION PERIOD Saturation of initial available porosity	
Part of tunnel	50% saturation	100% saturation
Tunnel floor (concrete/sand)	< 1 month	< 1 month
Sides (sand)	2 month	1 year and 7 months
Top fill (sand)	1 year	2 years and 4 months
Waste domain, storage area	2 months	1 year and 1 months

Table 15.9 BMA: Detailed model - Length of saturation period.

BMA	LENGTH OF SATURATION PERIOD Saturation of initial available porosity	
Part of tunnel	50% saturation	100% saturation
Tunnel floor (sand)	< 1 month	< 1 month
Filling at sides (sand)	2 month	11 months
Top fill (sand)	1 year	2 years and 4 months
Waste and encap. (concrete)	6 months	1 year and 6 months

Table 15.10 SILO: Detailed model - Length of saturation period.

SILO	LENGTH OF SATURATION PERIOD Saturation of initial available porosity	
Part of SILO	50% saturation	100% saturation
Bentonite at base	ca. 1 month	6 months
Bentonite at sides	2.5 years	13-16 years
Bentonite at top	0.5 years	2 years
Top filling (sand) above encap.	1.8 years	4 years
Inside of barriers, encap.& waste	9.2 years	23 years

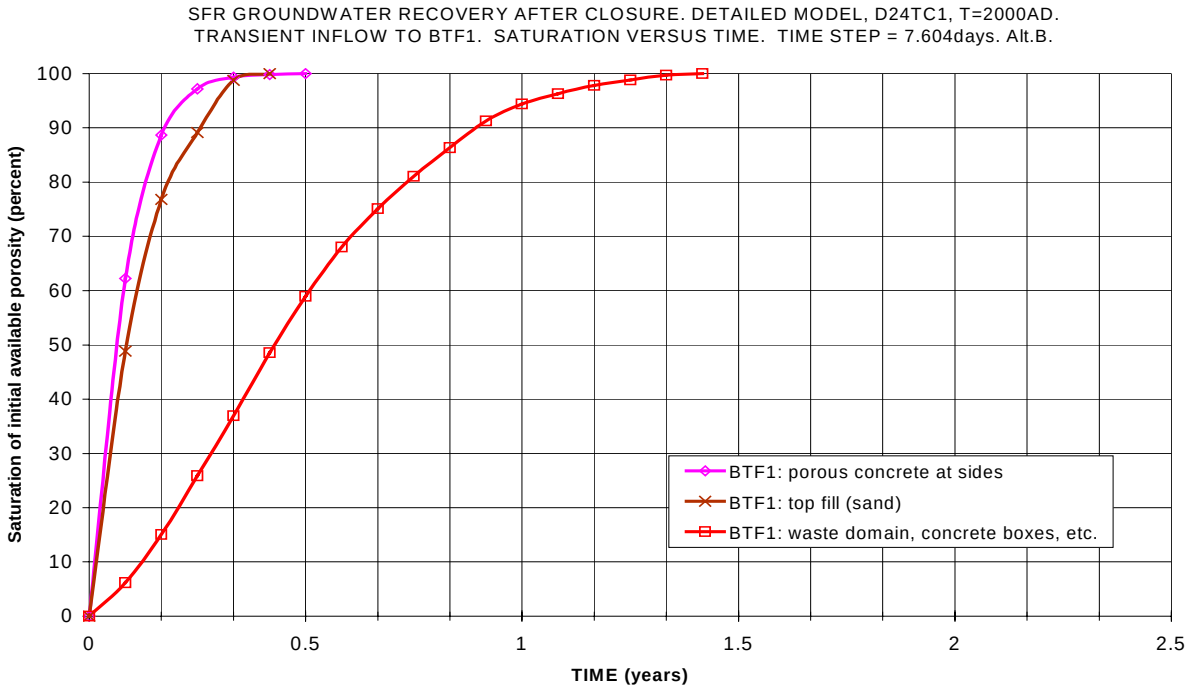

(i) *BTF1 Saturation versus time.*

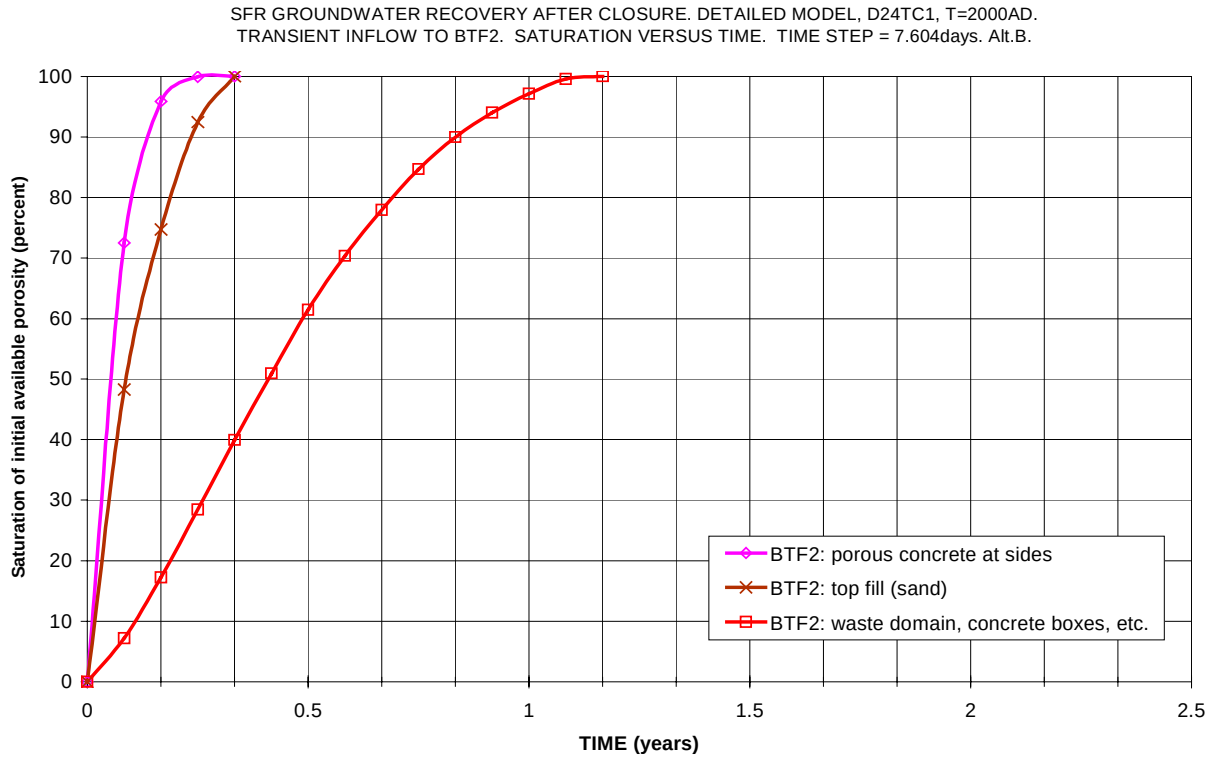

(ii) *BTF2 Saturation versus time.*

Figure 15.2 *Detailed model, BTF tunnels. Groundwater saturation of the tunnels after closure of repository (saturation of initial available porosity). Regional flow represents 2000 AD.*

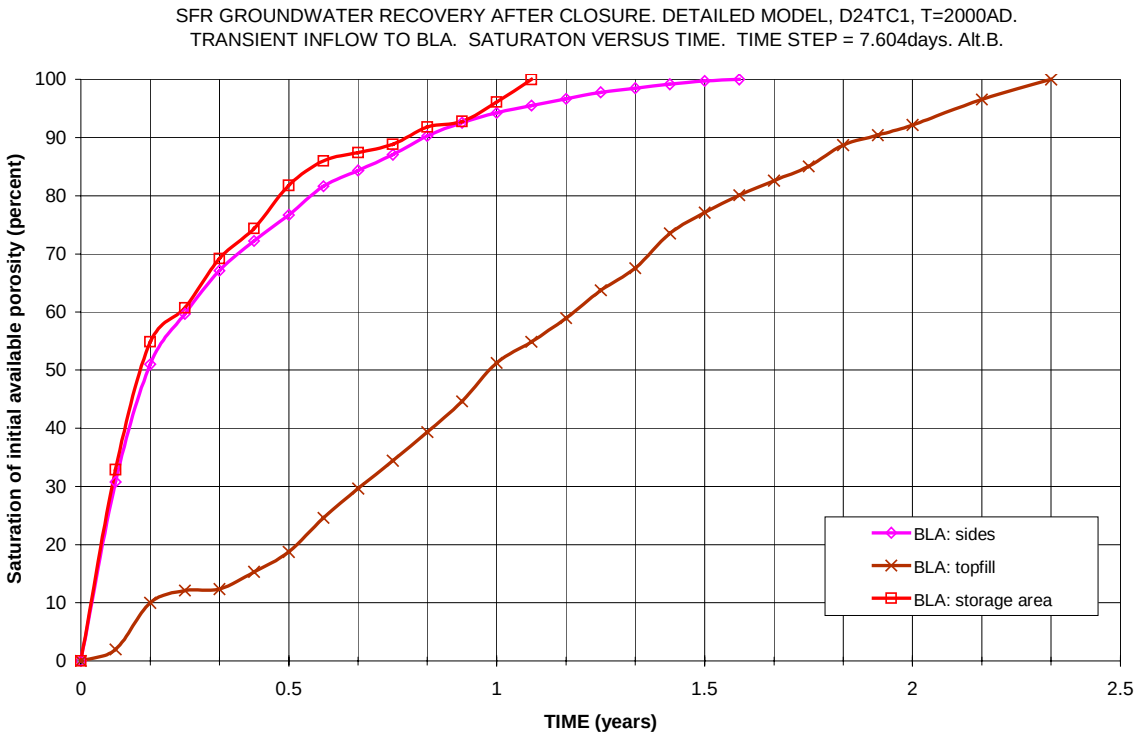

Figure 15.3 *Detailed model, BLA tunnels. Groundwater saturation of the tunnel after closure of repository (saturation of initial available porosity). Regional flow represents 2000 AD.*

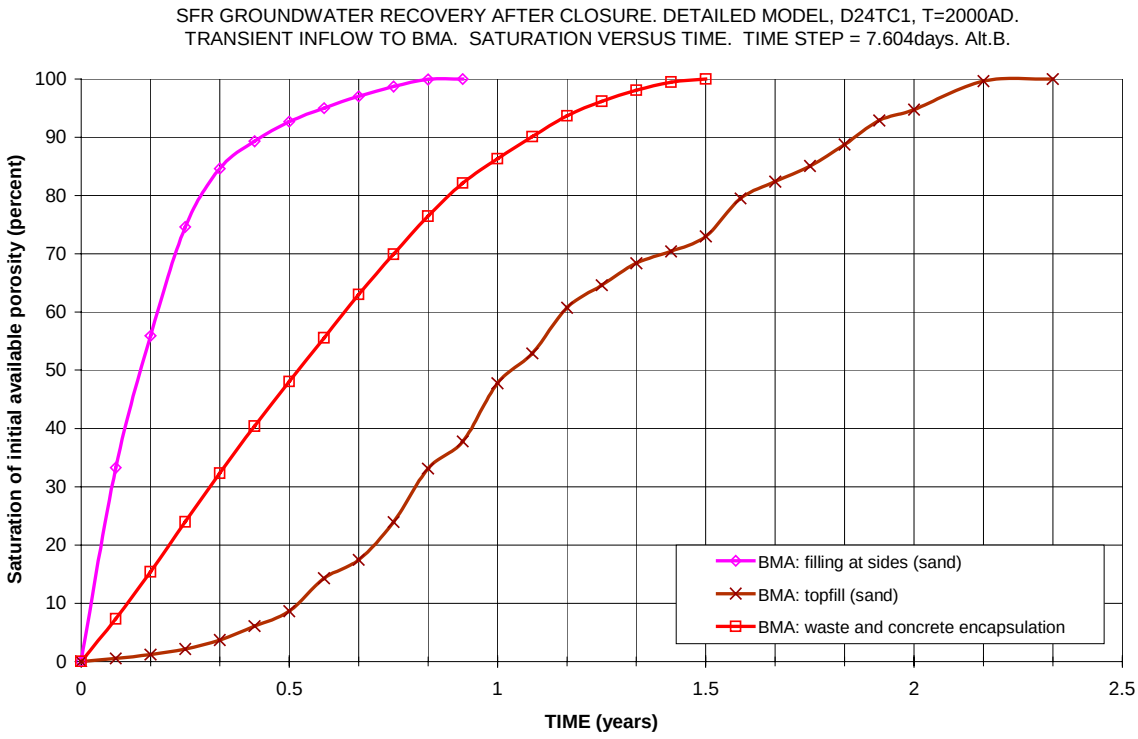

Figure 15.4 *Detailed model, BMA tunnels. Groundwater saturation of the tunnel after closure of repository (saturation of initial available porosity). Regional flow represents 2000 AD.*

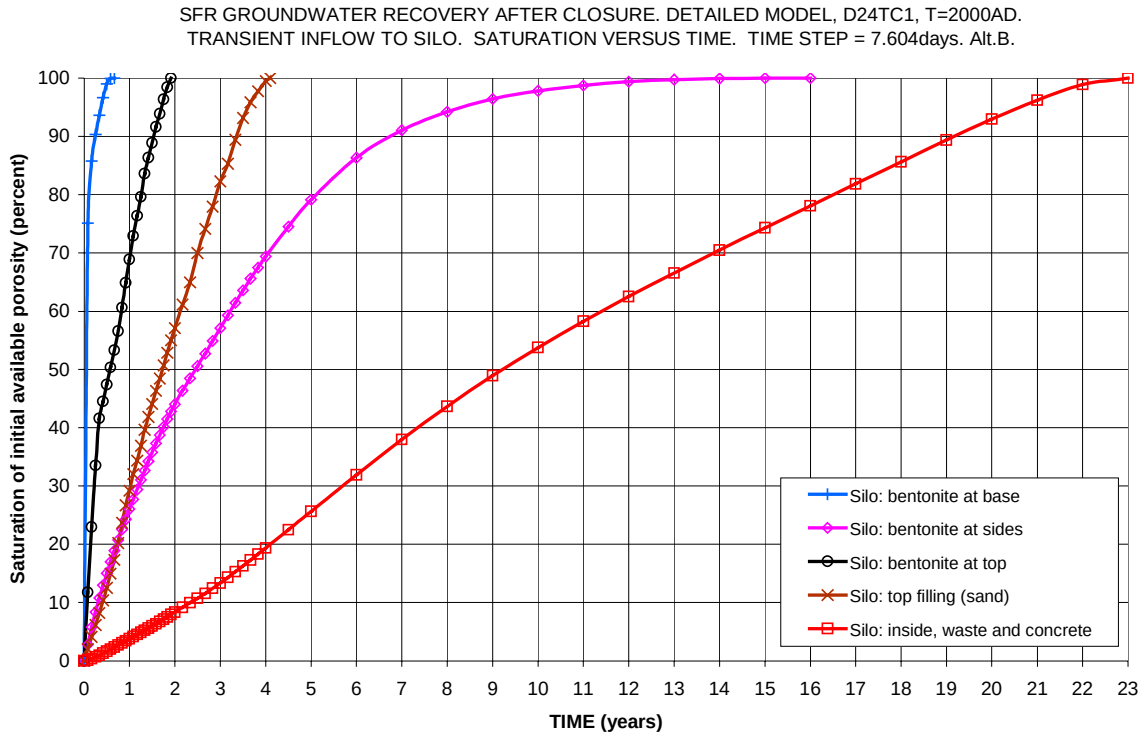

Figure 15.5 *Detailed model, the SILO. Groundwater saturation of the SILO after closure of repository (saturation of initial available porosity). Regional flow represents 2000 AD.*

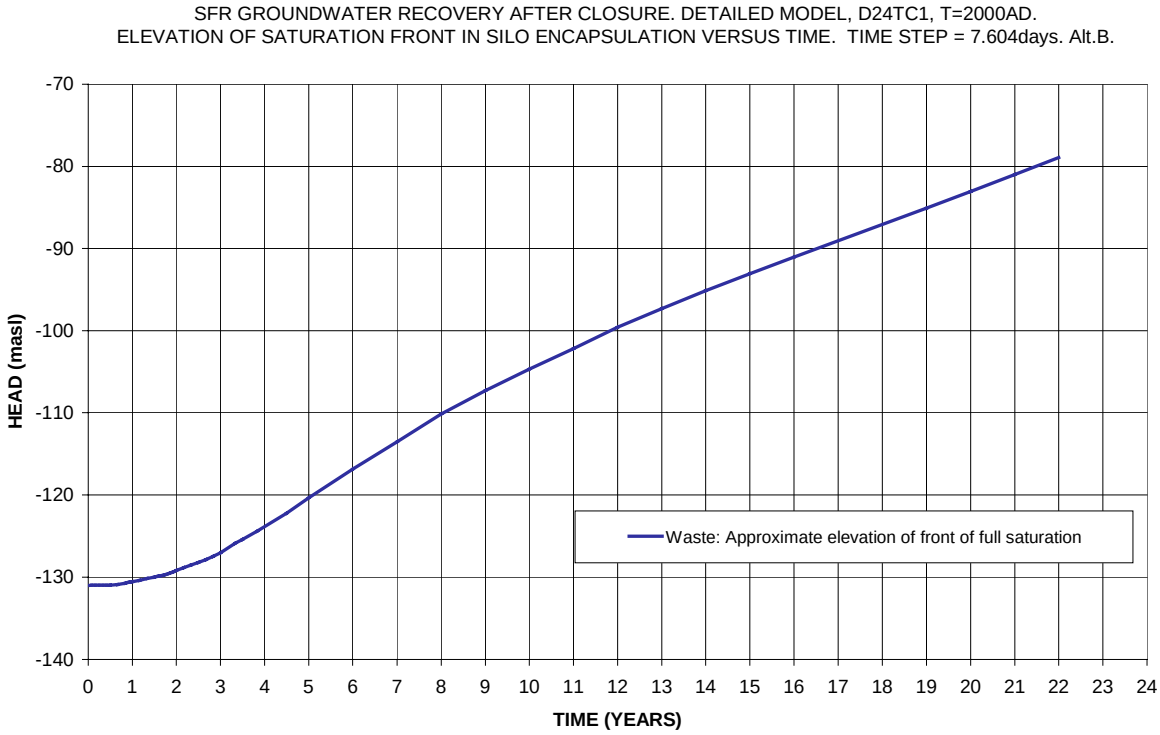

Figure 15.6 *Detailed model, the SILO. Approximate elevation of front of full saturation in encapsulation.*

15.7 Analytical estimate of transient inflow and length of saturation period

15.7.1 Purpose

A comparison is presented in this section, a comparison between a numerical and an analytical representations of the transient groundwater inflow to the SILO and the BLA tunnels, which will occur after these tunnels are abandoned and no longer kept dry. The purpose of this comparison is to demonstrate that no fundamental error has been included in the numerical model.

15.7.2 Presumptions and simplifications

In all of the following discussions and calculations we have used the same presumptions and simplifications as those presented in Section 15.3. Hence, this section is not a test of the applicability of those simplifications.

15.7.3 Theoretical discussion of inflow to an unsaturated domain

The groundwater inflow to an object (e.g. a tunnel) having a lower head than the groundwater head in the surroundings of the object depends on the size of the object, the conductivity, the head difference etc. Everything else being equal:

- The inflow to smaller tunnels is smaller than the inflow to larger tunnel.
- The inflow to a drained tunnel in a low permeable rock mass is smaller than the inflow to a drained tunnel in a more permeable rock mass.
- The lower the head in the tunnel, the larger the inflow to the tunnel.

By a drained tunnel we mean a tunnel that is completely drained, the extension of the sink is equal to the extension of the tunnel. However, if the sink only occurs at some part of the tunnel there will be a flow inside the tunnel towards the sink. Consequently, for such a system, the inflow to the tunnel may become dependent of the properties inside the tunnel, the conductivity of the tunnel itself (i.e. its backfill) as well as the size of the tunnel and the sink.

Consider the groundwater inflow to a tunnel that is slowly being filled with water, as the groundwater is stored in the tunnel. This is a transient process for which the initial condition is the inflow to a drained tunnel (as discussed above). The saturation period is the period during which the tunnel is filled with water. The water will be stored inside the tunnel, hence inside a tunnel there will be two different theoretical domains: (i) the saturated domain in which the water is stored, this domain increases in size with time, and (ii) the unsaturated domain, this is the sink of the system and it is reduced with time.

If the tunnel has an infinite conductivity, which is the same thing as a tunnel without backfill (an empty tunnel), there will be no resistance to flow inside the tunnel. For such a tunnel the size of the inflow to the tunnel is controlled by the conductivity of the surrounding rock mass, the envelope area of the tunnel and the head difference (between tunnel and surroundings). And as the change in head is normally small (se below), the change in inflow during the saturation period will be small as well. The

inflow will be close to constant, for as long as there are empty space left in the tunnel, when the tunnel is filled with water, the inflow will drop to zero. Darcy´s law can not represent the flow inside such a tunnel.

For all other tunnels with some sort of backfill giving a resistance to flow, the inflow during the saturation period will depend on the conductivity of the rock mass as well as that of the backfill. To significantly influence the inflow to a tunnel, the conductivity of the tunnel (the backfill) should be less than that of the rock mass or close to that of the rock mass. This is because the flow path, through the tunnel towards the unsaturated domain, is normally short compared to the flow path through the rock mass. However, the presence of a backfill will also have a second effect on the flow system, because there will be a moving interface between the saturated and unsaturated domains, and the size of this interface will be important for the flow.

For a tunnel with a backfill, it is not only the size of the tunnel that controls the inflow to the unsaturated domain in the tunnel, but also the envelope area of the unsaturated domain. Consider a tunnel that gets more and more filled with groundwater as it flows into the tunnel (more and more saturated). Inside the tunnel, the water will flow towards the sink of the system, which is the part of the tunnel that contains the lowest head. That part is the unsaturated domain of the tunnel, and that domain is becoming smaller with time as the water level rises in the tunnel and water is stored in the tunnel. Hence, as the tunnel is getting more and more saturated, it is not only the head difference, the conductivity of the rock mass and the tunnel as well as the size of the tunnel that determines the inflow, but also the envelope of the unsaturated domain. The following example illustrates this. Consider a system in which a tunnel has a backfill having the same hydraulic properties e.g. conductivity, as the surrounding rock mass. For such a system the size of the tunnel is of no importance, as it does not exist from a fluid mechanical point of view; it is the size of the envelope area of the unsaturated domain and the head inside this domain that controls the inflow.

The head differences between (i) the head inside the unsaturated domain of the object studied and (ii) the head in the surrounding flow medium; may not change very much during the course of saturation. That is because the head inside the unsaturated domain of a tunnel is normally given by the elevation of the unsaturated domain and a pressure near atmospheric pressure (we will in this discussion not consider the capillary forces of an unsaturated porous backfill). Hence, for an unsaturated domain under atmospheric pressure located inside a tunnel, the change in average head inside the unsaturated domain is not larger than the height of the tunnel. For example, consider the horizontal deposition tunnel of BLA. It has a maximum height of 12.5 m. The maximum head difference between a completely unsaturated BLA tunnel (under atmospheric pressure) and the sea is about 60 m; and when about 90% of the tunnel is filled with water, the head difference is about 50 m. Hence, during the course of saturation, the head difference has been reduced about 15%

Based on Darcy´s law we conclude the following equation for the inflow to an unsaturated domain:

$$Q = A\,K\,I$$

Where Q is the inflow to the unsaturated domain, A is the envelope area of the unsaturated domain, K is the conductivity and I is the gradient across the boundary between the saturated and unsaturated domains. If the conductivity of the tunnel is extremely large (i.e. an empty tunnel) the equation is not applicable (Darcy´s law has to be applicable).

For tunnels with a backfill, Darcy´s law together with the laws of mass-conservation and of flow-continuity indicates that the change of inflow to an unsaturated tunnel, which is getting more and more filled with water, must depend on the envelope area and size of the unsaturated domain. That is because when the unsaturated domain, in which the inflow of water is stored becomes smaller and finally cease to exist, the inflow must also become smaller and finally cease.

Figure 15.7 demonstrates how the inflow changes with the radius of different objects.

15.7.4 Transient analytical solutions

We have derived two different analytical transient formulations based on the equation by Thiem (1906). The two analytical solutions represent two-dimensional radial flow towards a cylinder in a homogeneous and isotropic flow medium. For both formulations, the cylinder will get more and more filled with water (saturated) with time, as water flows into the cylinder and will be stored in the cylinder. The volume of the dry (unsaturated) part of the cylinder is reduced with time. The cylinder itself has the same conductivity as the surroundings. It is assumed that the water enters the cylinder through the circular outer envelope of the cylinder and not through the gables. The analytical methods are given in Appendix C. Storage and release of fluid in the surrounding rock mass is not included in the analytical formulations.

- For the first analytical formulation it is assumed that the fluid is stored inside the cylinder along the radius of the cylinder –a radial storage from the outer limits of the cylinder and inwards. It follows that the radius of the unsaturated cylinder (e.g. the radius of the unsaturated domain of the SILO) decreases with time, as more and more of the cylinder gets saturated and more and more water is stored in the cylinder. The height of the cylinder is constant. See Figure 15.8.
- For the second analytical formulation it is assumed that the fluid is stored inside the cylinder along the axis (height) of the cylinder –an axial storage from the bottom of the cylinder and upward. It follows that the vertical extension of the unsaturated cylinder (e.g. the height of the unsaturated domain of the SILO) decreases with time as more and more of the cylinder gets saturated. The radius of the cylinder is constant. See Figure 15.8.

15.7.5 Numerical solution

The numerical solution is the local three-dimensional transient modelling carried out with the GEOAN model. The numerical model is based on a detailed description of the heterogeneous properties the rock mass and includes a description of all the different tunnels of the SFR. For this comparison we will use the local scale model (the local model) of SFR. For the local model the inside of all tunnels are defined as homogeneous.

15.7.6 Studied case - SILO

The SILO is a vertical cylindrical deposition tunnel at the SFR repository. The size of the cylinder representing the SILO, as defined in the analytical solutions and in the GEOAN model, is very close to the actual size of the SILO (height ca. 60 m and diameter ca. 30 m). The volume of the SILO is the same in both the analytical solutions and in the GEOAN model.

In this comparison, we will use a numerical solution, calculated by the GEOAN model, for this solution the SILO is defined in accordance to the first SILO definition (SD1), as given in Section 6.5.4.

In the GEOAN model, the SILO has an internal conductivity (1×10^{-8} m/s) that is larger than that of the rock mass (6.5×10^{-9} m/s), but barriers protects the SILO on all sides and these barriers has a conductivity (5×10^{-10} m/s and 1×10^{-9} m/s) that is less than that of the surrounding rock mass. A representative average conductivity, for the flow media surrounding the inside of the SILO (rock mass and barriers), is a value between that of the rock mass and that of the barriers. The calibration procedure of the analytical solutions could be looked upon as a way of deriving such a representative value. For the analytical solutions, we have assumed a homogeneous and isotropic flow medium and the conductivity of the analytical solution is the result of a calibration procedure. The calibrated analytical solutions predict the same inflow for a completely drained SILO, as the inflow predicted by the GEOAN model. The resulting conductivity (1.7×10^{-9} m/s) is less than that of the rock mass of the numerical model, but larger than that of the barriers of the numerical model, as these are defined in the GEOAN model. It follows from the analytical method that in the analytical solutions the SILO is set as having the same conductivity as the surrounding flow medium (rock mass).

The distance between the outer boundary of the analytical solutions and the centre of the cylinder representing the SILO is equal to the distance between the sea and the SILO in the GEOAN model. The head difference between the head in the SILO and the head of the outer boundary (the sea etc) of the analytical solutions is constant and approximately similar to the head difference in the GEOAN model. The head in the cylinder will not change with time in the analytical solutions, but the average head in the SILO of the GEOAN model will be increased with time, about 30%, as the SILO gets more and more saturated. For the analytical solutions, the porosity of the SILO is also similar to that of the GEOAN model. Hence, the analytical solutions represent a simplified system that as regards its main features is not so different from the description of the GEOAN model.

15.7.7 Comparison of results - SILO

Now, let us study Figure 15.9. As expected, no analytical solution could perfectly reproduce the inflow to the SILO as the GEOAN model predicts it. That is because the analytical solutions are simplified descriptions of the actual system represented by the GEOAN model. However, the general trends of the different phases of the saturation procedure, as predicted by the GEOAN model, are well imitated by the different trends of the two analytical solutions.

Time is less than 1 year.
The first part of the curve denoting the GEOAN model demonstrates an increase of the inflow to the SILO, that is not erroneous, but a consequence of surrounding tunnels getting saturated. As these tunnels get completely saturated, the flow inside and in the surroundings of these tunnels will get redirected towards the SILO, which increases the inflow to the SILO. This behaviour of the actual system can not be reproduced by the analytical solutions.

Time is between 1 and 5.5 years.
The second part of the curve denoting the GEOAN model demonstrates a decrease of the inflow to the SILO. The shape of the decreasing curve follows closely the shape of the second analytical solution. Hence, it is possible to conclude that during this period the unsaturated domain in the SILO is mainly reduced by a reduction of the vertical extension of this domain -the saturated domain starts at the base of the SILO and with time it is enlarged upwards.

Time is between 5.5 and 6.5 years.
The third part of the curve denoting the GEOAN model demonstrates a rapid decrease of the inflow to the SILO. The shapes of the decreasing curve resemblance the last part of the first analytical solution, but it has a less steep drop. It should be pointed out that the time step used in the GEOAN model was set to 7 days and it was checked that this time step was small enough not to influence the results. Hence, it is possible to conclude that during this period the unsaturated domain in the SILO is reduced in two ways: (i) a reduction of the vertical extension of this domain and (ii) a reduction of the radius of this domain. Hence, during the last year the saturated domain is enlarged all the way up to the top of the SILO and also during the last year, the saturated domain is enlarged inwards in a radial direction, as the last part of the SILO gets saturated.

15.7.8 Studied case - BLA

The BLA is a horizontal deposition tunnel at SFR repository. The size of the BLA tunnel, in the numerical model, is larger than its actual size. For the analytical solutions, the BLA tunnel was defined as having the same length and volume as the BLA tunnel in the numerical model, but with a different cross-section. For the analytical solutions the cross-sections is circular, but in the numerical model it is rectangular.

In the GEOAN model the BLA-tunnel is homogeneous and a backfill is defined in the tunnel. The conductivity of the back fill (1×10^{-5} m/s) is much larger than that of the surrounding rock masses (6.5×10^{-9} m/s). But the BLA is also intersected by fracture Zone 6, which has a conductivity (5×10^{-7} m/s) that is not so much smaller than that of the tunnel. About 50% to 75% of the inflow to BLA, is carried by this Zone. A representative average conductivity, for the flow medium surrounding the BLA tunnel (rock mass and Zone 6), is a value between that of the rock mass and that of Zone 6. The calibration procedure of the analytical solutions could be looked upon as a way of deriving such a representative value. For the analytical solutions, we have assumed a homogeneous and isotropic flow medium and the conductivity of the analytical solutions is the result of a calibration procedure. The calibrated analytical solutions predict the same inflow for completely drained BLA tunnel, as the inflow predicted by the GEOAN model. The resulting conductivity (2×10^{-8} m/s) is larger than that of the

rock mass and smaller than that of Zone 6, as these are defined in the GEOAN model. It follows from the analytical method that in the analytical solutions the BLA is set as having the same conductivity as the surrounding flow medium (rock mass).

The distance between the outer boundary of the analytical solutions and the centre of the BLA is equal to the distance between the sea and the BLA in the GEOAN model. The head difference between the head in the cylinder representing BLA and the head at the outer boundary (the sea etc) of the analytical solutions is constant and approximately similar to the head difference in the GEOAN model. The head in the cylinder will not change with time in the analytical solutions, but the average head in the BLA of the GEOAN model will be increased with time, about 15%, as the BLA gets more and more saturated. For the analytical solutions, the porosity of the BLA is also similar to that of the GEOAN model. Hence, the analytical solutions represent a simplified system that as regards its main features is not so different from the description of the GEOAN model.

15.7.9 Comparison of results - BLA

Now, let us study Figure 15.10. As expected, no analytical solution could perfectly reproduce the inflow to the BLA as the GEOAN model predicts it. That is because the analytical solutions are simplified descriptions of the actual system represented by the GEOAN model. However, the general trends of the saturation procedure, as predicted by the GEOAN model, are well imitated by the trends of the analytical solutions No.1. The only major difference is that during the last 2.5 months of the saturation period, the inflow to the BLA decreases more rapidly in the analytical solution than in the GEOAN numerical model. It should be pointed out that the time step used in the GEOAN model was checked that it was small enough not to influence the results. Hence, it is likely that for the last part of the saturation period, the inflow to the remaining unsaturated domain is not well represented by a two-dimensional radial flow in a homogeneous and isotropic flow medium. The actual flow in the GEOAN model is, for the last parts of the unsaturated domain, probably better represented by a three dimensional flow patter in a heterogeneous flow medium.

15.7.10 Analytical method - conclusions

The good agreement between (i) the inflow as predicted by the GEOAN model and (ii) the inflow as predicted by the analytical solutions, demonstrates that no fundamental error has been included in the numerical model.

The good estimates produced by the analytical solutions may lead to the conclusion that the numerical model is not necessary, that is however not correct. The analytical solutions are calibrated against values of inflow (see Sections 15.7.6 and 15.7.8) and these values of inflow are given by the numerical model, as the actual inflow is not measured for all tunnel explicitly. Furthermore, the analytical methods are not capable of producing detailed predictions of the saturation process inside the tunnels, for that we need a detailed numerical model (see Section 15.6).

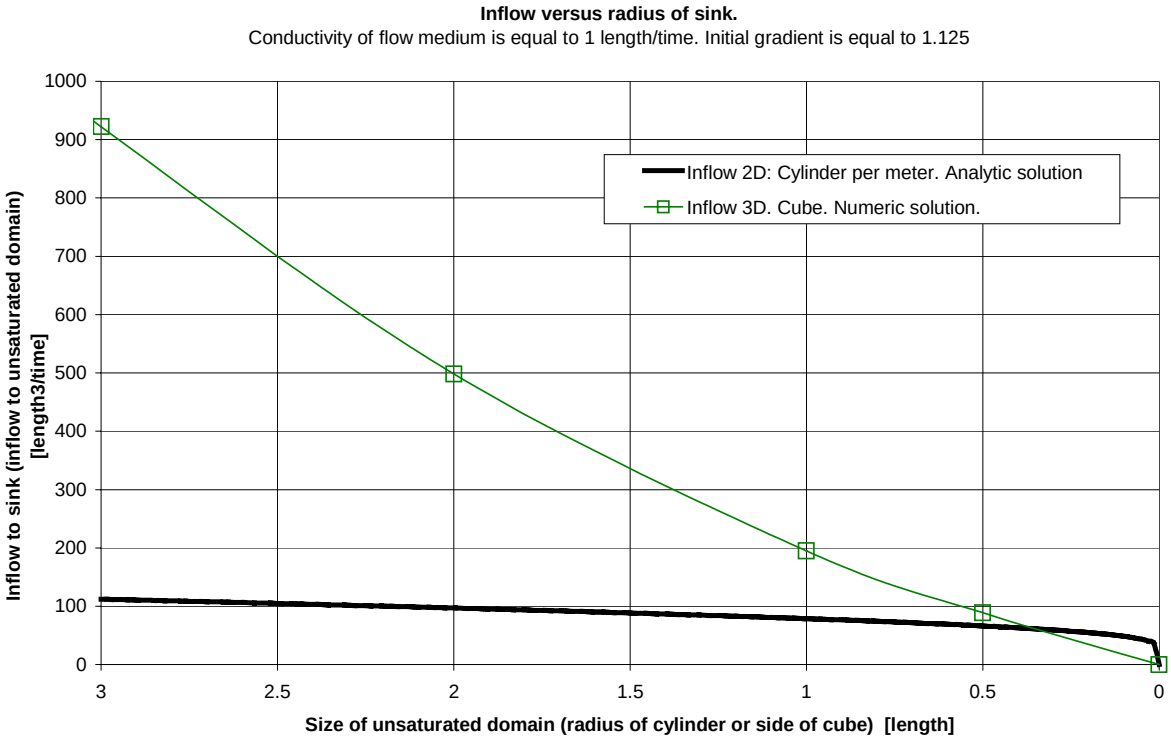

Figure 15.7 *Two and three-dimensional steady radial confined flow towards sinks (e.g. unsaturated domains) of different geometrical shapes and sizes. The head inside the sinks is the same regardless of size of sink. The inflow to the cylinder is a two-dimensional flow per meter of cylinder. The inflow to the cube is a three-dimensional flow towards all faces of the cube.*

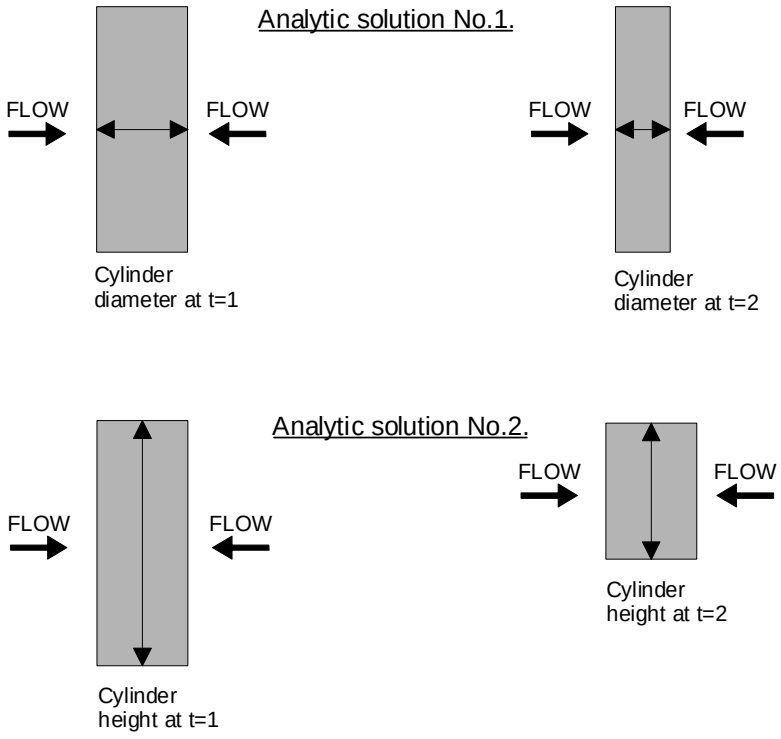

Figure 15.8 *Figure demonstrating the differences between the two analytical methods.*

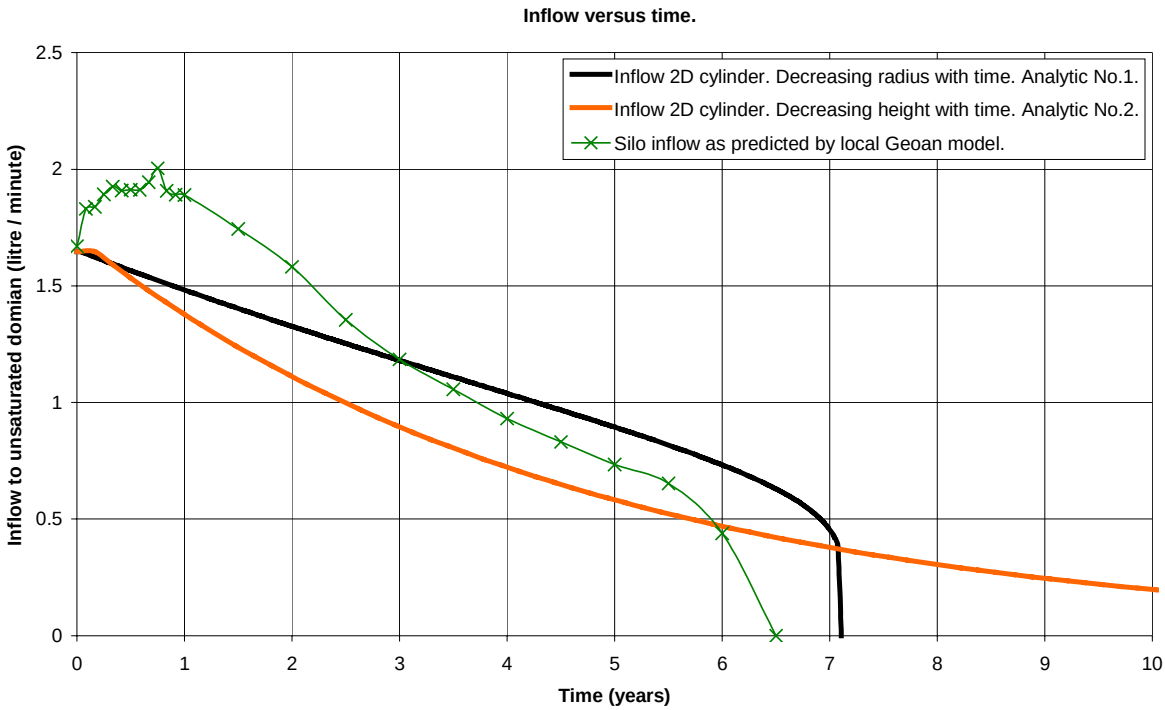

Figure 15.9 *Inflow to SILO during the saturation period.*

The figure presents a comparison of predicted inflows, predictions by analytical methods and by a numerical model (local model, first SILO definition, SD1).

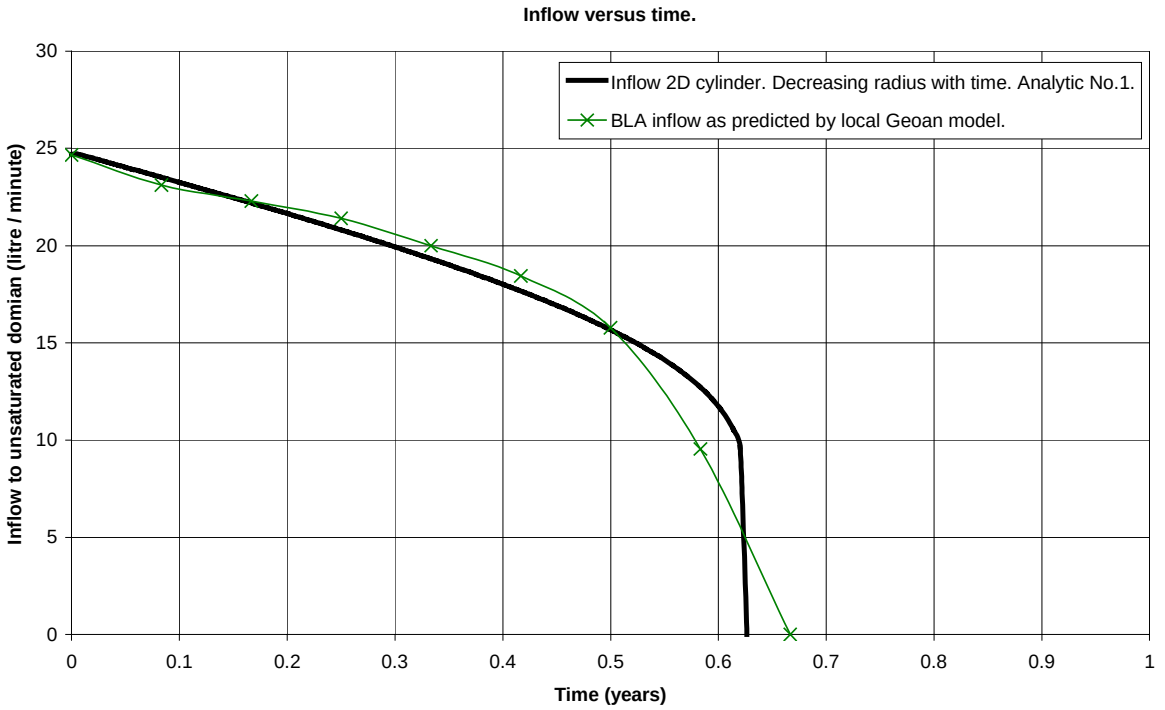

Figure 15.10 *Inflow to BLA during the saturation period.*

The figure presents a comparison of predicted inflows. Predictions by analytical methods and by a numerical model (local model).

16. Discharge areas, sediment accumulation and flow paths from the repository

16.1 Introduction

The current topography of the seabed in the area surrounding the SFR repository may not stay the same in the future. Considering a period of several thousands of years, changes in topography may take place because of erosion and/or accumulation of sediments. In addition to the geological and biological processes that continuously shape the landscape, for the area studied there will also be the process of the shore level displacement. Based on the assessment of the shore level displacement (see Sec. 2.6.2) we have assumed that the present seabed will in the future be dry land, as the shore level will move away from the repository. Such a dramatic change in conditions may in the long time perspective also lead to a change of the topography. Because the geological and biological processes will not be the same for (i) a topography below the sea, (ii) a topography close to the shore line and the sea level and (iii) a topography above the sea and perhaps also far away from the shoreline. It is also possible that human development (e.g. farming etc) of the old seabed will take place as it rises above the sea, and that such activities will lead to some changes of the topography.

We are aware of the fact that the geologic and biologic process that we will study in this chapter (accumulation of sediments) is difficult to quantify and will bring some uncertainty to the analysis, therefore such processes have not been included in the analyses of the previous chapters. Processes that in the future will change the topography are not included in the base case of this study, such a process is however studied in this chapter.

By sediments we mean both solid particles derived from rocks (created by weathering and erosion) as well as organic material (created by biological activity), and by sedimentation we mean the process of sediment deposition.

16.2 Purpose of simulations

The purpose of the following simulations is to estimate the effects of small changes in the topography, as regards flow paths from the repository. In the following simulations the change in topography is caused by accumulation of sediments at discharge areas. The detailed objectives are to estimate the positions of the areas where the groundwater, coming from the deposition tunnels of the repository, will discharge into the surface water system. These areas will change with time and will be affected by changes in the topography. For the base case with constant topography, the positions of the discharge areas for the flow paths from the repository are given in Chapter 11.8.

The type of landscape and biological environment where the flow paths from the repository discharges is of importance when calculating the effects of a release of radioactive nuclides. It is a purpose of this chapter to estimate the type of environment where this discharge will take place; we will present simple estimations based on how these discharge areas are located in relation to the shore line.

16.3 A qualitative assessment of the studied course

We will study a time period from 3000 AD and until a steady-state-like situation will take place for the groundwater system close to the repository, which will probably occur between 5000 AD and 7000 AD. A prerequisite for these simulations is the assessment of the shore level displacement (see Sec. 2.6.2). According to this assessment the present seabed will in the future become dry land, as the shore level will move away from the repository. The semilocal topography of the areas surrounding the SFR-repository is given in Figure 16.1, the piers, embankments and quays of the SFR-harbour is not included in this study. Considering the purpose of this study, the presence of these constructions are not very important, and it is possible that the piers and embankments of the SFR harbour will be removed, before the closure of the repository. At the present situation (2000 AD), the depth of the sea above the central parts of the repository is about 2 m - 5 m. The shoreline will be above the repository at about 2800 AD. And at 4800 AD the shoreline has moved about 1 km away from the repository and because of a topographic threshold, lakes and mires will be established about 1 km North and Northeast of the repository. The water level of these lakes and mires is somewhat uncertain, as it will depend on a future topographic threshold, however, in the models of this study the water level of these lakes is set to -15 masl (see Figure 16.1 and Figure 16.2).

Considering the current topography of the area in the surroundings of the repository, the groundwater that has passed the deposition tunnels will discharge into two different drainage basins (catchment areas), limited by surface water divides, see Figure 16.2 (the basins are denoted as No.**1** and No.**2** in the figure). The actual size of basin No.2 is somewhat larger than the area denoted in the figure, a small part of the actual basin is outside of the semilocal domain (East of area No.2). It should also be noted that only a small part of these basins are above the shoreline at 3000 AD, and as the sea withdraws the parts of these basins that are above the shoreline will increase in size. The large basin Northeast of the repository, which in the future will form a large lake, is denoted as No.**3** in the figure. It should be noted that there are uncertainties in the exact location of the surface water divides, especially in the close surroundings of the lakes that will be formed North of the repository.

As regards accumulation and reduction of sediments it is possible to divide the studied course into three periods. Because of the movement of the shoreline and the undulating topography, these three periods will take place at different times for different places. A qualitative assessment of the studied course is as follows.

- First period. The topography is below the sea. During this period sedimentation will take place at the seabed, primarily at low lying parts of the topography, however there

may also occur erosion and transport of sediments away from the area studied, due to the effects of moving water, i.e. underwater streams.

- Second period. The topography is close to the shoreline and close to the surface of the sea. This period is normally shorter than the other two periods, however it could be an important period, because during this period much erosion and transport may take place as a result of wave erosion. The impact of waves against an unprotected shore can be very large; but islands located close to the shore will protect the shore, and much reduce the effect of wave erosion.

- Third period. The topography is above the sea. During this period, accumulation of material may take place at low-lying parts of the topography, because of biological activity and by deposition of material carried by local small streams. There will also be some erosion, and material will be transported away from the area studied by local small streams. Because of the length of the time period studied (several thousands of years), accumulation of material could be significant at local basins, such as lakes and mires etc. For example, after a time period long enough most lakes will come to an end, as sedimentation and biological activity in the lake will lead to accumulation of material that will finally fill up the lake.

16.4 Assumptions – sediment accumulation and reduction

16.4.1 First and second periods – assumption of sedimentation

For the areas surrounding the repository, Brydsten (1999) has carried out an assessment of sedimentation and wave erosion by use of numerical models; the models simulated the retreat of the shoreline and different processes that will transport and redistribute sediments. No quantification of the change in topography was given in that study.

In this study we have assumed that the total effect of (i) the sedimentation below the sea during the first period and (ii) the wave erosion during the second period; will results in a situation for which the topography has not changed significantly when the third period starts. Hence, for the models used in this study, the topography will not change as long as the sea covers the topography.

16.4.2 Third period – assumption of sedimentation

Considering the third period, it is difficult to quantify at what rate and amount local small basins will accumulate sediment. A historical comparison with lakes, mires and peat bogs in the province of Uppland (SFR is located within Uppland) demonstrates that, partly due to biological activity, a small lake may become filled with peat and sediments after a period of less than 1000 years. Consequently, we have estimated that a possible accumulation of sediment in a local basin is in the range of a few millimetres up to about 10 millimetres per year. This means that a small lake having a depth of a few meters could be totally filled with sediments within less than 1000 years.

In the model we have assumed that accumulation of sedimentation will only take place at areas where groundwater discharges to the surface water system[§]. Such areas are found at low-lying parts of the topography, often at the bottom of local drainage basins, and often close to the shoreline. At such areas it is very likely that there will be a surplus of water available to biological activity throughout the year, and due to its topography (a basin) it is likely that sediments will accumulate at such areas. Groundwater discharge areas are found along fracture zones 3 and 9, North of the repository. For the base case presented in previous chapters, in which the topography does not change with time and no accumulation of sediments occurs, the positions of the discharge areas for the flow paths from the repository are primarily in connection to fracture zones 3 and 9 (see Chapter 11.8).

In the model we have applied the condition of sediment accumulation (at groundwater discharge areas) inside a limited domain only. This domain is within the local drainage basins for the groundwater flow from the repository. Considering the current topography of the area in the surroundings of the repository, the groundwater that has passed the deposition tunnels will discharge into two different drainage basins (denoted as **1** and **2** in Figure 16.2). The parts of these basins that are above the shoreline will increase in size with time, as the sea withdraws (see Figure 16.5). Accumulation of sediment will only take place at groundwater discharge areas within a limited domain inside these two local basins; the extension of the domain within which sediment accumulation will take place is given in Figure 16.2. For the large basin Northeast of the repository, which in the future will form a large lake (denoted as **3** in the figure), we have assumed that the accumulation of sediments will be less significant, because of the size of these lakes. In the model we have set the accumulation of sediments equal to zero for this area.

Thus, in the model when the sea has withdrawn and exposed new land, the topography of this new land will change somewhat at local basins, as sediments will accumulate at these areas. In the model the accumulation of sediments at a certain area will only continue as long as the area remains a discharge area for the groundwater. Due to the movement of the shoreline and/or due to the accumulation of sediments, it is possible that the discharge of groundwater ceases at a certain area; for such a situation the groundwater discharge moves to another area having a lower elevation. If the groundwater discharge ceases at a certain area, also the accumulations of sediments will cease at that area. In the model we have used different rates of sediment accumulation for different cases, either 5 mm/year or 10 mm/year.

16.4.3 Conductivity of sediments accumulated during the third period

The conductivity of the future sediments is difficult to predict, as they will contain both material derived from rocks (created by weathering and erosion) as well as organic material (created by biological activity). For the third period we have assumed an accumulation of sediments in small local basins, these sediments will primarily be of organic origin, therefore it is likely that they will have a low permeability, probably less than 1×10^{-7} m/s. In the model we have used different values for different cases.

[§] In this study, groundwater is defined as the groundwater of the fractured rock; it does not include the near surface groundwater of the quaternary deposits.

It should however be noted that it is not the permeability of the sediments that is the most important parameter as regards the objectives of this study (presuming that the conductivity is not extremely large), but the rate with which the sediments are accumulated. The rate is most important, because compared to the situation without sediments, a build up of sediments will cause a build-up in groundwater heads below the sediments, which will change the flow pattern of the groundwater below the sediments. The build-up of groundwater heads will take place for all plausible values of sediment conductivity, because for such values of conductivity the sediments will be saturated with water.

16.5 The semilocal model

16.5.1 Introduction

For the estimation of the effects of sediment accumulation, the model needs to be larger than the previously presented local model (see Sec. 6), but include the same level of details. For that reason we have established a model which is larger than the local model but smaller than the regional model, this model is called the semilocal model.

16.5.2 Size of semilocal model

The semilocal model represents a rectangular three-dimensional body. The horizontal area covered by the semilocal model is larger than the area covered by the previously presented local model, but the semilocal model is much smaller than the regional model. The semilocal model includes the same level of details as the local model. The primary differences, compared to the local model, are that the semilocal model is extended 1408 m towards Northeast and 983 m towards Northwest. The semilocal model covers a horizontal area of 2699 m x 3732 m (10.1 km^2). The depth of the model is the same as for the local model (490 m). The upper boundary of the model is the surface topography. The model has vertical sides and a base that is nearly flat. The horizontal extension and topography of the semilocal model and the local model is given in Figure 16.1.

16.5.3 Mesh

Three-dimensional cells of different sizes make up the model. The cells form a mesh. The mesh of the semilocal model, representing the tunnel system at SFR and surrounding rock masses, has 25 layers and contains 108 675 cells. Each cell represents one node in the mathematical model, placed at the center of the cell. The mesh is primarily optimized to match the layout of the deposition tunnels of the SFR; a secondary optimization was carried out for the access tunnels. Outside of the area where deposition tunnels are defined in the mesh, the size of the cells is increased towards the

outer boundaries of the model. For the areas where the local basins are and where the discharge occurs of water from the repository, the largest cells have a horizontal size of 75 m x 75 m. The mesh is given in Appendix A.

16.5.4 The fracture zones

In the semilocal model, the regional fracture zones are the same as in the regional model. The local fracture zones, as known today, are all in the close surroundings of the SFR. In the models, the position of the fracture zones is according to the updated structural geological model (Axelsson and Hansen 1997). The knowledge of these zones is based on information from exploratory drillings and information gathered during the construction of the repository. Hence, the local structural geological model is based on information gathered in the close surroundings of the present repository, and outside this area we have no information of other small fracture zones, because no detailed investigation has been carried out outside the close surroundings of the repository. For example, it is very likely that several more fracture zones exist close to the repository, but outside of the known local fracture zones. As the semilocal model is larger than the local model, two of the local fracture zones have been extended in the semilocal model; these zones are zones 3 and 9. They have been extended towards Northeast, and in the semilocal model they terminate towards the regional fracture zone D. No new local fracture zones have been introduced to the semilocal model. The fracture zones of the semilocal model is illustrated in Figure 16.1. Hence, the fracture zones of the semilocal model are identical to the zones of the local and regional model; except for the length of zones 3 and 9, these zones are extended towards Northeast in the semilocal model.

16.5.5 Regional properties contra local properties in the semilocal model

The semilocal model is larger than the local model, but smaller than the regional model; hence it includes parts of both the local and the regional domains. The part of the semilocal model that represents the same volume as the local model is defined with the same hydraulic properties (conductivity etc) as the local model. And the part of the semilocal model that represents the same volume as the regional model is defined with the same hydraulic properties as the regional model. This means that the rock mass of the semilocal model will have different values of conductivity, one value inside the local domain and another value inside the regional domain. The different values of conductivity reflect the discrepancy in the amount of known data - inside the local domain the local small fracture zones are known, but outside of the local domain no small fracture zones are known. The horizontal extension of the semilocal model and the local model is given in Figure 16.1.

Hence, inside the local domain, the conductivity of the rock mass of the semilocal model is equal to 6.5×10^{-9} m/s, as in the calibrated local model. And inside the regional domain, the conductivity of the rock mass of the semilocal model is equal to 1.5×10^{-8} m/s, as this is the effective conductivity of cases 2 and 4 of the regional model (see Sec.7.9). The rock mass of the semilocal model is defined as homogeneous, but with fracture zones.

16.5.6 Quaternary deposits

Investigations of the seabed at SFR have revealed that the fractured rock is mainly covered by a glacial till (morain) of varying thickness with a large amount of boulders and a small amount of fine grained material, Sigurdson (1987). At present a continuous layer of fine-grained sediments, e.g. clay, does not cover the seabed above the SFR. The hydraulic conductivity of the glacial till is estimated by Sigurdson (1987) to be within a range of 1×10^{-5} m/s through 1×10^{-8} m/s. This indicates that on the average, the quaternary deposits have a conductivity that is larger than the average conductivity of the rock mass. Where fracture zones intersect the rock mass, the conductivity of the quaternary deposit is smaller than or approximately the same as the conductivity of the fracture zones.

Quaternary deposits have not been explicitly included in the formal models (regional, semilocal and local models). The quaternary deposits are represented in the models as a part of the fractured rock. However, the accumulation of sediments during the third period (as discussed above) will be explicitly defined in the model.

16.5.7 Calibration of semilocal model

The semilocal model was not calibrated; as its hydraulic properties (e.g. conductivity) in the local domain are the same as for the calibrated local model, both the local and the semilocal models include the present tunnel system (see Chapter 6). Considering the flow through the deposition tunnels at different times, the local and the semilocal models predict flow values that are very close to each other.

16.5.8 Methodology, chain of simulations and boundary conditions

For the semilocal model, we can not use the same methodology as for the local model, because the process of accumulation of sediments needs to be represented as a fully time-dependent process. Hence, the semilocal model needs to be a fully transient model.

In the same way as for the local model, the semilocal model will be assigned boundary conditions (specified head) along the vertical sides and base of the model, which are taken from the regional model (from the time-dependent regional simulation, case 4). Hence, the semilocal models will have the specified head boundary condition at the base and at the vertical sides of the model. The actual head values assigned to the boundary nodes of the base and sides of the semilocal models are calculated based on a three-dimensional and time-dependent interpolation between the head values of the nodes of the regional model. Along the top of the model the boundary conditions will depend on the flow situation, by use of the method discussed in Sec. 7.4.1. This method will calculate the extension of discharge and recharge areas based on the topography and the state of groundwater flow system.

The chain of simulations is as follows:

1. Simulation with the regional model. The regional model case 4 has been used, it provides boundary conditions for the semilocal model.

2. Semilocal model, initial condition. The model needs an initial condition, which will be the start point for the transient simulations. The initial condition represents the flow situation at time equal to 3000 AD. The regional model gives the head values at the outer limits of the semilocal model, representing the regional flow situation at 3000 AD. The semilocal model is run under steady state conditions until a good convergence is reached. No accumulation of sediment is applied during this simulation.

3. Simulation with the semilocal model, transient conditions. The initial condition is the flow situation calculated by the semilocal model for 3000 AD (as discussed above). For the transient simulations, the semilocal model will be run under fully transient conditions. The head values at the outer limits of the semilocal model will change with time as well. These changing head values, along the base and sides of the semilocal model, are taken from the regional model, and they represent the transient flow situation as simulated by the regional model. The time step of the semilocal model was set to 5 years. This time step was selected based on a sensitivity analysis.

Thus, the simulations with the semilocal model will be carried out under time-dependent conditions (transient). In addition to the transient mode of the simulations, five different time-dependent processes are included in the semilocal model:

(i) Lowering of the sea water table, which simulates the land uplift.
(ii) Change in distribution of recharge and discharge areas.
(iii) Transport of surface water flows in the direction of the topographic gradient.
(iv) Accumulation of sediments at discharge areas at selected local basins, which causes changes of the topography.
(v) The change of head values at the base and sides of the model, which represents the time-dependent change in the regional groundwater flow.

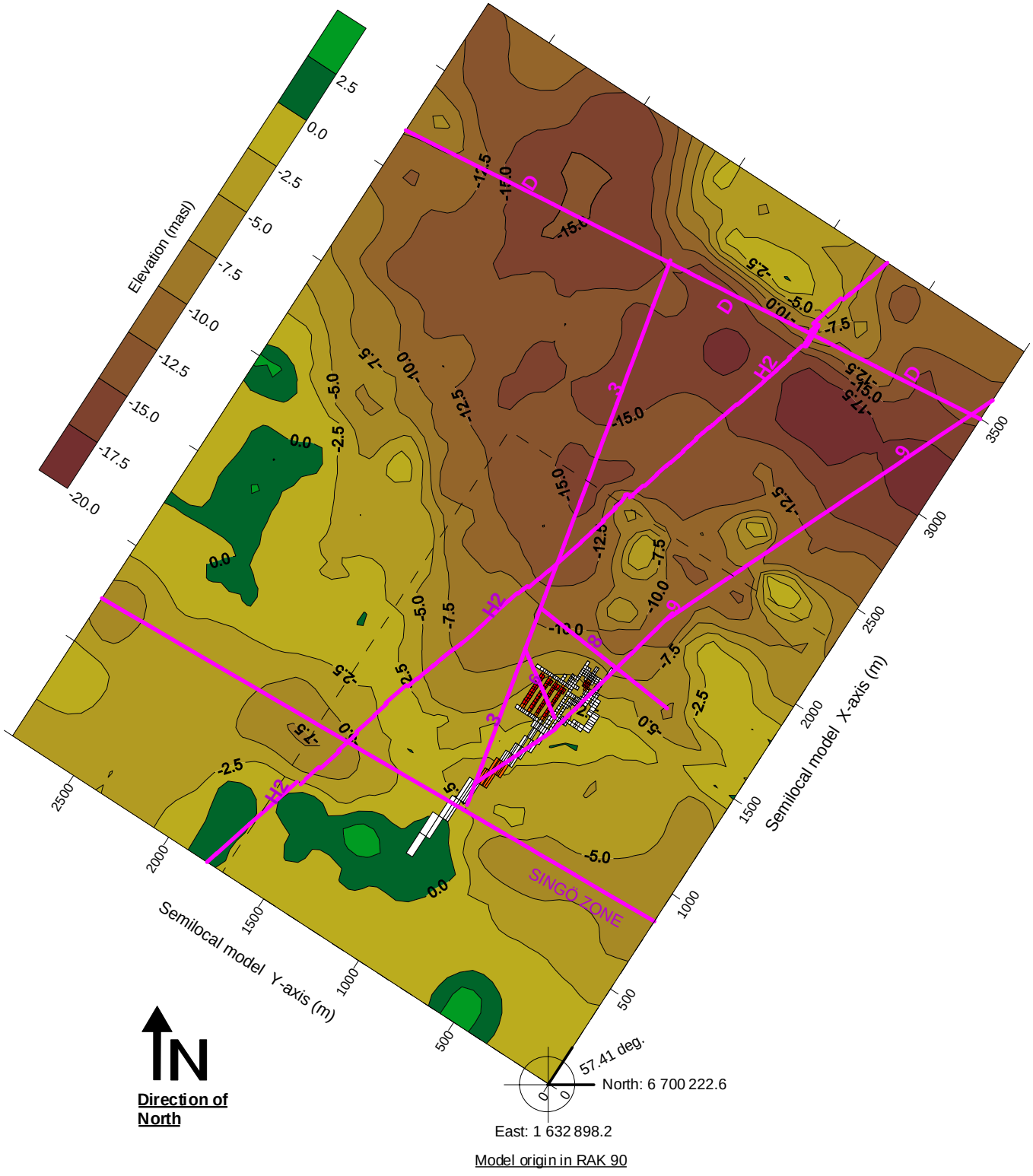

Figure 16.1 *The semilocal model, the topography and the surface positions of the fracture zones, as well as the SFR tunnel system.*

The extension of the local model is denoted by a dotted line.

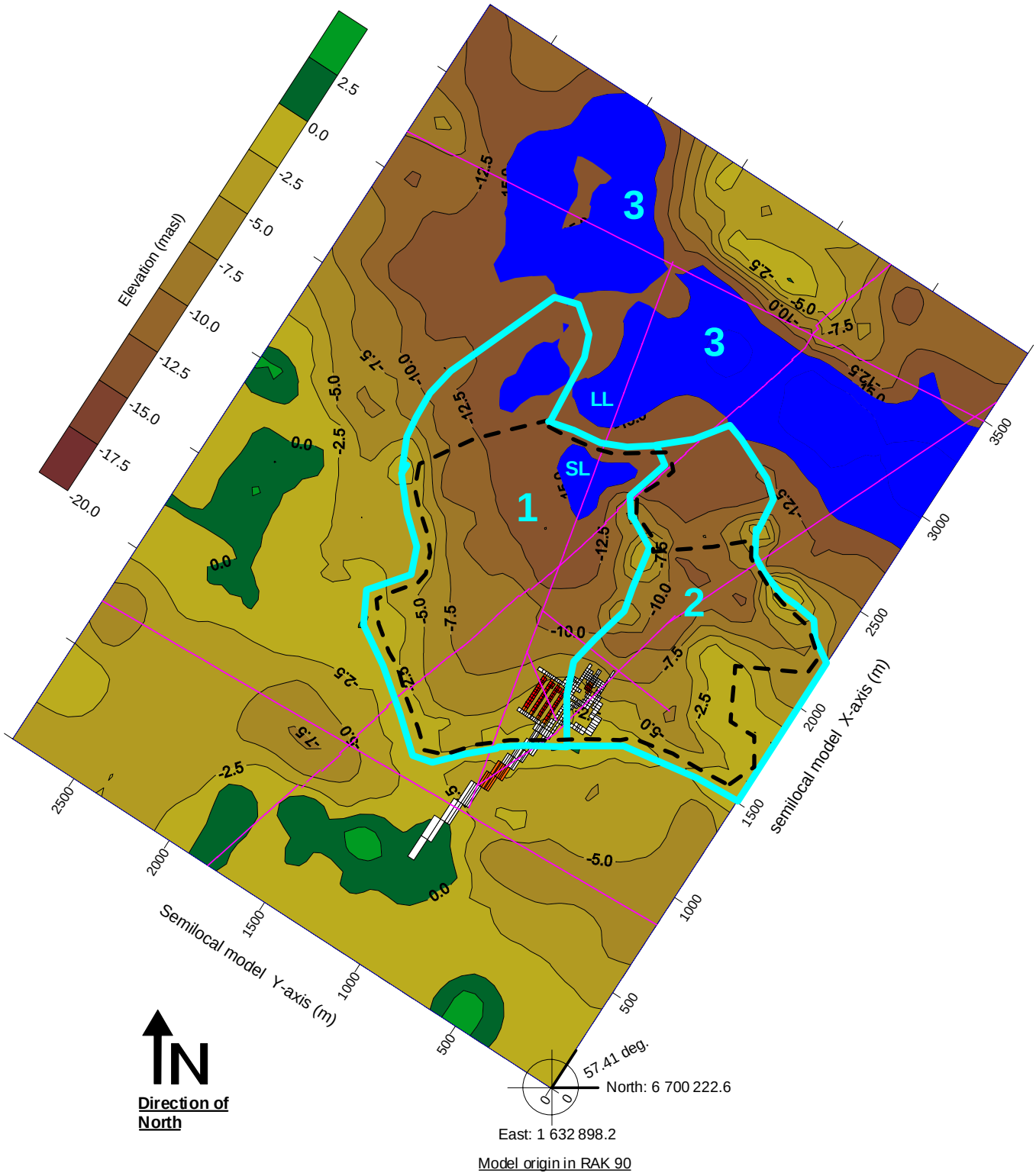

Figure 16.2 *The semilocal model, the topography and the local drainage basins (catchment areas).*

*The following are denoted in the figure. The drainage basins, within which the groundwater flow from the repository will discharge, are denoted by a thick light-blue line and denoted as areas No.**1** and No. **2**. Sediment accumulation is defined at groundwater discharge areas inside the domain surrounded by a dotted black line. The large lakes North and Northeast of the repository are denoted as No.**3**, their water level is at –15 masl, which represents the situation after 4800 AD. The small lake within basin No.**1** is denoted with **SL**. The part of the large lake, which is closest to basin No.**1**, is denoted as **LL**.*

16.6 Results

16.6.1 General behaviour of the system studied

The flow paths of the groundwater that has passed the repository will terminate at the ground surface, at discharge areas located North of the repository. The topography and the position of the sea primarily give the positions of these discharge areas. Due to the shore level displacement new land will rise above the sea. And as new land will rise above the sea, new recharge and discharge areas will be established at the new land. But also the old recharge and discharge areas will become affected by the retreating shoreline, presuming that the shoreline is close enough to affect the groundwater system close to these areas. The purpose of the simulations presented below is to estimate the effects of small changes in the topography, considering flow paths from the repository. In these simulations the change in topography is caused by accumulation of sediments at discharge areas above the shoreline.

Without any sediment accumulation, or any other change of the topography, the following development will take place. As the shoreline retreats the local groundwater system will be more and more influenced by the local topography and less influenced by the position and level of the sea. Hence, considering the area studied North of the repository, as the shoreline retreats from this area, the groundwater discharge areas for the flow paths coming from the repository will move and follow the shoreline, but as the shoreline retreats the importance of the local topography will increase. When the shoreline has moved to a certain distance from the area studied, its influence on the groundwater system at the area studied is negligible, and the local groundwater situation at the area studied has developed into a situation controlled by the local topography. For such a situation, the groundwater system at the area studied is at a local steady-state-like situation and the local recharge and discharge areas are stable and will not move, even if the shoreline continues to retreat. It should be noted that the discussion above concerns an annual average situation. The introduction of sediment accumulation at discharge areas will change the course discussed above, with sediment accumulation, the local flow system will not reach a local steady-state-like situation, but change as the shoreline retreats and as sediment accumulates.

In these simulations we have assumed that with time sediments will accumulate at the discharge areas North of the repository, as these areas rise above the sea, which will cause a build-up of the groundwater heads at these areas, which in turn will force the groundwater to discharge at other areas with lower groundwater heads, closer to the shoreline. Thus, the accumulation of sediments will change the position of the discharge areas of the flow paths coming from the repository, and slowly force these discharge areas to move with the retreating shoreline, thereby giving the flow paths coming from the repository a tendency to follow the retreating shoreline.

The retreating shoreline is caused by the shore level displacement (the sum of the land-rise and the sea level change); the change in the elevation of sea and land will cause a vertical and a horizontal movement of the shoreline. How closely the discharge areas will follow the retreating shoreline depends primarily on the velocity of the horizontal

movement of the retreating shoreline, in relation to the rate of the sediment accumulation. The steeper the topography, the slower the horizontal movement of the shore line. If the horizontal movement of the shoreline is slow, the flow paths coming from the repository may be able to follow the retreating shoreline. But if the horizontal movement of the shoreline is fast, the flow paths will not be able to follow the shoreline, because the rate of the sediment accumulation is not fast enough to create the necessary build-up of groundwater heads below the old discharge areas. Of course, in reality, also the rate of sediment accumulation depends on the topography, however, in these simulations we have assumed a constant rate within a limited domain. Hence, the way the groundwater discharge areas will move with the retreating shoreline is the result of a complicated interplay between: (*i*) the shore level displacement, (*ii*) the topography and (*iii*) the rate and extension of the sediment accumulation. This conclusion assumes everything else being equal and constant in time (e.g. groundwater recharge, hydraulic conductivity). Hence, for a constant rate of sediment accumulation at discharge areas, the undulation of the topography may cause the discharge areas to follow the shoreline for some periods and not to follow the shoreline for other periods.

The length of the flow paths will increase as the discharge area follows the retreating shoreline, and so will the break-through times of the transport of nuclides from the repository. However, in this chapter no such results will be presented in detail, a short discussion is given in Sec16.6.4. For the base case, details of flow path lengths, break-through times, etc have been calculated and is presented in Chapter 11. Also the flow through the deposition tunnels will be affected by sediment accumulation, typically the flow through the tunnels will decrease as sediment accumulate at the ground surface above the shoreline, but no such calculations will be presented in this chapter.

16.6.2 The different cases studied

We have studied five different cases (they are called Sel as in semilocal).

- Case Sel 0. This is the base case, for which no sediment accumulation has been defined; this case corresponds to the base case presented in previous chapters.
- Case Sel 7. For this case the maximum rate of sediment accumulation was set to 10 mm/year, at groundwater discharge areas, within the defined domain. The conductivity of the sediments was set to 1×10^{-9} m/s.
- Case Sel 8. For this case the maximum rate of sediment accumulation was set to 5 mm/year, at groundwater discharge areas, within the defined domain. The conductivity of the sediments was set to 1×10^{-9} m/s.
- Case Sel 5. For this case the maximum rate of sediment accumulation was set to 1 mm/year, at groundwater discharge areas, within the defined domain. The conductivity of the sediments was set to 1×10^{-9} m/s.
- Case Sel 9. For this case the maximum rate of sediment accumulation was set to 10 mm/year, at groundwater discharge areas, within the defined domain. The conductivity of the sediments was set to 1×10^{-7} m/s.

The only difference in the definitions of cases 7, 8 and 5 is the defined maximum rate of sediment accumulation; the only difference between cases 7 and 9 is the conductivity of the sediments.

16.6.3 General differences between the results of the different cases as regards the movement of the discharge areas

The positions of the discharge areas for the flow paths coming from the repository will move as the shoreline retreats, the distance between the repository and the discharge areas will increase with time. Examples of this is given in Figure 16.3 and Figure 16.4, which presents typical horizontal distances from the BTF2 tunnel to the discharge areas for the flow paths coming from this tunnel; for the different cases studied. Another example is given in Figure 16.5, which gives the positions of the discharge areas for the flow paths coming from the repository for case Sel 7, at four different times.

Comparison between cases Sel 7 and Sel 9. The results of cases 7 and 9 are very similar. This demonstrates that it is not the permeability of the sediments that is the most important parameter as regards the objectives of this study (presuming that the conductivity is not extremely large), but the rate with which the sediments are accumulated. The rate is most important, because compared to the situation without sediments, a build up of sediments will cause a build-up in groundwater heads below the sediments, which will change the flow pattern of the groundwater below the sediments. The build-up of groundwater heads will take place for all plausible values of sediment conductivity, because for such values of conductivity the sediments will be saturated with water. The movement of the discharge areas for the flow paths coming from the repository is the same for cases Sel 7 and Sel 9.

Comparison between cases Sel 7, Sel 8 and Sel 5. The difference between cases Sel 7, Sel 8 and Sel 5 are the different rates of maximum sediment accumulation. The rate of Sel 8 is half of the rate defined for Sel 7 and the rate of Sel 5 is one tenth of the rate defined for Sel 7. Therefore the build-up of groundwater heads caused by sediment accumulation is slower in Sel 8 and Sel 5 than in Sel 7. However, the maximum sediment accumulation rate is still large enough in Sel 8, to produce very much the same flow development as for case Sel 7. The movement of the discharge areas for the flow paths coming from the repository (see Figure 16.4) is very much the same for cases Sel 7 and Sel 8, however somewhat slower in Sel 8. For case Sel 5, the movement of the discharge areas for the flow paths coming from the repository is much slower than for the other two cases. Comparing case Sel 5 to the base case (with no sediment accumulation), reveals that no significant differences takes place before 4300 AD. However, the development in case Sel 5 is the same as for the other two cases (Sel 7 and Sel 8), but it takes place with a much slower pace.

16.6.4 Length of flow paths and break-through times

As the different cases predict different movements of the discharge areas, also the predicted lengths of the flow paths and the break-through times will be different for the cases studied. The following can be concluded based on the results presented in Figure 16.3 and Figure 16.4. The differences between the cases with a significant rate of sedimentation (Sel 7, 8 and 9) and the base case without any sedimentation (Sel 0), increases with time, as the shoreline retreats. At 3900 AD the differences are very small. At 5000 AD, for the cases with a significant rate of sedimentation a representative length of the flow paths is probably more than two times longer than for the base case with no sediment accumulation (Sel 0). Considering a representative break-through time, the differences between cases are probably even larger.

16.6.5 Size of drainage basins versus time

Considering the current topography of the area in the surrounding of the repository, the groundwater that has passed the deposition tunnels will discharge into two different drainage basins, see Figure 16.2 (the two basins are denoted as No.1 and No.2 in the figure). The parts of these basins that are above the shoreline will increase in size with time, as the sea withdraws (see Table 16.1).

16.6.6 The volume of run-off versus time

The precipitation and the run-off at the area studied are discussed in Sec. 4.2; based on estimates by SMHI, the run-off was set to 250 mm/year in the models. The run-off together with the size of the drainage basins above the shoreline gives an estimate of the total volume of surface and groundwater that will flow in the drainage basin above the shoreline. Such estimates of the total flows is somewhat uncertain, because the exact location of the surface water divides is uncertain, especially in the surroundings of the lakes that will be formed North of the repository (see Figure 16.2), and also due to groundwater flows that may take place across surface water divides. The estimated total flows are given in Table 16.1 through Table 16.4. The volume of run-off estimated in this way will not vary for the different cases studied, because the run-off is defined as a function of precipitation, evapotranspiration and the area of the basins that is above the shoreline, and we have assumed that these variables are the same for the different cases.

16.6.7 Sediment accumulation versus time

The calculated sediment accumulation for the different cases studied is given in Table 16.1 through Table 16.4, as average values considering the whole of the drainage basins (these average values are weighted based on cell-sizes) and also as maximum values (at a single cell).

16.6.8 Volume of groundwater discharge versus time

The volume of calculated groundwater discharge inside the drainage basins and above the shoreline varies between the different cases, because the accumulation of sediment will influence the groundwater flow. The general evolution of the groundwater discharge is the same for all cases studied, but for the cases with sediment accumulation, the discharge above the shoreline is less than with if no sedimentation takes place. This is because the accumulation of sediments will force a certain amount of the groundwater to discharge below the sea. The calculated groundwater discharge is given in Table 16.1 through Table 16.4.

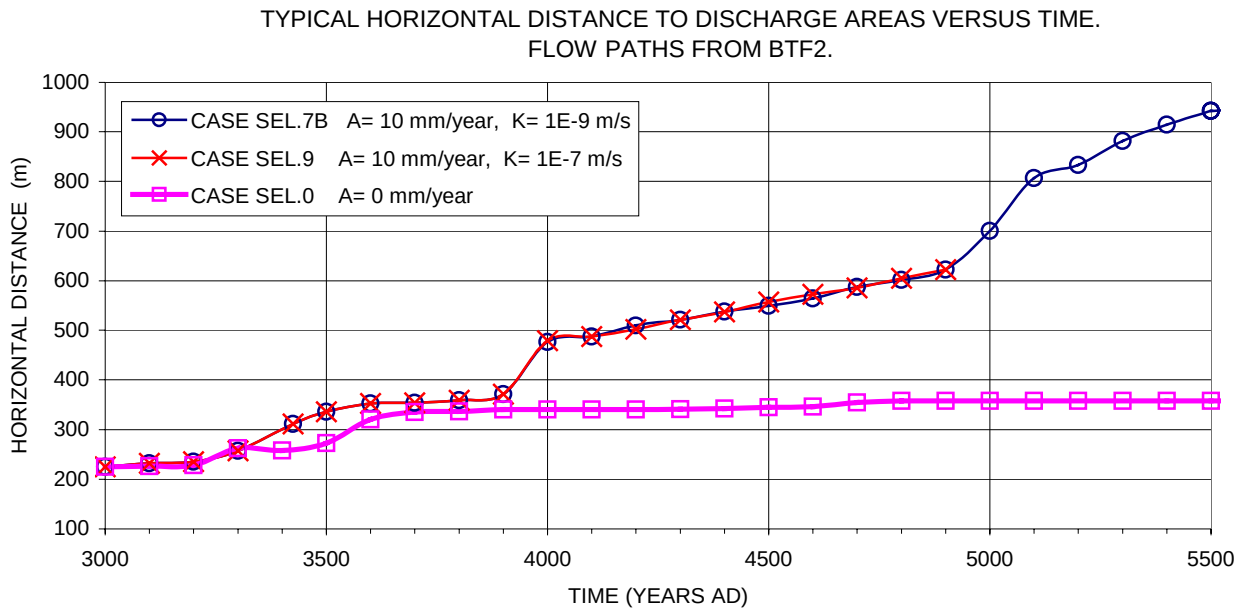

Figure 16.3 *Semilocal model. Typical horizontal distances from the BTF2 tunnel to the discharge areas for the flow paths coming from BTF2 tunnel, versus time.*

The figure gives the results for the cases with different values of conductivity as regards the accumulated sediments. In the legend of the figure, ***A*** *denotes the defined rate of maximum sediment accumulation and* ***K*** *denotes the conductivity of the sediments.*

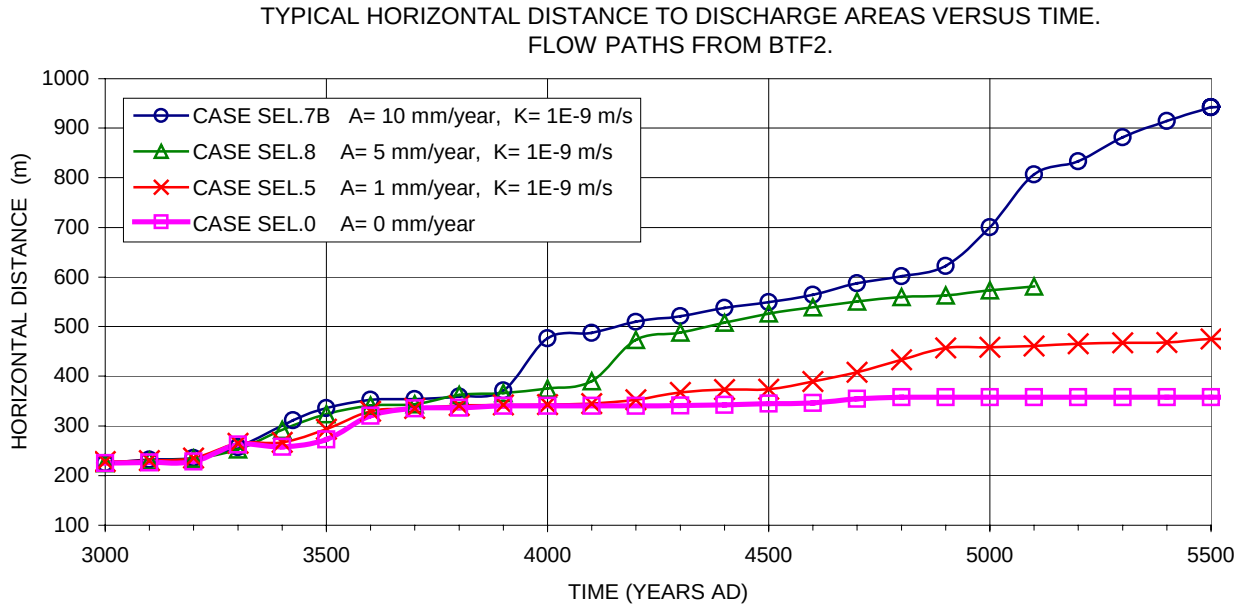

Figure 16.4 *Semilocal model. Typical horizontal distances from the BTF2 tunnel to the discharge areas for the flow paths coming from BTF2 tunnel, versus time.*

The figure gives the results for the cases with different rates of defined maximum sediment accumulation. In the legend of the figure, ***A*** *denotes the defined rate of maximum sediment accumulation and* ***K*** *denotes the conductivity of the sediments.*

Table 16.1 Semilocal model results for case Sel 0 (base case), no sediment accumulation for this case.

Case Sel 0 Time AD	Area (km2)	Run-off (m3/year)	Total sediment accumulation (1) Maximum (m)	Total sediment accumulation (1) Average (m)	Groundwater Discharge (m3/year) (2)
Drainage basin No.**1**					
3000	0.408	102000	0	0	1190
3400	0.591	147700	0	0	5280
3800	0.823	205700	0	0	13020
4000	0.958	239500	0	0	27000
4400	1.120	280000	0	0	12580
4800	1.460	365000	0	0	23190
5000	1.621	405250	0	0	28170
Drainage basin No.**2**					
3000	0.389	97170	0	0	640
3400	0.584	145900	0	0	2110
3800	0.698	174400	0	0	3060
4000	0.765	191200	0	0	3980
4400	0.915	228700	0	0	5360
4800	1.030	257600	0	0	11370
5000	1.049	262200	0	0	5500

(1) Average values considering the whole of the drainage basin area. Average values are weighted based on cell-sizes. Maximum values represent a single cell.
(2) Discharge of groundwater above the shoreline, groundwater coming from the fractured rock.

Table 16.2 Semilocal model results for case Sel 7.

Case Sel 7 Time AD	Area (km2)	Run-off (m3/year)	Total sediment accumulation (1) Maximum (m)	Total sediment accumulation (1) Average (m)	Groundwater Discharge (m3/year) (2)
Drainage basin No.**1**					
3000	0.408	102000	0.00	0.00	1190
3400	0.591	147700	3.25	0.30	5330
3800	0.823	205700	4.30	0.70	15200
4000	0.958	239500	5.70	1.10	20130
4400	1.120	280000	5.80	1.49	5890
4800	1.460	365000	5.80	1.97	12680
5000	1.621	405250	5.85	2.28	17650
Drainage basin No.**2**					
3000	0.389	97170	0.00	0.00	640
3400	0.584	145900	2.80	0.25	2060
3800	0.698	174400	4.05	0.51	1570
4000	0.765	191200	4.15	0.63	2240
4400	0.915	228700	4.95	1.10	2970
4800	1.030	257600	6.20	1.48	10590
5000	1.049	262200	6.30	1.62	2580

(1) Average values considering the whole of the drainage basin area. Average values are weighted based on cell-sizes. Maximum values represent a single cell.
(2) Discharge of groundwater above the shoreline, groundwater coming from the fractured rock.

Table 16.3 Semilocal model results for case Sel 8.

Case Sel 8 Time AD	Area (km2)	Run-off (m3/year)	Total sediment accumulation (1) Maximum (m)	Total sediment accumulation (1) Average (m)	Groundwater Discharge (m3/year) (2)
Drainage basin No.**1**					
3000	0.408	102000	0.00	0.00	1190
3400	0.591	147700	2.00	0.20	6080
3800	0.823	205700	3.08	0.47	16220
4000	0.958	239500	3.63	0.70	22700
4400	1.120	280000	4.30	1.03	7050
4800	1.460	365000	4.55	1.40	14580
5000	1.621	405250	4.78	1.62	19530
Drainage basin No.**2**					
3000	0.389	97170	0.00	0.00	640
3400	0.584	145900	1.98	0.17	2200
3800	0.698	174400	3.20	0.36	2070
4000	0.765	191200	3.65	0.45	2760
4400	0.915	228700	3.95	0.77	3390
4800	1.030	257600	4.50	1.07	10940
5000	1.049	262200	5.13	1.20	2910

(1) Average values considering the whole of the drainage basin area. Average values are weighted based on cell-sizes. Maximum values represent a single cell.
(2) Discharge of groundwater above the shoreline, groundwater coming from the fractured rock.

Table 16.4 Semilocal model results for case Sel 9.

Case Sel 9 Time AD	Area (km2)	Run-off (m3/year)	Total sediment accumulation (1) Maximum (m)	Total sediment accumulation (1) Average (m)	Groundwater Discharge (m3/year) (2)
Drainage basin No.**1**					
3000	0.408	102000	0.00	0.00	1190
3400	0.591	147700	2.95	0.26	5260
3800	0.823	205700	4.25	0.67	1450
4000	0.958	239500	5.45	1.07	19520
4400	1.120	280000	5.55	1.46	5750
4800	1.460	365000	5.55	1.94	12340
5000	1.621	405250	5.60	2.21	8260
Drainage basin No.**2**					
3000	0.389	97170	0.00	0.00	640
3400	0.584	145900	2.25	0.19	900
3800	0.698	174400	3.95	0.51	1630
4000	0.765	191200	4.10	0.62	2350
4400	0.915	228700	4.95	1.10	3030
4800	1.030	257600	6.20	1.48	10840
5000	1.049	262200	6.30	1.61	2660

(1) Average values considering the whole of the drainage basin area. Average values are weighted based on cell-sizes. Maximum values represent a single cell.
(2) Discharge of groundwater above the shoreline, groundwater coming from the fractured rock.

16.6.9 Location of discharge areas

For the base case, which is the case for which no sediment accumulation has been assigned to the model, the positions of the discharge areas are calculated by both the local model and the semilocal model. Both models give the same results. For the local model the position of the discharge areas are presented in Section 11.8.

As previously discussed, sediment accumulation may force the discharge areas to follow the retreating shoreline. An example demonstrating this is given in Figure 16.5, which presents the results of case Sel 7, the figure gives the positions of the discharge areas for the flow paths coming from the repository. For other cases, with a small or a large sediment accumulation, the positions of the discharge areas are very much the same, but the time when these positions are reached will not be the same, as this will depend on the rate of sediment accumulation. For the cases with sediment accumulation, the final positions of the discharge areas for the flow paths coming from the repository depend on the development of the lakes located North of the repository; these lakes will be established at about 4800 AD, and if these lakes remain as open bodies of water, i.e. they will not be filled up with sediments, for such a situation these lakes will be the final discharge areas for the flow paths coming from the repository. The situation at 5200 AD, given in Figure 16.5 represents such a situation.

If no sediment accumulation is assigned to the model (the base case) the flow paths coming from the SILO will discharge in local basin 2, and as the shore level retreats this discharge area will remain stable. Consequently, for the base case, the discharge from the repository will be split into two main areas, one area for the discharge coming from the BMA, BLA, and BTF tunnels and another area for the discharge coming from the SILO. However, for the cases with sediment accumulation, this situation will change as sediments accumulate in basin 2. The studied cases with a significant sediment accumulation (Sel 7, Sel 8 and Sel 9) demonstrate that until ca. 4300 AD the discharge will be split into two areas, but after that time, also the flow paths coming from the SILO will discharge at the same area as the paths coming from the BMA, BLA, and BTF tunnels (see Figure 16.5).

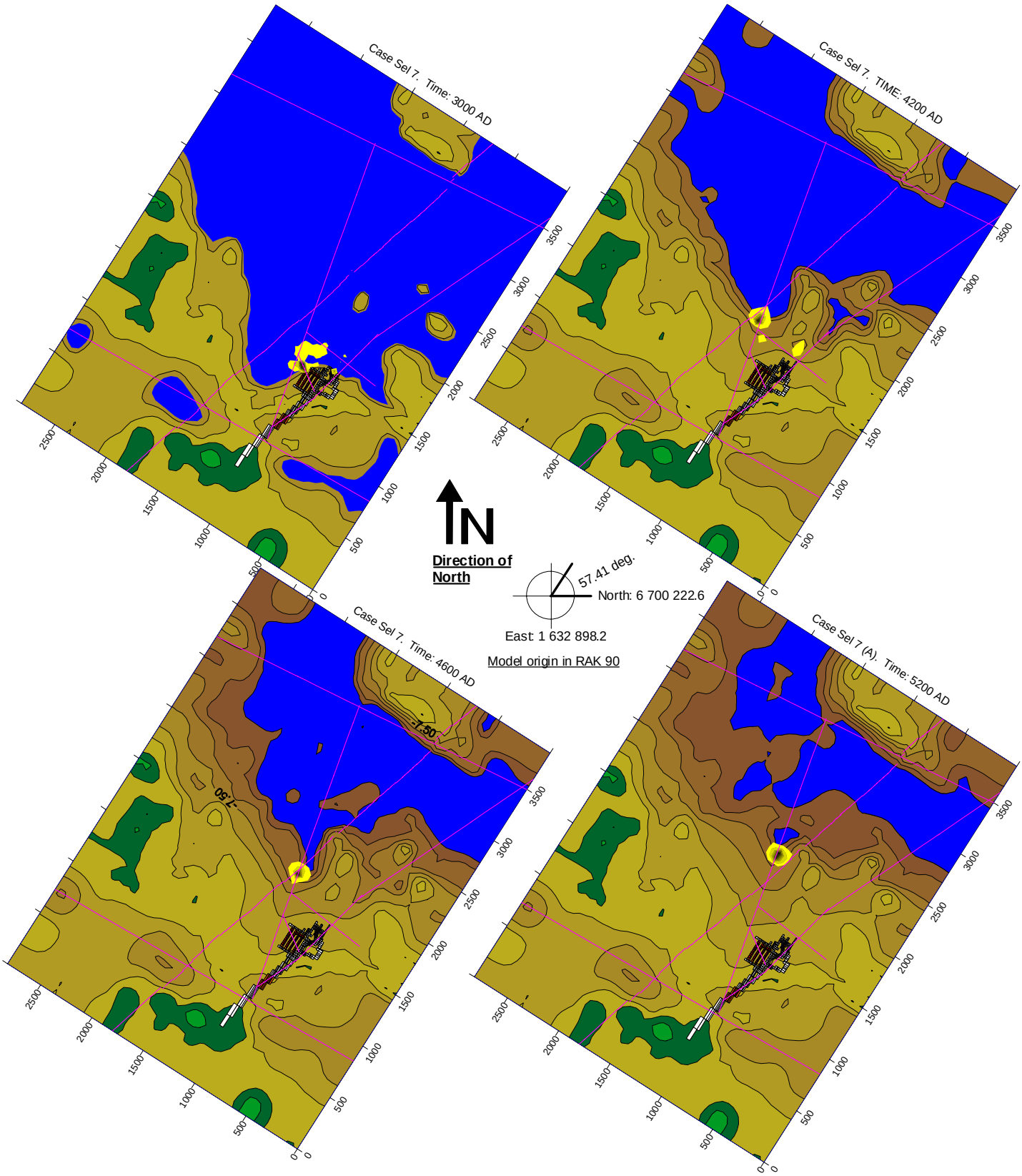

Figure 16.5 *Semilocal model case Sel 7, retreat of the shoreline.*

The retreat of the shoreline and the movement of the discharge areas for the flow paths from the repository (these areas are denoted as shades of yellow, at the figure's centre). The figures represents the following situations: upper left is 3000 AD, upper right is 4200 AD, lower left is 4600 AD and lower right is 5200 AD.

16.6.10 Type of environment at discharge areas

The type of landscape and biological environment where the discharge takes place is of importance when calculating the effects of a release of radioactive nuclides. As the locations of the discharge areas are different, with and without a significant sediment accumulation, the biological environment will not be the same for these two cases. Below we will present the location of the discharge areas for the flow paths coming from the repository, with consideration of the properties of the area where the paths will terminate. As a simple and robust approach we have divided the areas into six different types.

1. Below the sea. The discharge areas are located below the sea.

2. Shoreline. The discharge areas are located close to the shoreline, some flow paths will discharge below the sea and other paths will discharge above the sea, but all paths are close to the shoreline.

3. Land. The discharge areas are located above the shoreline on land, in connection to creeks and wetlands.

4. Small lake. The discharge areas are located at the small lake North of the repository (denoted as **SL** in Figure 16.2.).

5. Mire. The discharge areas are located at a mire, which use to be the small lake North of the repository, (denoted as **SL** in Figure 16.2). It is likely that sediment accumulations (partly due to biological activity) in this shallow lake will turn the lake into a mire, within a few hundreds of years.

6. Large lake. The discharge areas are located at the large lake North of the repository (denoted as **LL** in Figure 16.2.). No sediment accumulation has been assigned to this lake.

The different rates of sediment accumulations, defined for the different cases studied, will produce different developments of the discharge areas. For cases studied, the type of discharge area versus time is presented in a stacked bar diagram, see Figure 16.6. The different colours of the bars represent the different types of areas, as defined above.

No sediment accumulation, case Sel 0. This is the base case for which no sediment accumulation has been defined. For the period from 2000 AD and until ca. 2800 AD, the discharge areas are below the sea. From ca. 2800 AD and until ca. 3950 AD, the discharge areas will be at the shoreline. From ca. 3950 AD and onwards, the discharge will take place above the shoreline. For this case, the discharge area for the flow paths coming from the SILO will terminate within basin No.2, while the paths coming from the other deposition tunnels will terminate within basin No.1.

With sediment accumulation, cases Sel 7, 8 and 9. For the period from 2000 AD and until ca. 2800 AD, the discharge areas are below the sea. From ca. 2800 AD and until ca. 4300 AD, the discharge areas will be at the shoreline for the paths coming from the BMA, BLA, and BTF tunnels, while the paths coming from the SILO will be at the

shoreline or above the shoreline. Hence, during this period the discharge area for the flow paths from the SILO will be within basin No.2, while the flow paths from the other deposition tunnels will terminate within basin No.1. From ca. 4300 AD all flow paths will terminate at one area inside basin No.1, and there will no longer be two (or more) separate discharge areas. From ca. 4300 AD and until ca. 4600 AD, the discharge will be at the shoreline. From ca. 4600 AD and until ca. 5200 AD, the discharge will take place above the shoreline, but still close to the shore, the maximum distance to the shore being ca. 200 m. From ca. 5200 AD, the discharge will take place at a small lake (denoted as **SL** in Figure 16.2.). For the following development two alternatives have been analysed: (i) case Sel 7A assumes no sediments will accumulate in this lake and (ii) case Sel 7B assumes that sediments will accumulate in this lake, with the same rate as has been assigned for the other discharge areas within basin No.1. If no sediment accumulation will take place in this lake, this lake will be the final and stable discharge area, and this is the final condition for case Sel 7A. It is likely however, that sediment will accumulate in this shallow lake, which will turn the lake into a mire, within a few hundred years. Consequently, for case Sel 7B, from ca. 5350 AD and until ca. 5900 AD, the discharge will take place at a mire, which used to be the small lake. After ca. 5900 AD, the flow paths have moved all the way down to the large lake (denoted as **LL** in Figure 16.2.). And if no sediment accumulation will take place in this lake, this lake will be the final and stable discharge area, and this is the final condition for case Sel 7B.

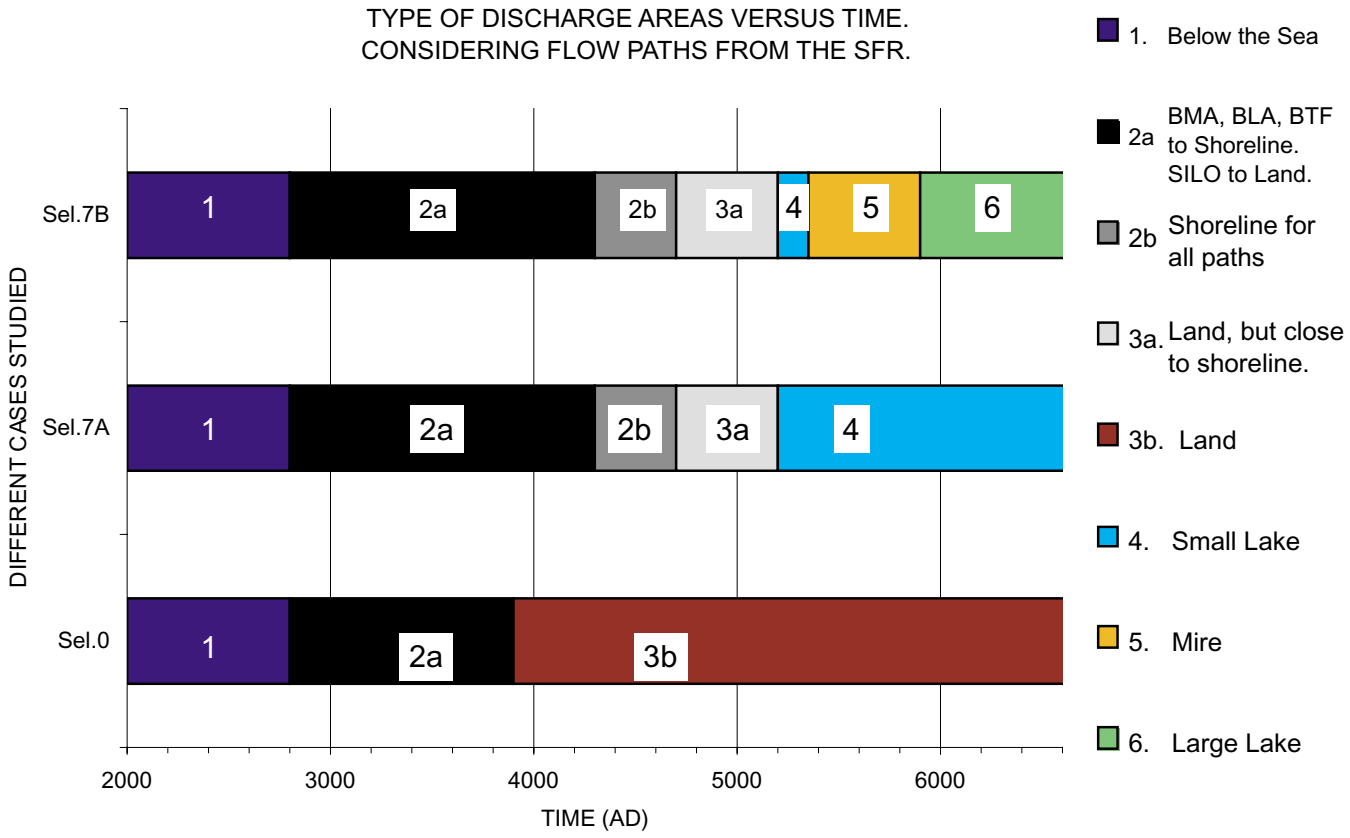

Figure 16.6 *Semilocal model, cases Sel 7 and Sel 0 (Sel 0 = base case), type of discharge area (environment) versus time; for the flow paths from the repository.*

17. Discussion of uncertainties

17.1 General

There are three sources of uncertainty influencing the results of the modelling:

(i) Uncertainties stemming from the limited knowledge of the system studied and how the system changes with time, i.e. uncertainties in the conceptual model.

(ii) Uncertainties stemming from generalisations and simplifications applied when establishing the formal models, i.e. establishing the mathematical model.

(iii) Uncertainties stemming from the numerical procedure i.e. the numerical procedure may not produce the correct solution to the mathematical problem.

Points (i) and (ii) above, will together cause prediction uncertainty due to the limited knowledge of the spatial variability of the properties of the flow system, and how the spatial variability is defined in the formal models. The heterogeneous properties of the rock mass will cause a spread in the results predicted by the model. However, the range of results is not only caused by the defined heterogeneity, but also the result of the limited knowledge of the actual heterogeneity. Or as stated by Freeze *et al.* (1990), "heterogeneity is in the geology, whereas uncertainty is in the mind of the analyst."

The formal models are based on the conceptual model. The conceptual model is primarily based on field investigations at the SFR and in its surroundings (see Chapter 2.6 and Chapters 3 through 5). The uncertainties in the results of these investigations are very difficult to estimate. The formal models are generalised and simplified interpretations of the conceptual model. The generalisations and simplifications are necessary when establishing the formal models, due to theoretical and practical limitations, but they will cause uncertainty in results predicted.

Thus, the uncertainty in the conceptual model and the uncertainty stemming from generalisations and simplifications applied in the formal models will give rise to uncertainty in the predictions. To minimise these uncertainties we have used calibration procedures and sensitivity analyses when establishing the formal models and when selecting the case used for detailed studies. The calibration procedure and sensitivity analysis will not eliminate the uncertainties, but will provide us with a plausible model, for which the uncertainties are limited considering the knowledge available for the system being studied. Sensitivity analysis will provide us with an estimate of the importance of different parameters.

Below we will present analyses of the uncertainty in some of the predictions given in previous chapters. This chapter will not present a complete uncertainty analysis, but only give a few interesting results.

17.2 Regional properties

The different cases studied by use of the regional model (Case 1 through Case 4) can be looked upon as a sensitivity analysis of the importance of the regional properties. Considering the flow through the deposition tunnels, the different cases demonstrate that the uncertainty in the regional properties gives a variation in flow equal to the flow of the base case (Case 4) plus/minus 25 percent.

17.3 Local properties – importance of fracture zones

For the purpose of studying the importance of the flow in the fracture zones, a case was established, identical to base case of the local model except that no fracture zones were included. This case was not calibrated and its purpose was solely to demonstrate the importance of the fracture zones. This case estimates the flow that will remain in the deposition tunnels when all fracture zones are replaced with rock mass.

In comparison to the previous presented predictions of the flow of the tunnels of the local model, the removal of the fracture zones will produce a smaller flow through the BMA, BLA and BTF tunnels and a larger flow through the SILO, see Figure 17.1. Most important for the horizontal tunnels is the removal of zone 6, Zone H2 is most important for the SILO.

Without the zones, the flow through the BMA and BLA, will be about 0.3 to 0.5 times the flow with the zones, dependent on the position of the sea. The flow through the BTF tunnels, will be about 0.6 to 0.4 times the flow with the zones, dependent on the position of the sea. For the BMA and BLA tunnels, the difference decreases with time, for the BTF tunnels the difference increase with time. As regards the SILO, the zones that surround it divert the flow away from the SILO. The removal of the zones will therefore lead to an increase in the flow through the SILO. Without the zones, the flow through the SILO will be about 3.0 to 1.2 times the flow with the zones, dependent on the position of the sea. The large difference occur when the regional flow is vertical (before 5000 AD), the small difference occur when the regional flow turns towards a more horizontal flow. This is mainly due to the importance of the sub-horizontal zone H2, which diverts a vertical regional flow away from the SILO, but has a smaller effect on a horizontal regional flow. This sensitivity study demonstrates that the uncertainty in the properties of the fracture zones is important for the flow through the SILO, even if a fracture zone does not intersect the SILO (especially the properties of zone H2). And as regards the flow through the BMA, BLA and BTF tunnels, the uncertainty in the properties of zone 6 is important. However, the calibration of the local model will to a great extent cover these uncertainties.

For the base case, in which the topography remains the same in the future, the removal of the fracture zones will only cause small changes in the locations of the discharge areas for the flow paths coming from the repository. Hence, the location of the discharge areas is mainly controlled by the topography and the position of the sea and not by the fracture zones. Another reason why the discharge areas are about the same is that the surface positions of the fracture zones of the models are in general located along small “valleys” that with or without the zones will form discharge areas. For times

beyond about 5000 AD, the discharge area will be extended further north without the zones than with the zones; nevertheless, the main discharge will take place at about the same place. The start points and the ends of the flow paths are approximately the same, with or without the fracture zones, hence the lengths of the flow paths will be roughly the same with and without the fracture zones. As regards the flow paths from the deposition tunnels and interaction with other tunnels, the access tunnel located Northeast of the horizontal deposition tunnels, will be very much used for transport if zone 6 is not included in the model. Without the fracture zones the breakthrough times will be very different compared to the previous presented results of the local model.

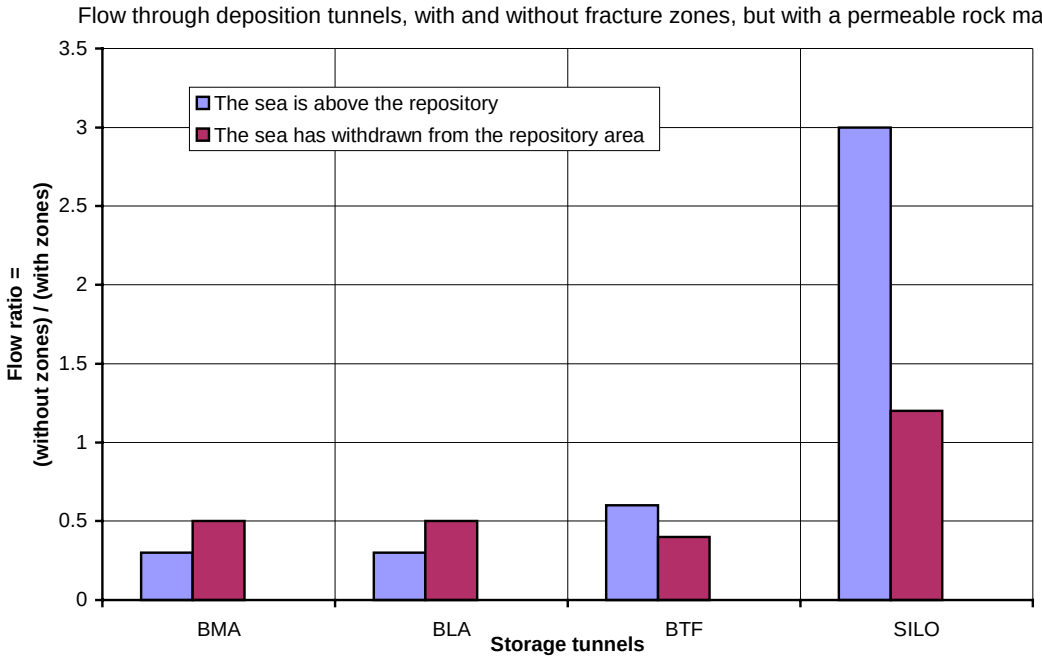

Figure 17.1 *Importance of fracture zones.*

The flow through the deposition tunnels of the local model, considering a flow medium with a permeable rock mass, but without fracture zones; in relation to a flow medium with fracture zones and a permeable rock mass. The figure gives the flow that remains in the deposition tunnels when the fracture zones are replaced with rock mass.

17.4 Local properties – importance of rock mass conductivity

For the purpose of studying the importance of the flow in the rock mass, a case was established, identical to the base case of the local model except that the rock mass was defined as having a negligible conductivity (less than 1×10^{-18} m/s). Hence, for this case all the flow will take place in the fracture zones, the case was not calibrated and its purpose was solely to demonstrate the importance of the flow in the rock mass.

In comparison to the previous presented results of the local model, the case with a negligible rock mass conductivity produced a smaller flow through all tunnels, see Figure 17.2. The largest changes are for the SILO and for the BMA tunnel.

No fracture zones intersect the SILO hence, if the rock mass has a negligible conductivity the flow through the SILO will be caused by the flow in the access tunnels only. With a negligible rock mass conductivity, the flow through the SILO will be less than 0.05 times the flow of the previous presented results of the local model. The horizontal deposition tunnels (BMA, BLA and BTF) are intersected by zone 6. As a part of the calibration of the local model (see Section 6.8, Table 6.3) a reduced conductivity (grouting/skin) was applied at the contact between the BMA tunnel and zone 6, consequently the direct hydraulic connection between Zone 6 and the BMA tunnel is not very effective. Therefore the flow through the rock mass is most important for the BMA tunnel. With a negligible rock mass conductivity, the flow through the BMA tunnel will be about 0.05 times the flow of the previous presented results of the local model; for the BLA and BTF tunnels the flow will be about 0.8 times the previous presented flow This sensitivity study demonstrates that the uncertainty in the properties of the rock mass is very important for the flow through the SILO and the BMA tunnel. However, the calibration of the local model will to a great extent cover the uncertainty in the properties of the rock mass.

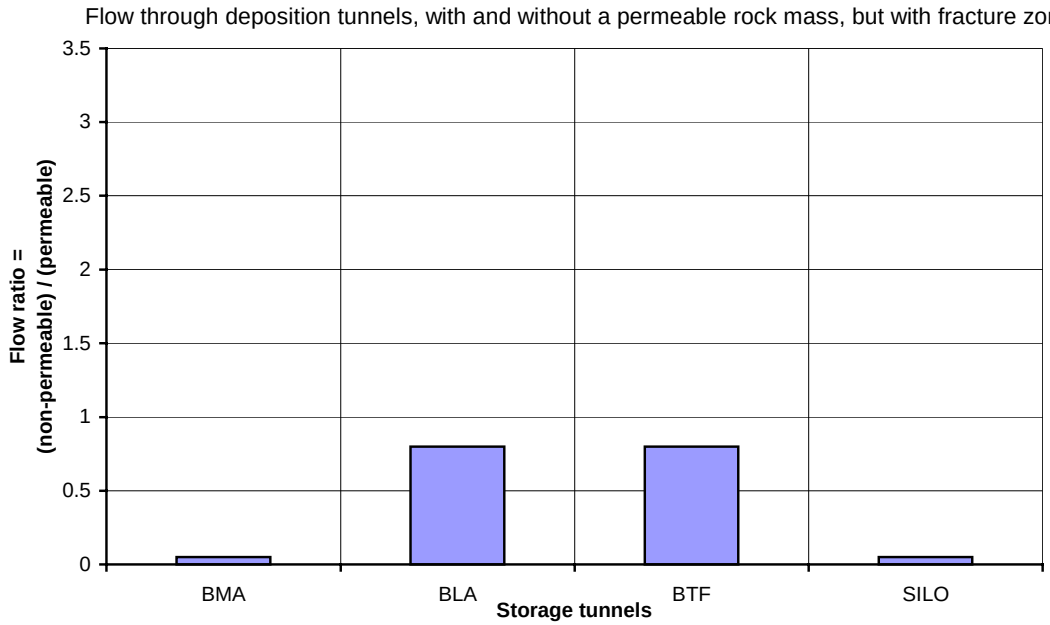

Figure 17.2 *Importance of rock mass permeability.*

The flow through the deposition tunnels of the local model, considering a flow medium with fracture zones, but with a non-permeable rock mass; in relation to a flow medium with fracture zones and permeable rock mass. The figure gives the flow that remains in the deposition tunnels when the rock mass is set as non-permeable.

For the base case, in which the topography remains the same in the future, the permeability of the rock mass is not very important as regards the positions of the discharge areas for the flow paths coming from the repository, presuming that the fracture zones remains the same. A case with a negligible rock mass conductivity will have approximately the same discharge areas as the base case (with a permeable rock mass). This is because primarily the flow paths will be inside the fracture zones. And in

general, the surface positions of the fracture zones of the models are located along small "valleys". The flow paths will primarily discharge along the fracture zones located in the small valleys, regardless of the rock mass conductivity. Hence, the topography and the position of the sea mainly control the location of the discharge areas.

With a negligible rock mass conductivity, the lengths of the flow paths will be somewhat different and so will the interaction with other tunnels, compared to the results of the base case (with a permeable rock mass). However, as the starting points and the ends of the flow paths are approximately the same for both cases, the lengths of the flow paths will be roughly the same as for both cases. Regarding flow paths from the deposition tunnels and interaction with other tunnels, a rock mass with a very small conductivity will increase the interaction between the deposition tunnels. With a negligible rock mass conductivity the breakthrough times will be very different compared to the previous presented results of the local model.

17.5 Importance of the measured excess head

Groundwater heads in the rock mass at SFR were measured before the construction of the repository, this is discusses in Section 5.6. For the bore holes that intersected the H2 sub-horizontal fractures zone, the results of the head measurements demonstrated, in relation to the mean sea water level, an excess head level in the bore holes, which was between +0.11 meters and +0.61 meters. From a theoretical point of view it is likely that there should be an excess head, but theoretical assessments gives no exact information of the size of the excess head, and the results of the actual measurements are uncertain. The uncertainty in the excess head brings an uncertainty to the predicted tunnel flow. The importance of the excess head as regards the predicted tunnel flow has been evaluated in Section 8.3. It was concluded in this analysis that the uncertainty in the measured and interpreted values of excess head, will only have a large influence on the predicted values of tunnel flow, for the period between 2000 AD and 3000 AD. For the predictions of tunnel flow, representing the situation at 2000 AD, the uncertain excess head brings an uncertainty to the flow predictions, equal to approximately plus/minus 30 percent of the flow predicted. For the predictions of tunnel flow, representing the situation after 4000 AD, the uncertain excess head brings an uncertainty to the flow predictions which is insignificant.

17.6 Importance of small changes in topography considering flow paths and discharge areas

The current topography of the seabed in the area surrounding the SFR repository may not stay the same in the future. Considering a period of several thousands of years, changes in topography may take place because of erosion and/or accumulation of sediments. In addition to the geological and biological processes that continuously shape the landscape, for the area studied there will also be the process of the shore level displacement. Such a dramatic change in conditions may in the long time perspective also lead to a change of the topography. Considering the length of the period studied, also a topographic change of a few millimetres per year may after a few thousands of

years have a significant effect on the flow system. In Section 16, we have estimated the effects of small changes in the topography, as regards flow paths from the repository. In the models, the change in topography was caused by a simulated accumulation of sediments at discharge areas. The detailed objectives of the simulations were to estimate the positions of the areas where the groundwater, coming from the deposition tunnels of the repository, will discharge into the surface water system. These areas will change with time and will be affected by changes in the topography.

Sediment accumulation will change the position of the discharge areas of the flow paths coming from the repository, and slowly force these discharge areas to move with the retreating shoreline, thereby giving the flow paths coming from the repository a tendency to follow the retreating shoreline. It was concluded, based on the results of the simulations, that even a small rate of sediment accumulation at discharge areas (a few millimetres per year) could have a significant effect.

The type of landscape and biological environment where the discharge takes place is of importance when calculating the effects of a release of radioactive nuclides. As the locations of the discharge areas are different, with and without a significant sediment accumulation, the biological environment will not be the same for these two cases. With no sediment accumulation, the final discharge area after ca. 4000 AD is above the shoreline, while for the case with a significant sediment accumulation the discharge areas will be at the shoreline for a much longer period.

As the cases studied, with and without sediment accumulation, predict different movements and locations of the discharge areas, also the predicted lengths of the flow paths and the break-through times will be different for the cases studied. The following can be concluded. The differences between the cases with a significant rate of sedimentation and the base case without any sedimentation, increases with time, as the shoreline retreats. At 3900 AD the differences are very small. At 5000 AD, for the cases with a significant rate of sedimentation, a representative length of the flow paths is probably more than two times larger than for the base case with no sediment accumulation. Considering a representative break-through time for the flow paths, the differences between cases are probably even larger.

Thus for the area studied, with its smooth topography and small differences in elevation, also small changes in the topography may have some significant influences on the movement and localisation of discharge areas, as well as on the lengths and break-through times of the flow paths from the repository. This will bring uncertainty to the results of the study. The uncertainty of the future topography is an example of uncertainty in the conceptual model, which is discussed in point (i) of Sec17.1. We are aware of the fact that the geologic and biologic process that may change the topography in the future (e.g. accumulation of sediments) are difficult to quantify, therefore such processes have not been included in the base case of this study.

17.7 Numerical uncertainty

The models use numerical methods for solving the differential equation that represents the flow of groundwater (except for the analytical estimates). The numerical methods used are iterative methods; these methods will only produce an estimate of the unknown solution to the differential equation. The mass balance is a measure of the goodness of the derived solution. The global mass balances of the local models and detailed models are good (divergences are much less than 0.05%). However, based on analyses of the mass balances of the deposition tunnels of the local model and the methods used (different meshes, time dependency, etc), the estimated numerical error in predicted flow, considering the flow through BMA, BLA and BTF tunnels, is within plus/minus 25 percent of the predictions given in the previous sections; for the SILO the error is less.

17.8 Uncertainty and sensitivity analysis - Conclusion

The predicted flows through the deposition tunnels should be regarded as estimates, and since we do not know the uncertainty in the conceptual model, it is not possible to estimate a confidence interval for these results. In the previous sections of this chapter we have discussed uncertainties due to unknown regional properties, the importance of fracture zones and the conductivity of the rock mass, as well as the uncertainty stemming from the numerical procedure. If we add these uncertainties together it is possible to estimate a probable total uncertainty for the flow through the deposition tunnels. The uncertainty is approximately plus 100 percent and minus 50 percent; it should however be noted that this is only an estimate.

For some of the objectives of this study, the unknown and not included heterogeneity of the rock mass (the heterogeneity that is not represented by the fracture zones), is of less importance -these objectives are the predictions of the flows inside the tunnels. The not included heterogeneity of the flow media outside of the tunnels is of less importance considering the flow inside of the tunnels, because the models will be calibrated to reproduce the actual measured inflow to the tunnels and because the flow inside the tunnels will be inside the tunnels (sic!) and for the tunnels the properties are known and included in the models.

For other objectives, the unknown and not included heterogeneity might be of more importance – such objectives are typically based on an analysis of simulated flow paths in the rock mass, e.g. length of flow paths from the repository to the discharge areas and breakthrough times. Considering the results of the flow path analysis, the approach used for the local domain, with a homogeneous rock mass between given fracture zones having different but homogeneous properties, will provide us with good estimates considering average representative results. However, the actual variation of results caused by the local heterogeneity of the rock mass and especially by the heterogeneity inside the fracture zones, is not included in this study. To calculate such a variation also the heterogeneity of the rock mass and the fracture zones need to be included and as such heterogeneity has not been included in this study no such variation is calculated.

For the locations of the discharge areas the uncertainties are small, presuming that the current topography will not change in the future. For all cases simulated, with or without fracture zones, or with a negligible rock mass conductivity (but with fracture zones), the discharge areas are approximately the same, presuming that the topography remains the same. Hence, the topography and the position of the shoreline are the main factors that determine the location of the discharge areas. This means that for a given topography, the uncertainty is limited when a calculated representative value of the flow path lengths is considered. However, in view of the length of the period studied, even small changes in the topography (a few millimetres per year) will lead to changes in the locations of the discharge areas and thereby in flow path lengths. The predictions of the breakthrough times are very uncertain, as they depend not only on length of flow paths and size of groundwater flows, but also on the effective porosity.

18. General conclusions

18.1 Introduction

This chapter contains general conclusions and results of this study; it is partly a summary of the results previously given in this study, but it is not a recapitulation of the detailed results. The executive summary given at the beginning of this report is based on this chapter; hence the executive summary and this chapter are very similar.

18.2 Flow through deposition tunnels

Generally, the models predict that as long as the sea covers the ground above the SFR, the regional groundwater flow as well as the flow in the deposition tunnels is small. However, due to shoreline displacement the shoreline will retreat, and in around 2800 AD the shoreline will be above the deposition tunnels. As a consequence of the retreating shoreline, the general direction of the groundwater flow at SFR will change, from vertically upward to a more horizontal flow; the size of the groundwater flow will increase as well. Hence, the predicted regional groundwater flow at SFR and the flow through the deposition tunnels will increase with time, but a steady-state-like situation will be reached in around 5000 AD.

The purpose of the detailed model is to predict the flow through the closed deposition tunnels in detail, considering the internal structures of the tunnels, such as flow barriers and encapsulations. The detailed model predicts that most of the water that flows in the deposition tunnels will flow in the highly permeable parts of the tunnels, e.g. in the top fills. These highly permeable structures will partly act as flow barriers and lead the flow away from the waste encapsulation. However, it is only in the BMA tunnel that highly permeable flow barriers surround the encapsulation on all sides; the BMA is the only tunnel at SFR that has a complete hydraulic cage protecting the waste encapsulation. The other deposition tunnel at SFR with an efficient system of flow barriers is the SILO, which is protected by low-permeable bentonite flow barriers on all sides. The tunnel with the least barriers is the BLA tunnel, which contains no waste encapsulation. The flow in the waste/encapsulation domains of the tunnels is about 1-40 percent of the flow in the top fillings, depending on deposition tunnel and time.

For the encapsulation in the SILO and the BMA tunnel, very small values of flow are predicted. For the BMA, this is the result of the efficient hydraulic cage that surrounds the BMA encapsulation. However, the hydraulic cage will only work efficiently if it surrounds the encapsulation on all sides. If, for example, the highly permeable gravel bed at the base of the BMA tunnel is replaced with a concrete floor, similar to that in the BTF and BLA tunnels, the flow through the BMA encapsulation will be about 20-40 times the flow of the present layout. In the models, the simulated hydraulic cage of the BMA tunnel is not optimised. The model predicts that conductivity contrasts, between the

encapsulation and the surrounding backfill, larger than that of the base case (an increase in conductivity contrast) will produce an inversely proportional change in encapsulation flow. For example, an increase of the contrast of one order of magnitude will produce a reduction of encapsulation flow of about one order of magnitude (presuming that Darcy´s law is applicable).

In the detailed model, total flow versus time has been calculated for the different internal structures of the deposition tunnels separately, the definition of the internal layout of the tunnels is given in Section 7. The flow of the different structures is given in Table 10.2 through Table 10.10 (pages 88 through 96), as well as in Figure 10.1 and Figure 10.2 (page 91).

A summary of the total flow as predicted by the established models and a comparison with the results of the previous modelling studies of the SFR is given in Table 10.12 (page 101). This study predicts much smaller flow values than the previous studies. This is partly a consequence of the much more detailed representation of the tunnel system in this modelling study, compared to the coarse representation used in previous studies.

18.3 Length of flow paths

The models predict that as long as the sea covers the ground above the SFR, the flow paths from the deposition tunnels are short and more or less vertical from the deposition tunnels to the ground surface. When the general direction of the groundwater flow changes, from a vertical to a more horizontal flow, the lengths of the paths increase, as the flow pattern becomes more complicated. For the five different deposition tunnels, the length of the flow paths versus time has been calculated for each tunnel separately. Considering the base case, in which the topography remains the same in the future, the results for time-independent flow paths are given in Figure 11.9 (page 113) as well as in Table 11.1 through Table 11.5 (pages 111 through 112).

18.4 Breakthrough times

Generally, the models predict that the shortest breakthrough times will be in around 3000 AD for BMA, BLA, BTF1 and BTF2, and in 4000 AD for the SILO; during this period there will be a large groundwater flow as well as short flow paths. Earlier, in 2000 AD, the flow paths are short, but the size of the groundwater flow is small too. In 4000-5000 AD and later, the flow is large but the flow paths are long as well. For the five different deposition tunnels, the breakthrough times of the flow paths versus time have been calculated for each tunnel separately. Considering the base case, in which the topography remains the same in the future, the results for time-independent flow paths are given in Figure 11.10 and Figure 11.11 (pages 119 and 120), as well as in Table 11.6 through Table 11.14 (pages 116 through 118).

18.5 Fracture zones as conductors of flow paths

By investigating which fracture zones occur along a predicted flow path, we can estimate the importance of the different zones as conductors of the flow from the deposition tunnels. The general trend is that the importance of the zones as conductors of flow paths increases with time. In 2000 AD, the only important zone is zone 6; in 7000 AD zones H2, 3, 6, 8 and 9 are all involved in the pattern of the flow paths from the deposition tunnels. The results for time-independent flow paths are given in Figure 11.12 and Figure 11.13 (pages 123 and 124). The figures present the results with a focus on the distribution of the flow in the different zones. Focusing on the distribution of flow from the deposition tunnels, the results are given in Table 11.16 through Table 11.20 (pages 121 and 122). The importance of fracture zones is also discussed in Section 17.3 (page 240)

18.6 Hydraulic interaction between deposition tunnels

By investigating which tunnels occur along a predicted flow path from a deposition tunnel, it is possible to estimate the hydraulic interaction between the different deposition tunnels. The general conclusion is that for the studied base case (with intact barriers etc.) the hydraulic interaction between the deposition tunnels is limited. To a limited extent, flow paths from BTF1 pass through BTF2, and flow paths from BTF2 and BMA pass through BLA. In the case studied, no more than 10 percent of the flow from a deposition tunnel will pass through another deposition tunnel. The largest interaction takes place between 3000 AD and 4000 AD. The results for time-independent flow paths are given in Figure 11.14 (page 126), as well as in Table 11.21 and Table 11.22 (page 125).

18.7 Origin of water in deposition tunnels

During the period from 2200 AD until 3000 AD, the retreating shoreline will pass above the SFR and as a consequence the groundwater flow pattern will change. Since the flow pattern of the groundwater changes, the origin of the groundwater that reaches the tunnels changes as well. And since the origin of the groundwater changes, the chemical composition of the groundwater that reaches the deposition tunnels also changes. The models predict that during the first 750 years of the lifetime of the SFR, the type of groundwater that will reach the deposition tunnels will change, from an old groundwater (e.g. high chloride content, low oxygen content) coming from great depth, to a young groundwater (e.g. no chloride, some oxygen) coming from recharge areas in the immediate surroundings of the SFR. The main change will take place between 2300 AD and 2750 AD. The situation with local recharge areas providing nearly all the groundwater (i.e. a young groundwater) flowing through the deposition tunnels will persist after 2750 AD as the sea (shoreline) continues to retreat. This will be the final situation as the groundwater flow system evolves into a steady-state-like condition. Details of the results discussed above are given in Section 11.7 and Figure 11.15 (page 129). The results are based on both steady and transient paths.

18.8 Location of, and dilution at, discharge areas

The models predict that the discharge areas for the flow paths from the deposition tunnels will change with time. This is because shoreline displacement will change the flow pattern of the groundwater. The most important factors for the location of the discharge areas are the topography and the position of the sea. The models predict that most discharge areas occur along low-lying parts of the topography. The greatest discharge occurs along permeable fracture zones and especially where permeable fracture zones intersect, at low-lying parts of the topography.

In 2000 AD, the main discharge area is directly above the deposition tunnels. With time the main discharge areas move north of the SFR. Considering the length of the period studied, it is possible that the topography will change somewhat due to different processes, e.g. sedimentation. In the base case of this study no such changes have been included. However, the effects of sedimentation are included in a special case discussed below (see Sec18.13). Assuming that the topography remains the same in the future (the base case), the main discharge area is approximately 500 m north of the deposition tunnels in 5000 AD (steady-state-like conditions). The discharge area for the SILO is not the same as the main discharge area, since the flow paths from the SILO and some flow paths from the BTF1 discharge in separate discharge areas east of the main discharge area. For the SILO there is also a separate discharge area above the SILO.

In the studied base case (in which the topography remains the same in the future), all discharge will be within a horizontal distance of approximately 700 m from the deposition tunnels. The results are given in Figure 11.16 and Figure 11.17 (pages 134 and 135).

The amount of flow from the deposition tunnels that discharges above and below the sea will be different at different times. In 2000 AD, all water from the repository will discharge below the sea. Assuming that the topography remains the same in the future (the base case), all discharge will take place above the sea in 4000 AD. In between, discharge will take place close to the shoreline. In discharge areas above sea level, where water from the repository will discharge, water that has not passed through the repository will also be discharged. The actual groundwater discharge will be a mixture of groundwater from the repository (polluted water) and groundwater that has not been inside the repository (non-polluted water). We have estimated the ratio between polluted water and non-polluted water in the discharge areas, and hence estimated the dilution that will take place in the discharge areas. However, as the groundwater finally discharges and forms a part of the surface water flows, there will probably be further mixing and dilution with non-polluted surface water flows; this dilution is not included in this study. The results of the estimate of groundwater dilution demonstrates that water from the deposition tunnels typically comprises only a few percent of the total discharge of groundwater in a discharge area. These results are average values for the whole areas where the flow paths from the deposition tunnels terminate. The results are given in Table 11.23 through Table 11.25 (pages 132 and 133).

18.9 Effects of wells at SFR

The purpose of the well-cases was to study the effects of a small well on the future groundwater flow field in the environs of the SFR; conclusions are given below. The conclusions below correspond to a situation when the sea has retreated from the areas surrounding the repository.

- In the case of a well located upstream of the SFR, the probability that such a well will be contaminated is very small, unless it is situated extremely close to the repository tunnels.
- In the case of a well located inside the SFR, it is likely that such a well will receive most of the contaminated water produced by the flow through the repository, but probably not all of it. A well inside the tunnel system will also give rise to a large increase of flow through the tunnels. Normally a well collects water along its entire length. However, if a well intersects a deposition tunnel and the well receives all its water from this tunnel only, which is very unlikely, all of the well discharge will be contaminated water, and no dilution will take place in the well. If the well intersects an access tunnel, dilution with non-contaminated water will take place in the well.
- If a well downstream of SFR is located along the flow routes from the repository or below a discharge point for the groundwater flow from the repository, it may intercept and collect contaminated water from the SFR, even if the well is a very weak sink. If such a well is a strong sink, it may collect a large amount of the water coming from the repository, but if the well is located outside of the flow paths and the discharge areas it will have to be a very strong sink to divert the natural flow field and receive water from SFR.

It is however unlikely that a single well will be capable of being a very strong sink and change the groundwater flow pattern on a large scale. This is due to the large potential recharge in the present climate and the small conductivity of the rock mass. In the base case in this study, we assume that the topography will remain the same in the future. For such a case it is not possible for a single well to collect all the contaminated water from the SFR, since the flow paths of the undisturbed flow from the deposition tunnels will spread out over a large domain. Dilution with uncontaminated water will also take place in a well, unless the well is located inside a deposition tunnel and collects all its water from that tunnel. A summary of the results is given in Table 12.14 and Table 12.15 (pages 159 and 160). For the positions of the wells studied see Figure 12.2 (page 143).

It is possible to define a risk area as the area within which a well might be contaminated with water coming from the SFR repository or an area within which a well may intersect the deposition tunnels. Based on a simple comparison between (i) the size of the risk area and (ii) the current well density in the SFR area, it is possible to estimate the probability that a well will be drilled within the risk areas (assuming that the well is located in a uniformly random way). The resulting probability of a well being located in a way that its discharge may become contaminated (Risk Area 1) is 0.06, which is the same as 6 percent. Consider a borehole intersecting a deposition tunnel. For a vertical bore hole (Risk Area 2) the resulting probability is 0.07 percent; and for an inclined borehole (Risk Area 3) the resulting probability is 4 percent. The values of probability given above correspond to the probability of a well being drilled within a given risk area. Hence it is not the same as the probability that a well discharge will be contaminated (Risk Area 1), or that a well will intersect a deposition tunnel

(Risk Areas 2 and 3). Risk Area 1 is an area for which there is a significant probability that a well located within this area will collect contaminated water, and Risk Areas 2 and 3 may be regarded as estimates of upper and lower bounds for the probability of a well intersecting a deposition tunnel. See Figure 12.6 (page 155) and Figure 12.7 (page 157)

18.10 Extended tunnel system at SFR

There are plans for expansion of the SFR repository to make place for the disposal of radioactive waste from the decommissioning of the nuclear power plants. The purpose of the model study of the extended tunnel system is to estimate the future flow through the closed deposition tunnels of the extended tunnel system. During the design and construction of the SFR repository, when the original layout of the extended tunnel system was determined, the occurrence and extent of the local fracture zones was not known to the same degree as it is today. The layout of the extended tunnel system was therefore not designed to avoid the local fracture zones (see Figure 13.3, page 167). Consequently, from a hydrogeological point of view, the layout of the new horizontal deposition tunnels is not optimal and can probably be improved. It follows that the groundwater flow through the new tunnels will be greater than for the old tunnels, and the flow paths from the new tunnels to the ground surface will also be shorter than for the old tunnels. The general trend of the flow in the extended tunnel system is the same as for the model representing the present tunnel system. Hence, the predicted regional groundwater flow at SFR and the flow through the deposition tunnels will increase with time, but a steady-state-like situation will be reached in around 5000–6000 AD. It should be noted that the presence of the new tunnels will influence the flow in the old tunnels. The flow in the new deposition tunnels is generally much larger than the flow in the old deposition tunnels. For the different deposition tunnels, total flow versus time has been calculated for each tunnel separately. The results are given in Table 13.2 (page 172).

18.11 Sensitivity case – failure of barriers

Tunnel flow and degradation of tunnel plugs

As a sensitivity case it is assumed that the plugs that separate the horizontal deposition tunnels from the access tunnels, as well as the plugs in the access ramp, will completely degrade over a given time period. During the period of degradation, the flow in the deposition tunnels will increase due to the evolution of the regional groundwater flow pattern, which is discussed in previous sections. In addition, the degradation of the plugs will produce a further increase of flow inside the tunnels. However, the degradation of the plugs will also change the direction of flow through the tunnels, which will also affect the size of the total flow.

- Considering the total flow through the whole of the tunnels, the detailed model predicts that complete degradation of the plugs will produce a total flow in the BMA, BLA and BTF tunnels that will be approximately two to three times the total flow in the same tunnels with intact plugs. In the SILO, the increase of flow in the top fill is much greater. The flow in the situation without the plugs will be 30 times the flow with plugs.

- Considering the total flow through the waste domains (encapsulations) in the tunnels, the detailed model predicts that the complete degradation of the plugs will produce a total flow in the tunnels as follows: In the BTF tunnel the flow wll be somewhat less than the flow with plugsas a result of the change in flow direction in the tunnels. In the BLA and BMA tunnels the flow will be two to three times greater than the flow with plugs. In the SILO the flow will be less than the flow with plugs, as long as the regional flow is vertical; in the case of horizontal regional flow (after 4000 AD) the flow will be somewhat greater than the flow with plugs.

The results are given in Table 14.1 through Table 14.5 (page 181 through 183). As the land above the access ramp rises above the sea, a water divide will be created in the access ramp. One consequence of the groundwater divide in the ramp is that the plugs in the ramp will be of little importance for the groundwater flow in the tunnels of the repository. Hence, with or without plugs in the ramp, the groundwater flow through the tunnel system will be nearly the same. Because of the groundwater divide in the access ramp, the large regional fracture zone (the Singö zone) will not have a great impact on the flow in the SFR tunnel system, even if all the plugs are completely degraded.

Flow in a failed SILO.

As a sensitivity case we have studied the flow through a failed SILO encapsulation. This case represents a situation in which the concrete barriers and the bentonite barriers of the SILO encapsulation have been breached. The groundwater flow through a failed SILO encapsulation is much greater than the flow through an intact encapsulation. But as the SILO after the collapse still has some resistance to flow; the flow through the failed SILO will not be the same as the flow through a completely empty SILO cavern. The detailed model predicts that a failed SILO, having a conductivity equal to 1×10^{-8} m/s, produces a total flow in the waste domain of the SILO between 3 and 10 times the total flow in the waste domain of an intact SILO, depending on the shoreline. The largest differences occur in 3000 AD. As far as the flow through the other deposition tunnels is concerned, the change in flow due to a failed SILO is very small if the other parts of the tunnel system are intact. Results of the detailed modelling of this sensitivity case are given in Table 14.7 (page 185) and Table 14.8 (page 186).

Flow in a failed or breached section of the BMA encapsulation.

The BMA encapsulation is divided into different sections separated by concrete walls. As a sensitivity case we have studied the flow through an assumed failed or breached section. Compared to the base case, the difference is that a limited part of the encapsulation, located close to Zone 6, is defined as having the same conductivity as the surrounding backfill (1×10^{-5} m/s). The groundwater flow through a breached section of the BMA encapsulation is greater than the flow in the same section with intact concrete walls, because a certain amount of the flow in the surrounding barriers will be redirected through the breached section. However, as the intact parts of the encapsulation are still low-permeable (separated by intact concrete walls), the size of the flow through the intact parts of the encapsulation will change very little. Hence, the change in flow will primarily take place in the breached section. The flow in the BMA will increase due to the evolution of the regional groundwater flow pattern, which is the same behaviour as in the base case discussed in previous sections. The flow in the intact

parts of the encapsulation is nearly the same as the flow in the encapsulation in the base case. Considering the flow in the breached section and the flow in the whole of the encapsulation, the detailed model predicts that the total flow in the breached section makes up about 97 percent of the total flow in the encapsulation. The model predicts that the breached section studied will cause a total flow in the encapsulation that is between 30 and 37 times the total flow in an intact encapsulation. When flow values calculated for other parts of the BMA tunnel – e.g. top fill, side fill etc. – are compared with the flow values of the base case, the change in flow values are small, because the properties of the surrounding materials are not changed. The effect of the breached section is mainly to redirect some of the flow that occurs in the backfill and hence provide a short cut through the encapsulation. When the predicted flow in other deposition tunnels is considered, the values predicted for this case are the same as the values predicted for the base case. The results of the detailed modelling of this sensitivity case are given in Table 14.10 (page 189).

Flow of a failed or breached section of the BTF1 tunnel.

As a sensitivity case we have studied the flow through a failed or breached section of the BTF1 tunnel. The flow through such a section is larger than the flow in the same section when intact, because a certain amount of the flow in the surrounding area will be redirected through the breached section. Compared with the base case of the detailed model, the difference is that a limited part of the BTF1 tunnel, located close to Zone 6, is assumed to be breached and is defined as having the same conductivity as the highly permeable top fill ($1x10^{-5}$ m/s). For this case we have studied two different alternatives, as regards to what extent the different barriers of the BTF1 tunnel are breached. In Alternative 1, only the waste domain (encapsulation) of the section studied is failed or breached; the floor and the side fills (concrete) are intact. In Alternative 2, all parts of the tunnel at the section studied are breached or failed, including the floor and the side fills. The results of the simulations demonstrate that the flow in BTF1 will increase due to the evolution of the regional groundwater flow pattern, which is the same behaviour as for the base case, discussed in previous sections.

- Considering Alternative 1, the total flow in the encapsulation increases with time and reaches a steady value in about 6000 AD. The total flow in the breached part makes up about 60 percent of the total flow of the encapsulation. In comparison with a completely intact encapsulation (the base case), the flow of the breached encapsulation is about 1.6 times larger (in 3000 AD the flow is 2.3 times larger).
- Considering Alternative 2, the total flow in the encapsulation increases with time and reaches a steady value in about 6000 AD. The total flow of the breached parts makes up about 90 percent of the total flow of the encapsulation. In comparison to a completely intact encapsulation (the base case), the flow of the breached encapsulation is about 5 times larger (in 3000 AD the flow is 6.3 times larger).

Considering the predicted flow in other deposition tunnels (SILO, BMA, BLA, BTF2), the values predicted for this sensitivity case are very close to the values predicted for the base case. The results of the detailed modelling of this sensitivity case are given in Table 14.12 and Table 14.13 (page 192)

18.12 Groundwater saturation of SFR

At present the tunnels of the SFR are kept dry; however, some time after the repository is abandoned, the tunnels will be filled with groundwater. One purpose of this study is to simulate the transition period during which the tunnels are being filled with water (the saturation period). We have estimated the length of the saturation period based on different analytical and numerical methods. The detailed model was defined with a porosity that varied for the different structures inside the tunnels (see Table 15.4, page 200). A transient numerical modelling of the saturation period was carried out by use of the complete chain of models (regional–local–detailed).

- The last part of the deposition tunnels to become saturated is the void inside the SILO encapsulation; it may take 25 years to saturate this structure.
- The time necessary for the complete saturation of the BMA, BLA and BTF tunnels is a few years.

The detailed results are given in the following tables and figures: Table 15.6 (page 203) through Table 15.10 (page 204), as well as Figure 15.2 (page 205) through Figure 15.6 (page 207).

Analytical solutions of the transient course of saturation have also been derived. The good agreement between (i) the inflow as predicted by the numerical GEOAN model and (ii) the inflow as predicted by the analytical solutions demonstrates that no fundamental error has been included in the numerical model.

18.13 Discharge areas, flow paths from the repository and sediment accumulation – effects of small changes in the topography

The flow paths of the groundwater that has passed the repository will terminate at the ground surface, in discharge areas located north of the repository. The topography and the sea level are the main factors determining the locations of these discharge areas. In the simulations in Chapter 16 (which starts at page 217) we have assumed that with time sediments of both of biological and geological origin will accumulate in the discharge areas north of the repository, as these areas rise above the sea, which will change the topography and cause a build-up of the groundwater heads in these areas, which in turn will force the groundwater to discharge in other areas with lower groundwater heads, closer to the shoreline. Thus, the accumulation of sediments will change the location of the discharge areas for the flow paths coming from the repository, and slowly force these discharge areas to move with the retreating shoreline. As a result, the flow paths coming from the repository have a tendency to follow the retreating shoreline.

The simulations of Chapter 16 demonstrate that that it is not the permeability of the sediments that is the most important parameter with regard to the movement of the discharge areas (assuming that the permeability is not extremely large), but the rate at which the sediments accumulate. The calculated total sediment accumulation for the different cases studied is dependent on the maximum rate of sediment accumulation, but

it is not directly equal to this rate, since in the model sediment accumulation will only take place in groundwater discharge areas, and only as long as the area remains a discharge area.

- The type of landscape and biological environment where the discharge takes place are of importance when calculating the effects of a release of radioactive nuclides. The flow paths from the repository will have a tendency to follow the retreating shoreline (especially if sediments accumulate in discharge areas). The different rates of sediment accumulation defined for the different cases studied resulted in different movements of the discharge areas. For the different cases of sediment accumulation studied , we have analysed which type of discharge area the flow paths from the repository will discharge into. As a rule, there are two different situations : the discharge will either be directly into large open bodies of surface water (discharge below the sea, at the shoreline or in a lake), or the discharge will be above the shoreline and not into a lake, but into creeks and wetlands etc.
- For the case with no sediment accumulation, the discharge will be into open water or at the shoreline between around 2000 AD and 3900 AD. From then on the discharge will take place above the shoreline, see Figure 16.6 (page 237)
- For the cases studied with significant sediment accumulation in discharge areas, the discharge will be into open water or at the shoreline between around 2000 AD and 4600 AD. Between around 4600 AD and 5200 AD, the discharge will be above the shoreline, but still close to the shore, the maximum distance to the shore being about 200 m. After around 5200 AD, the discharge will be into a small lake; from then on the situation will depend on the rate of sediment accumulation in this small lake. If sediment accumulation occurs in this small lake, the lake will probably turn into a mire (bog) within a few hundred years, which may force the flow paths from the repository to move to the larger lake located north of the small lake, see Figure 16.6 (page 237).

We are aware of the fact that the geological and biological process that was studied in Chapter 16 (accumulation of sediments) is difficult to quantify and will add some uncertainty to the analysis; such processes have therefore not been included in the other analyses of this study.

18.14 Uncertainties and sensitivity analysis

The uncertainty in the conceptual model and the uncertainty stemming from generalisations and simplifications applied in the formal models will give rise to uncertainty in the predictions. To minimise the uncertainties we have used calibration procedures and sensitivity analyses when establishing the formal models and when selecting the case used for detailed studies. The calibration procedure and sensitivity analysis will not eliminate the uncertainties, but will provide us with a plausible model for which the uncertainties are limited considering the knowledge available for the system being studied. Sensitivity analysis will provide us with an estimate of the importance of different parameters.

The predicted flows through the deposition tunnels should be regarded as estimates, and since we do not know the uncertainty in the conceptual model, it is not possible to estimate a confidence interval for these results. In Chapter 17 (page 239) we have

discussed uncertainties due to unknown regional properties, the importance of fracture zones and the conductivity of the rock mass, as well as the uncertainty stemming from the numerical procedure. If we add these uncertainties together it is possible to estimate a probable total uncertainty for the flow through the deposition tunnels. The uncertainty is approximately plus 100 percent and minus 50 percent; it should however be noted that this is only an estimate.

The uncertainties in the locations of the discharge areas are small, assuming that the current topography does not change in the future. The discharge areas are approximately the same for all the cases simulated, with or without fracture zones, or with a negligible rock mass conductivity (but with fracture zones), assuming the topography remains the same. Hence, the topography and the position of the shoreline are the main factors that determine the location of the discharge areas. This means that for a given topography, the uncertainty is limited when a calculated representative value of the flow path lengths is considered. However, in view of the length of the period studied, even small changes in the topography (a few millimetres per year) will lead to changes in the locations of the discharge areas and thereby in flow path lengths. The predictions of breakthrough times are very uncertain, as they depend not only on the length of flow paths and size of groundwater flows, but also on the effective porosity.

19. References

Ahokas H. and Herva S. (1993) “Summary of Hydrological Observations in Olkiluoto Area, Eurajoki.”, Work report PATU-92-35, TVO, Helsinki. (In Finnish).

Andersson J., Riggare P., Skagius K. (editors) (1998). “Project SAFE, Update of the SFR-1 safety assessment, Phase 1.” , SKB R-98-43, Swedish Nuclear Fuel and Waste Management Co., Stockholm.

Axelsson C-L. (1997) “Data for calibration and validation of numerical models at SFR Nuclear Waste Repository, Forsmark, Sweden”, SKB R-98-48, Swedish Nuclear Fuel and Waste Management Co., Stockholm.

Axelsson C.-L. and Hansen L.(1997) “Update of structural models at SFR nuclear waste repository, Forsmark, Sweden”, SKB R-98-05, Swedish Nuclear Fuel and Waste Management Co., Stockholm.

Bear J. and Verruit A., (1987) “Modeling groundwater flow and pollution”. D. Reidel publishing company, P.O.Box 17, 3300 AA Dorfrecht, Holland. ISBN 1-55608-014-X.

Bear, J., and Bachmat, Y., (1990) “Introduction to Modeling of Transport Phenomena in Porous Media.” Kluwer Academic Publishers, Dordrecht, The Netherlands. ISBN 0-7923-0557-4.

Bergman S., Isaksson H., Johansson R., Lindén A., Persson C. and Stephens M. (1996) “Förstudie Östhammar, jordarter, bergarter och deformationszoner”, Sveriges Geologiska Undersökning and GeoVista AB. (In Swedish).

Brandt M., Jutman T. and Alexanderson H. (1994) “Sveriges vattenbalans, Årsmedelvärden 1961-1990 av nederbörd, avdunstning och avrinning”, SMHI Hydrologi 49, Sveriges Meterologiska och Hydrologiska Institut, Norrköping. (In Swedish).

Brydsten (1999) “Change in coastal sedimentation conditions due too positive shore displacement in Öregrundsgrepen.”, SKB TR-99-37, Swedish Nuclear Fuel and Waste Management Co., Stockholm.

Carlsson L. and Gustafsson G. (1984) “Provpumpning som geohydrologisk undersökningsmetod”, Rapport R41: 1984, Byggforskningsrådet. (In Swedish).

Carlsson L., Winberg A. and Arnefors J. (1986) “Hydraulic modelling of the final repository for reactor waste (SFR). “Compilation and conceptualization of available geological and hydrological data” SKB PR SFR 86-03, Swedish Nuclear Fuel and Waste Management Co., Stockholm.

Carlsson L., Grundfelt, B., and Winberg, A., (1987) “Hydraulic modelling of the final repository for reactor waste (SFR). Evaluation of the groundwater flow situation at SFR“, SKB Progress Report SFR 86-07, May 1987. Swedish Nuclear Fuel and Waste Management Co., Stockholm.

Carslaw H.S., and Jaeger J.C. (1959) “Conduction of heat in solids”, (second edition), Oxford University Press, Walton Street, Oxford, OX2 6DP, IDBN 0 19 853303 9.

Christiansson R. (1986).”Geologisk beskrivning av zoner kring slutförvaret (Geological description of zones around the final repository)”, SKB Working Report SFR 86-02, Swedish Nuclear Fuel and Waste Management Co., Stockholm (In Swedish).

Darcy H., (1856) “Les Fontaines Publiques de la Ville de Dijon”, Dalmont, Paris, France.

Follin, S., (1992) “Numerical Calculations on Heterogeneity of Groundwater Flow” Department of Land and Water Resources, Royal Institute of Technology S-10044 Stockholm Sweden, (Dissertation), ISSN 0348-4955, ISBN 91-7170-077-3.

Freeze, R. A., Massmann, J., Smith, L., Sperling, T. and James, B., (1990) “Hydrogeological decision analysis, 1. A framework.” Ground Water, 28, 738-766.

Gustafson, G., R. Stanfors, and P. Wikberg, 1989: “Swedish hard rock laboratory evaluation of 1988 year preinvestigations and description of the target area, the island of Äspö”. SKB Technical Report 89-16, June 1989. Swedish Nuclear Fuel and Waste Management Co., Stockholm.

Hagconsult, (1982) “Geologiska undersökningar och utvärderingar för lokalisering av SFR till Forsmark” SFR 81-13 Del 1. Hagconsult AB, Stockholm Sweden (In Swedish).

Holmén J.G. (1992) “A three-dimensional finite difference model for calculation of flow in the saturated zone”, Department of quaternary geology, Uppsala University, Uppsala, Sweden, ISBN 91-7376-119-2, ISSN 0348-2979.

Holmén J.G. (1997).”On the flow of groundwater in closed tunnels. Generic hydrogeological modelling of nuclear waste repository, SFL 3-5”, Technical Report No. 97-10, Swedish Nuclear Fuel and Waste Management Co., Stockholm.

Kautsky U. (1998) “Variationer i biosfären från senaste istiden till nästa istid med speciell referens till Äspö”, PM 1998-02-10, Swedish Nuclear Fuel and Waste Management Co., Stockholm.

Marine Ecosystem Modeling group, (1996), http://data.ecology.su.se/baltic96/ February 20, 1998, Department of Systems Ecology Stockholm University, Sweden.

Neuman, S., P., (1987): “Stochastic continuum representation of fractured rock permeability as an alternative REV and fracture network concepts”, In: Farmer, I.W. *et al* (eds.) Proc. 28th U.S. Symp. Rock. Mech., 533-561, Balkema, Rotterdam.

Neuman, S., P., (1988): "A proposed conceptual framework and methodology for investigating flow and transport in Swedish crystalline rocks" SKB AR 88-37. Swedish Nuclear Fuel and Waste Management Co., Stockholm.

Nordic glossary of hydrology, Johanson I. (editor) 1984 “Nordic glossary of hydrology”, ISBN 91-22-00692-3, Almqvist & Wiksell, Uppsala.

Press W., Teukolsky S., Vetterling W. and Flannery B. (1992), “Numerical recipes in fortran. The art of scientific computing” (second edition), Cambridge University Press, ISBN 0-521-43064-X.

Påsse T. (1996) “A mathematical model of the shore level displacement in Fennoscandia”, SKB Technical Report TR 96-24, Swedish Nuclear Fuel and Waste Management Co., Stockholm.

Pollock, D.W. (1989) “Documentation of computer program to compute and display path lines using results from the U.S. Geological survey modular three-dimensional finite difference groundwater flow model”, (Modpath manual). US Geological survey, 411 National Centre Reston, VA 22092, USA.

SGU (2000) Swedish Geological Survey. Water Well Record Section (well archive). Uppsala, Sweden.

SKB (1993) “Slutförvar för radioaktivt driftavfall – SFR2. Slutlig säkerhetsrapport. Reviderad utgåva – Maj 1993”, (SKB Final repository for radioactive waste – SFR1. Final safety report. Revised edition – May 1993) SKB, Swedish Nuclear Fuel and Waste Management Co., Stockholm.

SKB (1999) “Deep repository for spent nuclear fuel. SR 97 - Post-closure safety”, SKB Technical Report TR-99-06, Swedish Nuclear Fuel and Waste Management Co., Stockholm.

SKI (1992) “Utvärdering av SKB:s fördjupade säkerhetsanalys av SFR-1”, SKI rapport 92:16, (in Swedish) Swedish Nuclear Power Inspectorate, Stockholm, Sweden.

SMHI, (1999): Data provided by SMHI through the internet: http://www.smhi.se/sgn0102/n0205/index.htm June 2, 1999, SMHI - the Swedish Meteorological and Hydrological Institute, Norrköping.

Stigsson M., Follin S. and Andersson J. (1998.) “On the simulation of variable density flow at SFR, Sweden” SKB R-98-08, Swedish Nuclear Fuel and Waste Management Co., Stockholm.

Studsvik Eco & Safety AB (2000), Information provided by Sara Karlsson, October 2000, Studsvik Eco & Safety AB, S-611 82 Nyköping, Sweden.

Thiem, G., (1906): “Hydrologische Methoden.” J. M. Gebhardt, Leipzig, Germany.

Walker, D., I. Rhen and I. Gurban (1997) “Summary of the hydrogeological conditions at Aberg, Beberg and Ceberg.” SKB Technical Report-97-23, Swedish Nuclear Fuel and Waste Management Co., Stockholm.

Westman P. (1997). “Saliniteten i Östersjön sedan istiden”, Kvartärgeologiska institutionen Stockholms Universitet. (In Swedish).

Wikberg, P. (ed), G. Gustafson, I. Rhén, and R. Stanfors, (1991) “Äspö Hard Rock Laboratory. Evaluation and conceptual modelling based on the pre-investigations 1986-1990”. SKB Technical Report 91-22, June 1991. Swedish Nuclear Fuel and Waste Management Co., Stockholm.

Appendix A

Different co-ordinate systems and meshes of numerical models

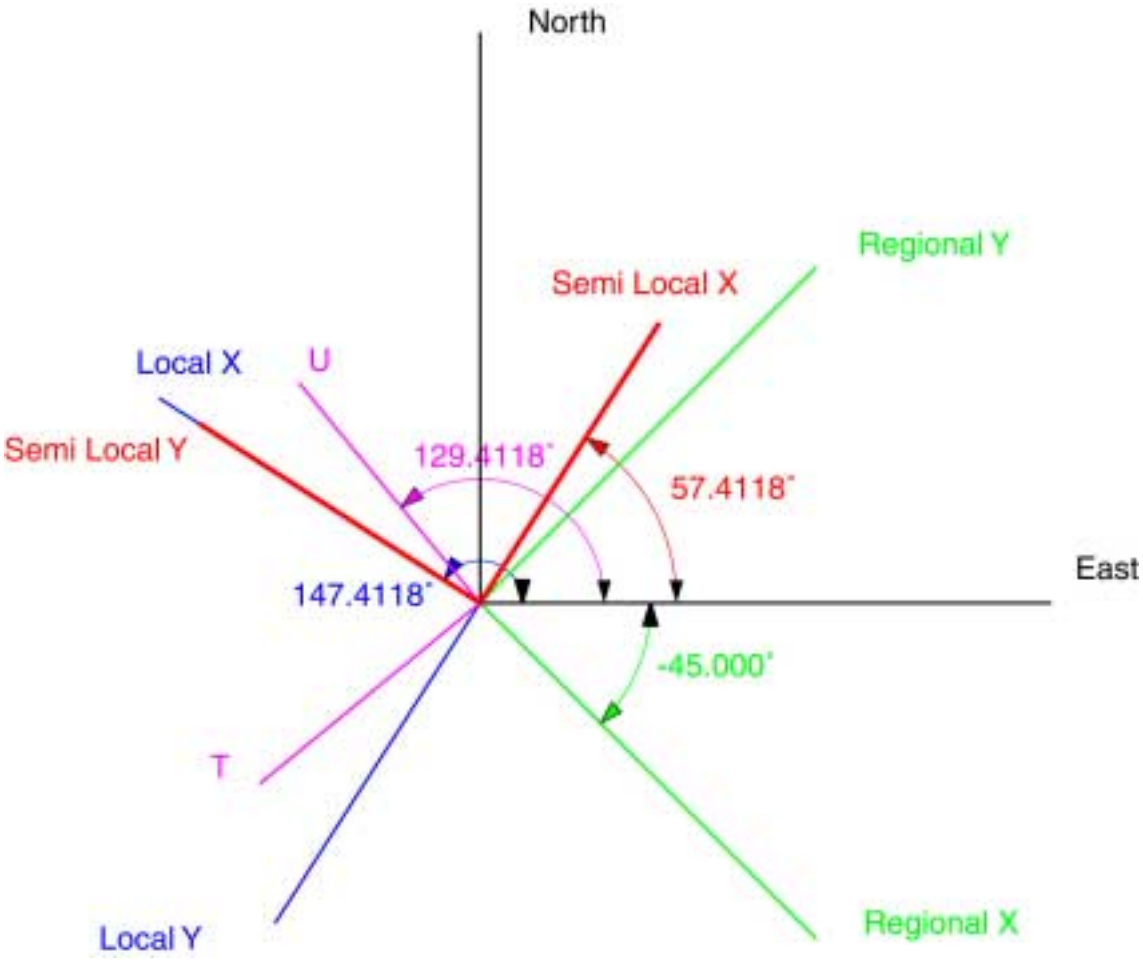

Figure A.1 *Vectors denoting the different directions of the co-ordinate systems of the different numerical models*

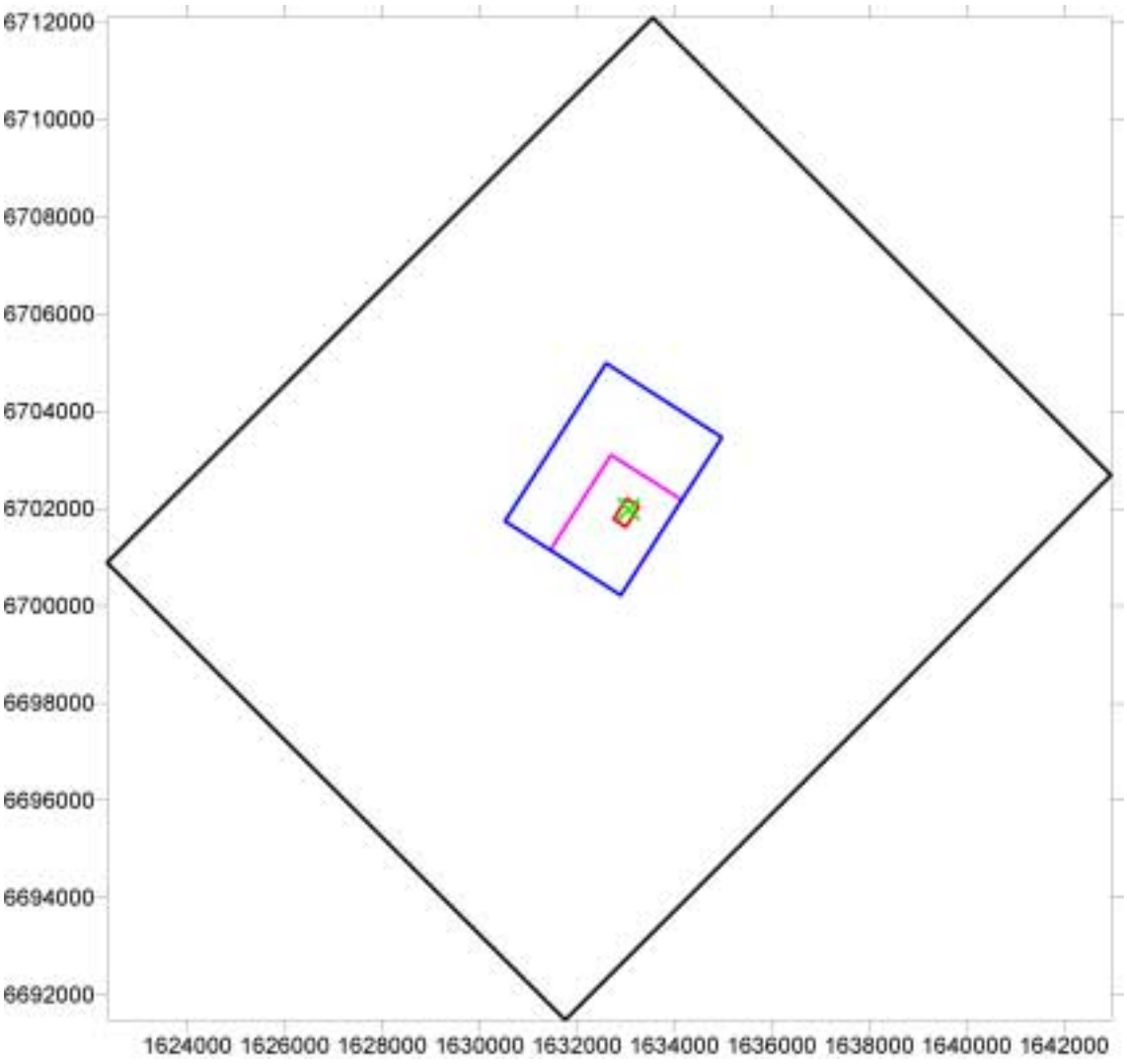

Figure A.2 *The extension of the different models. The smallest model is the detailed model, next in size is the local model, the semilocal model is larger than the local model and the largest model is the regional model.*

Transformation – Translation between models and RAK 90

Regional model:

Regionl co-ordinate system defined in RAK 90 system (rikets system).

East	North	Up	Angle
(16)22356.0	(6)700877.0	0	-45.0

Regional co-ordinate system defined in local model system.

X	Y	Up	Angle
9240.3	7442.3	0	167.5882 (-192.4118)

Regionl co-ordinate system defined in Semi local.

X	Y	Up	Angle
-5118.2	-9240.3	0	-102.4118

Local model:

Local co-ordinate system defined in RAK 90 system (rikets system).

East	North	Up	Angle
(16)34149.9	(6)702180.8	0	147.4118

Local co-ordinate system defined in regional model system.

X	Y	Up	Angle
7424.7	9254.4	0	-167.5882 (192.4118)

Local co-ordinate system defined in Semi local system.

X	Y	Up	Angle
2324.0	0	0	90.0

Local co-ordinate system defined in detailed system.

X	Y	Up	Angle
-585.0	-665.0	0	0

Detailed model:

Detailed co-ordinate system defined in RAK 90 system (rikets system).

East	North	Up	Angle
(16)33274.6	(6)702046.6	0	147.4118

Detailed co-ordinate system defined in regional model system.

X	Y	Up	Angle
6900.7	8540.6	0	-167.5882 (192.4118)

Detailed co-ordinate system defined in local system.

X	Y	Up	Angle
585.0	665.0	0	0

Detailed co-ordinate system defined in semi local system.

X	Y	Up	Angle
1659.0	585.0	0	90.0

Semi local model:

Semi local co-ordinate system defined in RAK 90 system (rikets system).

East	North	Up	Angle
(16)32898.2	(6)700222.6	0	57.4118

Semi local co-ordinate system defined in regional model system.

X	Y	Up	Angle
7924.3	6984.7	0	102.4118

Semi local co-ordinate system defined in local model system.

X	Y	Up	Angle
0	2324.0	0	-90.0

Semi local co-ordinate system defined in detailed system.

X	Y	Up	Angle
-585.0	1659.0	0	-90.0

Transformation between RT90 2.5^{g} V and local T-U co-ordinate system at the SFR

The general transformation between 2 orthogonal co-ordinate systems in the same plane is described by:

$$\begin{bmatrix} x' \\ y' \end{bmatrix} = \begin{bmatrix} \cos\alpha & \sin\alpha \\ -\sin\alpha & \cos\alpha \end{bmatrix} \begin{bmatrix} X - C1_X \\ Y - C1_Y \end{bmatrix} + \begin{bmatrix} C2_X \\ C2_Y \end{bmatrix}$$

$$\begin{bmatrix} X \\ Y \end{bmatrix} = \begin{bmatrix} \cos\alpha & -\sin\alpha \\ \sin\alpha & \cos\alpha \end{bmatrix} \begin{bmatrix} x' - C2_X \\ y' - C2_Y \end{bmatrix} + \begin{bmatrix} C1_X \\ C1_Y \end{bmatrix}$$

where:	x',y'	=	Co-ordinates in new system
	X,Y	=	Co-ordinates in old system
	α	=	Rotation angle between the systems (CCW)
	$C1_X$, $C1_Y$	=	Translation constants
	$C2_X$, $C2_Y$	=	Translation constants

The local system (T-U) at the SFR and the new RT90 are almost in the same plane, but there is a slight difference since they are calculated from different geoids. If it is assumed that they are in the same plane the error will be less than 3‰. The translation between the two co-ordinate systems can then be described by the equations:

$T = \cos(230.5882°)\cdot(X_{North}-6700000)+\sin(230.5882°)\cdot(Y_{East}-1630000)+6704.312$
$U = -\sin(230.5882°)\cdot(X_{North}-6700000)+\cos(230.5882°)\cdot(Y_{East}-1630000)+2087.350$

$X_{North} = \cos(230.5882°)\cdot(T-6704.312)-\sin(230.5882°)\cdot(U-2087.350)+6700000$
$Y_{East} = \sin(230.5882°)\cdot(T-6704.312)+\cos(230.5882°)\cdot(U-2087.350)+1630000$

Observe that both of the systems are left-handed, and that the angels then are positive in the CW direction.

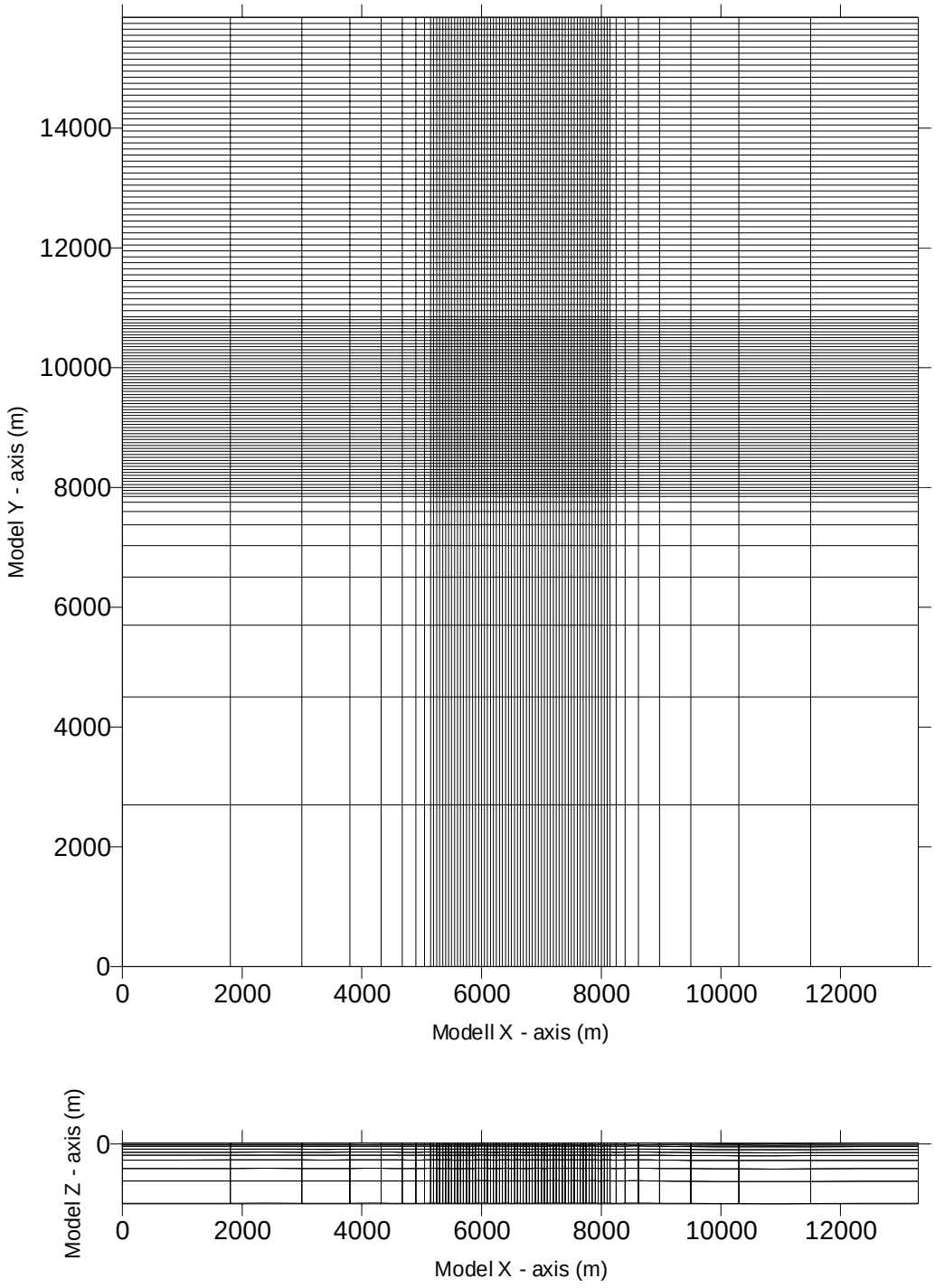

Figure A.3 *The finite difference mesh of the regional model. The mesh has 9 layers and contains 81 369 cells. The model represents a horizontal area of 13300 m x 15 850 m (210.8 km^2) and it has a depth of 1000 m. The X-axis of the regional model is pointing towards Southeast.*

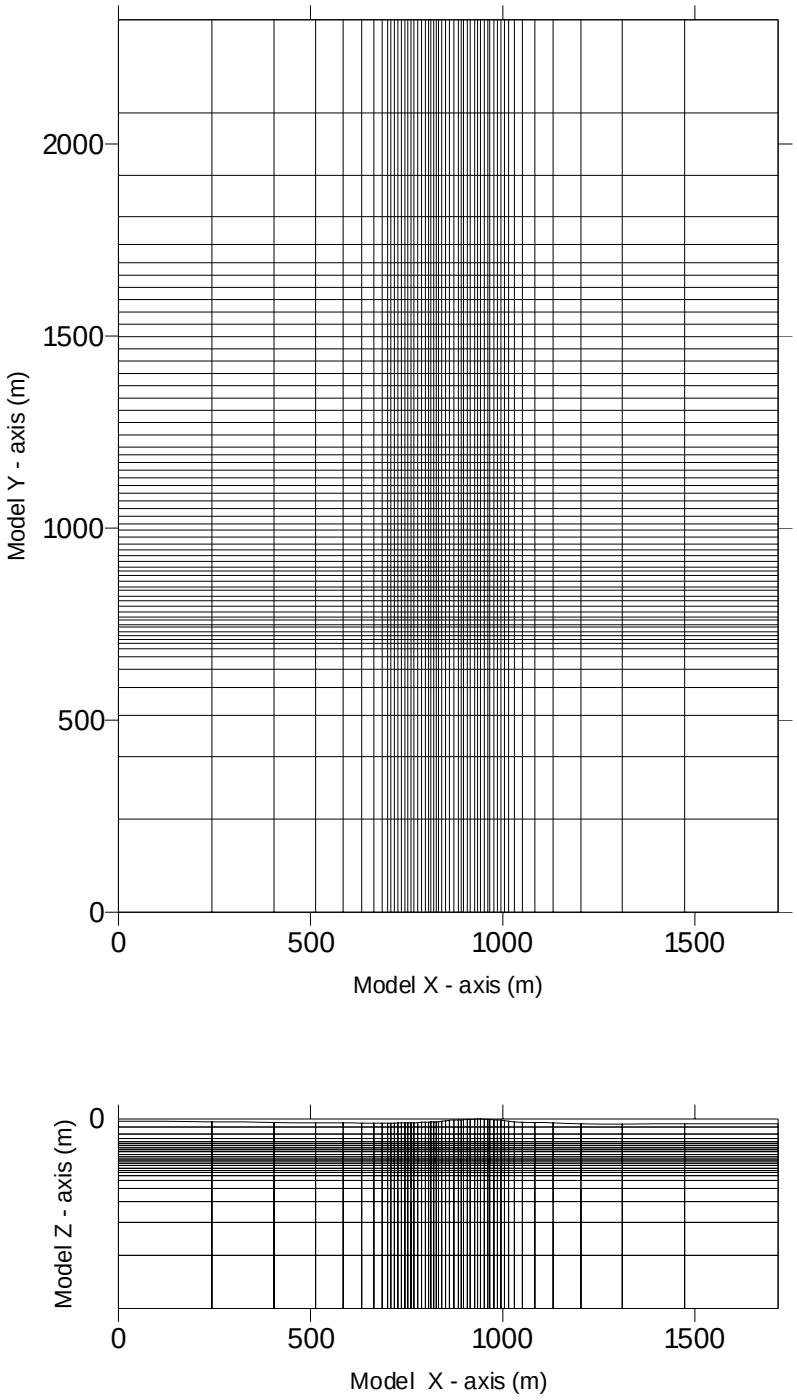

Figure A.4 *The finite difference mesh of the local model. The mesh has 25 layers and contains 80 600 cells. The mesh is optimised for the lay-out of the storage caverns. The model represents a horizontal area of 1716 m x 2324 m (4.0 km^2) and it has a depth of 490 m. The X-axis of the local model is pointing towards Northwest.*

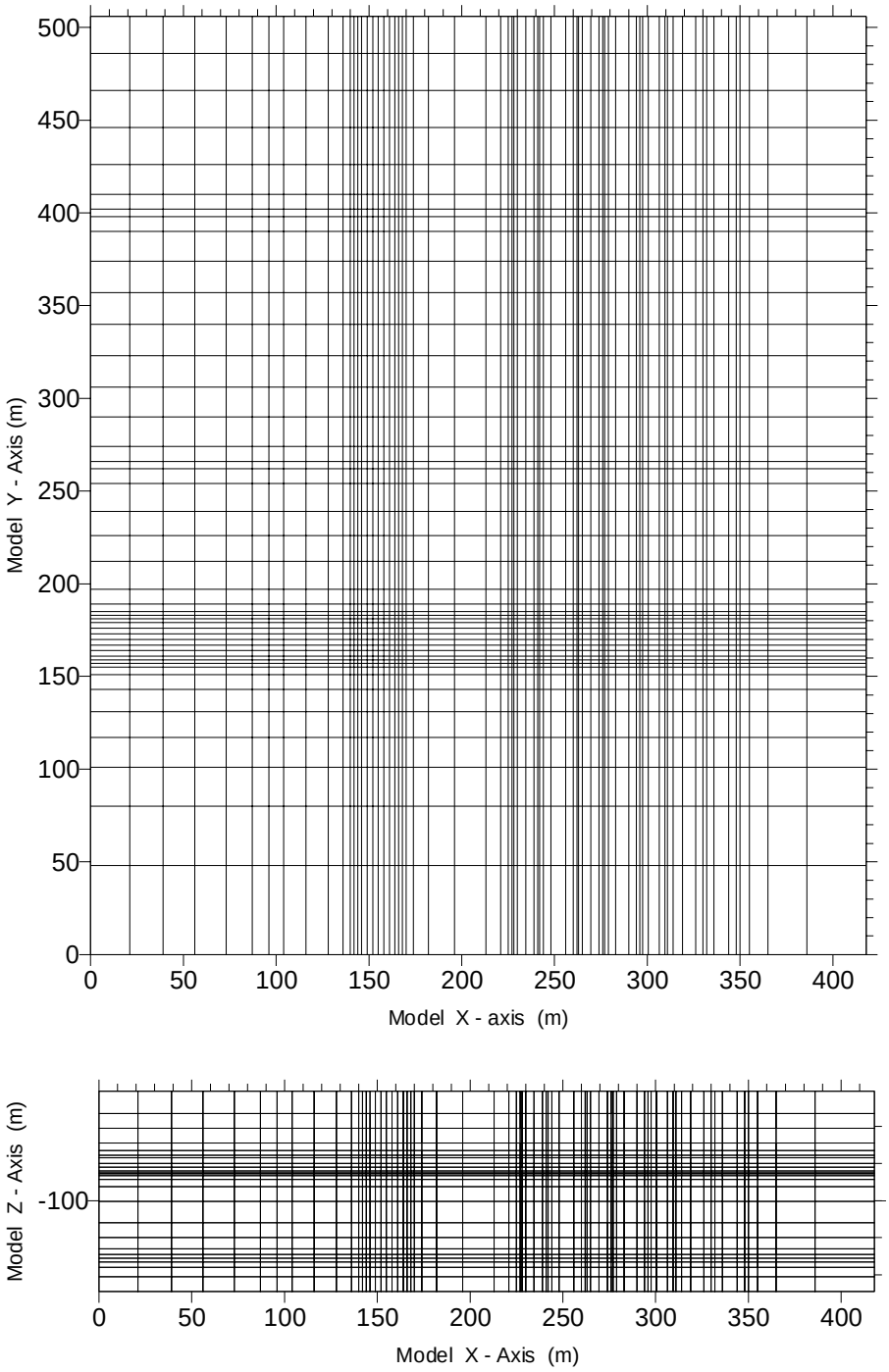

Figure A.5 *The finite difference mesh of the detailed model. The mesh has 24 layers and contains 73 920 cells. The mesh is optimised for the lay-out of the storage caverns. The model represents a horizontal area of 418 m x 506 m (0.21 km^2) and it has a depth of 108 m. The X-axis of the detailed model is pointing towards Northwest.*

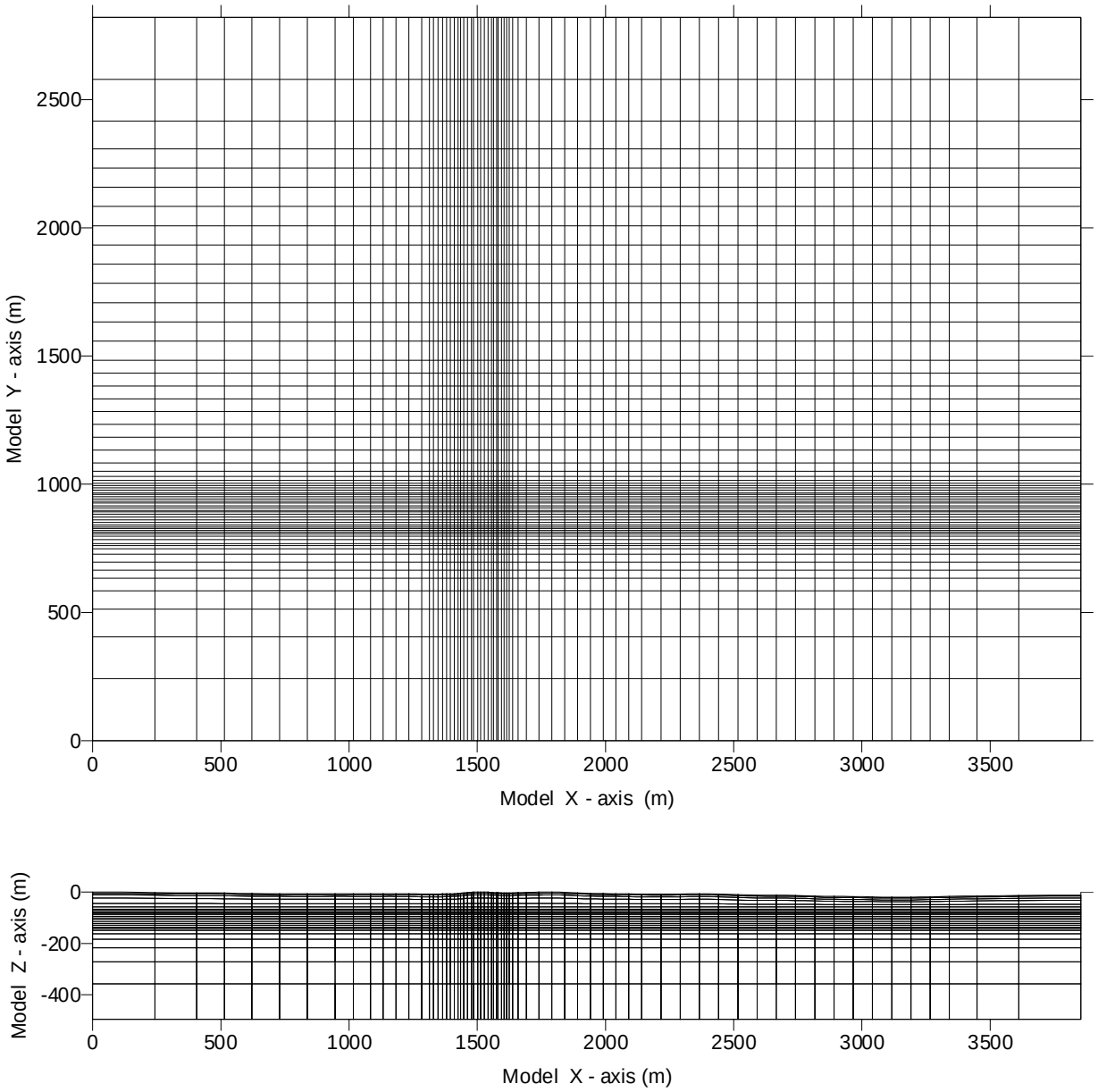

Figure A.6 *The finite difference mesh of the semilocal model. The mesh of the semilocal model, representing the tunnel system at SFR and surrounding rock masses, has 25 layers and contains 108 675 cells. The mesh is optimised for the lay-out of the storage caverns. The semilocal model covers a horizontal area of 2699 m x 3732 m (10.1 km^2). The depth of the model is the same as for the local model (490 m). The X-axis of the detailed model is pointing towards Northeast.*

Appendix B

Calculation of conductivity of tunnels for detailed model

USED FORMULAS

Addition of serial conductivities

$$\frac{L_1 + L_2 + ... + L_n}{\frac{L_1}{K_1} + \frac{L_2}{K_2} + ... + \frac{L_n}{K_n}} = K_{\text{equivalent}}$$

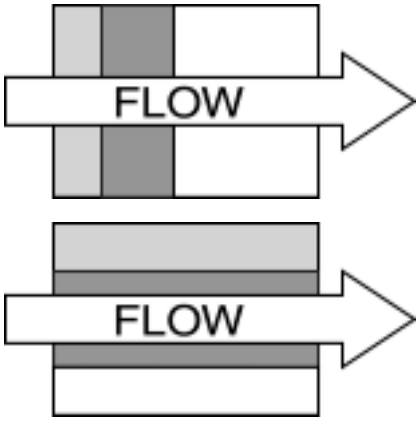

Addition of parallel conductivities

$$\frac{A_1}{A_{tot}} \cdot K_1 + \frac{A_2}{A_{tot}} \cdot K_2 + ... + \frac{A_n}{A_{tot}} \cdot K_n = K_{equivalent}$$

HIGH THRESHOLD

Below when discussing the conductivity of very permeable parts of the repository, e.g. a highly permeable back fill, we will use the concept of "high threshold". By this we mean that the material studied has a permeability that is so high that the material will not, in relation to the permeability of the surrounding rock mass, give any significant resistance to flow.

As an example, consider a small tunnel with a very permeable back fill. The flow in the tunnel will not depend on the permeability of the back fill, if the backfill permeability is large enough, because for such a situation the flow in the backfill is determined by the permeability of the surrounding rock mass. The surrounding rock mass will produce such a large resistance for the groundwater flow through the rock mass and the tunnel, that the material inside the tunnel, the very permeable backfill, will in comparison be of no importance for the flow through the tunnel.

However, the degree of permeability of a very permeable backfill is important when calculating the flow through a low permeable encapsulation, which is surrounded by a highly permeable backfill, i.e. a hydraulic cage. The amount of water that flows through the encapsulation depends on the contrast in conductivity between the surrounding backfill and the encapsulation. Hence, an increase of the permeability of the backfill will have a minimal effect on the flow in the backfill, but it will have an important effect on the flow through the encapsulation.

1. BMA TUNNEL

1.1 WASTE ELEMENTS

1.1.1 Along the tunnel

Number of concrete walls à 40 cm: 14
Length between walls: 9.9 m
Area1: $15.1 \cdot 7.3 = 110.23$ m^2
Area2: $15.9 \cdot 8.1 - 15.1 \cdot 7.3 = 18.56$ m^2

Conductivity of concrete walls: $8.3 \cdot 10^{-10}$ m/s
Conductivity of containers: ∞

Assumed Conductivity Part 1: $$\frac{14 \cdot 0.4 + 13 \cdot 9.9}{\frac{14 \cdot 0.4}{8.3 \cdot 10^{-10}} + \frac{13 \cdot 9.9}{\infty}} = 2.0 \cdot 10^{-8} \text{ m/s}$$

Assumed Conductivity Part 2: $8.3 \cdot 10^{-10}$ m/s

Assumed conductivity along the tunnel: $$2 \cdot 10^{-8} \cdot \frac{110.23}{128.79} + 8.3 \cdot 10^{-10} \cdot \frac{18.56}{128.79} = \mathbf{1.72 \cdot 10^{-8}} \text{ m/s}$$

1.1.2 Perpendicular to the tunnel

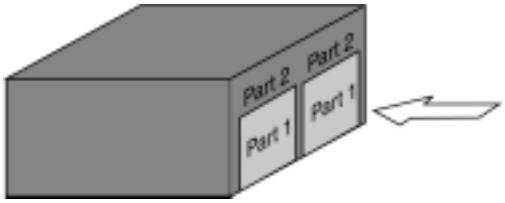

Number of concrete walls à 40 cm: 2
Length between walls: 15.1m
Conductivity of concrete walls: $8.3 \cdot 10^{-10}$ m/s
Conductivity of containers: ∞
Area1: $9.9 \cdot 7.3 = 72.27$ m^2
Area2: $10.3 \cdot 8.1 - 9.9 \cdot 7.3 = 11.16$ m^2

Assumed Conductivity Part 1: $$\frac{2 \cdot 0.4 + 1 \cdot 15.1}{\frac{2 \cdot 0.4}{8.3 \cdot 10^{-10}} + \frac{15.1}{\infty}} = 1.6 \cdot 10^{-8} \text{ m/s}$$

Assumed Conductivity Part 2: $8.3 \cdot 10^{-10}$ m/s

Assumed conductivity perpendicular to the tunnel:
$$1.6 \cdot 10^{-8} \cdot \frac{72.27}{83.43} + 8.3 \cdot 10^{-10} \cdot \frac{11.16}{83.43} = \mathbf{1.44 \cdot 10^{-8}} \text{ m/s}$$

1.1.3 Vertical through the tunnel

Number of concrete lids à 80 cm: 1
Height of the construction: 7.3 m
Conductivity of concrete lids: $8.3 \cdot 10^{-10}$ m/s
Conductivity of containers: ∞
Area1: $15.1 \cdot 9.9 = 149.49$ m^2
Area2: $10.3 \cdot 15.9 - 15.1 \cdot 9.9 = 14.28$ m^2

Assumed Conductivity Part 1:
$$\frac{0.8 + 7.3}{\frac{0.8}{8.3 \cdot 10^{-10}} + \frac{7.3}{\infty}} = 8.4 \cdot 10^{-9} \text{ m/s}$$

Assumed Conductivity Part 2: $8.3 \cdot 10^{-10}$ m/s

Assumed conductivity vertical through the tunnel:
$$8.4 \cdot 10^{-9} \cdot \frac{149.49}{163.77} + 8.3 \cdot 10^{-10} \cdot \frac{14.28}{163.77} = \mathbf{7.74 \cdot 10^{-9}} \text{ m/s}$$

1.2 WASTE ELEMENTS definition 2

If the waste is assumed to have the same conductivity as concrete backfill, i.e. $8.3 \cdot 10^{-9}$ m/s, instead of an infinite value, the Hydraulic conductivity in the different directions will be:

Assumed conductivity along the tunnel: **$5.3 \cdot 10^{-9}$ m/s**
Assumed conductivity perpendicular to the tunnel: **$5.1 \cdot 10^{-9}$ m/s**
Assumed conductivity vertical through the tunnel: **$4.1 \cdot 10^{-9}$ m/s**

1.3 SIDES, BACKFILL ON TOP & OTHER VOLUMES

High threshold

2. BLA TUNNEL

2.1 WASTE ELEMENTS

High threshold

2.2 CONCRETE FLOOR

2.2.1 Horizontally

Thickness of element: 0.5 m
Thickness of concrete: 0.2 m
Thickness of sand 0.2 m
Thickness of rockmass 0.6 m
Conductivity of concrete: $8.3 \cdot 10^{-10}$ m/s
Conductivity of sand $1 \cdot 10^{-7}$ m/s
Conductivity of rockmass $6.5 \cdot 10^{-9}$ m/s

Assumed conductivity: $$8.3 \cdot 10^{-10} \cdot \frac{0.2}{0.5} + 1 \cdot 10^{-7} \cdot \frac{0.2}{0.5} + 6.5 \cdot 10^{-9} \cdot \frac{0.1}{0.5} = \mathbf{4.2 \cdot 10^{-8}} \text{ m/s}$$

2.2.2 Vertically:

Thickness of element: 1m
Thickness of concrete: 0.2 m
Thickness of sand 0.2 m
Thickness of rockmass 0.6 m
Conductivity of concrete: $8.3 \cdot 10^{-10}$ m/s
Conductivity of sand $1 \cdot 10^{-7}$ m/s
Conductivity of rockmass $6.5 \cdot 10^{-9}$ m/s

Assumed conductivity: $$\frac{0.2 + 0.2 + 0.1}{\frac{0.2}{8.3 \cdot 10^{-10}} + \frac{0.2}{1 \cdot 10^{-7}} + \frac{0.1}{6.5 \cdot 10^{-9}}} = \mathbf{1.3 \cdot 10^{-9}} \text{ m/s}$$

2.3 SIDES, BACKFILL ON TOP AND OTHER VOLUMES

High threshold

3. BTF

3.1 WASTE ELEMENTS

3.1.1 Along the tunnel

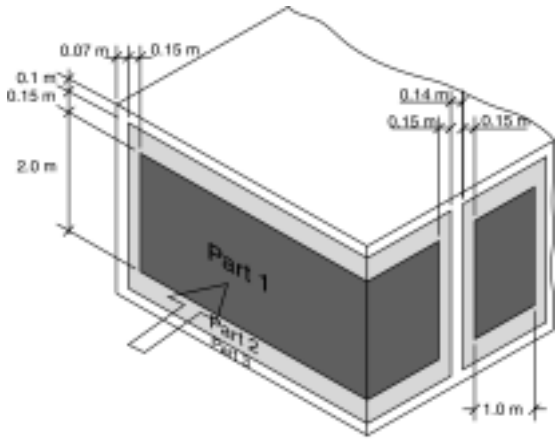

Part1

Thickness concrete wall 2·0.15m
Thickness Waste: 1·1.0m
Thickness concrete backfill 1·0.14m
Conductivity Concrete wall $8.3 \cdot 10^{-10}$ m/s
Conductivity Waste: ∞
Conductivity concrete backfill: $8.3 \cdot 10^{-9}$ m/s

Assumed Conductivity K_{part1}:

$$\frac{2 \cdot 0.15 + 1.0 + 0.14}{\frac{2 \cdot 0.15}{8.3 \cdot 10^{-10}} + \frac{1.0}{\infty} + \frac{0.14}{8.3 \cdot 10^{-9}}} = 3.8 \cdot 10^{-9}$$

Part 2

Thickness concrete wall: 1·1.3m
Thickness concrete backfill: 1·0.14m
Conductivity Concrete wall $8.3 \cdot 10^{-10}$ m/s
Conductivity concrete backfill: $8.3 \cdot 10^{-9}$ m/s

Assumed Conductivity K_{part2}:

$$\frac{1.3 + 0.14}{\frac{1.3}{8.3 \cdot 10^{-10}} + \frac{0.14}{8.3 \cdot 10^{-9}}} = 9.1 \cdot 10^{-10}$$

Part 3

Thickness concrete backfill: 1·1.44m
Conductivity concrete backfill: $8.3 \cdot 10^{-9}$ m/s

Part 1-3

Area Part 1 $2 \cdot 3 = 6 m^2$
Area Part 2 $(3.3 \cdot 2.3) - (3 \cdot 2) = 1.59 m^2$
Area Part 3 $(3.44 \cdot 2.5) - (3.3 \cdot 2.3) = 1.01\ m^2$

Assumed conductivity along the tunnel:

$$3.8 \cdot 10^{-9} \cdot \frac{6}{8.6} + 9.1 \cdot 10^{-10} \cdot \frac{1.59}{8.6} + 8.3 \cdot 10^{-9} \cdot \frac{1.01}{8.6} = \mathbf{3.8 \cdot 10^{-9}}\ \text{m/s}$$

3.1.2 Perpendicular to the tunnel

Part 1

Thickness of Concrete wall: 2·0.15m
Thickness of waste: 1·3.0m
Thickness of concrete backfill: 1·0.14m
Conductivity Concrete wall $8.3 \cdot 10^{-10}$ m/s
Conductivity Waste: ∞
Conductivity concrete backfill: $8.3 \cdot 10^{-9}$ m/s

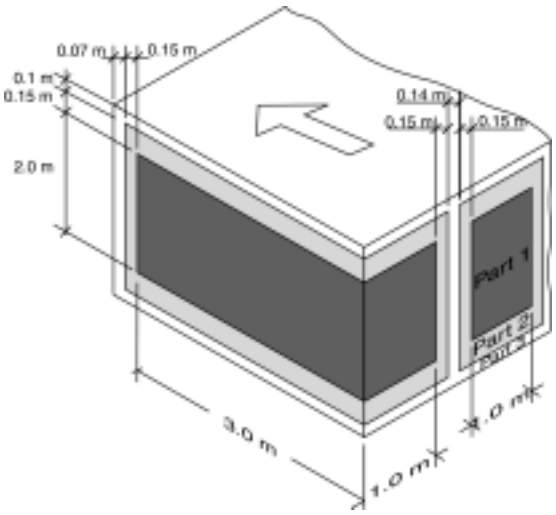

Assumed Conductivity K_{part1}:

$$\frac{2 \cdot 0.15 + 3.0 + 0.14}{\frac{2 \cdot 0.15}{8.3 \cdot 10^{-10}} + \frac{3.0}{\infty} + \frac{0.14}{8.3 \cdot 10^{-9}}} = 9.1 \cdot 10^{-9}$$

Part 2

Thickness of Concrete wall: 1·3.3m
Thickness of concrete backfill: 1·0.14m
Conductivity Concrete wall $8.3 \cdot 10^{-10}$ m/s
Conductivity concrete backfill: $8.3 \cdot 10^{-9}$ m/s

Assumed Conductivity K_{part2}:

$$\frac{3.3 + 0.14}{\frac{3.3}{8.3 \cdot 10^{-10}} + \frac{0.14}{8.3 \cdot 10^{-9}}} = 8.6 \cdot 10^{-10}$$

Part 3

Thickness of concrete backfill: 1·3.44m
Conductivity concrete backfill: $8.3 \cdot 10^{-9}$ m/s

Part 1-3

Area Part1 $1 \cdot 2 = 2 m^2$
Area Part2 $(1.3 \cdot 2.3) - (2 \cdot 1) = 0.99 m$
Area Part3 $(1.44 \cdot 2.5) - (1.3 \cdot 2.3) = 0.61 m$

Assumed conductivity perpendicular to the tunnel

$$9.1 \cdot 10^{-9} \cdot \frac{2.0}{3.6} + 8.6 \cdot 10^{-10} \cdot \frac{0.99}{3.6} + 8.3 \cdot 10^{-9} \cdot \frac{0.61}{3.6} = \mathbf{6.7 \cdot 10^{-9}}$$

3.1.3 Vertically through the tunnel

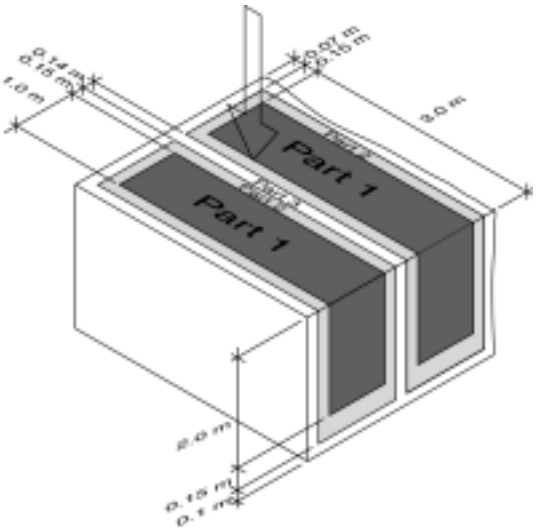

Part 1
Thickness of Concrete wall: 2·0.15m
Thickness of waste: 1·2.0m
Thickness of concrete backfill: 2·0.1m
Conductivity Concrete wall $8.3 \cdot 10^{-10}$ m/s
Conductivity Waste: ∞
Conductivity concrete backfill: $8.3 \cdot 10^{-9}$ m/s

Assumed Conductivity

K_{part1}: $$\frac{2 \cdot 0.15 + 2.0 + 0.2}{\frac{2 \cdot 0.15}{8.3 \cdot 10^{-10}} + \frac{2.0}{\infty} + \frac{0.2}{8.3 \cdot 10^{-9}}} = 6.5 \cdot 10^{-9}$$

Part 2
Thickness of Concrete wall: $1 \cdot 2.3$m
Thickness of concrete backfill: $1 \cdot 0.2$m
Conductivity Concrete wall $8.3 \cdot 10^{-10}$ m/s
Conductivity concrete backfill: $8.3 \cdot 10^{-9}$ m/s

Assumed Conductivity K_{part2}: $$\frac{2.3 + 0.2}{\frac{2.3}{8.3 \cdot 10^{-10}} + \frac{0.2}{8.3 \cdot 10^{-9}}} = 8.9 \cdot 10^{-10}$$

Part 3
Thickness of concrete backfill: $1 \cdot 2.5$m
Conductivity concrete backfill: $8.3 \cdot 10^{-9}$

Part 1-3
Area Part 1 $1 \cdot 3 = 3m^2$
Area Part 2 $(1.3 \cdot 3.3) - (1 \cdot 3) = 1.29$
Area Part 3 $(3.44 \cdot 1.44)(1.3 \cdot 3.3) = 0.66$m

Assumed conductivity vertically through to the tunnel

$$6.5 \cdot 10^{-9} \cdot \frac{3.0}{4.95} + 8.6 \cdot 10^{-10} \cdot \frac{1.29}{4.95} + 8.3 \cdot 10^{-9} \cdot \frac{0.66}{4.95} = \mathbf{5.3 \cdot 10^{-9}}$$

3.2 CONCRETE FLOOR

Same as for the concrete floor in the BLA, see section 2.2.1 and 2.2.2.

3.3 SIDES

Conductivity concrete backfill: $8.3 \cdot 10^{-9}$

3.4 BACKFILL ON TOP AND OTHER VOLUMES

High threshold

4. SILO

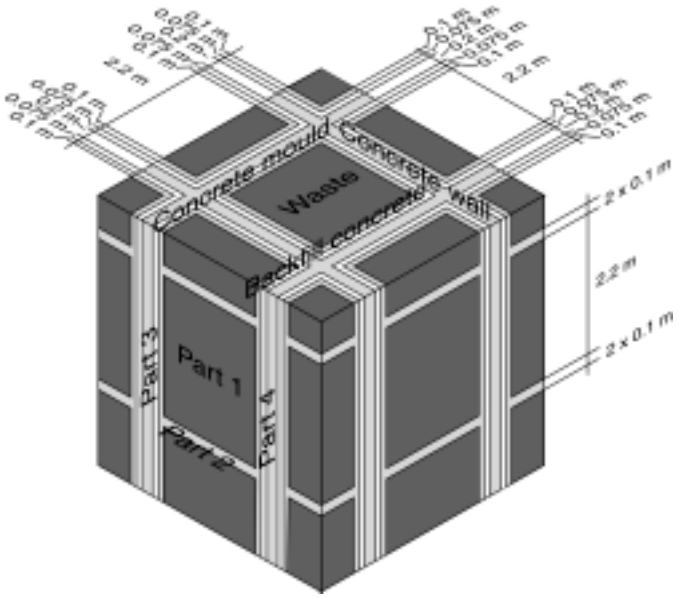

4.1 ENCAPSULATION

4.1.1 Horizontally

Part 1

Thickness of Concrete walls:	2·0.10 +0.2m
Thickness of Waste:	2.2m
Thickness of backfill concrete:	2·0.075m
Conductivity Concrete wall	$8.3 \cdot 10^{-10}$ m/s
Conductivity Waste:	∞
Conductivity concrete backfill:	$8.3 \cdot 10^{-9}$ m/s

Assumed Conductivity K_{part1}:

$$\frac{2 \cdot 0.1 + 0.2 + 2.2 + 2 \cdot 0.075}{\frac{2 \cdot 0.1 + 0.2}{8.3 \cdot 10^{-10}} + \frac{2.2}{\infty} + \frac{2 \cdot 0.075}{8.3 \cdot 10^{-9}}} = 5.5 \cdot 10^{-9}$$

Part 2

Thickness of Concrete walls:	2.6m
Thickness of backfill concrete:	2·0.075m
Conductivity Concrete wall	$8.3 \cdot 10^{-10}$ m/s
Conductivity concrete backfill:	$8.3 \cdot 10^{-9}$ m/s

Assumed Conductivity K_{part2}:

$$\frac{2.6 + 2 \cdot 0.075}{\frac{2.6}{8.3 \cdot 10^{-10}} + \frac{2 \cdot 0.075}{8.3 \cdot 10^{-9}}} = 8.7 \cdot 10^{-10}$$

Part 3

Thickness of Concrete walls:	2·0.1m
Thickness of backfill concrete:	2.55m
Conductivity Concrete wall	$8.3 \cdot 10^{-10}$ m/s
Conductivity concrete backfill:	$8.3 \cdot 10^{-9}$ m/s

Assumed Conductivity K_{part3}:

$$\frac{0.2 + 2.55}{\frac{0.2}{8.3 \cdot 10^{-10}} + \frac{2.55}{8.3 \cdot 10^{-9}}} = 5.0 \cdot 10^{-9}$$

Part 4

Thickness of Concrete walls:	1·2.75m
Conductivity Concrete wall	$8.3 \cdot 10^{-10}$ m/s

Part 1-4

Area Part1	2.2·2.2= 4.84m
Area Part 2	2.4·2.4-2.2·2.2= 0.92m
Area Part 3	2.4·0.15=0.36 m
Area Part 4	2.4·0.2=0.48 m

Assumed conductivity

$$5.5 \cdot 10^{-9} \frac{4.84}{6.6} + 8.7 \cdot 10^{-10} \cdot \frac{0.92}{6.6} + 5 \cdot 10^{-9} \cdot \frac{0.36}{6.6} + 8.3 \cdot 10^{-10} \cdot \frac{0.48}{6.6} = \mathbf{4.5 \cdot 10^{-9}}\ \text{m/s}$$

4.1.2 Vertically

Part 1
Thickness of Concrete walls: 2·0.10 m
Thickness of Waste: 2.2 m
Conductivity Concrete wall $8.3 \cdot 10^{-10}$ m/s
Conductivity Waste: ∞

Assumed Conductivity K_{part1}:

$$\frac{2 \cdot 0.1 + 2.2}{\frac{2 \cdot 0.1}{8.3 \cdot 10^{-10}} + \frac{2.2}{\infty} +} = 1 \cdot 10^{-8} \text{ m/s}$$

Part 2
Thickness of Concrete walls: 2.4m
Conductivity Concrete wall $8.3 \cdot 10^{-10}$ m/s

Part 3
Thickness of backfill concrete: 2.4m
Conductivity concrete backfill: $8.3 \cdot 10^{-9}$ m/s

Part 4
Thickness of Concrete walls: 2.4m
Conductivity Concrete wall $8.3 \cdot 10^{-10}$ m/s

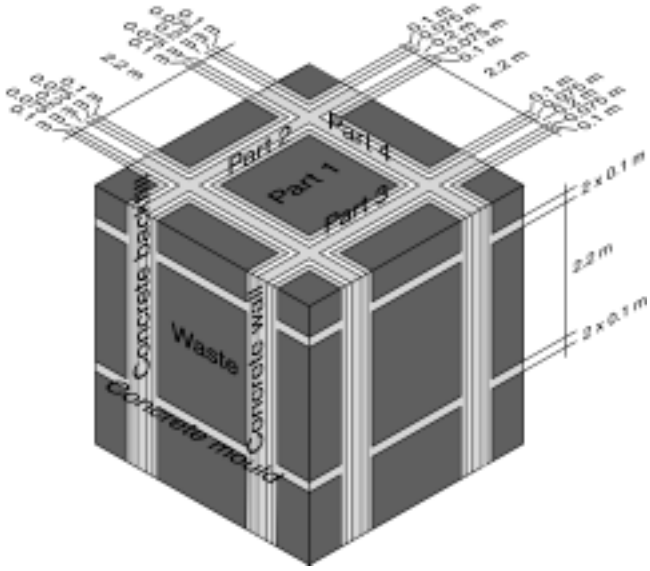

Part 1-4
Area Part 1 $2.2 \cdot 2.2 = 4.84 m^2$
Area Part 2 $(2.4 \cdot 2.4) - (2.2 \cdot 2.2) = 0.92 m$
Area Part 3 $(2.55 \cdot 2.55) - (2.4 \cdot 2.4) = 0.74 m$
Area Part 4 $(2.75 \cdot 2.75) - (2.55 \cdot 2.55) = 1.06 m$

Assumed conductivity

$$1 \cdot 10^{-8} \frac{4.84}{7.56} + 8.3 \cdot 10^{-10} \cdot \frac{0.92}{7.56} + 8.3 \cdot 10^{-9} \cdot \frac{0.74}{7.56} + 8.3 \cdot 10^{-10} \cdot \frac{1.06}{7.56} = \mathbf{7.4 \cdot 10^{-9}} \text{ m/s}$$

4.2 Silo walls – Barriers

4.2.1 Horizontally

Thickness of concrete: 0.8m
Thickness of Bentonite: 1.2m
Conductivity Concrete $8.3 \cdot 10^{-10}$ m/s
Conductivity bentonite $6 \cdot 10^{-12}$ m/s

Assumed conductivity:

$$\frac{0.8 + 1.2}{\frac{0.8}{8.3 \cdot 10^{-10}} + \frac{1.2}{6 \cdot 10^{-12}}} = \mathbf{1.0 \cdot 10^{-11}} \text{ m/s}$$

4.2.2 Vertically

Thickness of concrete: 0.8m
Thickness of Bentonite: 1.2m
Conductivity Concrete $8.3 \cdot 10^{-10}$ m/s
Conductivity bentonite $6 \cdot 10^{-12}$ m/s

Assumed conductivity: $8.3 \cdot 10^{-10} \cdot \frac{0.8}{2} + 6 \cdot 10^{-12} \cdot \frac{1.2}{2} = \mathbf{3.4 \cdot 10^{-10}}$ m/s

4.3 Silo base - Barriers

4.3.1 Horizontally

Tickness of contrete: 1m
Thickness of Sand/Bentonite: 1.5m
Conductivity Concrete $8.3 \cdot 10^{-10}$ m/s
Conductivity sand/bentonite $1 \cdot 10^{-9}$ m/s

Assumed conductivity: $8.3 \cdot 10^{-10} \cdot \frac{1}{2.5} + 1 \cdot 10^{-9} \cdot \frac{1.5}{2.5} = \mathbf{9.3 \cdot 10^{-10}}$ m/s

4.3.2 Vertically

Tickness of contrete: 1m
Thickness of Sand/Bentonite: 1.5m
Conductivity Concrete $8.3 \cdot 10^{-10}$ m/s
Conductivity sand/bentonite $1 \cdot 10^{-9}$ m/s

Assumed conductivity: $\frac{1+1.5}{\frac{1}{8.3 \cdot 10^{-10}} + \frac{1.5}{1 \cdot 10^{-9}}} = \mathbf{9.2 \cdot 10^{-10}}$ m/s

Appendix C

Analytical solutions for estimation of length of saturation period

The purpose of this appendix is to present a pseudo-analytic method that represents the transient inflow of water to the Silo at SFR. As the Silo has the shape of a cylinder we will simplify the actual three dimensional flow towards the Silo and represent it as a two dimensional flow towards the circular envelope of a cylinder (no flow through the gables). We will also simplify the actual heterogeneous flow medium (the rock mass) and assume homogeneous and isotropic hydraulic properties for the flow medium. Furthermore, it is assumed that the air inside the Silo can escape out of the Silo, as the Silo becomes filled with water, without influencing the inflow of groundwater or change the pressure inside the Silo. The pressure inside the unsaturated domain of the Silo is assumed to be constant and represent atmospheric pressure. These are a simplification of the actual system, which makes it possible to handle the course of saturation as a problem concerning one phase only i.e. the groundwater.

An equation giving the head at a well, for a given steady state discharge, was derived by Thiem (1906). The equation describes radial and steady, two-dimensional flow, under confined conditions, towards a circular sink of a given height (a cylinder). The flow and the radius of the sink must be given as well as the head at a specified head boundary, at a given radius from the sink. The development of this equation from Darcy´s law is well known and will not be presented here, see e.g. Strack (1989) Thiem's equation is given as Equ. 1. Note that a flow into the sink (the well discharge) should be given as a negative flow (a flow out of the system).

Equ. 1

$$\phi = \phi_0 + \frac{Q}{2\pi K T} \ln \frac{r}{R}$$

ϕ = Head at circular sink
ϕ_0 = Head at a defined outer boundary
Q = Flow at circular sink (discharge of well)
K = Hydraulic conductivity
T = Thickness of flow medium and height of cylinder (circular sink)
r = Radius of cylinder (circular sink)
R = Radius to outer boundary

Solving Equ. 1 for the flow gives the following equation.

Equ. 2

$$Q = 2\pi K T \frac{\phi - \phi_0}{\ln \frac{r}{R}}$$

We will formulate the equation above as time dependent, by including a time dependent storage of fluid inside the cylinder (inside the well), as well as a time dependent change of the size of the cylinder. We will simplify the problem and not consider storage of fluid in the flow medium outside of the cylinder. Because for a crystalline rock mass under confined conditions, the storage due to pressure changes is normally very small, especially compared to the storage inside the cylinder. The storage of fluid inside a cylinder may occur as a storarge of fluid along the radius of the cylinder – a radial storage, or as a storarge of fluid along the height of the cylinder – an axial storage. Based on these two alternatives we have derived two different formulations: Analytic solution No.1 and Analytic solution No.2.

Analytic solution No.1.

For the first analytic formulation it is assumed that the fluid is stored inside the cylinder along the radius of the cylinder – a radial storage from the outer limits of the cylinder and inwards. It follows that the radius of the unsaturated cylinder (the radius of the unsaturated domain in the Silo) decreases with time, as more and more of the cylinder gets saturated and more and more water is stored in the cylinder. The height of the cylinder is set as constant. The following equation defines the volume inside the cylinder that is available for storage during the time period between t_1 and t_2

Equ. 3

$$V_{avail} = (\pi r_{t1}^2 T - \pi r_{t2}^2 T)\, \eta_{cyl}$$

V_{avail} = *Volume available for storage*
r_{t1} = *Radius of cylinder at time equal to* t_1
r_{t2} = *Radius of cylinder at time equal to* t_2
η_{cyl} = *Available porosity of cylinder*

The volume of inflow during the time step between t_1 and t_2 is equal to the following integral:

Equ. 4

$$V_{in} = \int_{t1}^{t2} Q_{(t)}\, dt$$

We will use an iterative method to solve the final equation and for small values of the time step the equation above can be simplified as below.

Equ. 5

$$V_{in} = \int_{t1}^{t2} Q_{(t)}\, dt \quad \approx \quad Q_{t1}\, \Delta t$$

V_{in} = *Volume of inflow during the time period of* Δt
$Q_{t\,1}$ = *Inflow at time equal to* t_1
Δt = *Time step*

The law of mass-conservation and of flow-continuity tells us that V_{in} is equal to V_{avail} . Therefore, we will set Equ. 3 equal to Equ. 5 and get the following equation:

Equ. 6

$$Q_{t1}\,\Delta t = (\pi r_{t1}^2 T - \pi r_{t2}^2 T)\,\eta_{cyl}$$

Solving for the radius of the cylinder produces the following equation:

Equ. 7

$$r_{t2} = \sqrt{r_{t1}^2 - \frac{Q_{t1}\,\Delta t}{\pi T\,\eta_{cyl}}}$$

Substituting Equ. 7 into Equ. 2 produces the following equation.

Equ. 8

$$Q_{t2} = 2\pi K T \frac{\phi - \phi_0}{\ln \frac{\sqrt{r_{t1}^2 - \frac{Q_{t1}\,\Delta t}{\pi T\,\eta_{cyl}}}}{R}}$$

Q_{t2} = *Inflow at time equal to* t_2

The equation above has to be a part of an iterative algorithm. The initial condition for the iterations should be the steady state condition, as given by Equ. 2. By use of a sufficient small time step, the inflow at any later time (t_2) could be reached by iterations. This is the analytic solution No.1.

Analytic solution No.2.

For the second analytic formulation it is assumed that the fluid is stored inside the cylinder along the axis (height) of the cylinder – an axial storage from the bottom of the cylinder and upward. It follows that the vertical extension of the unsaturated cylinder (the height of the unsaturated domain in the Silo) decreases with time as more and more of the cylinder gets saturated. The radius of the cylinder is set as constant. The following equation defines the volume inside the cylinder that is available for storage during the time period between t_1 and t_2

Equ. 9

$$V_{avail} = (\pi r^2 T_{t1} - \pi r^2 T_{t2})\,\eta_{cyl}$$

V_{avail} = *Volume available for storage*
T_{t1} = *Vertical extension of cylinder at time equal to* t_1
T_{t2} = *Vertical extension of cylinder at time equal to* t_2
η_{cyl} = *Available porosity of cylinder*

The volume of inflow during the time step between t_1 and t_2 is equal to the following integral:

Equ. 10

$$V_{in} = \int_{t1}^{t2} Q_{(t)}\, dt$$

We will use an iterative method to solve the final equation and for small values of the time step the equation above can be simplified as below.

Equ. 11

$$V_{in} = \int_{t1}^{t2} Q_{(t)}\, dt \quad \approx \quad Q_{t1}\, \Delta t$$

V_{in} = Volume of inflow during the time period of Δt
$Q_{t\,1}$ = Inflow at time equal to t_1
Δt = Time step

The law of mass-conservation and of flow-continuity tells us that V_{in} is equal to V_{avail}. Therefore, we will set Equ. 11 equal to Equ. 9 and get the following equation:

Equ. 12

$$Q_{t1}\, \Delta t = (\pi r^2 T_{t1} - \pi r^2 T_{t2})\, \eta_{cyl}$$

Solving for the vertical extension of the cylinder produces the following equation:

Equ. 13

$$T_{t2} = T_{t1} - \frac{Q_{t1}\, \Delta t}{\pi\ r^2\, \eta_{cyl}}$$

Substituting Equ. 13 into Equ. 2 produces the following equation.

Equ. 14

$$Q_{t2} = 2\pi K \left(T_{t1} - \frac{Q_{t1}\, \Delta t}{\pi\ r^2\, \eta_{cyl}} \right) \frac{\phi - \phi_0}{\ln \frac{r}{R}}$$

Q_{t2} = Inflow at time equal to t_2

The equation above has to be a part of an iterative algorithm. The initial condition for the iterations should be the steady state condition, as given by Equ. 2. By use of a sufficient small time step, the inflow at any later time (t_2) could be reached by iterations. This is the analytic solution No.2.

References

Strack, O., (1989): "Groundwater Mechanics" Prentice-Hall Inc., Englewood Cliffs, New Jersey, 07632 USA.

Thiem, G., (1906): “Hydrologische Methoden.” J. M. Gebhardt, Leipzig, Germany.